Machine Learning and Reaction Chemistry for Efficient Thermal Conversion of Waste Plastic

A Thesis Presented

by

Elizabeth Rose Belden

Submitted to the Graduate School of

Worcester Polytechnic Institute in partial fulfillment

of the requirements for the degree of

DOCTOR OF PHILOSOPHY

March 2024

Department of Chemical Engineering

Machine Learning and Reaction Chemistry for Efficient Thermal Conversion of Waste Plastic

A Thesis Presented

by

Elizabeth Rose Belden

Approved as to style and content by:

Dr. Michael T. Timko Chemical Engineering, WPI	Dr. Nikolaos Kazantzis, Member Chemical Engineering, WPI
Dr. N. Aaron Deskins, Member Chemical Engineering, WPI	Dr. Randy C. Paffenroth, Member Mathematical Sciences, Data Science, Computer Science, WPI
Dr. Susan Roberts, Department Head Chemical Engineering, WPI	

Acknowledgements

There are so many people who have encouraged and helped me throughout my PhD and I will try to do justice thanking them here. Firstly, I want to thank my advisor Mike Timko who has provided unending support and guidance throughout my years. Being your first primarily computational student was an adventure that almost didn't happen. Thank you for pushing back during my first year when I said I wanted to be 100% experimental in my research. You acknowledged and fostered my computational skill set and I truly can't see my thesis ending up any other way than it has. Regardless of how weird my brain described a new idea, you took the time to understand what I meant and taught me how to explain my science to a wider audience.

I also want to thank the Timko and Teixera groups, especially Heather LeClerc, Maddie Reed, Karen Agro and David Kenney. You have all helped me not only with research, through endless discussions and brainstorming sessions, but also emotionally by listening when I just needed to vent! I want to thank Heather in particular, I really don't know what I would have done my first year (or any other year) without you as a resource to guide me through all things PhD and a friend to help me adjust to graduate school. I also can't forget the countless other friends at WPI who have made my grad school experience unforgettable including, Lily Gaudreau, Cam Armstrong, Fatou Diop, Sydney Packard, Esai Lopez and Muntasir Shahabuddin. Finally (for this section), I want to thank my best friend, Meg Marchione. You have been there for me through the ups and downs of my PhD, listened to countless complaining and celebrated all the wins, even small ones I struggled to celebrate.

Additionally, I want to thank my collaborators and committee members for sharing their knowledge with me, teaching me new techniques and supporting me throughout my various

projects. In particular, I want to thank Dr. Geoff Tompsett and Dr. Alex Maag for answering my seemingly endless stream of questions as I tried to learn experimental techniques. You never made me feel dumb, even when my questions probably were. You always made time for me when I needed help in lab, wanted to run ideas by you, vent about frustrations or just chat. Your aid has been invaluable to me throughout my PhD. I also want to thank Dr. Nikolaos Kazantzis and Dr. Randy Paffenroth for teaching me all I know about modeling techniques and encouraging me to continue exploring ways to apply them to my research. Thank you Randy for always listening to my, sometimes crazy, ideas of new ways to apply machine learning to my work and helping me achieve it. Thank you to the rest of my committee and collaborators who have aided in guiding me through my PhD and always shared their expertise.

Finally, I want to thank my family, particularly my parents and sister, for always supporting and encouraging me to achieve my goals. I never would have made it this far in my PhD, or in life, without you. You have been there for me through everything, encouraged my love of math and science from an early age and supported me when graduate school or life got tough. I am so happy I was able to do my PhD so close to home and see you so often. I truly could not have done this without you and love you so much!

Abstract

Waste plastic is an ever-growing environmental concern with millions of tons of plastic entering the environment every year. The strongly bonded carbon backbone of plastics combined with their low recyclability results in an accumulation of this recalcitrant polymer with limited viable options for reuse. Thermal depolymerization technologies are one of the promising methods capable of chemically recycling waste plastics. Hydrothermal liquefaction (HTL) and pyrolysis use high temperatures, with or without the presence of oxygen, respectively, to break the strong covalently bonded polymer chain to create smaller molecules such a fuel grade oils and platform chemical monomers. Regardless of the thermal method, research has shown that thermal depolymerization performance is highly dependent on feedstock composition, which requires experimental studies of each new feedstock.

In this work, computational and experimental studies are combined to provide a detailed understanding of feedstock compositional effects and thermodynamic and economic potential of thermal conversion of waste plastic to fuel and chemicals. The use of thermodynamic Monte Carlo modeling revealed the thermodynamic feasibility of self-powered cleanup of oceanic waste plastics via conversion into marine fuel, termed “Blue Diesel”. In addition to being thermodynamically feasible, it was shown the existing plastic present in the Great Pacific Garbage Patch could be entirely cleaned within 50 years, if new plastic input to the ocean can be eliminated. Stopping plastic waste in rivers before they can enter the ocean is a major step to turning off plastic input to the ocean. To understand the thermodynamic potential of river-based conversion systems, machine learning models were developed such that the oil yields from any new feedstocks can be predicted and incorporated into thermodynamic models. This work indicated that even in mildly polluted rivers, river-based conversion systems were thermodynamically feasible and that machine

learned models could be used to analyze the impact of feedstock composition on reaction performance. Along with thermodynamic potential, machine learning models were also used to predict the oil yield potential of land-based pyrolysis of waste plastic to oil in all 50 states. These predictions were incorporated into a technoeconomic analysis, showing an average minimum selling price of $170/ton. These models allow for the rapid analysis of new feedstocks without the necessity of new experimental studies. Further improvement to the economic potential of thermal conversion of waste plastics was studied experimentally through the creation of high value oxygenated products from radical induced-HTL of polystyrene. These experiments combined with traditional HTL experiments began to shed light on the effect of water on the depolymerization mechanism of polystyrene, a mechanism that is not currently known in the literature. Economic potential was further analyzed computationally to understand depolymerization kinetics of model compounds to target high value products. The work done in this thesis expands the fields knowledge of the exceptional potential of thermal conversion technologies to change how the world handles end of life waste plastics.

Authorship

The work in this thesis could not have been completed without the collaboration of the many. A summary of collaborators and their affiliations can be found below.

Chapter 2 – Thermodynamic feasibility of shipboard conversion of marine plastics to blue diesel for self-powered ocean cleanup

Nikolaos K. Kazantzis[1], Christopher M. Reddy[2], Hauke Kite-Powell[3], Michael T. Timko[1], Dudley R. Herschback[4]

Chapter 3 – Machine learning predictions of oil yields obtained by plastic pyrolysis and application to thermodynamic analysis

Matthew Rando[1], Owen G. Ferrara[1], Eric T. Himebaugh[1], Christopher A. Skangos[1], Nikolaos K. Kazantzis[1], Randy C. Paffenrith[5,6], Michael T. Timko[1]

Chapter 4 – Predictive machine learning for thermal depolymerization of plastics and application to economic analysis of municipal recycling facilities

Bernardo Castro-Dominguez[7], Michael T. Timko[1]

Chapter 5 – Oxygenated monomer production from the depolymerization of polystyrene in the presence of a radical source

Alex R. Maag[1], Christopher M. Reddy[2], Robert K. Nelson[2], Michael T. Timko[1]

Chapter 6 – Data driven discovery of reaction pathways for understanding catalytic cracking of hydrocarbons in the presence of catalyst

Randy C. Paffenroth[5,6], Michael T. Timko[1]

Chapter 7- Use of Machine Learning and Monte Carlo Analysis to Various Applications

Project 1

Accuracy of predictions made by machine learned models for biocrude yields obtained from hydrothermal liquefaction

Feng Cheng[1], Elizabeth R. Belden, Wenjing Li[5], Muntasir Shahabuddin[1], Randy C. Paffenroth[5,6], Michael T. Timko[1]

Project 2

Mechanochemical pretreatment for waste-free conversion of bamboo to simple sugars: Utilization of available resources for developing economies

Nneka B. Ekwe[1,8,9], Maksim V. Tyufekchiev[1], Ali A. Salifu[8,10,11], Geoffrey A. Tompsett[1], Heather O. LeClerc[1], Elizabeth R. Belden, Emmanuel O. Onche[8], Klaus Schmidt-Rohr[12], Shichen Yuan[12], Zhaoxi Zheng[12], Winston O. Soboyejo[8,10,11], Michael T. Timko[1]

Project 3

Thermodynamic and economic analysis of a deployable and scalable process to recover monomer-grade styrene from waste polystyrene

Madison R. Reed[1], Elizabeth R. Belden, Nikolaos K. Kazantzis[1], Michael T. Timko[1], Bernardo Castro-Dominguez[7]

Affiliations

1. Worcester Polytechnic Institute, Department of Chemical Engineering, 100 Institute Road, Worcester, MA 01069, USA.
2. Department of Marine Chemistry and Geochemistry, Woods Hole Oceanographic Institution, Woods Hole, MA, 02543
3. Marine Policy Center, Woods Hole Oceanographic Institution, Woods Hole, MA, 02543
4. Department of Chemistry and Chemical Biology, Harvard University, Cambridge, MA 02138, USA
5. Department of Mathematical Sciences, Worcester Polytechnic Institute, 100 Institute Rd., Worcester, MA 01609, USA.
6. Department of Computer Science, and Data Science Program, Worcester Polytechnic Institute, 100 Institute Rd., Worcester, MA 01609, USA.
7. Department of Chemical Engineering, University of Bath, Bath, UK
8. Department of Materials Science and Engineering, African University of Science and Technology (AUST), Abuja, Nigeria
9. Department of Chemical Engineering, University of Abuja, Abuja, Nigeria
10. Department of Biomedical Engineering, Worcester Polytechnic Institute, 60 Prescott Street, Gateway Park Life Sciences and Bioengineering Center, Worcester, MA, 01609 USA
11. Mechanical Engineering Department and Materials Science and Engineering Program, Worcester Polytechnic Institute, 100 Institute Road, Worcester, MA, 01609 USA
12. Department of Chemistry, Brandeis University, 415 South Street, Waltham, MA, 02453 USA

Table of Contents

Table of Figures

Table of Tables

Chapter 1: Background and Motivation

1.1 Prevalence of Waste Plastic

Global production of plastics reached 368 million metric tons in 2019 with only an estimated 9% being recycled and 12% being incinerated for energy recovery[1, 2]. The reaming 79% of plastic waste is destined for landfills, with a significant amount ending up in the natural environment due to mismanagement of waste. Of the six major classes of plastics, termed the "Big Six" (polystyrene (PS), high density polyethylene (HDPE), low density polyethylene (LDPE), polypropylene (PP), polyvinyl chloride (PVC) and polyethylene terephthalate (PET)) only PET, HDPE and PP can be easily recycled[3]. Compounding the recycling problem is the fact that these plastic only have a recycling rate of approximately 30%[4]. Low recycling rates for these polymers are attributed to a range of factors including, mismanagement of waste by end users (i.e. putting plastic waste in the trash or littering), limited recycling facilities[5] and issues sorting plastics. In order to produce a high-quality recycled product the plastics must be sorted into individual pure plastic streams[3]. Sorting individual plastic types is not trivial and is often complicated further due to contaminants such as residual product, labels and polymer additives[3].

HDPE, PET and PP account for approximately 55% of the waste polymer in the US as seen in **Figure 1-1**, leaving 45% of all plastic waste with no recycling options. Being able to handle these other polymers, as well as the reaming 70% that is not recycled from PET, HDPE, and PP is critical to addressing the plastic waste problem in the world. It is also critically important to develop technologies that can handle mixed waste streams to further increase our recycling capabilities by eliminating the need for sorting and reducing the impact of contaminants. One promising family of technologies are thermal techniques that convert plastics into fuels and other

byproducts as they can handle these mixed wastes creating a diesel grade fuel or converting single polymers into high value byproducts.

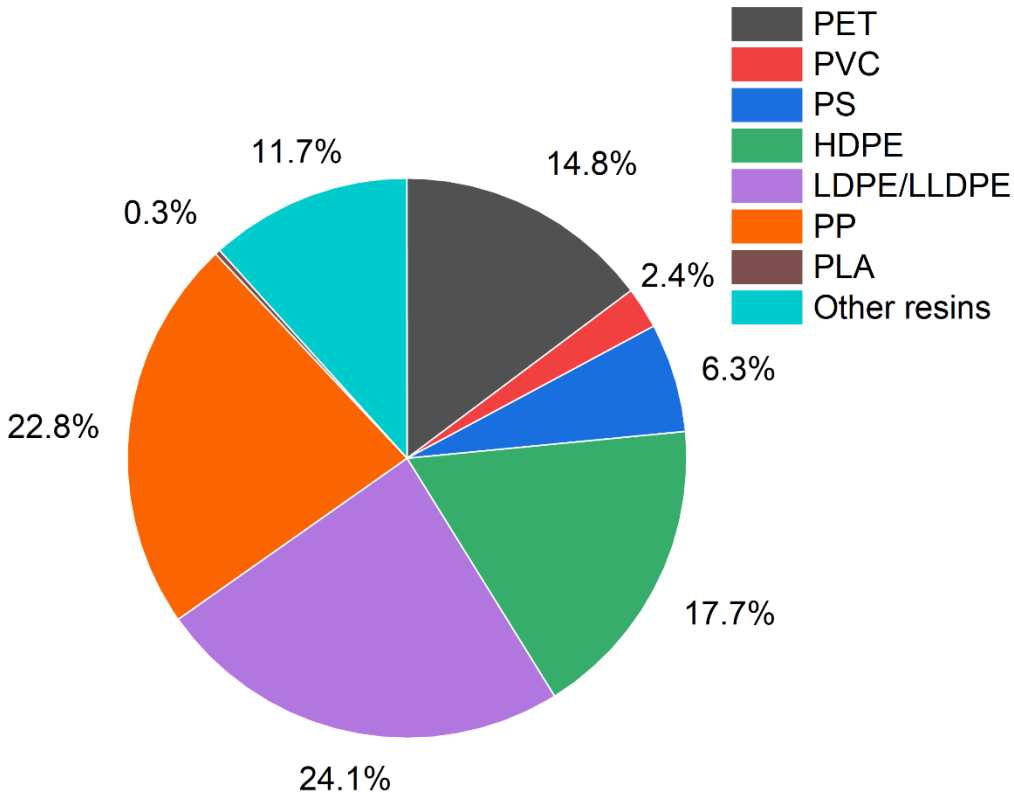

Figure 1-1 Distribution of plastic types in municipal solid waste in the United States in 2018[4]. PLA stands for polylactide and LLDPE stands for linear low-density polyethylene.

1.2 Environmental Fate of Plastics

Mismanagement of waste plastic throughout history and continuing today has resulted in a huge amount of plastic in the environment. This waste comes from mismanagement at all levels, from consumers littering, and waste escaping from landfills to some countries in the world practicing environmental disposal methods[6]. This results in plastic appearing at all levels of the environment and creating a massive cleanup problem.

Oceans

Perhaps the most daunting reservoir of waste plastic existing in the environment exists floating in oceans all around the world. Although the amount of plastic already in the ocean is not

known, it is estimated 4.8 to 12.7 million tons enters the ocean annually [7]. Oceanic waste plastic comes from two primary sources, waste entering the ocean from land-based streams, primarily rivers, and waste from the fishing industry[8]. Once in the ocean that plastic is at the mercy of ocean currents, resulting in much of the plastic being accumulated in areas called gyres. Gyres are natural current formations in the ocean that currents flow into but that have very little current themselves[9]. The currents push plastic into these gyres where it gets stuck and creates what is often referred to as "plastic islands", the largest of which is the Great Pacific Garbage Patch (GPGP)[10], estimated to have approximately 80,000 tons of plastic[11]. The plastic found in these patches is comprised primarily of polyethylene, polypropylene and occasionally polystyrene, as these plastics will float on water and other types will sink due to their densities[11].

Outside of gyres waste plastics can be found throughout the water column, close to shore and in the middle of the ocean[12-14]. There is well documented impact to sea life from the consumption of plastics[15], with plastic being found in fish[16], marine birds[17] and other sea life such as sea turtles[18]. Plastic also poses a large risk of entanglement for sea life which can have fatal results[19]. Although a daunting task clearing the ocean of plastics is critical to ensuring the longevity of critically important ecosystems around the world.

Rivers

Clearing the oceans of plastic is without a doubt an important task, but if new plastic waste cannot be prevented entering the ocean, cleaning the ocean will be a never-ending battle. As previously highlighted, one of the key mechanisms for plastic entering the ocean is through rivers. Rivers act like plastic highways into the ocean[20] and if the highways can be closed, a huge amount of plastic can be prevented from entering the ocean. It has been estimated that between 1.15 and 2.41 million tons of plastic flow into the ocean from rivers every year[21]. Along with transporting

massive quantities of plastic into oceans, similar negative impact to ecosystems and wildlife has been seen from river-based waste plastic through ingestion and entanglement, among others[20].

Although research on the composition and quantity of plastic in rivers around the world is lacking, wastes from rivers have been found to have a higher diversity in polymer type[22] and exist as both macro (>5mm) and micro-plastics (<5mm)[23-27]. This increased diversity indicates that more of the plastic can be collected in the smaller depth rivers. Along with an increase in plastic diversity, collecting plastic from rivers before it enters the ocean allows for the capture of micro-plastics. Micro-plastics are wildly thought to be un-collectable in the ocean, due to the scale and complexity of the world's oceans. Collecting plastics from river sources will eliminate a massive ocean input source term, as well as be technologically easier while advanced collection methods are developed for the ocean.

1.3 Material Recovery Facilities

The plastic found in oceans and rivers throughout the world comes from many sources, one of which is leakage from landfills[6]. Plastic ends up in landfills either from disposal in the trash or disposal from Materials Recovery Facilities (MRFs). There are approximately 420 MRFs across the US that accept co-mingled wastes containing on average 67% paper/paperboard, 4.5% wood, 13% metals, 4% glass, 6% rubbers/textiles and 4.5% plastics[4, 5]. This MSW is sorted at the MRF by category and can further sorted by type within each category (i.e. by polymer type); plastic that can be recycled is cleaned to remove contaminants and any plastic that cannot be adequately purified is disposed of. Plastics that do not have recycling mechanisms but were accidentally put in a recycling receptacle are disposed of, eventually ending up in landfills. The sorting steps at MRFs are non-trivial and often expensive, greatly increasing the cost of any material made from recycled materials[28, 29]. To reduce the amount of sorting necessary MRFs restrict the type of

plastics they accept, however the type of plastics accepted by MRFs varies from town to town, city to city, often causing confusion for end users and reducing the amount of plastic actually recycled[30]. Developing new technologies that can be used to recycle mixed plastic feeds will eliminate the need for extensive pre-processing and increase the types and amounts of plastics that can be recycled.

1.4 Recycling Techniques

Recycling of plastics can be done in multiple ways. The most commonly practiced is mechanical recycling, however new research has led to the rise of chemical recycling as a valid recycling technique. **Table 1-1** outlines the four key recycling terms and provides examples. The following sections will expand on mechanical and chemical recycling techniques.

Table 1-1 Definitions and examples of plastics recycling[31, 32]

ASTM D5033 definitions	*Equivalent ISO 15270 (draft) definitions*	*Examples*
Primary recycling	Mechanical recycling	One to one closed-loop recycling
Secondary recycling	Mechanical recycling	Downgrading to lower value product
Tertiary recycling	Chemical recycling	Pyrolysis or Hydrothermal liquefaction
Quaternary recycling	Energy recovery	Incineration with energy recovery

Mechanical Recycling

Mechanical recycling is the most prevalent form of recycling today. There are multiple ways to perform mechanical recycling but the most common is extrusion technology. Extrusion can be performed at large-scale, does not need solvents and can be used for multiple types of plastic, all of which make it so popular[32]. Drawbacks of mechanical recycling methods like extrusion include degradation of the polymer structure and properties[33] preventing one to one closed loop recycling. One to one closed loop recycling is when a plastic product can be recycled

and converted back into the original product, like turning a PET water bottle back into a PET water bottle. When degradation of the polymer occurs, primary recycling is no longer possible and secondary recycling is the only option. Methods have been developed to limit this mechanical destruction of polymer properties, but it cannot be prevented entirely.

Another drawback to mechanical recycling techniques are that they are most effective when used on single polymer types. This means the plastics must be sorted prior to recycling. Sorting is typically achieved through both automated and manual techniques. Near infrared (NIR) can be used to sort select plastics by determining polymer type and sorting clear and colored plastics[34]. NIR can only determine the properties of the bulk polymer, so polymer blends or multi layered polymers cannot be identified through this technique. Research and patents have been published for developing systems able to distinguish and mark all polymer types, but they are not commercially available at this time[32]. Although polymer mixtures can be recycled using mechanical recycling methods the products formed typically have poor mechanical properties[32]. The final limitation of mechanical recycling is that there is a finite number of times a polymer can be recycled before its physical properties are too degraded to be used for either primary or secondary recycling[35] The need for recycling techniques that can handle mixed plastic feeds that cannot be separated and recycle end of life polymers that would otherwise be landfilled has led to the rise in research and development of chemical recycling technologies.

Chemical Recycling

Thermal conversion technologies, also known as chemical recycling, have been studied for the conversion of waste plastic for over 50 years. Thermal conversion technologies work by using high temperature (>300 ˚C) and sometimes high pressures (>24 MPa) to break the bonds in the

backbone of polymer chains creating smaller molecules. Depending on the reaction operating conditions these molecules can vary in size from low molecular weight polymers to monomers of the polymer. This variability indicates a strong dependence on reaction conditions but also a potential tunability of the products to target desired outputs, either as oils or valuable by-products if the processes can be well understood. Although, these technologies are increasingly being studied there still exists gaps in the literature.

1.4.2.1 *Pyrolysis*

Pyrolysis is a thermal technology that utilizes high temperature (>450 ˚C) in the absence of oxygen to convert polymers into smaller molecules[36]. Pyrolysis of plastic has been studied in the literature both experimentally and through various modeling techniques. Pyrolysis can be operated as either a catalytic or non-catalytic process and under fast or slow pyrolysis conditions[36, 37]. Oil yields of greater than 90 wt% have been reported for single stream plastics[38-40] and 50 wt% for select plastic mixtures under optimized conditions[41, 42].

1.4.2.2 *Hydrothermal Liquefaction*

Hydrothermal liquefaction (HTL) is the second thermal technology of interest. HTL also operates at high temperatures and high pressures but unlike pyrolysis uses sub- or supercritical water[43] to create a bio-oil with properties similar to diesel fuel[44]. HTL is a promising technology for wet feedstocks, as drying, a high-cost process, is not required. For this reason, significant research has been done on HTL for the conversion of wet organic biomass feedstocks, with only recent focus on this technology for the conversion of plastics, a traditionally dryer feedstock. Where there is an abundant source of water HTL offers potential benefits over pyrolysis as the temperatures necessary for depolymerization are lower. Recent work in the literature has studied the use of HTL for the conversion of single stream plastics into oils [45-50] to optimize the oil yields.

For these single streams, oil yields of 80% and above were achieved, a significant and promising result. While promising, the literature has focused on polymers like PET, PE and PP, and data for PS and polycarbonates is lacking. There has also been limited research on the conversion of mixed plastic streams. The studies that have been done have shown significantly lower conversions to oil, approximately 50% [47], and required higher reaction temperatures (~500 ˚C or higher). Decreasing the reaction conditions and increasing the oil yields will be critical for deployment of these technologies on a large scale.

Along with single stream polymers and full mixed waste streams studies have also considered polymer mixtures of two to three plastics. Acquiring these polymer mixtures may be more feasible than single plastic streams. Some known plastic waste sources are primarily composed of only a few plastics, such as the plastic found on the surface of the Great Pacific Garbage Patch in the Pacific Ocean which is a majority PE and PP[11]. Partial separation of polymers at MRF's is also possible by utilizing the density differences between plastics such as PE, PP and PS with those of PET and PVC allowing for floatation separation, a relatively simple and cost-effective process. Advancing the fields knowledge and understanding of these thermal conversion technologies will require both experimental and computational study to provide a comprehensive analysis.

1.5 Modeling Techniques

Monte Carlo Modeling

Thermodynamics, economics and environmental impacts are all critical factors for understanding the potential of hydrothermal and pyrolytic technologies. However, there are many unknown variables required to calculate the impact of these factors. Traditionally, a value based on the literature, and chemical knowledge of the system is chosen for an unknown variable. Although a valid way to model the system, the model results are specific to the decisions made

about these variables. To address this limitation Monte Carlo (MC) simulation techniques can be used. MC techniques allow the process variables to be a range of values in a known distribution (such as uniform or triangular) instead of single points. This allows the whole range of possible results to be modeled and the probability of different results studied. MC techniques have been proven useful for handling uncertainties in similar types of analyses [51].

MC techniques also allow for new information to be easily incorporated into models when it becomes available. This is important for studying depolymerization reactions, as the field is constantly producing new information.

Machine Learning Techniques

Waste plastics is an active field currently, with a significant number of studies being published every year. This wealth of published data can be utilized to create datasets that can be analyzed with various machine learning techniques. Analyzing these datasets can help to predict desired reaction features, such as oil yield, and aid in the optimization of these reactions. Although a significant amount of data exists in the literature the amount of data points (~300-500) is significantly less than the size of data traditionally used in machine learning (>100,000) [52, 53]. This means that the machine learning techniques utilized must be carefully selected and validated to ensure that there is not overfitting, as this is the common challenge faced in these low data problems [54, 55].

One promising algorithm for handling small datasets is Random Forest regression (RF) which is an ensemble method that utilizes multiple decision trees and bootstrapping to predict the value of the desired dependent variable [56]. By bootstrapping the data, RF allows each decision tree to only see a small subset of the data and reduces the correlation between each tree which results in an overall more accurate predication [57]. RF models can be developed to take the specific reaction conditions, such a feed composition, temperature and reaction time and predict the reaction yields

(oil, gas and char). With a well-developed model, predictions can be made to understand how changing specific reaction conditions or feedstock composition effects the desired yields. This allows for the exploration of many more conditions than could be performed in a lab and also can aid in determining which experiments should be further studied experimentally.

Random forest techniques have been proven successful with small datasets as explained previously, however some real data, such as kinetic time series, have even less data than the small datasets discussed above. They also suffer from the fact that when each reaction product is tracked over time the data has significantly more columns than it does rows which is a critical flaw in most regression algorithms. Therefore, in order to be able to do any sort of machine learning on such data, regression must be ruled out. These datasets are not large enough to make accurate regression predictions, however if studying the features of the dataset alone is important, techniques such as dendrograms can be used. Dendrograms are a form of hierarchical clustering that represent data from dimensional space as a tree with the height of the tree representing similairty[57]. Such a technique can be used to identify similarities in the products of the kinetic time series data even with very few data points. Understanding the similarity of products can aid in the development of group type kinetic reaction models and targeting of high value reaction products.

1.6 Research Objectives

Addressing waste plastics from oceans to rivers and materials recovery facilities will require a multifaceted approach from fundamental thermodynamics to developing new technologies. To understand the potential of chemical recycling techniques for efficient recycling of waste plastic, this work aims to address the following objectives:

1. Understand the fundamental thermodynamic potential of thermal conversion of waste plastic to fuel

2. Demonstrate how machine learning can be integrated into chemical recycling problems

3. Develop enhanced knowledge of thermal depolymerization pathways for optimization of reaction products.

To this end, computational methods were combined with experimental knowledge and data to create a complete picture of waste plastic depolymerization through pyrolysis and hydrothermal liquefaction. Fundamental thermodynamic modeling and Monte Carlo modeling methods were utilized in Chapter 2 to understand if fuel generated from oceanic waste plastic on board a ship could produce enough energy to fuel the conversion system and ship itself. The learnings from the thermodynamic analysis were then applied to a case study to understand how long cleaning up an area of the ocean would take utilizing a self-powered ocean cleanup vessel.

Chapter 2 highlights the need to not only cleanup the ocean, but also prevent new plastics entering the ocean. Chapter 3 combines the thermodynamic modeling developed in Chapter 2 with machine learning techniques to understand the exergy potential of waste plastic to fuel systems based next to polluted rivers. Machine learning techniques allow for the utilization of all of the data that has already been published in the literature and create decision aiding tools that eliminate the need for extensive and wasteful experimental work. Chapter 4 will further expand upon the power of the machine learning models developed by increasing the type of reaction that can be modeled, in order to study the reduction of landfill waste from Material Recovery Facilities (MRFs). Reducing the amount of waste plastic that ends up in landfills will also reduce the amount of plastic escaping into the environment and therefore ending up in rivers and oceans. Chapter 4 will further advance the capabilities of machine learning by incorporating machine learning estimations with a technoeconomic analysis that will predict the minimum selling price of product required for cost effective conversion of waste plastics in all 50 states in the US through pyrolysis.

Finally, Chapters 5 and 6 will address the need for a better understanding of the products produced from thermal depolymerization. Enhanced understanding of the mechanisms controlling thermal depolymerization will allow for the creation of higher value products further advancing the potential of these technologies. Chapter 5 will utilize an external radical source to create valuable oxygenated single ring aromatic products. Suggestions are made both in Chapter 5 and Chapter 8 as to how these external radicals can be used to advance the understanding of how radicals interact in hydrothermal environments. Chapter 6 aims to advance the knowledge of product production during thermal degradation by studying a polyethylene model compound, dodecane, and utilizing machine learning to do group type kinetic modeling. The use of machine learning allows for the parsing of complex kinetic datasets while still producing accurate kinetic predictions capable of tracking specific molecules of interest.

Chapter 2: Thermodynamic feasibility of shipboard conversion of marine plastics to blue diesel for self-powered ocean cleanup[58]

2.1 Introduction

An estimated 4.8 to 12.7 million tons of plastic enter the ocean each year, distributing widely across the ocean's surface and water column, settling into sediments, and accumulating in marine life [7, 11, 59]. Numerous studies have shown plastics contribute to sublethal and lethal damages to marine life and birds, therefore motivating introduction of effective mitigation and removal measures [60]. Reducing or eliminating the amount of plastic waste generated is critically important, especially when the current loading may persist for years to even decades [7, 61, 62].

As a highly visible part of an integrated approach for removing plastics from the environment, [7, 61, 62] efforts are underway to collect oceanic plastic from accumulation zones in gyres formed by ocean currents [59, 63]. Present approaches to remove plastic from the open ocean utilize a ship that must store plastic on board until it returns to port often thousands of kilometers away to unload the plastic, refuel, and resupply.

Optimistic evaluation of cleanup time using the harvest-return approach indicates that at least 50 years will be required for full plastic removal [63]; more conservative estimates suggest that partial removal will require more than 130 years [63, 64]. Cleanup times of decades mean that environmental degradation may have already reduced the existing plastics to microscopic and smaller forms that can no longer be harvested before cleanup is completed [7, 60, 64]. These considerations underscore the massive challenge of removing plastics from the ocean and naturally raise the following question: can any approach remove plastics from the ocean faster than they degrade?

Some current plastic removal strategies involve accumulation via a system of booms, consisting of semi-circular buoys fit with a fine mesh extending below the ocean surface [63, 65]. These booms are positioned so that prevailing currents brings plastic to the boom, where it then accumulates. The currently envisioned approach is for a ship to steam to the boom system, collect plastic, and then return to port to offload and refuel before resuming collection activities.

The time required for recovering plastics could be reduced if return trips to refuel and unload plastic were eliminated. Indeed, the harvested plastic has an energy density similar to hydrocarbon fuels; harnessing this energy to power the ship could thereby eliminate the need to refuel or unload plastic from the ship, reducing fossil fuel usage and potentially cleanup times.

Self-powered harvesting may be the only way to accomplish cleanup using the passive boom collection approach at timescales less than environmental degradation. Unfortunately, cleanup itself is a moving target, as technology improves [63] and especially as plastic continues to accumulate. What is required therefore is a framework to evaluate the impact of self-powered harvesting on cleanup time and fuel usage. The framework can then be updated as more data become available.

To be valuable, the cleanup framework must be reducible to practice using actual technology. A viable technology for converting plastics into a usable fuel is hydrothermal liquefaction (HTL), which utilizes high temperature (300-550 °C) and high pressure (250-300 bar) to transform plastics into monomers and other small molecules suitable as fuels [45, 46, 66]. Oil yields are typically >90% even in the absence of catalysts and, unlike pyrolysis, yields of solid byproducts – which would need to be stored or burned in a special combustor – are less than 5% [45, 46, 66], thus conferring certain comparative advantages to HTL. Ideally, a vessel equipped with an HTL-based plastic conversion system could fuel itself, creating its fuel from recovered materials. The result could be

termed “blue diesel”, to reference its marine origin and in contrast with both traditional marine diesel and “green diesel”, derived from land-based renewable resources [67].

To make the HTL approach feasible, the work produced from the plastic must exceed that required by the process and, ideally, the ship’s engines so that fuel can be stockpiled during collection for later use. Exergy analysis provides a framework to determine the maximum amount of work that a complex process is capable of producing without violating the fundamental laws of thermodynamics [68]. The reliability of an exergy analysis depends on the reliability of the data it uses as inputs, and key parameters describing HTL performance and ocean surface plastic concentration are currently not known with certainty. A rigorous and statistically meaningful analysis of shipboard plastic processing must therefore integrate uncertainty [69]. Here, the Monte Carlo (MC) simulation method, which has proven its usefulness for similar type of analyses, is the appropriate tool for handling the uncertainties inherent to the current application [51] and allows for the integration of new information and data as further study of oceanic surface plastic is completed.

Accordingly, the thermodynamic performance of a shipboard HTL process was evaluated to determine if (and when) the process could provide sufficient energy to power itself plus the ship. A framework was then developed to evaluate the implications of shipboard plastic conversion on fuel use and cleanup times. The results provide valuable insight into the potential use of shipboard conversion technologies for accelerating removal of plastics from the ocean and the framework should prove useful for guiding future work in this area.

2.2 Results

Thermodynamic Analysis of Shipboard HTL Plastic Conversion

The first step was a thermodynamic analysis of a realistically configured plastic conversion process. **Figure 2-1** provides a schematic of the proposed plastic conversion system that includes components to collect and shred the plastic, remove salts and other impurities, and convert the

plastic feed into blue diesel, a marine plastic derived fuel with similar energy density and volatility to marine diesel [70]. Details can be found in Appendix A (Section 2.5.2 and **Table 2-1**). The entire process is self-contained and can easily fit on a ship, selected here as 40 meters – smaller than current vessels in use for the removal of ocean plastics [63] since the ship with on-board conversion does not need to store plastic that it collects.

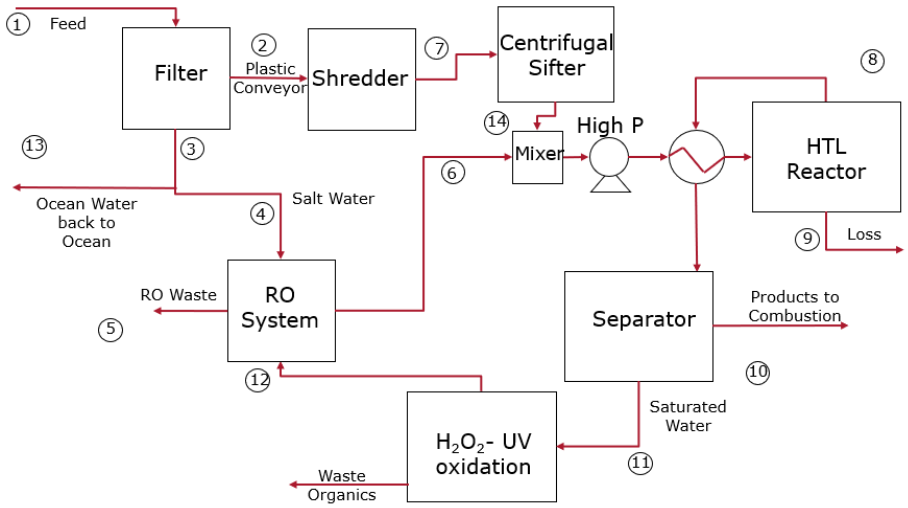

Figure 2-1 Conceptual design of a shipboard HTL-based process for converting ocean-borne plastics into usable fuel: a) process flow diagram. The entire process is designed to fit within a standard 20 ft shipping container.

Thermodynamic performance of the HTL reactor itself is determined by oil yield and heating value obtained at a given reaction temperature. The relationship between oil yield and temperature depends on the composition of the plastic feed and is measured experimentally. Accordingly, simulations were performed for two individual pure plastics commonly found in the ocean [11], polypropylene (PP) and polyethylene (PE), as well as a "mixed feed" based on the typical composition of marine plastics (2:1 polyethylene: polypropylene) [11]. The operating temperature, overall conversion, and product yield for each plastic feed were taken from previous work [45, 46, 66] and are listed in Appendix A **Table A.2-4** and **Table A.2-5** (section 2.5.3). Performance in the

PP/PE mixed feed case was especially promising as HTL of this feed resulted in 85% oil yield at modest temperature (400 °C) and with no solid byproduct.

HTL produces chemical energy in a form usable by the engine. All peripheral equipment detracts from the ideal thermodynamic performance. Parasitic losses required for operation of the peripheral equipment required for shredding, heating, pumping, and separations were included in the system-level analysis (See Appendix **Table A.2-3**). Performance of the system consisting of both the HTL reactor and the ship itself was evaluated for operation of the ship at either what is termed normal speed or extra slow steaming, a speed that is recommended for minimizing fuel consumption [71].

Published performance, thermodynamic properties, and equipment specifications provide a basis for a comprehensive exergy model of the HTL-based process. However, most of the required parameters are not known with accuracy; projecting them to scale introduces additional uncertainty. Accordingly, the uncertainties of key parameters were included in the exergy model using a Monte-Carlo (MC) sampling approach. [72].

After testing the effects of several parameters, the six shown in **Table 2-1** were chosen for inclusion in the uncertainty analysis. **Table A.2-6** *(*Appendix section 2.5.4*)* provides justifications for the ranges selected for the values of these parameters. Model input uncertainty was then propagated through the aforementioned exergy model to derive a probability distribution profile and statistically characterize a range of possible performance outcomes rather than generating single point estimates as in conventional approaches.

Table 2-1 Uncertain Thermodynamic Model Variables and their Uniform Probability Distribution Ranges.

Parameter	Uniform Probability Distribution Ranges
Weight Percent Plastic in Reactor	10-30%
Surface Ocean Temperature	17-30 °C
Heat Exchanger Efficiency	50-80%
Engine Power	1,800-2,200 hp
Engine Efficiency	35-40%
Heat of Combustion Variance	0.98-1.02

The MC-based model does not include uncertainty in the loading of plastic on the ocean surface, a key parameter governing performance. Unfortunately, the plastic loading has only been roughly estimated and varies from location to location [11, 61]. Accordingly, to account for uncertainty in the plastic loading we combined the aforementioned MC process simulation with a traditional sensitivity analysis of plastic loading by simulating the performance over a range of plastic loadings.

Figure 2-2 shows the probability of shipboard HTL producing more exergy than the process and the ship itself consume, when the ship travels at full engine power (**Figure 2-2**a) and optimized engine power (1/3 engine power) (**Figure 2-2**b) to conserve fuel. The PE decomposition

temperature is greater than PP yet has similar oil yields, accounting for the difference in performance predicted for PE compared with PP.

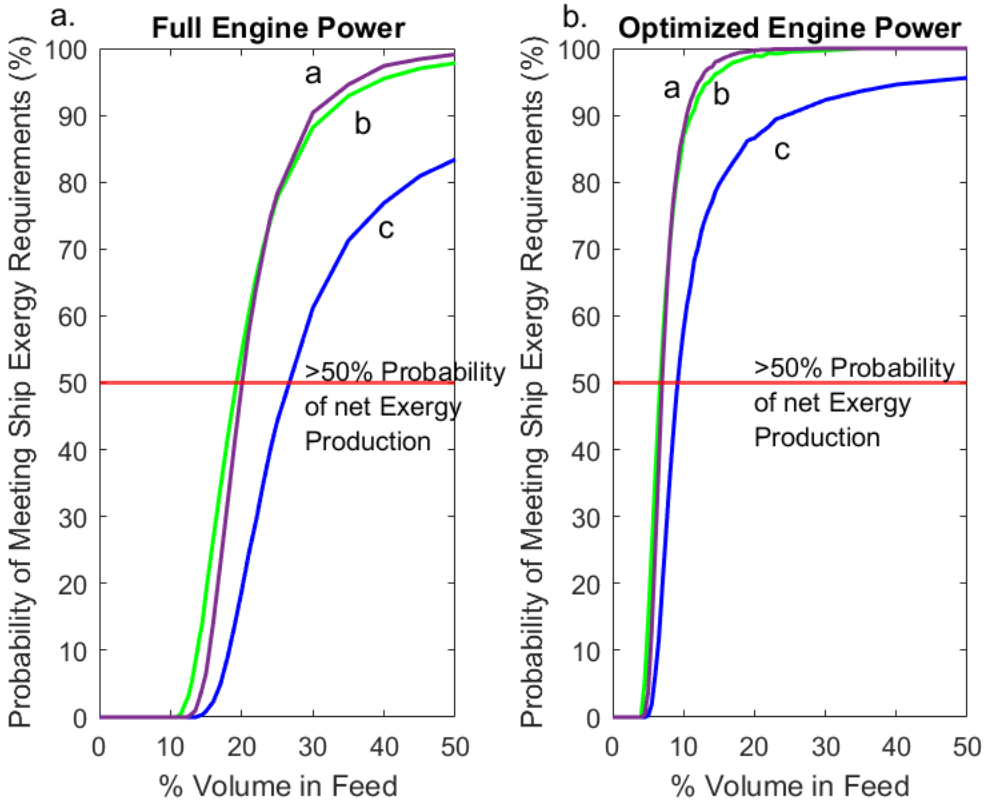

Figure 2-2 Probability of producing more exergy than is consumed by the combination of the HTL process itself and the ship's engine for a.) a 2:1 polyethylene to polypropylene mixture b.) polypropylene and c.) polyethylene for full engine power and optimized engine power (15 knots, 1/3 engine power [71]) conditions to simulate worse case (full engine power) and more realistic (1/3 engine power) exergy consumption.

Interestingly, performance profiles in the PP and the PE/PP mixture cases are similar to one another, a promising finding given that the PE/PP mixture is most representative of the composition of plastic present in the GPGP [7]. Based on previous modeling of the depolymerization

of mixtures, the likely explanation for the favorable performance observed for PE/PP is an auto-catalytic effect arising from radicals formed by PP pyrolysis [66].

The point in **Figure 2-2** at which the probability of net exergy production is greater than 50% takes specific importance as it represents an interesting condition that balances the risk of producing insufficient exergy with the benefit of self-powered cleanup (Appendix A section 2.5.5 contains further details). **Figure 2-2b** shows that the break-even point is reached when the ship operates at optimized engine power for all plastic loadings <10%. A plastic loading of 10% is within the range predicted for collection by a boom placed within a gyre [64] . However, the break-even point loading is much greater than is expected without a boom, meaning that HTL conversion is not self-powering in the open ocean.

Figure 2-2 shows a range in predicted outcomes that is the result of current level of uncertainties in HTL thermodynamics and conversion rates. Improved data and predictive models will reduce the range of predicted outcomes, thereby de-risking investment in the approach. Figure 2 also suggests that optimizing engine power (1/3 engine power [71]) is necessary for thermodynamically favorable processing of mixed plastic streams.

Figure 2-1 provides more detail on the exergy consumed by the various sub-processes, taken at the point of >50% probability of producing net exergy. In all cases, the ship itself is the main source of exergy consumption followed by heating the feed to the HTL reactor.

Pyrolysis was also considered as a possible technology option for self-powered ocean cleanup. Like HTL, pyrolysis is a thermal depolymerization process that yields an oil product that can be used as fuel. Unlike HTL, pyrolysis requires a dry feed, meaning that exergy is required to dry the ocean plastic stream prior to pyrolyzing it. Similarly, pyrolysis produces greater yields of solid byproducts than HTL; these solid byproducts must be stored on board – which reduces one

of the main benefits of shipboard conversion – or burned for heat in a dedicated burner. On the other hand, HTL requires pre-heating of the liquid water feed, only part of which can be recovered from the product stream. Thermodynamic analysis is required to evaluate these tradeoffs.

Figure A.2-6 provides a comparison of HTL and pyrolysis for the mixed PE/PP stream. Interestingly, thermodynamic performance profiles of HTL and pyrolysis are very similar to one another, indicating that the differences in drying, heating, and oil yields obtainable by the two processes nearly offset one another [66, 73]. From a strictly thermodynamic standpoint, therefore, either pyrolysis or HTL could be a viable shipboard technology. That stated, the pyrolysis oil yield is much less than obtained from HTL (65 compared with 85%), meaning the byproduct disposal is much more difficult for pyrolysis than HTL [73]. These byproducts consisting of gasses and chars will have to be flashed, stored or burned in solids combustors. The pyrolysis footprint will be greater than that required for HTL to accommodate the dryer required for pyrolysis. These secondary considerations indicate that HTL is the more promising technology for shipboard conversion; however, pyrolysis remains a viable option should HTL prove difficult to implement.

Scale is an important consideration, and in addition to the base case, which assumed a flowrate of 3.6 $m^3\ h^{-1}$, a second case was also considered for the mixed plastic stream with a flow rate of 36 $m^3\ h^{-1}$. The benefit of increasing the exergy output for a ship of a fixed size more than counter-balanced the increased energy requirements of the peripheral equipment, shifting the 50% probability point from 20 to 2.2 vol% (**Figure A.2-7**). Accordingly, thermodynamic considerations encourage scaling the process as large as practically possible within size, weight, and economic constraints of a given vessel. This suggests a logical extension of the present work: the joint optimization of vessel and process size, and vessel endurance, with detailed considerations of space and energy needs of the crew and all onboard systems.

A Framework to Evaluate the Implications of Shipboard HTL Conversion on Ocean Cleanup

The previous section (Thermodynamic analysis) predicts that shipboard HTL enables self-powered harvesting of plastics that have first been collected by a boom placed within a natural oceanic gyre. Accordingly, the impact of shipboard HTL conversion was projected within a cleanup framework for a concrete application: estimating the yearly removal of plastics from the Great Pacific Garbage Patch (GPGP), a gyre located in the central portion of the Pacific Ocean [11].

Figure 2-3a locates the port of San Francisco CA, far from the GPGP. **Figure 2-3b** and **Figure 2-3c** show the deployment of the boom array and the filling of a single boom due to ocean current respectively and **Figure 2-3d** shows the conversion of plastic into the "blue diesel" replacement fuel. As shown in **Figure 2-3**, the framework requires the following parameters: the size of each boom, the number of booms, the distance between booms, and the distance from the booms to the vessel's home port.

Existing boom designs (which consist of a series of semi-circular floating buoys equipped with a fine mesh extending several feet below the ocean surface) [65] collect plastic at a rate that depends on the loading of incoming plastic, and the speed of the local ocean current, as shown in **Figure 2-3c**. Shipboard conversion does not directly change the values of any of these parameters compared with an approach consisting of collecting the plastic, storing it on board, and returning to port to unload. However, shipboard conversion can reduce the frequency of return trips, allowing more booms to be deployed and emptied every year than would be possible with the collect-store-return approach.

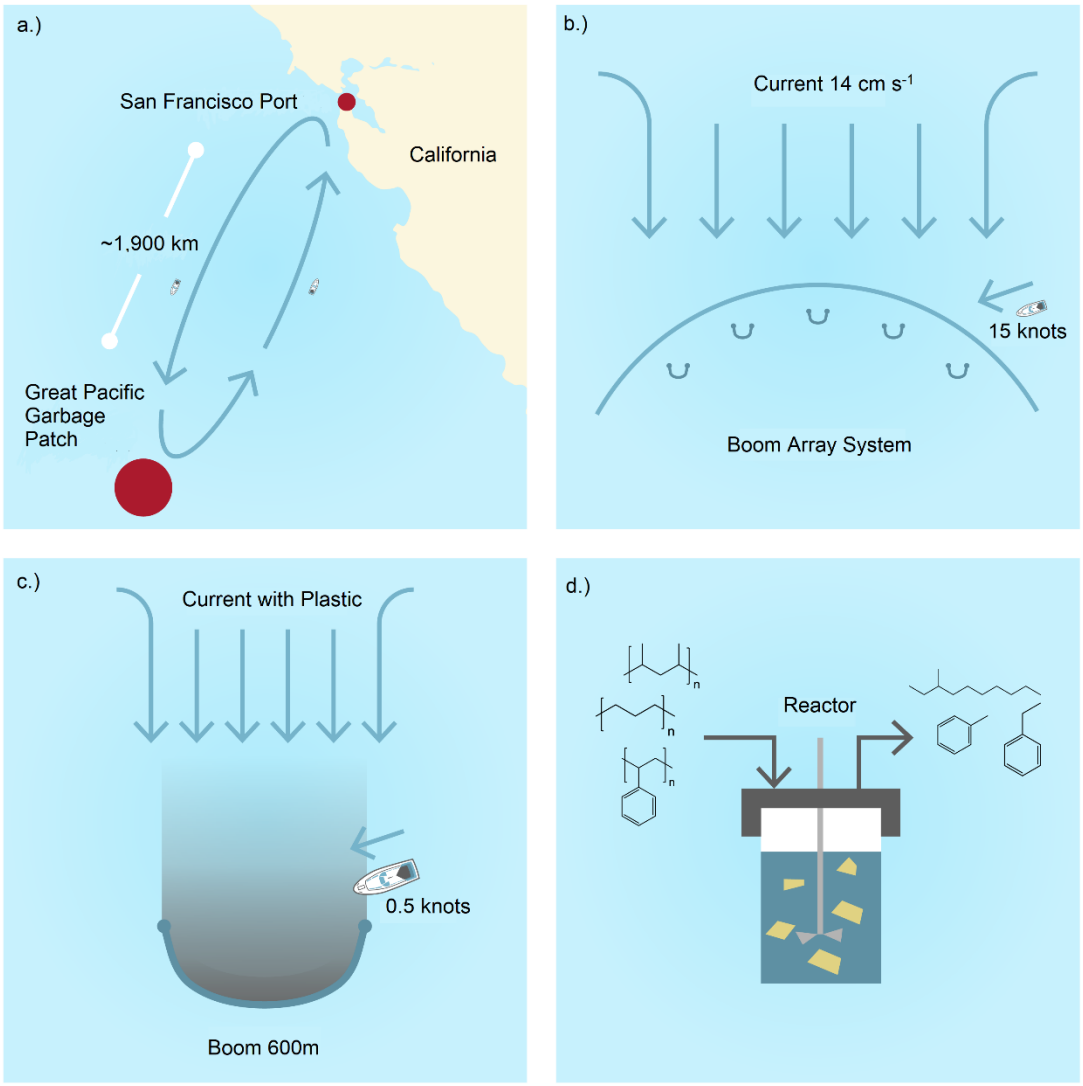

Figure 2-3 Overview of the process for plastic removal out of the Great Pacific Garbage Patch showing a.) the total system overview, b.) part of the system of collection booms, c.) a single collection boom and d.) the HTL reactor.

Shipboard conversion suggests a second potential advantage over the collection-storage-return approach. While plastic harvesting is typically performed manually to minimize fuel use (with workers manually scooping the plastic out of the booms and into small bags [63]), shipboard conversion makes practical automated plastic collection where the ship can pass through the plastic in the boom and feed it to the conversion process via a conveyor [63]. The continuous collection rate

is then related to the speed of the ship and the concentration of plastic trapped by the boom. Due to its efficiency, continuous collection was modeled for cases with shipboard conversion. A potential problem with automated scooping is dispersion of the plastic. To minimize wake effects and fuel usage, the ship speed during collection was set to 0.5 knots and the collection efficiency was set to 70% to account for partial dispersion from the ship's wake during collection.

The quantity of plastic that could be removed was then calculated for shipboard conversion of plastics to fuel. We assumed the booms are deployed at a distance of 25 km from one another. This distance was selected to minimize boom-boom interactions that would decrease collection efficiency and because 25 km spacing corresponds to the maximum number of booms that can be deployed in the GPGP based on space and be serviced by a single ship in a single year. Details of all of these assumptions and calculations can be found in Appendix A, **Table A.2-7** and **Equations A.1-A.7**.

Using this framework and corresponding assumptions, 2,500 booms could be harvested per year when shipboard conversion was used. A year was assumed to consist of at most 240 days, with 16-hour days to account for maintenance down time, weather, sea state, and time off for the crew. Using this value for the number of booms that could be harvested per year and the boom-boom separation distance, the total amount of plastic that could be removed from the GPGP by a single ship yearly at several distinct values of the plastic surface concentration was calculated [7, 11]. The results are summarized in **Table 2-2**, showing that 1.2×10^7 kg could be removed for the case with the greatest value of plastic surface concentration (2,500 g km^{-2}) [7]. As plastic surface concentration decreases the amount of plastic removed decreases, a consequence of the effect of plastic surface concentration on collection in the booms.

Table 2-2 Plastic removed and total project lifetime for removal of plastic from the GPGP using shipboard HTL

Plastic Concentration in GPGP (g km^{-2})[a]	Plastic Removed Per Year (kg)[b]	Percentage of Plastic Derived Fuel Consumed Yearly (%)[c]
2,500	$1.2*10^7$	580
1,000	$4.6*10^6$	230
500	$2.3*10^6$	120
200	$9.2*10^5$	50
50	$2.3*10^5$	12

(a) Surface concentration of plastic in the GPGP [7] for a fixed value of 79,000 tons of plastic contained in the GPGP [11]
(b) Plastic removed from 2,500 booms per year with a 70% collection efficiency
(c) Percentage of total required fuel consumption that can be covered with plastic derived fuels assuming a fuel density of 0.84 kg/L, a conversion range of 60% and fuel consumption of 90 GPH.

By eliminating trips to port and by replacing marine diesel with blue diesel, shipboard conversion reduces fuel requirements and especially fossil fuel requirements, as shown in **Table 2-2**. Specifically, for the highest concentrations, enough plastic can be collected to generate fuel with an excess of 480% that can be stored and used for trips to and from the GPGP, eliminating the need for the use of any fossil fuels. Three of the five concentrations can create an excess of fuel, indicating that areas of low plastic concentration can be supplemented with fuel from higher concentration areas.

A key assumption in this analysis is that HTL feed rate and conversion rates are equal to the plastic collection rate so that the ship need not pause periodically to allow time for plastic conversion. This assumption is generally met for the HTL reactor described in the previous section. At the high end of the range of plastic loadings shown in **Table 2-2**, the ship will require 2-3 reactors to match conversion rates with collection rates, which should be easily managed.

Table 2-2 paints an optimistic picture of GPGP cleanup using shipboard HTL conversion, at least if plastic concentration is present in the higher end of the range of current estimates. On the other hand, if plastic concentrations are on the lower end of the estimated range, cleanup is daunting when considering the current total amount of plastic in the GPGP; the effects of continued accumulation make these estimates even less attractive. Similarly, the size of the ship, or the power rating of the engine, must be carefully selected and its speed controlled for the process to be thermodynamically favorable. The effect of the composition of the plastic in the GPGP on the thermodynamics of the HTL process adds an extra degree of uncertainty.

2.3 Discussion

Based on the aforementioned considerations, shipboard conversion of oceanic plastic wastes to fuels using HTL is predicted to produce enough exergy to power itself, power the ship, and generate surplus fuel for later use when booms are used within a gyre – but not in the open ocean or within a gyre lacking booms. Unfortunately, using the results from **Table 2-2** to calculate cleanup times show times at the edge or beyond what is practical for a single ship to accomplish (7-340 years, see Appendix A **Equations A.1-A.6** and

Table A.2-8). **Table 2-2** is based on a 25-km boom-boom separation distance, the distance that corresponds to the maximum number of booms deployed in the GPGP that a single ship can service per year. Accordingly, the framework used to generate estimates in **Table 2-2** was used to

evaluate the effects of increasing the number of booms and ships on estimated GPGP cleanup times assuming that no new plastic enters the GPGP during the cleanup operation.

The net effect of decreasing boom-boom separation is to increase the number of booms in the GPGP and hence reduce the cleanup times. The boom-boom separation distance must be sufficient so that upstream booms do not negatively impact the collection efficiency of downstream booms. The minimum distance that avoids the shadow effect is not currently known [74], meaning that boom-boom separation distance can be considered as a parameter in the framework. For a given GPGP area, the boom-boom distance then controls the number of booms deployed and hence the amount of plastic that accumulates – and thereby the estimated cleanup time.

Figure 2-4 shows estimated cleanup times as a function of the distance between booms. Estimates are included for both an optimistic scenario and a conservative one, with the difference being the concentration of plastic currently residing within the GPGP [7]. **Figure 2-4** shows that the time required to clear the GPGP is strongly dependent on the boom-boom distance, with times less than one year estimated in the optimistic scenario for distances ≤10 km. However, **Figure 2-4** also shows short clean up times correspond to huge numbers of deployed booms, a trade off in cost and practicality that must be considered. Likewise, the boom-boom interactions certainly will impact performance at some separation distance, and this effect should be included in future versions of this framework.

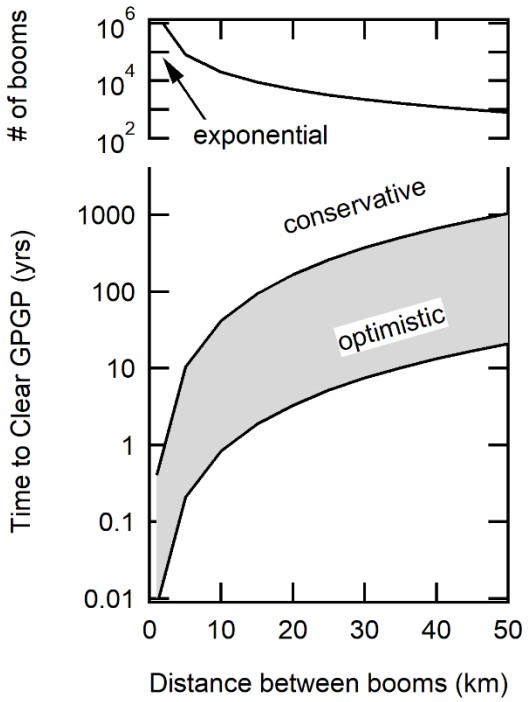

Figure 2-4 Estimation of the time required to completely clear the Great Pacific Garbage Patch based on high (2,500 g km^{-2}) and low (50 g km^{-2}) concentration estimations [7] for plastic within the GPGP for deployment distance between booms of 1 to 50 km and the corresponding number of booms deployed.

Thermodynamic performance, boom-boom distance, and boom-boom interaction will influence economic and environmental performance. Previous techno-economic analysis indicates that HTL can produce fuels at approximately $4 per gallon of gasoline equivalent [75], a cost that is more than competitive with commercial prices given the fuel savings predicted for self-powered cleanup.

The current analysis has thus far focused on cleanup of the oceanic gyres as areas of high plastic concentration. However, the cleanup times estimated here, which are constrained by the number of booms that can be deployed in the GPGP, either are similar in magnitude as environmental degradation timescales [62] or require thousands of deployed booms. Given the cleanup timescales and costs, efforts might be better placed on interception at locations of high

plastic flux to prevent plastic reaching the patches in the first place [64]. River mouths are one potential location where a boom and collection system could be more strategically deployed than at the oceanic gyres [64]. Similarly, boom systems might be placed to protect especially fragile or valuable ecosystems, such as breeding grounds. Alternative approaches involving mobile collection technologies are possible, but these options do not appear to reduce collection times sufficiently to justify the greater technological complexity. More details are provided in the SI.

The current analysis shows that collection of plastics that have already entered the environment is at most part of a multi-layered approach to mitigate environmental damage from plastics. Other key elements include reducing plastic use, [76] improving the recyclability of plastics, or increasing the biodegradability of plastics [77]. Implementing a plastic waste harvesting technology, whether it is based on HTL, pyrolysis, or some other technology, will require understanding details that include engine performance and emissions characteristics [78] and fuel delivery system integrity [79] when running on the plastic-derived fuel.

This analysis has focused on HTL as a technologically deployable method suitable for plastic conversion. However, the results presented here can reasonably be extended to other conversion methods. Enzymatic conversion [80, 81], which has been the subject of several recent studies, could be especially attractive for conversion at low temperatures, thereby improving thermodynamic efficiency and reducing hazards to the crew. Since HTL already produces sufficient energy to power the process and the ship, the thermodynamic benefit of enzymatic conversion will be incremental rather than transformative. Similarly, enzymatic conversion rates are slower than HTL rates, meaning that larger reactor vessels are required for enzyme-based conversion reactions than required for HTL [80]. Accordingly, the transformative impact of the enzymatic conversion would be for degradation of the plastics into harmless products in the ocean

without harvesting them. The current analysis indicates that research of in situ enzymatic decomposition of plastics to harmless products is warranted.

Converting marine plastics into fuel will ultimately release the carbon they contain as greenhouse gas (GHG) emissions. That stated, the quantities of released CO_2 are a small percentage of the global emissions budget, currently ~485 PgC [82]. If the system ran continuously for 10 years the total percentage would be less than 0.02% of the global carbon budget. On the other hand, converting the plastic into fuel eliminates new fossil emissions while simultaneously cleaning the oceans and reducing the amount of plastic being recycled in land-based operations. Converting the plastic to fuel also eliminates unnecessary congestion at ports and reduces the chance of a nearshore oil spill. Unlike petroleum fuels, plastic-derived fuels have low sulfur content, meaning that their combustion will not release sulfur oxides [83, 84], which is a desirable outcome given the importance of SO_2 in the formation of pollutants [85] and new regulations limiting sulfur content in fuels [86].

The results of this work provide a strong argument for continued study to advance current understanding of the factors that affect marine plastic depolymerization in real systems. Advances in the scientific knowledge of depolymerization thermodynamics, rates, and product distributions of ocean-borne plastics are required to reduce uncertainty around the HTL approach. Similarly, the cleanup framework can be improved by filling gaps in current estimates of marine plastic concentrations, quantities, and fluxes to reduce uncertainties in deployment outcomes. Finally, the results of this work show the immense challenge facing the prospect of cleaning up the ocean and argue for the need to change current plastic use and recycling strategies. Accordingly, the sound probability analysis and framework presented here can be incorporated with risk analysis to insightfully and reliably inform future decision making and policy responses in this important area.

2.4 Methods

@Risk Model

All the uncertain model input variables were modeled using appropriately selected uniform distributions in the absence of any accumulated operating experience and pertinent historical data. Monte Carlo simulation runs were conducted using the @Risk software [87] with 10,000 iterations for each volume percent of plastic in the inlet stream.

Process Details

Table A.2-3 includes a list of the equipment and their energy requirements. Salt is removed from the feed to protect the reactor and other materials from corrosion. Residual salt is removed using a reverse osmosis system (operating at 99% efficiency) to reduce the salt concentration in the system to levels that are compatible with high grade stainless steel (<1 weight percent (wt %)) [88]. To increase the effectiveness of depolymerization and permit feeding to the reactor, the plastics must be shredded at the process intake [89, 90]. **Table A.2-4** shows reaction conditions met by the equipment for the plastics studied. The shredded plastic is then combined with desalinated water to 10-30 wt% solids, preheated in the heat exchanger, pumped to pressure and heated to reaction temperature. The stream exiting the reactor is cooled to form organic and water-rich products [45, 46, 66] which are separated in a gravity separator. Residual organics in the aqueous phase are removed in a hydrogen peroxide/UV oxidation system prior to recycling. The HTL product oil (composition seen in **Table A.2-5**) is fed to an engine, to generate power, operating at an efficiency of 35 to 40%.

Exergy Calculations

The exergy of each sub-process was individually calculated and then summed and normalized based on the mass of plastic in the inlet.

Chemical Exergies and Combustion

The chemical exergies and exergy of combustion of the stream were calculated as the weighted average of the Gibbs Free energy of each product including water and the weighted average based on the enthalpy of combustion and their published yields respectively. Thermodynamic data for pure plastics and products were taken from the literature [91-94] and NIST [95] and yields were found in the pertinent literature [45, 46, 66]. When the thermodynamic values (enthalpy and entropy) of the products could not be found, correlations based on carbon number were used to estimate them (see Appendix A **Equation A.8-A.13**). It was assumed that 100% of the oil formed from HTL could be directly combusted without upgrading.

UV/Hydrogen Peroxide System

A UV sub-process was modeled for organic removal using a 300 nm lamp. The solubility values of the products of polystyrene in water were found in the pertinent literature [96-99]. Further details of this calculation can be found in the SI (Appendix A section 2.5.6).

2.5 Appendix A

Model Details

Table A.2-3 lists each piece of equipment seen in **Figure 2-1** needed for the conversion of plastic waste into fuel. The table also contains the power requirements, manufacturer and model number for each piece of equipment that was used in the model development.

Equipment/System Details

Table A.2-3 Process Equipment Energy Requirements

Equipment	Power Requirement (kW)	Manufacturer	Model Number	Manufacturer Website
Conveyor Belt	0.37	Titan Conveyors	Model 118	https://www.titanconveyors.com/
Shredder	7.5	Franklin Miller	Taskmaster TM1600 Shredder	https://franklinmiller.com/
Centrifugal Sifter	1.49	Kason	Centri-Sifter	https://www.kason.com/
RO System	18.6	Pure Aqua, Inc.	SWI Series Model # SW-16K-1480	https://pureaqua.com/
Pump	0.75	Goulds Water Technology	3642/3742 model	https://pureaqua.com/
UV/H_2O_2 System	4.14	Calculated (not from a manufacturer)	N/A	N/A

2.5.2.1 *Process Equipment Details*

Individual pieces of equipment were chosen among available commercial options to meet the desired process conditions (400-520 ˚C, 30 MPa, 3.6 m^3 hr^{-1} (i.e. a 30-minute residence time), selected from the literature [45, 46, 66]). Two filters at the process inlet remove 99% of the water from the plastics, correspondingly removing ~99% of the salt from the plastic-water mixture. Combined with the reverse osmosis system the residual salts in the system are reduced to levels that negate the need for higher-cost nickel-based alloys [100].

The feed was pre-heated by heat recovery from the product stream and additional heat to reach the reactor temperature. Heat capacity was approximated as the average value of water over the range of temperatures relevant for each plastic studied here and as explained in more detail in the appendix. The final assumption made in this calculation was that heat could be released to the ocean, which was modeled as an infinite thermal reservoir of fixed temperature. For the UV/H_2O_2 system the exergy requirement was modeled off of the power requirements to remove the organics from water after formation of aromatics. Polystyrene was considered in the model as its products had the highest solubility in water and it was the most previously studied compound in the literature [96, 101]. This assumption will likely result in overestimating the exergy requirements for the other plastics and the waste plastic mixture, suggesting that this part of the analysis is probably conservative.

Reaction Details

Table A.2-4 and **Table A.2-5** show the plastics modeled and their reaction parameters including their reaction temperature, conversions, calculated average heat capacity and product yields. A sample calculation for the average heat capacity values can also be found after **Table A.2-5**.

Table A.2-4 Reaction Conditions of Studied Plastics: Chosen to maximize conversion to oil and minimize conversion to gas and residue.

Plastic	Molecular Weight (Da)	Reaction Temperature (˚C)	Conversion to Oil	Conversion to Gas	Average Heat Capacity (J g^{-1} K^{-1})	Source
Polypropylene	250,000	420	60-100%	0%	5.73	[45]
Polyethylene	117,000	520	60-80%	10-20%	5.80	[46]
2:1 PE:PP Mixture	Mixture	460	70-90%	10-30%	5.86	[66]

Table A.2-5 HTL Product Selectivity Values for Conditions shown in Table SI.2

Product	**Phase**	**Selectivity**
Polypropylene [45]		
C6-C13, Alkene	Oil	95%
C6-C11, Alkane	Oil	5%
Polyethylene [46]		
C7-C11, Alkene	Oil	15.1%
C7-C11, Alkane	Oil	4.1%
C12-C18, Alkene	Oil	22.3%
C12-C18, Alkane	Oil	6.1%
C19-C24, Alkene	Oil	8.3%
C19-C24, Alkane	Oil	2.3%
>C24, Alkene	Oil	3.0%
>C24, Alkane	Oil	0.82%
Waste	Gas	25%
2:1 PE:PP Mixture		
C7, Alkenes	Oil	1.98%
C7, Alkanes	Oil	1.82%
C8, Alkenes	Oil	0%
C8, Alkanes	Oil	2.43%
C9, Alkenes	Oil	10.33%
C9, Alkanes	Oil	0%
C10, Alkenes	Oil	1.54%

C10, Alkanes	Oil	3.75%
C11, Alkenes	Oil	0%
C11, Alkanes	Oil	2.94%
C12, Alkenes	Oil	3.25%
C12, Alkanes	Oil	3%
C13, Alkenes	Oil	1.69%
C13, Alkanes	Oil	2.91%
C14, Alkenes	Oil	1.73%
C14, Alkanes	Oil	2.86%
C15, Alkenes	Oil	4.29%
C15, Alkanes	Oil	2.98%
C16, Alkenes	Oil	1.46%
C16, Alkanes	Oil	2.97%
C17, Alkenes	Oil	4.8%
C17, Alkanes	Oil	2.81%
C18, Alkenes	Oil	0.56%
C18, Alkanes	Oil	2.67%
C19, Alkenes	Oil	1.67%
C19, Alkanes	Oil	4.13%
C20, Alkenes	Oil	0%
C20, Alkanes	Oil	10.84%
C21, Alkenes	Oil	0%
C21, Alkanes	Oil	2.36%
C22, Alkenes	Oil	1.22%
C22, Alkanes	Oil	0%
C23, Alkenes	Oil	1.07%
C23, Alkanes	Oil	0%
C24, Alkenes	Oil	2.23%
C24, Alkanes	Oil	2.71%
C25, Alkenes	Oil	0%
C25, Alkanes	Oil	2%
C26, Alkenes	Oil	0%
C26, Alkanes	Oil	2.97%
C27, Alkenes	Oil	0%
C27, Alkanes	Oil	1.21%

2.5.3.1 *Sample Calculation for Determining Average Heat Capacities*

To capture the change in the heat capacity of water with heating, the heat capacity curve of water at 30 MPa [102] was integrated to find an average value that incorporates the spike at the critical point as well as the rest of the temperature range. A 30 MPa value was chosen to reduce the discontinuity of the heat capacity curve as it approached the critical point. An average heat

capacity was found for every model in order to accurately represent the varying operating temperatures between the different plastics.

Model Development

Table A.2-6 restates the probability distribution ranges for the uncertain model input variables considered in the analysis performed as seen in **Table 2-1**. It also provides the justification for each of the ranges, providing a brief explanation of why each range was chosen. A more detailed explanation of the ocean temperature range and different scenarios is also provided after the table.

Table A.2-6 Probability Distribution Profiles of the Uncertain Model Input Variables

Parameter	Uniform Probability Distribution Ranges	Justification
Weight Percent Plastic in Reactor	10-30%	Maintain realistic pumping capabilities
Ocean Temperature	17-30 ˚C	Account for varying ocean temperature based on location and season
Heat Exchanger Efficiency	50-80%	Based on average heat exchanger efficiencies
Engine Power	1,800-2,200 hp	Engine size of an average large fishing trawler with a 10% variance to account for variable weather conditions and engine power draws
Engine Efficiency	35%-40%	Based on current engine technology efficiencies
Heat of Combustion Variance	0.98-1.02	Account for slight variance in selectivity of products and therefore variance in heat of combustion

The effect of ocean temperature on thermodynamic performance was studied to evaluate the impact of operation in different waters (e.g., North Atlantic compared with South Pacific). Within the proposed analytical framework, additional simulation runs suggest that the difference

between the Atlantic and Pacific Ocean temperature generates an almost negligible shift of only a few percentage points in the respective probability curves. It is however also interesting to note that the probability of net exergy production was found to be higher in the lower temperature Atlantic Ocean case due to the fact that the exergy benefit of lowering the dead state temperature outweighs the higher exergy consumption attributed to the lower initial temperature in the exergy of heating.

Expanded Results and Analysis

Figure 2-2 shows the results of the comprehensive thermodynamic model developed in this work. From this figure it can be seen that the 50% probability metric is reached for plastic loading values between 19 and 27 vol% for the PP, PE, and PE/PP mixture when the ship operates at full power; operating the ship at extra slow steaming conditions shifts the 50% point to <10 vol% for all plastic streams. These values should be achievable for plastics that have accumulated in booms, displaying a plastic concentration factor of almost 2600 relative to the open ocean [7]; however, they cannot be realistically achieved in the open ocean or even in natural gyres that lack booms.

Of the plastics modeled, the process behaves similarly for PP and the PE/PP mixture, with 50% probability of net exergy production occurring at nearly identical values of the plastic loading under both conditions. Performance for pure polyethylene is the least favorable of the feeds considered here, consistent with HTL of this particular mixed stream yielding less oil than the two streams [47]. These differences are readily explained by the thermodynamic stability of the different feeds, with the least stable plastics resulting in the most favorable performance. The sensitivity of the analysis to depolymerization thermodynamics – especially the temperature at which depolymerization to useful fuels occurs – is a clear gap that must be addressed in future work. Similarly, HTL of mixed plastics must be understood more thoroughly for this and similar applications.

Figure A.2-5 shows the individual exergy contributions of each step of the model for all three feeds that were studied. Under all cases, engine power and heating were the main exergy consuming processes and fuel combustion was the main exergy producing process.

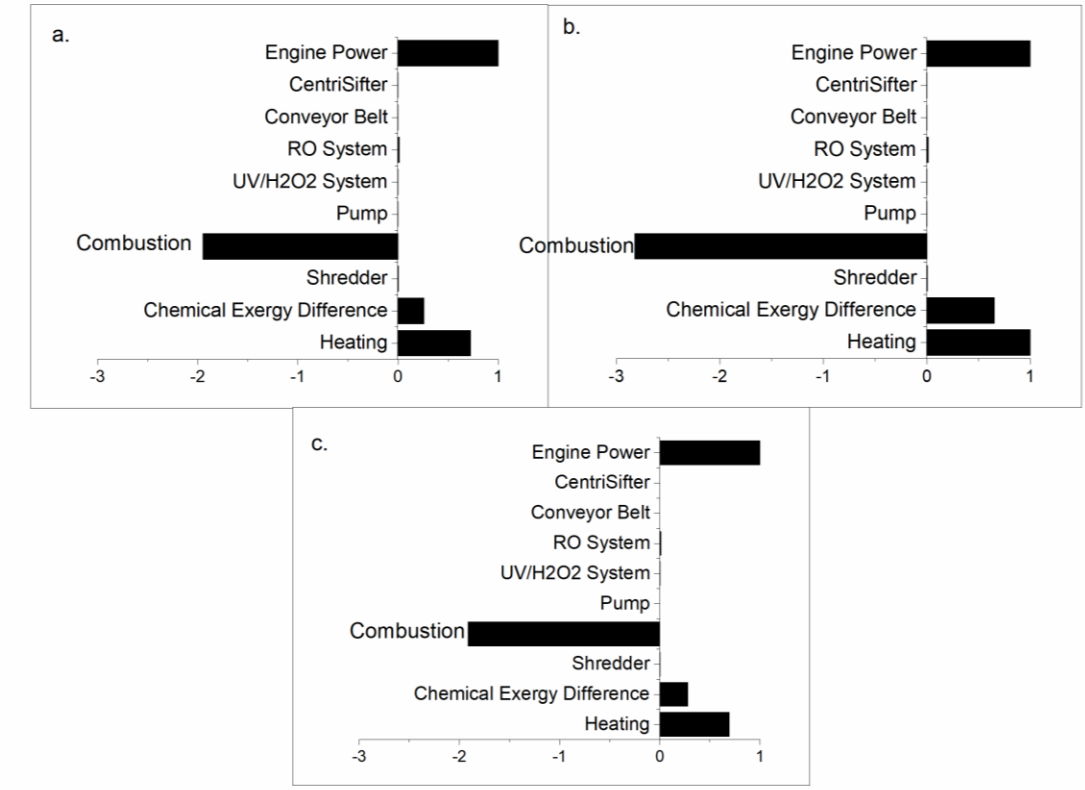

Figure A.2-5 Individual exergy contribution normalized to be unitless by the engine power at full steam of a.) polypropylene b.) polyethylene c.) 2:1 PE/PP mixture

Figure A.2-6 shows the comparison between HTL and pyrolysis for the 2:1 PE/PP mixed stream. Both methods have similar performance profiles in terms of exergy. Although HTL requires significantly more energy to heat the feed to reaction temperatures due to the presence of large amounts of water, the high conversion to oil and the oil produced in HTL almost entirely offsets this higher heating exergy requirement.

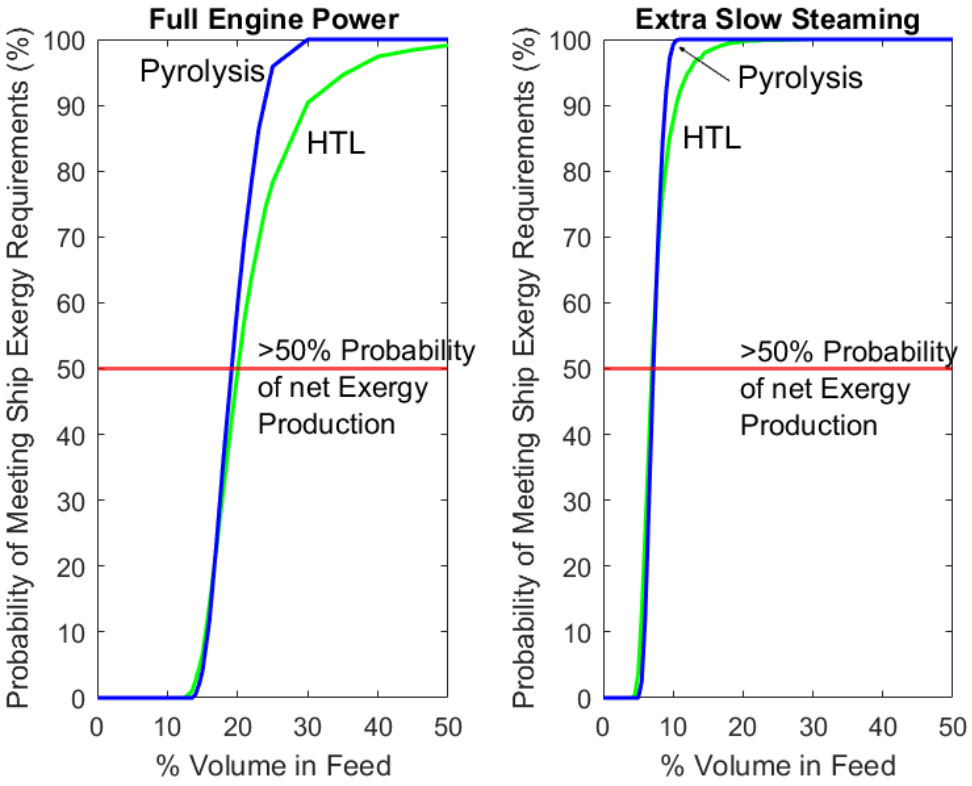

Figure A.2-6 Probability of producing net exergy for a feed of 2:1 PE to PP for pyrolysis and HTL as full engine power and extra slow steaming (1/3 engine power).

Figure A.2-7 shows the effect of changing the scale on the exergy analysis results. As it can be seen increasing the flowrate of plastic through the system, creates a more favorable exergy result. The total system and ship can be powered at a lower plastic concentration making the proposed option more appealing.

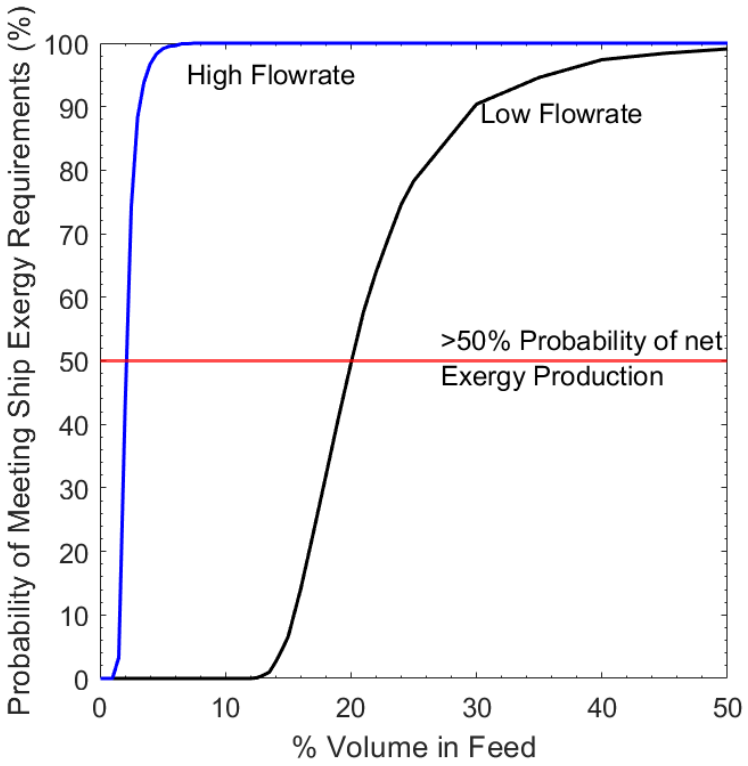

Figure A.2-7 Probability distributions for different feed rates of the PE/PP mixture, either 3.6 m^3 h^{-1} (low flowrate, used as the base case elsewhere) or 36 m^3 h^{-1} (high flowrate) for full engine power.

The following tables and sample calculations were used in the creation of **Table 2-1**. **Table A.2-7** provides all of the pertinent variables and their respective values used in the calculations

Table A.2-7 Parameters used in **Table 2-1** and **Figure 2-4** calculations and assumptions

Variable	**Nomenclature**	**Value**
Collection Speed	S_c	0.5 knots
Boom Length	L	600 m
Cruising Speed between Booms	S_T	15 knots
Distance Between Booms	d_b	25 km
Distance to GPGP	d_G	1930 km
Total Plastic in GPG	P_t	79,000 tonnes [11]
Plastic Concentration in GPGP	C	50-2500 g/km^2 [2 7]
Speed of GPGP Current	S_p	14 cm s^{-1}
Plastic Density	P	0.9 kg/L
Fuel Density	ρ_f	0.84 kg/L

Conversion	Z	60%
Days of Operation Per Year*	T	240
Hours of Operation Per Day	H	16
Size of GPGP [t]	A	$1.6^{*}\ 10^{6}$ km^2
Capacity of Boom	-	infinite
Max Boat Speed	S_m	25 knots
Engine Power with HTL (calculated)	E_1	2000 hp
Booms per Trip w/o HTL	B	10

*To allow for maintenance and crew days off

[t] Geometry of GPG was assumed to be circular

Equation A.1

$$Total\ Plastic\ Collected\ per\ year\ per\ boom(P) = \left(L * S_p\right) * C$$

Equation A.2

$$Booms\ per\ year\ with\ HTL\ (x_1) = (\frac{L}{S_c} + \frac{d_b}{S_T} + \frac{(d_G * 2)}{S_T})/(h)/(t)$$

Equation A.3

$$Years\ to\ Clean(T) = \left(\frac{P_t}{\left(\frac{P}{1000}\right) * x_1}\right)$$

Equation A.4 [103]

$$Boat\ Fuel\ Comsption\ (F_1) = 0.75 * E_1 * \left(\frac{185}{\rho_f}\right) * 0.001 * \frac{1}{3.785}$$

Equation A.5

$$Yearly\ Fuel\ Requirements\ (U) = \left(\frac{L}{S_c} + \left(\frac{d_b}{S_T} + \frac{(d_G * 2)}{S_T}\right) * F_1\right)$$

Equation A.6

$$Percent\ Fuel\ From\ Plastic = \frac{P * \rho * z * \frac{1}{3.785}}{U} * 100$$

Table A.2-8 Plastic removed and total project lifetime for removal of plastic from the GPGP using shipboard HTL

Plastic Concentration in GPGP (g km^{-2})[a]	Plastic Removed Per Year (kg)[b]	Total Time (years)[c]
2,500	$1.2*10^7$	7
1,000	$4.6*10^6$	18
500	$2.3*10^6$	35
200	$9.2*10^5$	86
50	$2.3*10^5$	340

(a) Surface concentration of plastic in the GPGP [7] for a fixed value of 79,000 tons of plastic contained in the GPGP [11]
(b) Plastic removed from 2,500 booms per year with a 70% collection efficiency
(c) Total time required to clean up the GPGP using a single ship

A second scenario was considered to see if towing a boom behind 2 ships could reduce not only the number of booms needed but also the total fuel consumption and total cleanup times. Towing the boom can increase the collection rate per boom by as much as 10-times that possible for a boom that relies on current alone. The speedup factor is estimated from the safe towing speed of the ship, 2-3 knots, compared with that of the ocean current, which is approximately 0.3 knots [64]. Travel at the maximum speed considered safe (3 knots) would require >500 booms to replicate the cleanup speed possible with 2,500 booms relying on current. While reducing the number of booms by a factor of 5 clearly has advantages, the towed boom approach would require at least one ship per boom, and probably two. Given the cost of each ship and its crew, booms that rely on current and that are serviced by a single ship may prove more economically feasible than a fleet of towed booms.

Equation A.7

$$\boldsymbol{Boom\ Knot\ (relative\ speed) = x_1 * S_x}$$

Where S_x can either be S_p (14 cm^{-1}, ~0.3 knots) or S_T

Extended Methods Section

2.5.6.1 *Thermodynamic Correlations based on Carbon Number:*

For alkenes where x is the Carbon Number: $\Delta H_f = -25940x + 85202$ Eq (A.8)

$$\Delta H_c = -653548x - 83571 \quad \text{Eq (A.9)}$$

$$S° = 30.224x + 119.99 \quad \text{Eq (A.10)}$$

For Alkane's where x is the Carbon Number: $\Delta H_f = -25538x - 45603$ Eq (A.11)

$$\Delta H_c = -654899x - 222305 \quad \text{Eq (A.12)}$$

$$S° = 33.031 + 95.283 \quad \text{Eq (A.13)}$$

2.5.6.2 *UV/H_2O_2 Oxidation System*

The chemical exergy difference within the hydrogen peroxide reaction was found assuming there was double the amount of hydrogen peroxide [96] in the system compared to the amount of organics remaining in the water after the separation step for polystyrene.

Chapter 3: Machine Learning Predictions of Oil Yields Obtained by Plastic Pyrolysis and Application to Thermodynamic Analysis[104]

3.1 Introduction

Every year approximately 370 million tons of plastic are generated globally[105]. In the US, approximately 9% of plastic is recycled, 15% is combusted with energy recovery, and the remaining 75% is landfilled [106]. In other locations, environmental disposal is common practice, and combined with losses during transport and loss from landfills, results in an estimated release of 10 to 20 million tons of plastic per year into the world's oceans[107]. Once in the environment, waste plastics have negative impacts on plant and animal life [108], with eventual negative impacts on human health [109].

Increased recycling is an obvious solution to the problem of environmental release. Although recent recycling initiatives have increased the amounts of plastic that are recycled, global recycling capabilities are limited by the need for single plastic streams for effective recycling and further sensitivity to the presence of contaminants like dyes, additives and residual products[31]. Switching to biodegradable plastics has potential to reduce the negative impacts of plastics released to the environment, but biodegradable plastics that duplicate the properties of synthetic ones are not available[110]. Without increasing the worlds recycling capabilities or replacing synthetic plastics with biodegradable ones, landfilled wastes will continue to end up in the environment outside of landfills and in oceans and rivers globally[11].

Reducing the amount of plastics that ends up in landfills and the environment is therefore a priority and one area of specific concern is plastic that is transferred into rivers, as it not only pollutes the rivers but is also transported to the world's oceans where it accumulates and becomes an environmental threat [77, 111]. Recently, a handful of highly industrialized river systems, including

the Yangtze, Ganges and Xi, have been identified as especially problematic [21] Because of the limitations of recycling and slow progress in replacing synthetic plastics with biodegradable versions, new and innovative technologies are needed to valorize waste plastics and reduce their flow into the environment [112, 113].

Different plastic valorization techniques have been developed over the years, falling mainly in to two categories, mechanical and chemical recycling. A key advantage of chemical recycling techniques is they are more compatible with mixed waste plastics than mechanical recycling. The end products of chemical recycling are fuels, chemicals, or monomers, depending on the feed and the specific process technology[114]. Although many dozens of plastics are in use, many of these are used in low-volume, niche applications. Six plastic types account for >85% of all plastic used today[115], meaning that reducing plastic waste should prioritize these plastics, which include poly(ethylene terephthalate) (PET), high density polyethylene (HDPE), polyvinyl chloride (PVC), low density polyethylene (LDPE), polypropylene (PP), and polystyrene (PS). Collectively, these plastics can be termed the "big six", since they are denoted numerically in the U.S. recycling system in this order from one to six [2].

Recent focus has shifted to circular economy for plastics, with emphasis on "upcycling", a term used to describe processes that yield products that are more valuable than the virgin plastics themselves[116]. Chemical recycling can qualify as upcycling, in certain cases, especially when performed in the presence of a catalyst[117]. On the other hand, recycling to products with value equal to the virgin plastic or even down cycling to produce products of less value than the original plastic can play an important role. Products such as chemicals, fuels, and monomers are undoubtedly more valuable than waste plastics[118] and this type of chemical recycling can help

reduce plastics entering landfills or the environment. Unlike upcycled products, the market size for chemicals, fuels, and monomers is commensurate with the size of the waste plastic feed.

Of the different forms of chemical recycling, thermal depolymerization techniques such as pyrolysis and hydrothermal liquefaction (HTL) have been especially promising for their ability to handle mixed wastes, their compatibility with contaminates, and their ability to achieve high oil product yields without using a catalyst[47]. Pyrolysis heats plastics to high temperatures in the absence of oxygen to break the carbon-carbon bonds within polymers to return them to their monomer states [119]. HTL operates similarly to pyrolysis but in the presence of sub- or supercritical water [120]. Both pyrolysis and HTL have the ability to convert plastics into oils with conversion rates of greater than 90%, depending on the process conditions and the plastic feed[66, 73]. Results like these have spurred significant research into thermal depolymerization of plastics [114].

Although previous studies show the great promise of thermal depolymerization, a technological problem of pyrolysis reactor design is that different polymers have very different thermal reactivities. Accordingly, the composition of a given plastic waste stream significantly affects both the oil yield and the overall conversion [121]. Given the number of potential feed streams, an inability to predict oil yields hampers prioritization of resources to the situations that are most promising for investment. Further, for every new feed of polymers the operating parameter matrix must be reoptimized, which is time consuming and potentially cost prohibitive, especially when the oil yields are unknown. An efficient way to determine the oil yield obtainable from a given plastic waste stream would permit allocation of finite resources to streams most likely to be thermodynamically and economically favorable.

Models that describe plastic depolymerization have been available for over 20 years[122-124]. These models are full kinetic networks that track polymer chain length using the method of

moments and formation of key products using systems of ordinary differential equations[122-124]. While providing accuracy and reliability, full kinetic models are computationally expensive, require years to develop for new plastics or plastic mixtures, and are not available for anything more than binary plastic mixtures[122-124]. Fortunately, the level of resolution offered by full kinetic models is not always required for process design, opening an opportunity for lower-resolution yet accurate methods of predicting key reaction outcomes, such as pyrolysis oil yields.

Machine learning techniques have the potential to predict reaction results, such as yield and conversion, with significantly less development time and less computational expense than full kinetic models. Unlike full kinetic models, which require detailed measurements of polymer chain length and key product and intermediate formation rates as a function of conversion, machine learning models use abundant historical data to train models capable of predicting outcomes of new situations [57]. Machine-learned models are black box, meaning they do not provide information about the chemistry that is occurring during reaction, yet they have been shown to accurately predict the results from thermal depolymerization for complex waste mixtures, such as food waste[125-127]. A handful of machine-learned models have been developed specifically for plastics, especially in the classification of polymer types [128-130]. The handful of studies that have used machine learning to predict depolymerization reactions, have focused on single plastics and not mixtures[131] or understanding properties of single phases [132]. The few studies that have looked at mixed plastic streams have focused on specific, and narrow, ranges of operating conditions like temperature [133] or specific reactor types [134] and have utilized very little data to train and validate the models (<<100 data points).

The pertinent literature contains many hundreds of data points on plastic pyrolysis, and thus utilizing all of the published literature data can improve the accuracy of machine-learned

models as well as expand the range of conditions and reactor types that can be studied. Naturally, utilizing the full range of published data requires an approach that can handle differences in feed, reaction conditions, reactor type, and the presence of catalyst. Fortunately, modern regression techniques have established ways to handle both numerical data as well as categorical data, such as reactor type or presence of catalyst[135]. Emerging methods for filling gaps in the values of dependent values – which are not uniformly reported – offer a way to maximize available data and harmonize between different reporting standards. The K nearest neighbor (KNN) method has proven especially versatile for data harmonization in other fields, but has yet to be applied in a plastic pyrolysis case [136]. Using models and methods such as these allows for efficient analysis of real waste streams and identification of promising experiments and conditions for future work.

The objective of this study is the development of machine-learned models for prediction of oil yields obtained by pyrolysis of common plastics and their mixtures over a wide range of conditions. Unlike previously reported studies, the current effort attempts to harmonize pyrolysis data arising from many different polymers – all of the "big six" – and for pyrolysis in different reactor types with and without the use of catalysts. The performance of seven different machine learning methods was comprehensively evaluated for accuracy. In particular, each of these models was trained, optimized, and validated using a dataset curated from the open literature encompassing a wide range of possible reaction conditions. The accuracy of model predictions was assessed with a test set that was set aside from the data set prior to training. The most accurate of these seven models was then used to predict the oil yields obtainable from pyrolysis of real plastic waste streams representative of U.S. Municipal Recycling Facilities (MRFs) and present in the Rhine River, a river with a high and well characterized plastic load [137, 138]. As a further example, the utility of the model was evaluated for making thermodynamic feasibility predictions of plastic

pyrolysis. Finally, the machine-learned models and the proposed approach to develop them could become useful evaluative tools for advancing plastic pyrolysis as part of a comprehensive strategy to reduce plastic waste.

The paper is organized as follows: Section 2 encompasses the conceptual, methodological and computational aspects of the proposed modeling and simulation framework. The study's main results are presented in Section 3 followed by a pertinent discussion. Finally, a few concluding remarks are provided in Section 4.

3.2 Methods

Overview

The aim of this work is to develop a rigorous method for creating, validating, and applying machine-learned models to predict the yields that can be obtained from pyrolysis of waste plastics and their mixtures. **Figure 3-1** shows the overall approach used for model development, refinement, selection, and application. The most important step is generation of the data set itself. Specifically, the data set was generated by retrieval of data published in the open literature, with attempts to be inclusive up until the start of 2022. Once the data were collected and pre-preparation steps completed, seven different machine learning algorithms were tested and then validated using K-fold cross validation. These models were then used for predicting oil yields and understanding how polymer type in the feed affects the oil yields. Future sections will describe each of these steps in more detail.

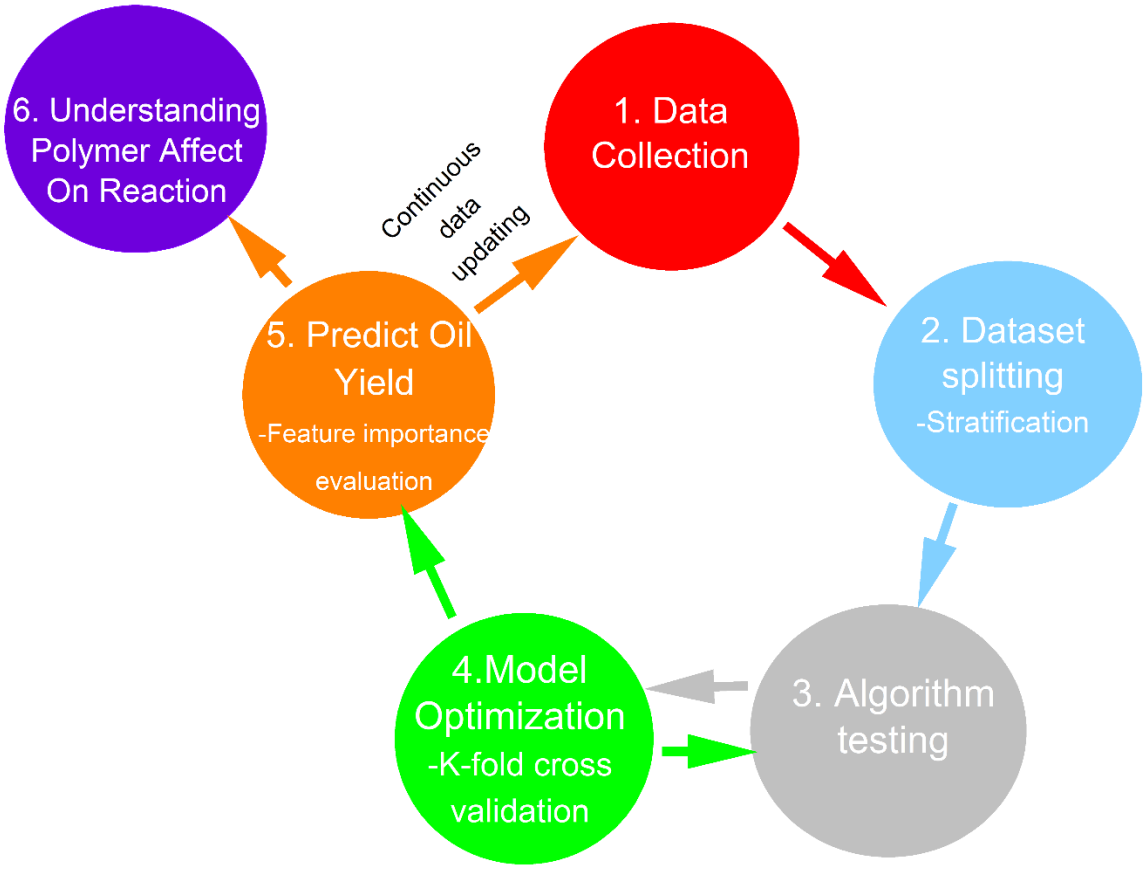

Figure 3-1 Outline of model development and deployment including validation process for building and validating a robust model capable of predicting plastic pyrolysis oil yields.

Data Collection and Preparation

The data set was collected from the open literature and consists of 325 individual data points corresponding to 39 papers, as seen in the Appendix B . Studies describing pyrolysis of any of the "big six" plastics ((polystyrene (PS), high- and low-density polyethylene (HDPE and LDPE), polypropylene (PP), polyvinyl chloride (PVC) and polyethylene terephthalate (PET)) were included in the retrieval effort, with pyrolysis defined as experiments performed in different reactor types with and without a catalyst. The data was collected from reliable sources as described in pertinent peer reviewed journal publications. In particular, the data set was derived from studies of both pure plastics and plastic mixtures, and the distribution of data points corresponding to

different types of pure plastics and mixed plastic streams is shown in **Figure 3-2**a. Of the plastics considered here, HDPE and LDPE along with PP are the most abundant in the current data set.

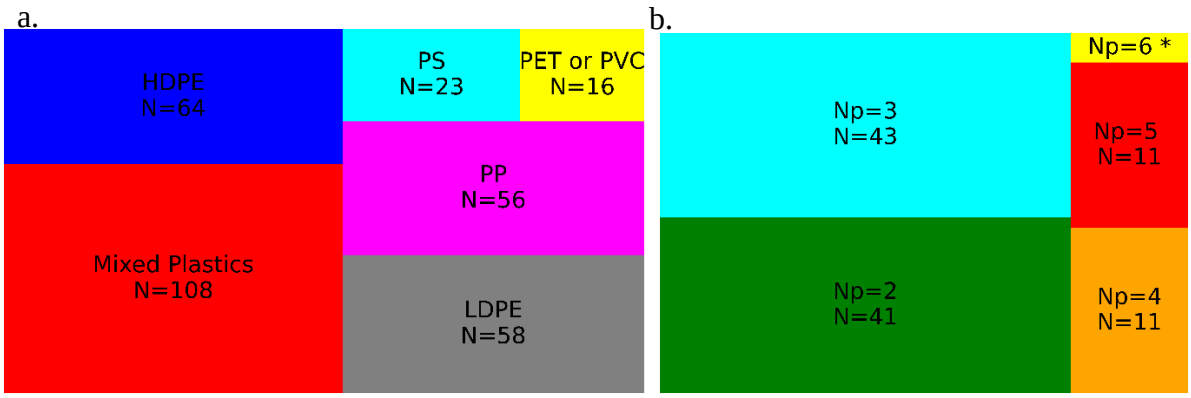

Figure 3-2 Visual representation of the 325 data point pyrolysis data set, showing a.) the distribution between pure plastic studies and mixed plastic studies where, N is the number of data points and b.) the number of plastics in the mixed plastic studies where Np is the number of plastics present in the mixture. Np=6 corresponds to 2 data points.

Studies on mixed plastic streams account for about one third of the entire data set. **Figure 3-2**b shows the distribution of the mixed plastic data in terms of the number of plastics in the mixture. Binary and ternary mixtures are the most commonly studied mixtures but several studies of mixtures including all of the "big six" plastics appear in the data set as well. For studies involving waste mixtures, the mass fraction in percent of each plastic type in the feed became its own independent variable input to the model. For pure streams, the mass fraction of the plastic being pyrolyzed was set to 100 while all other mass fractions were set to 0.0.

Along with the concentration of each of the plastics present in the feed, six other reaction parameters were also recorded in the data set and used as independent variables (called features): Pyrolysis reaction temperature, heating rate, particle size, amount of feed utilized, catalyst, and reactor type. Pyrolysis reaction temperature, heating rate, particle size, and amount of feed utilized are all numerical and can be handled using typical regression methods. After careful deliberation,

reaction time was not included as an independent variable, as reaction time is not well-defined for different reactor types. More detail is provided in the Discussion section.

Unlike the quantitative variables, catalyst and reactor type are categorical variables, which require special treatment. In order for the model to be able to handle these categorical variables they were one-hot encoded[135]. For example, catalyst was used as an independent variable with its value set to either 0 or 1 to represent the absence and presence of a catalyst, respectively. The model includes no information on the type of catalyst. Similarly, the reactor type was divided into five categories (batch, fixed bed, fluidized bed, horizontal tube and semi-batch) and each of these was described by its own independent one-hot encoded variable.

One potential drawback of using data from many different papers is inconsistencies in data reporting from lab to lab. The upshoot of data reporting inconsistencies is data gaps. To avoid this problem for dependent variables, pyrolysis oil yield was selected as the sole dependent variable as all studies of plastic pyrolysis report gravimetric oil yield. Oil yield was taken as the mass of liquid products recovered at room temperature and pressure. The phase behavior of the oil mixture depends on composition and as a rough guide it extends from products that are less volatile than pentane to compounds that melt at temperatures less than octadecane. Non-ideal phase behavior and solvation effects mean that this range can only be used as a guideline. Since oil composition varies from study to study and is not uniformly reported in the literature and since oil recovery protocol also vary from study to study, reported oil yield data display natural variability that influences model predictability. Data gaps in the independent variables are unavoidable, as not all studies report the six operating parameters selected for this study. Two common ways to handle data gaps are often used; omitting the data points that have missing data or using a data imputation algorithm such as K-nearest neighbor (KNN) to fill in the data gaps[139]. Although omitting data

with incomplete independent variable reporting is the more conservative of these approaches, preliminary tests found that eliminating even a handful of data points significantly and negatively impacted model performance, as seen in the Appendix B. Therefore, this work used the KNN method to fill in the above data gaps. The KNN algorithm works by looking at K of the nearest data points to that which is unknown and making an educated prediction based on the votes of each of these points. K can be chosen in a multitude of ways, but the conventional approach is to use the square root of the number of data points [140]:for this data set K was 17 for the training set size of 292 data points. KNN was needed to fill gaps for heating rate, particle size, and feed size. It should be pointed out that improved consistency of data reporting in future studies could potentially reduce the need for methods to handle data gaps.

Model Evaluation Metrics

Within the context of the present study, the Mean Absolute Error (MAE) criterion was used to evaluate model accuracy. Equation 3.1 shows how MAE is calculated:

$$\boldsymbol{MAE = \frac{\sum_{i=1}^{N} |x_i - \hat{x}_i|}{N}} \qquad \textbf{(3.1)}$$

where N is the number of data points, x_i is the predicted value of x and $\hat{x}_i$ is the experimental (true) value of x. Compared to other potentially viable alternatives such as the root-mean square error and mean relative error criteria, MAE is the most widely used and easiest to interpret. The units of MAE in this work corresponds to the units of oil yield (wt%).

Machine Learning Models

Seven different machine learning algorithms were evaluated in this study. Of the seven, three were linear methods and four were non-linear methods. The linear methods are linear regression (LR), linear regression with Lasso regression (LR-Lasso), and linear regression with Ridge regression (LR-Ridge). Both Lasso and Ridge regression are forms of linear regression that use penalty functions to shrink the model to fewer parameters [57]. The non-linear models that are

studied are decision tree (DT), eXtreme Gradient Boosting (XGBoost), random forest (RF) and artificial neural networks (ANN). Decision tree, XGBoost and random forest are all tree methods[57], with decision tree using a single tree while XGBoost and random forest methods rely on a series of trees to improve accuracy.

Each of the models that were tested were run and optimized using Python 3.6 [141] and scikit-learn 1.1.0 packages [142]. Model optimization involves tuning internal parameters, termed hyper parameters. The optimal hyper parameters for each model can be found in the appendix B **Table B.3-3**. For all methods other than the tree models the data had to be normalized due to the large difference in the values for the different reaction parameters (i.e. particle size ranges from microns to mm and feed sizes from mg to thousands of g). When normalization was required a Z transform was performed on the data including all of the model features. Equation 3.2 shows how the Z transform of a variable is calculated,

$$\boldsymbol{Z_i = \frac{x_{i,j} - \bar{x}_i}{\sigma_i}} \qquad \textbf{(3.2)}$$

where Z_i is the new value, $\bar{x}_i$ is the mean of feature i and σ_i is the standard deviation of feature i. Decision tree methods by nature are not sensitive to these differences and unscaled data were used for these model types [57].

Data Splitting

Development of rigorous, predictive machine learned models requires training the model on a data set followed by testing its accuracy for prediction of a separate data set. These two data sets are called the training and testing sets. For the current study, 10% of the data was removed prior to model optimization, placed into a "vault", and not touched again until all of the models were optimized in order to be able to test the models on "new" data that was not "seen" during model development. The remaining 90% of the data was used for KNN and model training.

Dividing data into training and test sets is common practice to prevent over fitting; inadvertent use of test data for model optimization is termed " data snooping" and can reasonably be expected to result in over fitting[57]. The splitting of the data set into training and test sets is done through random selection.

Model optimization on the training data utilized a method of validation, which further separates the training data into separate sub-sets. The model validation method selected is termed K-fold cross validation, which separates the training data into K sub-sets. Here, K was set equal to 10, meaning that the training data was split into 10 equal groups. Nine of these groups were used to train the model (training dataset) and 1 was used to validate (validation data set). This was repeated sequentially until all 10 groups had acted as the validation set. Cheng et.al. (2021) provided a visual representation of how the K-fold method works [125]. K-fold cross validation helps to prevent overfitting, or fortuitus fitting as the model must be trained on all of the data and the final result represents an average of all 10 models.

One of the potential pitfalls of working with small data is ensuring representative splitting into test and training data sets. For example, relatively few studies are published that include low-yield data, which means that random splitting into test and training sets may result in a training set that completely lacks low-yield data. The result is a model that cannot accurately predict data with low yields. To prevent the problem of non-representative data splitting, the data set was stratified based on yield prior to splitting. Stratification grouped data by reported oil yield to create a set of bins each with an equal number of data points (10 here). During splitting, at least one data point from each bin was included in the test set to ensure that it was representative of the full range of data present in the training set. The data were then re-randomized prior to training and validation.

3.3 Results/Discussion

The goal of this study was to use published data to develop a data-driven, machine-learned model to predict oil yields obtained from plastic pyrolysis. A data-driven model has the advantage that its predictions do not require detailed understanding of chemical mechanisms. Instead, reaction conditions can be used as the independent variables, or features, and inputs to a regression-type model that does not require knowledge about the underlying chemistry.

In addition to pyrolysis, the kindred method of hydrothermal liquefaction (HTL) has been reported for conversion of waste plastics to useful oils [143]. A universal tool that can predict HTL or pyrolysis yields obtainable from waste plastics could be very useful. Unfortunately, most studies on HTL have focused on plastics other than those in common commercial use, meaning that the HTL and pyrolysis data sets have minimal overlap and rendering simultaneous modeling of HTL and pyrolysis impractical at present.

After initial tests, reaction time was not included as an independent variable, due to the fact that reaction time is a fundamentally different concept depending on the reactor type. For example, reaction time is well-defined as the residence time in a closed, batch reactor on the one extreme and in a plug-flow continuous reactor on the other. For the most common pyrolysis reactors, including spouted bed reactors, swept-batch or semi-continuous reactors, and fluidized bed reactors, residence time of the plastic within the reactor is either poorly defined or impossible to compare with other types of reactors. Excluding certain reactor types limits the amount of data available for the model. Since the model already is pushing the lower boundary of how much data is required for robust predictions, all reactor types were included as independent variables and reaction time was excluded. In fact, preliminary tests (seen in the Appendix B*)* that conflated the different types or reaction times did not provide accurate predictions of pyrolysis oil yield.

Many different types of machine-learned models have been published in the literature for a range of different engineering applications [125-134]. Accordingly, a wide variety of model types were evaluated, as the ideal model for a given data set cannot be predicted *a priori*. The seven models studied included three linear models (Linear Regression, Ridge Regression and Lasso Regression), three non-linear tree models (Decision Tree, Random Forest and Xtreme Gradient Boosting) and one non-linear model (Artificial Neural Network). These seven were chosen as they are representative of successful model types previously studied in the literature for similar problems [125-127]. Linear regression represents the simplest starting point and is a good basis of comparison. Lasso and Ridge regressions are well-known modifications of the standard linear regression model that add an error function intended to improve accuracy [57]. Decision tree is the simplest Boolean model and Random Forest and XGBoost in particular were chosen because their use of multiple trees as well as subsets of the data improves their accuracy, especially when working with small data sets [144].

Each of the seven models consists of multiple parameters (termed "hyper parameters" in the machine learning literature [145]), which the user must select based on the application at hand. Hyper parameter values are optimized during cross validation to minimize model error. The optimal model hyper parameters for each individual model can be found in the Appendix B **Table B.3-3**.

After model optimization, prediction accuracy was assessed for both the validation and test sets. MAE was used as the error metric in this work. The most accurate model should minimize MAE, exhibit minimal change between the validation and test-set MAEs, and have low standard deviation arising from validation. Each of these plays an important role. MAE of the test-set is the truest measure of the predictive accuracy of the model. Agreement between the test-set and

validation MAEs as well as minimal validation standard deviation guard against over fitting and fortuitous division between validation and test sets. Using validation set MAE as the sole basis for model selection therefore risks model overfitting, which detracts from accuracy of predictions for new data not included in the original data set.

Figure 3-3 shows both the validation-set and test-set MAE for all seven models as well as the standard deviation of the validation set error. The MAE of the benchmark linear regression model is approximately 14, for both validation and test set analysis. The corresponding standard deviation of the validation set MAE is nearly 3. While the agreement between validation set and test set MAE is reassuring, the absolute value of these MAEs is not sufficient for most applications and the large standard deviation of the validation set MAE suggests that the regression is prone to errors due to fortuitous data selection. The Lasso and Ridge modifications of linear regression offer no benefit, indicating that the addition of an error function is insufficient to capture what is inherently a highly non-linear data set. Accordingly, linear models should not be expected to provide accurate pyrolysis yield predictions, except possibly over very narrow ranges of conditions where the problem might be nearly linear.

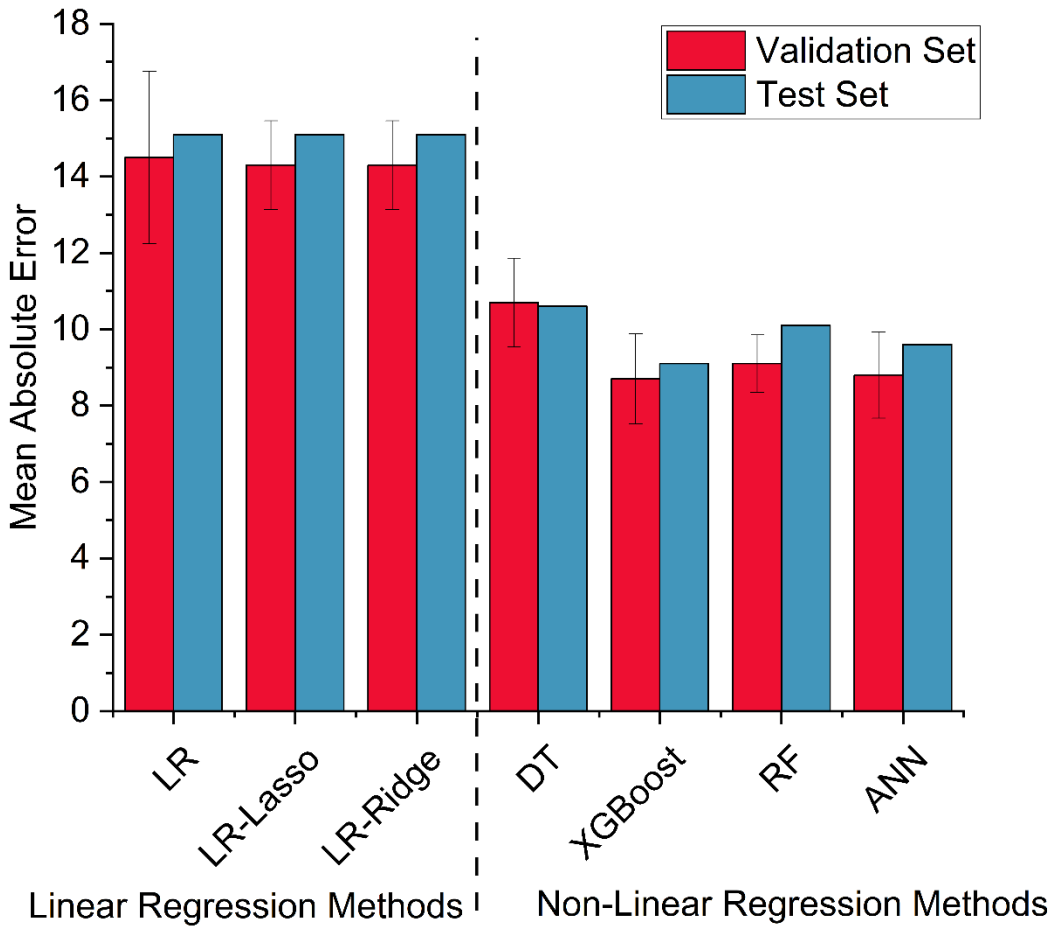

Figure 3-3 Mean absolute error (MAE) of the validation and test sets for linear regression (LR), Lasso regression (LR-Lasso), ridge regression (LR-Ridge), decision tree, eXtreme Gradient Boosting (XGBoost), random forest (RF) and artificial neural network (ANN)

All of the nonlinear models tested here provided superior performance compared to the linear models. Of the four non-linear methods, the MAE provided by the Random Forest, XGBoost and ANN models are less than the Decision Tree model. While the decision tree model fits the validation data better than the linear methods, the MAE of the validation and test sets along with the validation set standard deviation of Decision Tree is greater than the other three non-linear models. In comparison, the modest value of validation set standard deviation observed for Random Forest indicates it is much less sensitive to the subset of data it is trained on than any of the other models tested here. The comparison of validation set standard deviations recommends selection of RF over ANN or XGBoost, especially since all three methods yield similar values of MAE. The performance of RF, ANN and XGBoost are nearly identical and therefore any method could justifiably be used for further analysis. In this work XGBoost was chosen for future model applications due to its relative simplicity; low MAE for validation and test sets (8.7% and 9.1% respectively); and low standard deviation in validation (±1.2 %). A parity plot of the experimental vs predicted oil yields of the test for the optimal XGBoost model can be found in the Appendix B **Figure B.3-7**. The majority (67%) of predictions fall within ±10% of the experimentally reported values, with the remainder contributing to the observed value of MAE (9.1%) as seen in Table SI.3.

The MAE of the XGBoost model captures the residual error of the current dataset, as it was extracted from the literature. Residual error likely arises from several factors and reducing the error can be achieved in several ways. First, the available data set (<500 data points) is at the lower limit of what can be studied using machine learning. Increasing the amount of data – for example, by updating the model periodically as new data appear in the literature – should improve accuracy over time[53]. Second, the experimental data themselves are subject to experimental uncertainty,

which is on the order of several percent. Experimental uncertainty detracts from model accuracy and reducing the inherent experimental error should reduce the MAE that the model can achieve. Experimentalists should adopt methods such as mass balance and carbon balance closure to ensure data quality and reduce uncertainty. Third, different studies use slightly different methods – including reactor types, as previously discussed, and also analytical methods for recovering and quantifying oil yields. Differences in methodology give rise to systematic differences between oil yields reported in different studies. Greater consistency in analytical methods, especially in recovery conditions and oil yield definitions (e.g., instead of reporting total gravimetric yield, reporting yield obtained over a certain distillation range), should improve consistency in the data set and help to reduce uncertainty. Application of XGBoost-based regression on a single, uniform data set – of sufficient size (>500 data points) – can realistically be expected to achieve MAE values less than seen here. That data set does not exist in the public domain at this time.

A common analysis of regression error is to determine the statistical significance of the various features. For linear models, a common method is the F test [146]. For decision tree models, the corresponding metric is feature importance. **Figure B.3-8** provides the feature importance extracted from the XGBoost model. Plastic type and particle size have similar levels of importance (~10%), indicating that they have statistically significant effects on model predictions. Interestingly, the feature importance of catalyst was negligible compared with the other features. Effectively, the pyrolysis oil yields obtained using a catalyst may often be reproduced by increasing the pyrolysis temperature. However, other studies find that catalyst use has minimal or even negative effects on yields and instead mainly effects product distribution [147] – a dependent variable not considered here, outside of how product distribution affects oil yield. Data on the use of catalysts may be biased to lower temperatures that accentuate the perceived benefit on yield. In

these cases, the benefit of using a catalyst is not so much as to increase oil yields, but to lower the temperature at which an acceptable yield can be obtained. The net effect of catalyst use in these cases is to improve energy yield, an outcome that is not explicitly predicted by the models presented here.

The feature importance also highlights that the influence on oil yield of pyrolysis of plastics falls into two categories: factors that capture chemical reactivity and factors that are related to heat transfer. The chemical reactivity factors include plastic type, temperature, and presence of catalyst, and together they account for 57.2% of the observed correlation. Heat transfer factors include particle size, plastics loading, and heating rate, combine to account for 40% of the correlation. The importance of chemical reactivity and heat transfer factors is consistent with intuition[148], which is a comforting result for a data-driven model that is ignorant of physics.

Of all of the features considered in the present study, the value of the feature importance assigned to temperature was the greatest (43.6%), indicating that temperature had the most significant effect on pyrolysis yields. Due to the high feature importance of temperatures, understanding how temperature appears in the current data set is critical to understand before the corresponding model can be used to make predictions of new systems. Since model predictions can only be trusted for conditions that fall within the limits established by the data set, the temperature limits where model predictions can be trusted are based on the appearance of temperature in the data set. As a temperature-activated process, pyrolysis temperatures will naturally be biased to values that result in appreciable oil yields. Researchers use their knowledge of the system to determine the temperatures at which they run their experiments, meaning that temperatures much less and much greater than optimal do not appear in the literature. The result is that predictions for conditions that fall outside of the limits appearing in the data set cannot be

trusted. Because each plastic has its own temperature which optimizes pyrolysis oil yields, the available data set must be evaluated to understand the temperature range over which each plastic has been studied.

Figure 3-4 plots the temperature range covered by each of the plastics included in this study, as well as the temperature range covered by pyrolysis of mixtures, as a box-line plot where the box represents the 25% and 75% limits of the available data and the line represents the absolute limits. As expected, the temperature range studied for each plastic varies with the plastic, with PP, PS, and PET tending to be studied at low temperatures and PE at higher ones. PVC pyrolysis has been studied at a single temperature (700 °C). Fortunately, in aggregate, the temperature range over which pyrolysis yields are optimized, from 400 to 700 °C, is well covered in the data set – provided that pure PVC is excluded from the analysis. PVC is generally regarded as an unsuitable feed for plastic pyrolysis, due to the formation of hydrochloric acid during pyrolysis. Hydrochloric acid is corrosive and chlorine contamination detracts from fuel properties[149]. Hence, a predictive model that is appropriate for pure or mixed plastics, with the exception of PVC, in the range from 400 to 700 °C is valuable for many applications. Predictions made outside this range are not physically realistic, with the consistent over prediction of pyrolysis oil yields at temperatures less than 400 °C.

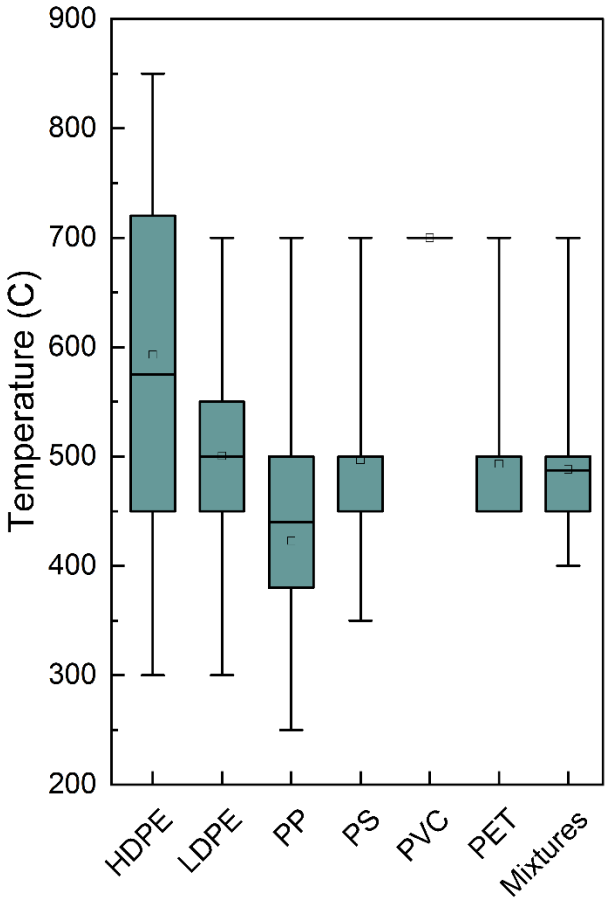

Figure 3-4. Temperature distribution for each polymer and mixtures in the data set showing the 25 %-75% range (box), the min-max range (line), the median line and the mean (▫).

Figure 3-3 and **Figure 3-4** indicate that an XGBoost model can make accurate pyrolysis oil yield predictions, in the temperature range from 400 to 700 °C. The next step was to demonstrate the method for two realistic applications: pyrolysis of plastics collected at municipal recycling facilities (MRFs) and pyrolysis of plastics present in river outflows to the ocean.

A major benefit of pyrolysis co-located with MRFs is that they exist in centralized locations where plastic is collected. Although the exact composition of plastics at these facilities can change from location-to-location representative averages exist for different countries/areas. These averages can vary significantly from country to country and therefore the expected oil yields from

converting the plastic to fuels are also expected to vary. The machine-learned model can predict oil yields for these different streams. To ensure reliable model predictions, the model was run in a batch reactor and at a constant temperature of 500 °C, well within the limits suggested by Figure 4.

Table 3-1 provides average compositions and corresponding predictions of oil yields for municipal solid waste (MSW) collected in both the U.S. and E.U. The two plastic streams vary considerably, especially in their relative ratios of HDPE and LDPE and their amounts of PS and PVC. These composition differences translate into predicted oil yields that differ by almost 15% from one another, with the oil yield predicted for pyrolysis of E.U. plastic waste being greater than that predicted for U.S. waste. That difference is likely related to the greater PS content of E.U. waste than U.S. waste, since PS is more easily pyrolyzed to obtain high oil yields than PP or PE [150].

Table 3-1 Comparison of Plastic in European and American Municipal Solid Waste and their Predicted Oil Yields

Location	***HDPE***	***LDPE***	***PP***	***PS***	***PVC***	***PET***	***Predicted Oil Yield***
US [115]	17.86%	24.08%	22.78%	6.29%	2.4%	14.79%	35.3%
Europe [47]	44.4%	0%	21.2%	13.3%	12.2%	8.9%	48.9%

The XGBoost model can be used to explore the benefits of partial separation for optimizing oil yields. In addition to PVC, oil yields obtained from pyrolysis of PET are generally less than those obtained from HDPE, LDPE, PS, and PP [150, 151]. Consistent with this expectation, the XGBoost model predicts that pyrolysis of pure PET at 500 °C results in 28% oil yield, much less than that predicted for PP, PS, or HDPE at the same conditions (74, 70, and 63%, respectively, as

seen in Appendix B **Figure B.3-9**). Similarly, whereas HDPE, LDPE, PS, and PP are all hydrocarbon plastics that yield oils with properties similar to hydrocarbon fuels, PET is an oxygenate that yields small oxygenated compounds, especially ethylene groups and benzoic acid [152], that are more suitable for use as monomers than as fuels. Finally, of the six commonly used plastics, PET has the most robust recycling market, meaning that recycled PET has an existing valorization channel that the other plastics lack [153]. For these reasons, separation of PET prior to pyrolysis is worth evaluating. Both new and existing [154] technologies can be used for PET separation.

To evaluate the effect of PET on pyrolysis oil yields, the XGBoost model was run many times for different ratios of PET in a PP and HDPE mixture and separately for PET in a PP and PS mixture. The combinations of plastics shown in Figure 5 were chosen due to the prevalence of HDPE, PP and PS in both US and European MSW [47, 115]. The result of these simulations are ternary diagrams relating composition to predicted oil yields, as shown in **Figure 3-5**. The oil yield analysis was performed for a mixture of LDPE, PP and PET and results can be found in the Appendix B as **Figure B.3-9**.The general trend observed in Figure 5 is that oil yields decrease with increasing PET content, strongly recommending PET removal prior to pyrolysis. Some interesting areas of potential synergy exist, for example mixtures of approximately 80% PET and 20% PP.

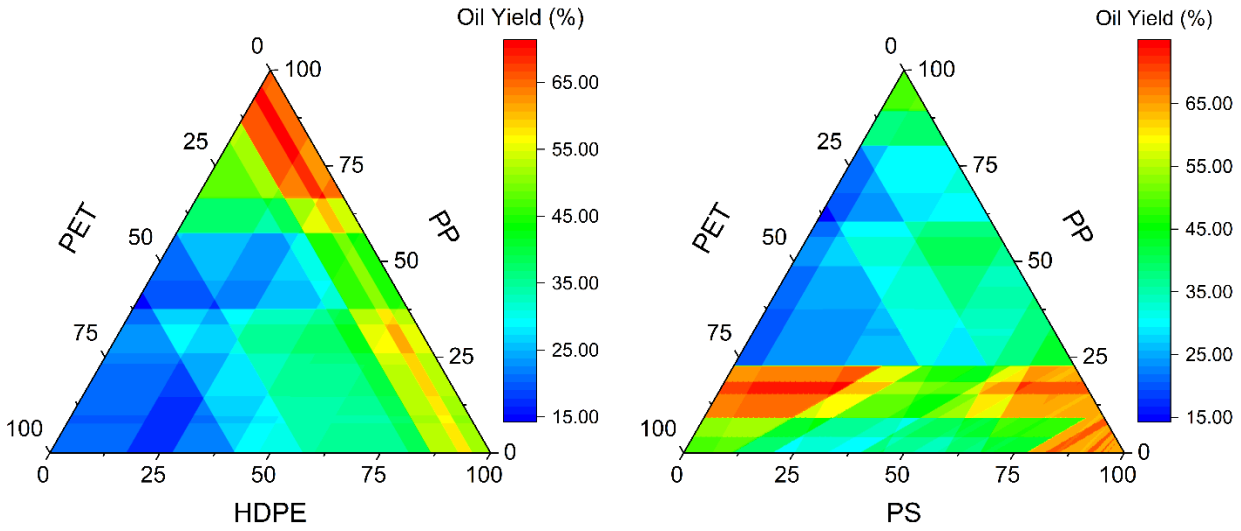

Figure 3-5 Predicted oil yields for mixtures of HDPE, PP and PET and PS, PP, and PET pyrolyzed in a horizontal tube reactor at 500 ˚C, with a heating rate of 10 ˚C/min, a particle size of 13mm, plastics loading of 200g without catalyst.

In addition to waste already collected at MRFs, significant waste ends up in the environment. Waste plastic in rivers throughout the world is especially damaging as it not only pollutes the river ecosystems, but also eventually pollutes the ocean as rivers act like highways to transport waste plastic to the ocean [111]. Rivers polluted with waste plastic exist all over the world, [21] and targeting these rivers as sources of plastic for conversion to oil could cut off these plastic highways into the world's oceans. The complete system would include a mechanism to collect the plastic, remove it from the river, feed it to the pyrolysis process, pyrolyze the plastic, and recover the oil, similar to a system designed for ocean plastics[58].

The composition of plastics varies significantly from river to river,[22] due to differences in regional industry and community usage. The natural consequence of these differences in composition is differences in oil yields obtainable by pyrolysis. Prioritizing specific rivers to implement plastic capture and conversion systems allows for optimal use of finite resources. One

way to prioritize rivers is to predict the oils yields that can be obtained for pyrolyzing the plastic present in them, potentially feeding those predictions into economic models to optimize return on investment. Alternatively, prioritization could be based relative ecological importance (i.e., proximity to fragile ecosystems), in which case predictions of oil yields are necessary to build a business model.

As a concrete example, the XGBoost model was used to predict the oil yields obtainable from pyrolysis of plastic found in the Rhine River in Europe. This river was chosen for the abundantly available data about plastic type and concentrations found along the length of the river [137, 138]. The Rhine River waste plastic consists of mainly HDPE, PP and PS (27, 37 and 26% by mass respectively). This average composition was then used along with a common set of reaction parameters (found in the Appendix B **Table B.3-5** and **Table B.3-6**) to predict an oil yield range of 44.1 to 56.7% for pyrolysis temperatures from 400 to 650 °C, comparable to the value observed for the MRF present in the E.U. The predicted oil yields for each temperature can be found in the Appendix B **Table B.3-7**.

The predicted oil yields were then input to a stochastic process model that utilizes the Monte Carlo (MC) technique for evaluating thermodynamic outcomes[58] of a plastic recovery and conversion process as a function of pyrolysis temperature and feed rate. In addition to the pyrolizer itself, the process includes pumps, shredders, blowers, filters, and other peripheral equipment. Modifications to the model previously published by Belden, et. al. can be found in the SI. In brief, the system consists of collection, shredding, pyrolysis, and oil recovery steps. The energy requirements for all auxiliary steps was taken from manufacturer specifications and assumed not to allow turn down to less than full power consumption. The energy requirement of the pyrolysis step was taken from thermochemical analysis of the enthalpy of reaction.

A major unknown in the analysis is the amount of plastic exiting the river that can be harvested. Accordingly, simulations were performed over a range of plastic feed rates with the goal of identifying under what conditions the process can be expected to be self-sufficient. All equipment in the process were off-the-shelf parts, and their energy consumption was based on vendor specifications and did not scale with plastic feed rate. The exergy required for the pyrolysis reactor was based on the heat of reaction and the exergy of the oil product was the process output; both of these values scaled linearly with the mass flow rate of plastic entering the process. To handle parameter uncertainty, the pyrolysis oil yield was handled as a stochastic variable in the Monte Carlo simulation; its value was varied to reflect the observed model MAE (± 9.1%). The remaining stochastic variables can be found in the Appendix B **Table B.3-7**.

Figure 3-6 shows the results of this analysis as a function of flow rate over a range of realistic temperatures as the probability of producing more exergy (based on fuel heating value) than is consumed ("net exergy production"). For feed rates of 1.0 and 2.0 kg/hr, the process is unlikely to produce more exergy than it consumes (<20%), since the energy required by the peripheral equipment is predicted to be greater than that in the fuel product. Between a feed rate of 2.0 kg/hr and 2.5 kg/hr and for temperatures less than 550 °C, the probability of net exergy production increases by a factor of 4; this sharp increase corresponds to the point at which the exergy embodied in the pyrolysis oil exceeds that required by the auxiliary equipment (~5 kW of fixed consumption). Increasing from 2.5 kg/hr to 3.0 kg/hr results in >80% probability of net exergy production for pyrolysis temperatures less than 550 °C.

In general, the model predicts that thermodynamic efficiency decreases with increasing pyrolysis temperature, a consequence of the high reactivity of the Rhine River plastic mixture. The exception to this trend is that the probability of net exergy production predicted at 500 °C is greater

than that predicted at 450 °C. Here, the model predicts that the oil yield at 450 °C is slightly less than at 500 °C (53% compared to 55.2%), accounting for the counter-intuitive finding. In fact, this difference in oil yield is within model uncertainty, meaning that the model indicates operating in the range between 400 and 500 °C for optimal thermodynamic efficiency. This range can be then used to minimize time spent in the evaluation of process performance with actual plastic mixtures.

Figure 3-6 can be interpreted to predict that pyrolytic conversion of Rhine River plastic is very likely to be energy self-sufficient, assuming that 100% of the plastic carried by the river can be captured. An estimated 20 to 30 tons of plastic is discharged from the Rhine annually[155], which corresponds to plastic flowrates of ~ 2 to 3 kg/hr, right in line with the predictions seen here for thermodynamically self-contained capture and pyrolytic conversion. Lower ends of this plastic exit rate may argue for the accumulation of plastic and the semi-continuous operation of the conversion system to permit modest process scale-up to achieve energy self sufficiency – or for re-design to improve efficiency. The analysis shown in Figure 6 assumes fixed power requirements for peripheral equipment, whereas the energy required for pyrolysis and embodied in the fuel scale with plastic feed rate. If the energy consumed by peripheral equipment can somehow be scaled to the feed rate – i.e., less energy might be consumed by the shredder for a dilute mixture than a concentrated one – then more favorable outcomes can be achieved for lower flow rates than are shown here. The analysis presented here for the Rhine River also suggests that other rivers with higher plastic discharge rates, including the Yangtze, Ganges and Xi [21], may yield self-sustaining plastic removal and pyrolysis systems, especially when complete capture of plastics is not possible, even accounting for the possibility that the oil yields for those rivers may be less favorable than predicted for the Rhine.

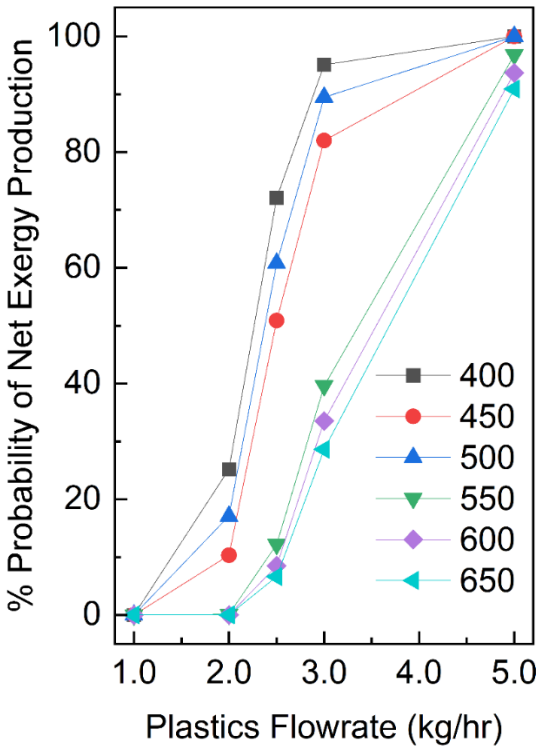

Figure 3-6 Percent probability of net exergy production for the Rhine River from 1 to 5 kg/hr flowrates and over a pyrolysis temperature range of 400 ˚C to 650 ˚C.

The examples of MRF and Rhine River plastic pyrolysis demonstrate how the current model can be used. The emphasis has been placed on predicting pyrolysis oil yields, with the end application of replacing petroleum-derived fuels. Because the origin of synthetic plastics is petroleum, combustion of plastic-derived fuels releases the same amount of CO_2 into the atmosphere as does combustion of petroleum-derived fuels. Using estimates of the global use of plastics[156] minus PVC and PET and the current model, approximately 130 million metric tons of plastic-derived fuel can be produced annually. Using typical emissions factors[157], combustion of this plastic-derived fuel would be equivalent to 230 million tons/year of CO_2, approximately 1% of annual emissions[158]. That stated, on a per mass basis, the environmental impact of plastic

entering the environment is almost certainly greater than that of CO_2, despite the threat of climate change.

Nonetheless, the CO_2 emissions analysis indicates that using pyrolysis to produce fuels incurs unacceptable climate penalties. Therefore, pyrolysis to fuel should be used as part of a comprehensive strategy, which includes pyrolysis for chemical production, increased recycling, and increased use of biodegradable plastics, to prevent plastic entering landfills or the environment. Similarly, the climate impact of using plastic-derived fuels can be minimized if they are reserved for use in applications that are difficult to decarbonize using available technologies, such as shipping or air transport[159]. Alternatively, to avoid new CO_2 emissions entirely, pyrolysis can be used to produce products other than fuels, such as lubricants, monomers, or other chemicals. The current model method can easily be adapted for these alternative products, provided that data are available.

The results presented here indicate that the accuracy of the current model is sufficient for many practical applications. More generally, the accuracy of the model with the available data set indicates substantial scope for improvement, as more data become available. Some of the uncertainty of the current model likely arises from incomplete reporting of independent variables – necessitating the use of KNN to fill data gaps – and a lack of a uniform way to report oil yields. A consistently used volatility-defined measure of oil yield, based on simulated distillation or thermogravimetric analysis of the product, would improve data quality and model predictability. More uniform and quantitative reporting of individual product yields would allow the model to be adapted for predictions of chemicals production.

3.4 Conclusions

Seven machine-learned models were optimized and evaluated for predicting oil yields obtained from pyrolysis of the big six plastics using feed composition, reaction conditions, reactor

type, and the presence or absence of catalyst as independent variables. Of these seven models, the accuracy profile of non-linear models was found to be superior to the one associated with conventional linear models included in the study, with XGBoost providing the most accurate predictions based on the Mean Absolute Error (MAE) criterion. Because of the content of the specific data set used to train the proposed machine-learned models, they are expected to be accurate in the temperature range from 400 to 700 °C, inclusive.

As a demonstration, the eXtreme Gradient Boosting model was used to predict the oil yields expected from pyrolysis of U.S. and E.U. plastic recycling waste, with the finding that E.U. waste appears to be a superior feed candidate for pyrolysis. The same regression model was used as part of a probabilistic Monte Carlo-based thermodynamic analysis that was performed on a process to remove plastic from the Rhine River, shred it, feed it to a pyrolyzer, and convert it into fuel. Thermodynamic analysis indicated that the process could be a net exergy producer under realistic conditions, provided that the scale of the pyrolyzer was sufficient to produce enough oil to offset fixed energy requirements associated with the peripheral equipment.

The model used here is therefore deemed sufficient for many practical applications involving waste plastic pyrolysis, and in particular can be used in conjunction with thermodynamic analysis to evaluate feasibility. As more data are reported, the model can gradually be refined and its predictive and performance evaluative capacity considerably enhanced. In addition to pyrolysis, the general methodological, modeling and simulation framework proposed in the present study could be readily applied to different technology options as well as inform strategies and policy responses for plastic waste reduction and management.

3.5 Appendix B

3.5.1.1 *Data*

Table B.3-2 Data set of 325 data points used in modeling

HDPE (wt%)	LDPE (wt%)	PP (wt%)	PS (wt%)	PVC (wt%)	PET (wt%)	Temperature (°C)	Heating Rate (°C/min)	Particle Size (mm)	Feed Size (g)	Catalyst	Reactor Type	Oil Yield (wt%)	Source
0	100	0	0	0	0	500	10	2.5	-	No	Fixed Bed	95	160
0	100	0	0	0	0	400	10	2.5	-	Yes	Fixed Bed	84	160
0	100	0	0	0	0	450	10	2.5	-	Yes	Fixed Bed	81	160
0	100	0	0	0	0	500	10	2.5	-	Yes	Fixed Bed	80	160
0	100	0	0	0	0	550	10	2.5	-	Yes	Fixed Bed	76	160
0	100	0	0	0	0	600	10	2.5	-	Yes	Fixed Bed	71	160
0	100	0	0	0	0	400	10	2.5	-	Yes	Fixed Bed	83	160
0	100	0	0	0	0	450	10	2.5	-	Yes	Fixed Bed	80	160
0	100	0	0	0	0	500	10	2.5	-	Yes	Fixed Bed	77	160
0	100	0	0	0	0	550	10	2.5	-	Yes	Fixed Bed	72	160
0	100	0	0	0	0	600	10	2.5	-	Yes	Fixed Bed	70	160
0	100	0	0	0	0	500	-	-	-	No	Fluidized Bed	81.2	161
0	100	0	0	0	0	550	-	-	-	No	Fluidized Bed	73.9	161
0	100	0	0	0	0	550	-	-	-	No	Fluidized Bed	72.7	161
0	100	0	0	0	0	550	-	-	-	No	Fluidized Bed	65.3	161
0	100	0	0	0	0	550	-	-	-	No	Fluidized Bed	64.7	161
0	100	0	0	0	0	600	-	-	-	No	Fluidized Bed	28.5	161

HDPE (wt%)	LDPE (wt%)	PP (wt%)	PS (wt%)	PVC (wt%)	PET (wt%)	Temperature (°C)	Heating Rate (°C/min)	Particle Size (mm)	Feed Size (g)	Catalyst	Reactor Type	Oil Yield (wt%)	Source
100	0	0	0	0	0	500	5	3	100	No	Fixed Bed	62	162
100	0	0	0	0	0	550	5	3	100	No	Fixed Bed	71	162
100	0	0	0	0	0	600	5	3	100	No	Fixed Bed	69	162
100	0	0	0	0	0	650	5	3	100	No	Fixed Bed	68	162
100	0	0	0	0	0	700	5	3	100	No	Fixed Bed	69	162
100	0	0	0	0	0	750	5	3	100	No	Fixed Bed	63	162
100	0	0	0	0	0	800	5	3	100	No	Fixed Bed	64	162
0	100	0	0	0	0	400	5	0.5	0.6	No	Batch	93.1	39
100	0	0	0	0	0	400	5	0.5	0.6	No	Batch	84.7	39
0	100	0	0	0	0	550	5	0.5	0.6	Yes	Batch	18.3	39
100	0	0	0	0	0	550	5	0.5	0.6	Yes	Batch	17.3	39
0	100	0	0	0	0	550	5	0.5	0.6	Yes	Batch	61.6	39
100	0	0	0	0	0	550	5	0.5	0.6	Yes	Batch	41	39
0	68	16	16	0	0	430	-	3	-	No	Batch	93	163
0	16	68	16	0	0	430	-	3	-	No	Batch	90	163
0	16	16	68	0	0	430	-	3	-	No	Batch	92	163
0	100	0	0	0	0	430	-	3	-	No	Batch	90	163
0	0	100	0	0	0	430	-	3	-	No	Batch	92	163
0	0	0	100	0	0	430	-	3	-	No	Batch	95	163
0	33	33	33	0	0	430	-	3	-	No	Batch	91	163
100	0	0	0	0	0	450	6.5	-	-	No	Batch	84	164
100	0	0	0	0	0	400	20	-	20	No	Batch	11.2	165

HDPE (wt%)	LDPE (wt%)	PP (wt%)	PS (wt%)	PVC (wt%)	PET (wt%)	Temperature (°C)	Heating Rate (°C/min)	Particle Size (mm)	Feed Size (g)	Catalyst	Reactor Type	Oil Yield (wt%)	Source
100	0	0	0	0	0	450	20	-	20	No	Batch	23.96	165
100	0	0	0	0	0	500	20	-	20	No	Batch	72.25	165
100	0	0	0	0	0	550	20	-	20	No	Batch	79.08	165
0	0	0	100	0	0	450	5	1.5	10	No	Batch	95.77	150
0	0	0	100	0	0	450	10	1.5	10	No	Batch	95.79	150
0	0	0	100	0	0	450	15	1.5	10	No	Batch	92.75	150
0	0	0	100	0	0	450	20	1.5	10	No	Batch	92.65	150
0	100	0	0	0	0	450	5	1.5	10	No	Batch	81.65	150
0	100	0	0	0	0	450	10	1.5	10	No	Batch	81.33	150
0	100	0	0	0	0	450	15	1.5	10	No	Batch	72.63	150
0	100	0	0	0	0	450	20	1.5	10	No	Batch	61.24	150
0	0	0	0	0	100	450	5	1.5	10	No	Batch	39.02	150
0	0	0	0	0	100	450	10	1.5	10	No	Batch	35.4	150
0	0	0	0	0	100	450	15	1.5	10	No	Batch	29.71	150
0	0	0	0	0	100	450	20	1.5	10	No	Batch	29.16	150
0	0	100	0	0	0	450	5	1.5	10	No	Batch	83.34	150
0	0	100	0	0	0	450	10	1.5	10	No	Batch	82.67	150
0	0	100	0	0	0	450	15	1.5	10	No	Batch	82.92	150
0	0	100	0	0	0	450	20	1.5	10	No	Batch	68.06	150
26.2	31.1	8.2	13	0	0	500	20	2.5	400	No	Fixed Bed	29	166
17.8	19.6	13.9	8.7	0	0	500	20	2.5	400	No	Fixed Bed	26.33	166
3.5	25	22.2	4	0	0	500	20	2.5	400	No	Fixed Bed	44.62	166

HDPE (wt%)	LDPE (wt%)	PP (wt%)	PS (wt%)	PVC (wt%)	PET (wt%)	Temperature (°C)	Heating Rate (°C/min)	Particle Size (mm)	Feed Size (g)	Catalyst	Reactor Type	Oil Yield (wt%)	Source
17	34	15.4	12.4	0	0	500	20	2.5	400	No	Fixed Bed	43.2	166
100	0	0	0	0	0	500	-	3	50	No	Batch	81	167
100	0	0	0	0	0	600	-	3	50	No	Batch	79.1	167
100	0	0	0	0	0	700	25	-	-	No	Fixed Bed	79.72	143
0	100	0	0	0	0	700	25	-	-	No	Fixed Bed	84.25	143
0	0	100	0	0	0	700	25	-	-	No	Fixed Bed	84.44	143
0	0	0	100	0	0	700	25	-	-	No	Fixed Bed	83.77	143
0	0	0	0	100	0	700	25	-	-	No	Fixed Bed	31.69	143
0	0	0	0	0	100	700	25	-	-	No	Fixed Bed	41.3	143
31.25	31.25	7.29	13.5	11.46	5.21	700	25	-	-	No	Fixed Bed	75.12	143
43	43	9.7	0	0	0	500	35	3.5	40	No	Horizontal Tube	63.91	168
43	43	9.7	0	0	0	550	50	3.5	40	No	Horizontal Tube	56.08	168
43	43	9.7	0	0	0	550	50	3.5	40	No	Horizontal Tube	59.21	168
43	43	9.7	0	0	0	550	20	3.5	40	No	Horizontal Tube	59.7	168
43	43	9.7	0	0	0	450	50	3.5	40	No	Horizontal Tube	48.38	168
43	43	9.7	0	0	0	550	20	3.5	40	No	Horizontal Tube	60.48	168
43	43	9.7	0	0	0	450	50	3.5	40	No	Horizontal Tube	13.61	168
43	43	9.7	0	0	0	450	20	3.5	40	No	Horizontal Tube	46.79	168
43	43	9.7	0	0	0	450	20	3.5	40	No	Horizontal Tube	15.4	168
43	43	9.7	0	0	0	550	35	3.5	40	No	Horizontal Tube	58.97	168
43	43	9.7	0	0	0	450	35	3.5	40	No	Horizontal Tube	34.94	168
43	43	9.7	0	0	0	500	50	3.5	40	No	Horizontal Tube	63.41	168

HDPE (wt%)	LDPE (wt%)	PP (wt%)	PS (wt%)	PVC (wt%)	PET (wt%)	Temperature (°C)	Heating Rate (°C/min)	Particle Size (mm)	Feed Size (g)	Catalyst	Reactor Type	Oil Yield (wt%)	Source
43	43	9.7	0	0	0	500	20	3.5	40	No	Horizontal Tube	66.51	168
43	43	9.7	0	0	0	500	35	3.5	40	No	Horizontal Tube	64.56	168
43	43	9.7	0	0	0	500	35	3.5	40	No	Horizontal Tube	64.22	168
29.3	29.3	26.9	8.8	0	5.6	500	10	-	-	No	Batch	75.8	37
29.3	29.3	26.9	8.8	0	5.6	500	20	-	-	No	Batch	82	37
0	0	100	0	0	0	250	-	-	2	No	Batch	57.27	169
0	0	100	0	0	0	300	-	-	2	No	Batch	69.82	169
0	0	100	0	0	0	350	-	-	2	No	Batch	67.74	169
0	0	100	0	0	0	400	-	-	2	No	Batch	63.23	169
100	0	0	0	0	0	300	-	-	2	No	Batch	30.7	169
100	0	0	0	0	0	350	-	-	2	No	Batch	80.88	169
100	0	0	0	0	0	400	-	-	2	No	Batch	54.17	169
0	0	100	0	0	0	460	-	-	10	No	Batch	86	170
0	34	66	0	0	0	460	-	-	10	No	Batch	84	170
0	66	34	0	0	0	460	-	-	10	No	Batch	63	170
0	100	0	0	0	0	460	-	-	10	No	Batch	95	170
0	66	34	0	0	0	460	10	-	10	Yes	Batch	67	170
0	34	66	0	0	0	460	10	-	10	Yes	Batch	62	170
0	0	100	0	0	0	460	10	-	10	Yes	Batch	57	170
0	100	0	0	0	0	460	10	-	10	Yes	Batch	50	170
0	100	0	0	0	0	500	6	2	-	No	Batch	80.41	171
0	100	0	0	0	0	500	8	2	-	No	Batch	79.64	171

HDPE (wt%)	LDPE (wt%)	PP (wt%)	PS (wt%)	PVC (wt%)	PET (wt%)	Temperature (°C)	Heating Rate (°C/min)	Particle Size (mm)	Feed Size (g)	Catalyst	Reactor Type	Oil Yield (wt%)	Source
0	100	0	0	0	0	500	10	2	-	No	Batch	76.45	171
0	100	0	0	0	0	500	12	2	-	No	Batch	74.32	171
0	100	0	0	0	0	500	14	2	-	No	Batch	71.11	171
0	0	0	0	0	100	500	6	2	-	No	Batch	38.89	171
0	0	0	0	0	100	500	8	2	-	No	Batch	34.16	171
0	0	0	0	0	100	500	10	2	-	No	Batch	32.13	171
0	0	0	0	0	100	500	12	2	-	No	Batch	30.33	171
0	0	0	0	0	100	500	14	2	-	No	Batch	29.14	171
0	0	100	0	0	0	500	6	2	-	No	Batch	82.12	171
0	0	100	0	0	0	500	8	2	-	No	Batch	81.32	171
0	0	100	0	0	0	500	10	2	-	No	Batch	80.65	171
0	0	100	0	0	0	500	12	2	-	No	Batch	79.41	171
0	0	100	0	0	0	500	14	2	-	No	Batch	78.26	171
100	0	0	0	0	0	430	3	-	10	No	Batch	84.7	172
0	100	0	0	0	0	430	3	-	10	No	Batch	84.3	172
0	100	0	0	0	0	430	3	-	10	No	Batch	84.6	172
50	50	0	0	0	0	430	3	-	10	No	Batch	83.7	172
0	0	0	100	0	0	450	10	-	1000	No	Batch	80.8	173
50	50	0	0	0	0	450	10	-	1000	No	Batch	25	173
0	0	100	0	0	0	450	10	-	1000	No	Batch	42	173
0	0	50	50	0	0	450	10	-	1000	No	Batch	25	173
25	25	0	50	0	0	450	10	-	1000	No	Batch	54	173

HDPE (wt%)	LDPE (wt%)	PP (wt%)	PS (wt%)	PVC (wt%)	PET (wt%)	Temperature (°C)	Heating Rate (°C/min)	Particle Size (mm)	Feed Size (g)	Catalyst	Reactor Type	Oil Yield (wt%)	Source
25	25	50	0	0	0	450	10	-	1000	No	Batch	24	173
12.5	12.5	25	50	0	0	450	10	-	1000	No	Batch	49	173
10	10	20	40	0	20	450	10	-	1000	No	Batch	40	173
0	100	0	0	0	0	450	7.5	-	17	No	Batch	79.8	174
100	0	0	0	0	0	450	7.5	-	17	No	Batch	79.8	174
0	100	0	0	0	0	450	7.5	-	17	No	Batch	79.1	174
0	0	100	0	0	0	450	7.5	-	17	No	Batch	85	174
0	50	50	0	0	0	450	7.5	-	17	No	Batch	79.4	174
33.3	33.3	33.3	0	0	0	450	7.5	-	17	No	Batch	82.4	174
25	50	25	0	0	0	450	7.5	-	17	No	Batch	79.7	174
34.6	34.6	9.6	9.6	10.6	1.1	450	7.5	-	17	No	Batch	75.4	174
25	50	25	0	0	0	450	-	-	17	No	Batch	79.7	175
0	100	0	0	0	0	450	-	-	17	No	Batch	79.1	175
44.4	0	21.2	13.3	12.2	8.9	500	5	7.5	35	No	Batch	48.7	176
100	0	0	0	0	0	500	5	3.5	35	No	Batch	93	176
0	0	100	0	0	0	500	5	3.5	35	No	Batch	95	176
0	0	0	100	0	0	500	5	3.5	35	No	Batch	71	176
0	0	0	0	0	100	500	5	3.5	35	No	Batch	15	176
0	100	0	0	0	0	500	5	3	-	No	Fluidized Bed	89.2	177
0	100	0	0	0	0	550	5	3	-	No	Fluidized Bed	78.6	177
0	100	0	0	0	0	600	5	3	-	No	Fluidized Bed	75.8	177
0	100	0	0	0	0	650	5	3	-	No	Fluidized Bed	59.9	177

HDPE (wt%)	LDPE (wt%)	PP (wt%)	PS (wt%)	PVC (wt%)	PET (wt%)	Temperature (°C)	Heating Rate (°C/min)	Particle Size (mm)	Feed Size (g)	Catalyst	Reactor Type	Oil Yield (wt%)	Source
0	100	0	0	0	0	700	5	3	-	No	Fluidized Bed	28.6	177
100	0	0	0	0	0	640	10	-	-	No	Fluidized Bed	68.5	178
100	0	0	0	0	0	680	10	-	-	No	Fluidized Bed	39.6	178
100	0	0	0	0	0	730	10	-	-	No	Fluidized Bed	18	178
100	0	0	0	0	0	780	10	-	-	No	Fluidized Bed	9.6	178
100	0	0	0	0	0	850	10	-	-	No	Fluidized Bed	16.2	178
50	50	0	0	0	0	500	10	5	2	No	Fixed Bed	83	179
0	0	100	0	0	0	500	10	5	2	No	Fixed Bed	81	179
0	0	0	100	0	0	500	10	5	2	No	Fixed Bed	97	179
0	0	0	0	0	100	500	10	5	2	No	Fixed Bed	38.5	179
30	30	13	18	0	0	500	10	5	2	No	Fixed Bed	80	179
30	30	13	18	0	0	500	10	5	2	No	Fixed Bed	88	179
100	0	0	0	0	0	500	10	-	2	Yes	Fixed Bed	57	179
0	0	100	0	0	0	500	10	-	2	Yes	Fixed Bed	51	179
0	0	0	100	0	0	500	10	-	2	Yes	Fixed Bed	93	179
0	0	0	0	0	100	500	10	-	2	Yes	Fixed Bed	43	179
30	30	13	18	0	0	500	10	-	2	Yes	Fixed Bed	51	179
30	30	13	18	0	0	500	10	-	2	Yes	Fixed Bed	57	179
29.4	29.4	26.9	8.7	0	5.6	450	20	20	200	No	Batch	78	180
29.4	29.4	26.9	8.7	0	5.6	500	20	20	200	No	Batch	80.5	180
29.4	29.4	26.9	8.7	0	5.6	550	20	20	200	No	Batch	82	180
29.4	29.4	26.9	8.7	0	5.6	600	20	20	200	No	Batch	84	180

HDPE (wt%)	LDPE (wt%)	PP (wt%)	PS (wt%)	PVC (wt%)	PET (wt%)	Temperature (°C)	Heating Rate (°C/min)	Particle Size (mm)	Feed Size (g)	Catalyst	Reactor Type	Oil Yield (wt%)	Source
100	0	0	0	0	0	645	-	0.225	-	No	Fluidized Bed	79.7	181
100	0	0	0	0	0	640	-	0.225	-	No	Fluidized Bed	78.9	181
100	0	0	0	0	0	650	-	0.225	-	No	Fluidized Bed	68.5	181
100	0	0	0	0	0	650	-	0.225	-	No	Fluidized Bed	72.3	181
100	0	0	0	0	0	685	-	0.225	-	No	Fluidized Bed	33.4	181
100	0	0	0	0	0	685	-	0.225	-	No	Fluidized Bed	39.6	181
100	0	0	0	0	0	700	-	0.225	-	No	Fluidized Bed	32.1	181
100	0	0	0	0	0	685	-	0.225	-	No	Fluidized Bed	40.7	181
100	0	0	0	0	0	730	-	0.225	-	No	Fluidized Bed	19.6	181
100	0	0	0	0	0	725	-	0.225	-	No	Fluidized Bed	20.7	181
100	0	0	0	0	0	715	-	0.225	-	No	Fluidized Bed	19.2	181
100	0	0	0	0	0	730	-	0.225	-	No	Fluidized Bed	13.5	181
100	0	0	0	0	0	780	-	0.225	-	No	Fluidized Bed	15.3	181
100	0	0	0	0	0	780	-	0.225	-	No	Fluidized Bed	9.6	181
100	0	0	0	0	0	780	-	0.225	-	No	Fluidized Bed	13.4	181
100	0	0	0	0	0	800	-	0.225	-	No	Fluidized Bed	13.7	181
100	0	0	0	0	0	850	-	0.225	-	No	Fluidized Bed	11.4	181
100	0	0	0	0	0	850	-	0.225	-	No	Fluidized Bed	16.2	181
100	0	0	0	0	0	850	-	0.225	-	No	Fluidized Bed	15.4	181
100	0	0	0	0	0	850	-	0.225	-	No	Fluidized Bed	12.2	181
0	0	0	100	0	0	450	5	3.5	10	No	Fluidized Bed	97.6	182
0	0	0	100	0	0	500	5	3.5	10	No	Fluidized Bed	96.4	182

HDPE (wt%)	LDPE (wt%)	PP (wt%)	PS (wt%)	PVC (wt%)	PET (wt%)	Temperature (°C)	Heating Rate (°C/min)	Particle Size (mm)	Feed Size (g)	Catalyst	Reactor Type	Oil Yield (wt%)	Source
0	0	0	100	0	0	550	5	3.5	10	No	Fluidized Bed	95.3	182
0	0	0	100	0	0	600	5	3.5	10	No	Fluidized Bed	98.7	182
0	0	0	100	0	0	650	5	3.5	10	No	Fluidized Bed	90.7	182
0	0	0	100	0	0	700	5	3.5	10	No	Fluidized Bed	90.2	182
0	100	0	0	0	0	425	10	2	10	No	Batch	89.5	183
0	100	0	0	0	0	450	10	2	10	No	Batch	72.4	183
0	100	0	0	0	0	500	10	2	10	No	Batch	37.5	183
0	0	0	100	0	0	350	10	2	10	No	Batch	99	183
0	0	0	100	0	0	450	10	2	10	No	Batch	79.4	183
0	0	0	100	0	0	500	10	2	10	No	Batch	67.1	183
0	70	0	30	0	0	400	10	2	10	No	Batch	96	183
0	70	0	30	0	0	425	10	2	10	No	Batch	90.2	183
0	70	0	30	0	0	450	10	2	10	No	Batch	83.7	183
0	0	100	0	0	0	380	3	-	10	No	Batch	64.9	147
0	0	100	0	0	0	380	3	-	10	No	Batch	80.1	147
0	0	100	0	0	0	380	3	-	10	Yes	Batch	54.5	147
0	0	100	0	0	0	380	3	-	10	Yes	Batch	68.8	147
0	0	100	0	0	0	380	3	-	10	Yes	Batch	78.3	147
0	0	100	0	0	0	380	3	-	10	Yes	Batch	47	147
0	0	100	0	0	0	380	3	-	10	Yes	Batch	75.4	147
0	0	100	0	0	0	380	3	-	10	Yes	Batch	80.6	147
0	0	100	0	0	0	380	3	-	10	Yes	Batch	86.4	147

HDPE (wt%)	LDPE (wt%)	PP (wt%)	PS (wt%)	PVC (wt%)	PET (wt%)	Temperature (°C)	Heating Rate (°C/min)	Particle Size (mm)	Feed Size (g)	Catalyst	Reactor Type	Oil Yield (wt%)	Source
0	0	100	0	0	0	380	3	-	10	Yes	Batch	85.4	147
0	0	100	0	0	0	380	3	-	10	Yes	Batch	83.3	147
0	0	100	0	0	0	380	3	-	10	Yes	Batch	83.7	147
0	0	100	0	0	0	380	3	-	10	Yes	Batch	83	147
100	0	0	0	0	0	430	3	-	10	No	Batch	69.3	147
100	0	0	0	0	0	430	3	-	10	Yes	Batch	67.8	147
100	0	0	0	0	0	430	3	-	10	Yes	Batch	74.3	147
100	0	0	0	0	0	430	3	-	10	Yes	Batch	49.8	147
100	0	0	0	0	0	430	3	-	10	Yes	Batch	71.1	147
100	0	0	0	0	0	430	3	-	10	Yes	Batch	81.4	147
100	0	0	0	0	0	430	3	-	10	Yes	Batch	80.1	147
100	0	0	0	0	0	430	3	-	10	Yes	Batch	81.9	147
100	0	0	0	0	0	430	3	-	10	Yes	Batch	75.2	147
0	0	100	0	0	0	250	-	50	1000	No	Batch	51.76	184
0	0	100	0	0	0	300	-	50	1000	No	Batch	68.98	184
0	0	100	0	0	0	350	-	50	1000	No	Batch	79.68	184
0	0	100	0	0	0	400	-	50	1000	No	Batch	80.14	184
0	0	100	0	0	0	250	-	50	1000	No	Batch	52.31	184
0	0	100	0	0	0	300	-	50	1000	No	Batch	69.32	184
0	0	100	0	0	0	350	-	50	1000	No	Batch	85.06	184
0	0	100	0	0	0	400	-	50	1000	No	Batch	88.86	184
25	35	40	0	0	0	400	12	1.4	-	No	Fixed Bed	18.89	185

HDPE (wt%)	LDPE (wt%)	PP (wt%)	PS (wt%)	PVC (wt%)	PET (wt%)	Temperature (°C)	Heating Rate (°C/min)	Particle Size (mm)	Feed Size (g)	Catalyst	Reactor Type	Oil Yield (wt%)	Source
25	35	40	0	0	0	500	12	1.4	-	No	Fixed Bed	30.66	185
25	35	40	0	0	0	450	12	1.4	-	No	Fixed Bed	26.68	185
25	35	40	0	0	0	475	12	1.4	-	No	Fixed Bed	28.26	185
25	35	40	0	0	0	500	12	1.4	-	No	Fixed Bed	32.8	185
25	35	40	0	0	0	525	12	1.4	-	No	Fixed Bed	28.8	185
25	35	40	0	0	0	500	12	1.4	-	No	Fixed Bed	28.8	185
25	35	40	0	0	0	500	12	1.4	-	No	Fixed Bed	30.37	185
40	0	35	18	4	3	460	20	3	100	No	Semi Batch	72	186
40	0	35	18	4	3	500	20	3	100	No	Semi Batch	65.2	186
40	0	35	18	4	3	600	20	3	100	No	Semi Batch	42.9	186
0	100	0	0	0	0	300	-	3.5	100	Yes	Fixed Bed	53.5	187
0	90	10	0	0	0	560	10	4	22.5	Yes	Batch	29	188
0	70	30	0	0	0	560	10	4	22.5	Yes	Batch	68	188
0	50	50	0	0	0	560	10	4	22.5	Yes	Batch	70	188
0	30	70	0	0	0	560	10	4	22.5	Yes	Batch	78	188
0	10	90	0	0	0	560	10	4	22.5	Yes	Batch	80	188
10	90	0	0	0	0	560	10	4	22.5	Yes	Batch	55	188
30	70	0	0	0	0	560	10	4	22.5	Yes	Batch	75	188
50	50	0	0	0	0	560	10	4	22.5	Yes	Batch	78	188
70	30	0	0	0	0	560	10	4	22.5	Yes	Batch	75	188
90	10	0	0	0	0	560	10	4	22.5	Yes	Batch	61	188
10	0	0	90	0	0	560	10	4	22.5	Yes	Batch	81	188

HDPE (wt%)	LDPE (wt%)	PP (wt%)	PS (wt%)	PVC (wt%)	PET (wt%)	Temperature (°C)	Heating Rate (°C/min)	Particle Size (mm)	Feed Size (g)	Catalyst	Reactor Type	Oil Yield (wt%)	Source
30	0	0	70	0	0	560	10	4	22.5	Yes	Batch	68	189
50	0	0	50	0	0	560	10	4	22.5	Yes	Batch	70	189
70	0	0	30	0	0	560	10	4	22.5	Yes	Batch	80	189
90	0	0	10	0	0	560	10	4	22.5	Yes	Batch	81	189
0	0	100	0	0	0	500	20	2.5	20	No	Batch	83	189
0	0	100	0	0	0	500	20	2.5	20	Yes	Batch	84	189
0	0	100	0	0	0	500	20	2.5	20	Yes	Batch	85	189
0	0	100	0	0	0	500	20	2.5	20	Yes	Batch	83	189
0	0	100	0	0	0	500	20	2.5	20	Yes	Batch	77	189
0	100	0	0	0	0	500	20	2.5	20	No	Batch	76	189
0	100	0	0	0	0	500	20	2.5	20	Yes	Batch	78	189
0	100	0	0	0	0	500	20	2.5	20	Yes	Batch	82	189
0	100	0	0	0	0	500	20	2.5	20	Yes	Batch	75	189
0	100	0	0	0	0	500	20	2.5	20	Yes	Batch	68	189
100	0	0	0	0	0	500	20	2.5	20	No	Batch	78	189
100	0	0	0	0	0	500	20	2.5	20	Yes	Batch	79	189
100	0	0	0	0	0	500	20	2.5	20	Yes	Batch	80	189
100	0	0	0	0	0	500	20	2.5	20	Yes	Batch	79	189
100	0	0	0	0	0	500	20	2.5	20	Yes	Batch	73	189
33.3	33.3	33.3	0	0	0	500	20	2.5	20	No	Batch	77	189
33.3	33.3	33.3	0	0	0	500	20	2.5	20	Yes	Batch	79	189
33.3	33.3	33.3	0	0	0	500	20	2.5	20	Yes	Batch	80	189

HDPE (wt%)	LDPE (wt%)	PP (wt%)	PS (wt%)	PVC (wt%)	PET (wt%)	Temperature (°C)	Heating Rate (°C/min)	Particle Size (mm)	Feed Size (g)	Catalyst	Reactor Type	Oil Yield (wt%)	Source
33.3	33.3	33.3	0	0	0	500	20	2.5	20	Yes	Batch	78	189
33.3	33.3	33.3	0	0	0	500	20	2.5	20	Yes	Batch	76	189
0	0	100	0	0	0	400	-	25	1000	No	Batch	78	190
0	0	100	0	0	0	450	-	25	1000	No	Batch	79.6	190
0	0	100	0	0	0	500	-	25	1000	No	Batch	81	190
0	0	100	0	0	0	400	-	25	1000	Yes	Batch	78.4	190
0	0	100	0	0	0	450	-	25	1000	Yes	Batch	75.5	190
0	0	100	0	0	0	500	-	25	1000	Yes	Batch	53.2	190
0	0	90	0	0	10	400	-	25	1000	Yes	Batch	73	190
0	0	75	0	0	25	450	-	25	1000	Yes	Batch	54.7	190
0	0	65	0	0	35	500	-	25	1000	Yes	Batch	45	190
0	0	0	100	0	0	450	5	20	1000	Yes	Batch	70	191
0	0	0	100	0	0	450	10	20	1000	Yes	Batch	60	191
50	50	0	0	0	0	450	10	20	1000	Yes	Batch	40	191
50	50	0	0	0	0	450	10	20	1000	Yes	Batch	42	191
0	0	100	0	0	0	450	10	20	1000	Yes	Batch	40	191
0	0	100	0	0	0	450	10	20	1000	Yes	Batch	54	191
0	50	0	50	0	0	450	10	20	1000	Yes	Batch	44	191
0	50	0	50	0	0	450	10	20	1000	Yes	Batch	52	191
0	0	50	50	0	0	450	10	20	1000	Yes	Batch	54	191
0	0	50	50	0	0	450	10	20	1000	Yes	Batch	34	191
0	50	50	0	0	0	450	10	20	1000	Yes	Batch	44	191

HDPE (wt%)	LDPE (wt%)	PP (wt%)	PS (wt%)	PVC (wt%)	PET (wt%)	Temperature (°C)	Heating Rate (°C/min)	Particle Size (mm)	Feed Size (g)	Catalyst	Reactor Type	Oil Yield (wt%)	Source
0	50	50	0	0	0	450	10	20	1000	Yes	Batch	40	191
0	25	25	50	0	0	450	10	20	1000	Yes	Batch	44	191
0	25	25	50	0	0	450	10	20	1000	Yes	Batch	40	191
0	20	20	20	0	20	450	10	20	1000	Yes	Batch	28	191
0	20	20	20	0	20	450	10	20	1000	Yes	Batch	30	191
0	100	0	0	0	0	450	55	0.5	15	Yes	Semi Batch	34.5	192
0	100	0	0	0	0	500	55	0.5	15	Yes	Semi Batch	56.53	192
0	100	0	0	0	0	550	55	0.5	15	Yes	Semi Batch	53	192
0	100	0	0	0	0	600	55	0.5	15	Yes	Semi Batch	48.97	192
0	17	0	17	0	66	450	6	100	60	No	Semi Batch	10	151
0	17	0	66	0	17	450	6	100	60	No	Semi Batch	36	151
0	100	0	0	0	0	450	6	100	60	No	Semi Batch	30	151
0	100	0	0	0	0	450	6	100	60	No	Semi Batch	32	151
0	0	0	0	0	100	450	6	100	60	No	Semi Batch	4	151
0	50	0	0	0	50	450	6	100	60	No	Semi Batch	8	151
0	33	0	33	0	33	450	6	100	60	No	Semi Batch	33	151
0	50	0	50	0	0	450	6	100	60	No	Semi Batch	52	151
0	0	0	0	0	100	450	6	100	60	No	Semi Batch	2	151
0	0	0	100	0	0	450	6	100	60	No	Semi Batch	49	151
0	0	0	50	0	50	450	6	100	60	No	Semi Batch	27	151
0	67	0	17	0	17	450	6	100	60	No	Semi Batch	34	151
0	0	0	100	0	0	450	6	100	60	No	Semi Batch	40	151

3.5.1.2 *Initial Testing*

Preliminary tests eliminated all data that had a data gap in one or more features, resulting in a dataset consisting of 149 data points. Although the corresponding MAE of the stripped-down validation set was 8.0% for Random Forest and 8.5% for XGBoost (less than what was found for the final models recommended here), the standard deviations on the validation sets were 1.5% and ±1.8%, much greater than the recommended models which indicates a strong dependence on the data used for training. Further, the test set MAE values were 9.9% for RF and 11.5% for XGBoost, and the corresponding differences between validation and test set MAE were 1.9 and 3, much greater than observed for the final models recommended here. Taken together, these observations indicate that the stripped-down data set led to a much stronger reliance on selection of training data and a much greater propensity for over fitting than observed in the models recommended here.

Instead of data removal and to develop more robust models that were less prone to overfitting, the K nearest neighbor (KNN) method was used to populate gaps in the reported values of features.

Further testing that tried to conflate the different reactor types or reaction times yielded a Random Forest validation set MAE of 9.6% and a test set MAE of 8.8%. The fact that the test set MAE is lower than the validation set indicates in this case that the model has been over specified and the accuracy of the predictions cannot be trusted.

3.5.1.3 *Model Parameters*

Each of the seven models studied in this work were optimized such that their hyper parameters gave rise to the minimum MAE for that model. The optimal hyper parameters can be seen below for each of the seven models in **Table B.3-3**.

Table B.3-3 Optimal Model Hyper Parameters for Seven Models Studied

Model	*Hyper Parameters*			
Linear Regression	Random State			
	50			
Lasso Regression	Random State	Alpha	Max iterations	
	10	0.0001	5000	
Ridge Regression	Random State	Alpha	Max iterations	
	50	0.001	5000	
Decision Tree	Random State	Max Features	Max Depth	
	55	11	16	
XGBoost	Random State	Number of Estimators	Learning Rate	
	50	640	0.05	
Random Forest	Random State	Number of Estimators	Max Features	Max Depth
	100	108	5	16
Artificial Neural Network	Random State	Max Iterations	Hidden Layer Sizes	Batch Size
	25	3000	(640,)	190

3.5.1.4 *Additional Model Results and Figures*

Figure B.3-7 shows the parity plot for the reported experimental oil yield vs the oil yields predicted by the optimal XGBoost model, along with the 1:1 line and the ±10% region.

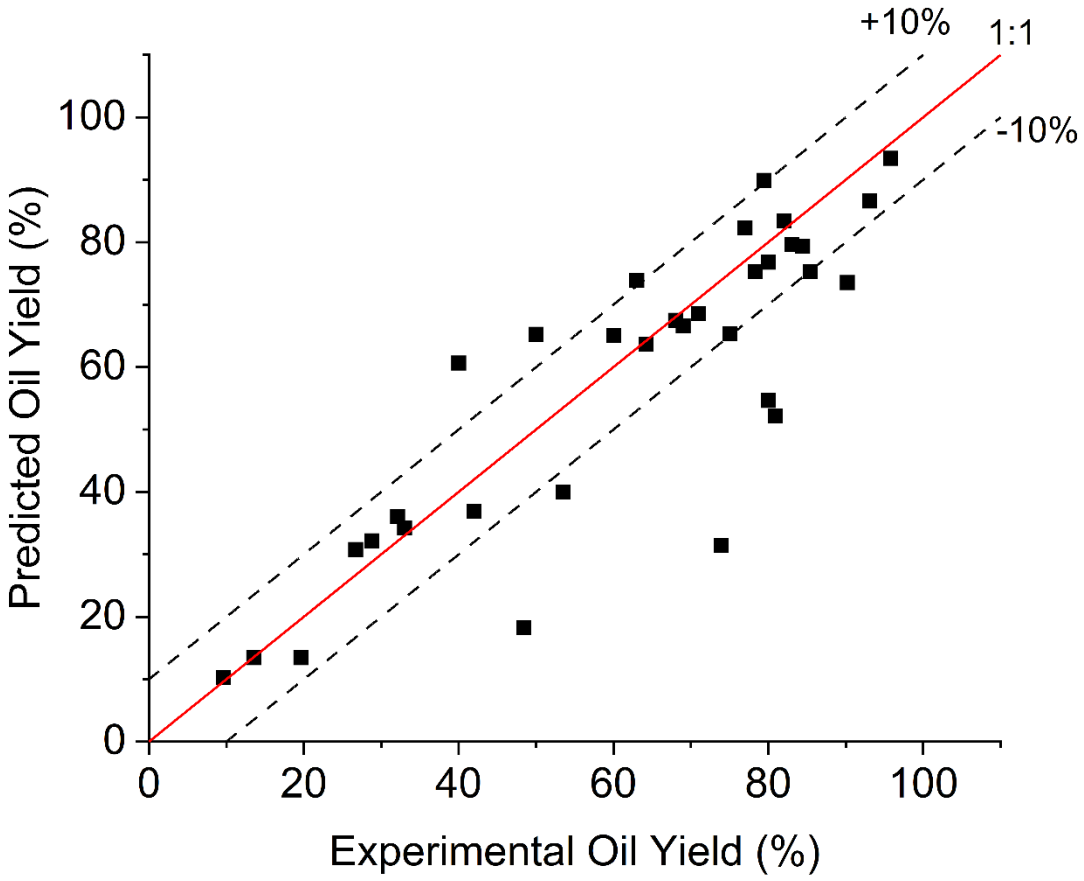

Figure B.3-7 Parity plot for the reported experimental oil yield vs the oil yield predicted by the optimal XGBoost model for the test set.

For the data points in the test set that lay outside of the ± 10% region **Table B.3-4** Analysis of conditions for outliers from **Figure B.3-7** evaluates the reaction conditions in order to determine if there was any systematic error. As can be seen from this table there is no trend that can be identified and no indication of any systematic error.

Table B.3-4 Analysis of conditions for outliers from **Figure B.3-7**

Difference in Prediction	*Plastic Type*	*Temperature*	*Reactor Type*	*Catalyst*	*# of KNN Predicted Features*
16.6	PS	700	Fluidized Bed	No	0
28.7	HDPE	350	Batch	No	2
25.4	LDPE	500	Fixed Bed	Yes	1
-10.5	PS	450	Batch	No	0
42.4	LDPE	550	Fluidized Bed	No	2
-10.9	2:1 LDPE:PP	460	Batch	No	2
13.5	LDPE	300	Fixed Bed	Yes	1
-15.3	LDPE	460	Batch	Yes	1
30.1	43:43:9.7 HDPE:LDPE:PP	450	Horizontal Tube	No	0
-20.6	PP	450	Batch	Yes	0

Figure B.3-8 shows the feature importance of each of the model features from the optimal XGBoost model. The plastic types each have their own feature importance but were grouped in **Figure B.3-8** due to their relatively small values and for simplicity.

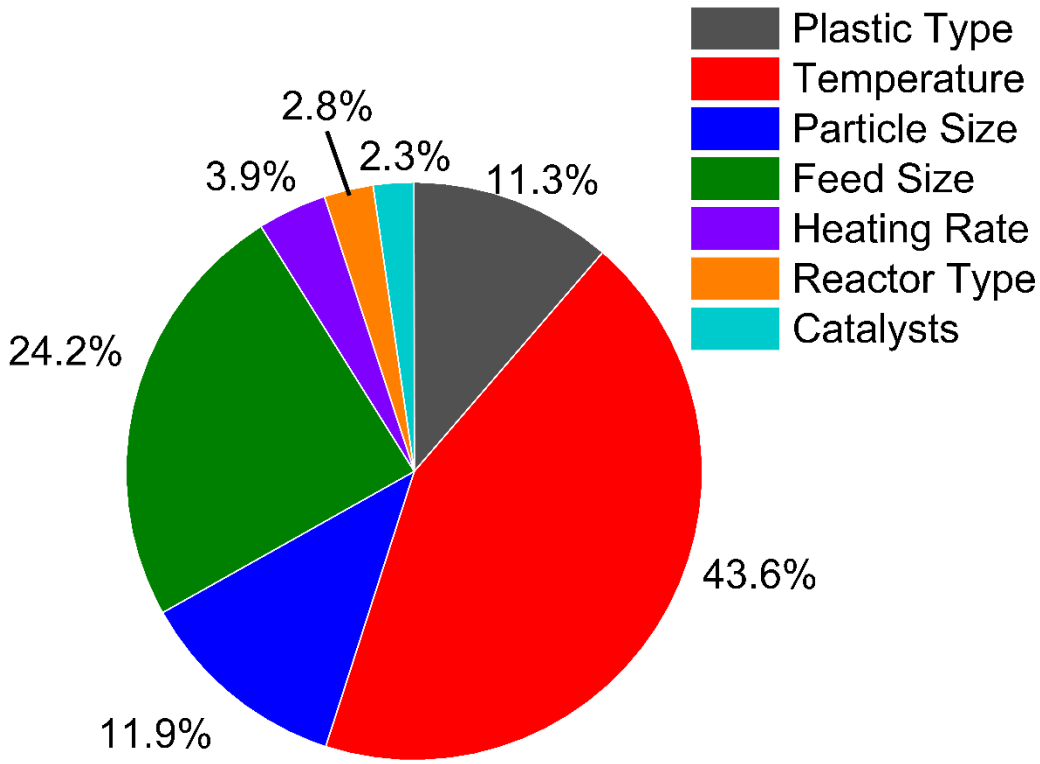

Figure B.3-8 Feature Importance for each feature included in the final optimal XGBoost Model. Plastic types are lumped into one category for simplicity

Figure B.3-9 shows the oil yields predicted for pyrolysis of pure plastics at 500 °C. The other features were chosen as representative values and are found in **Table B.3-6**.

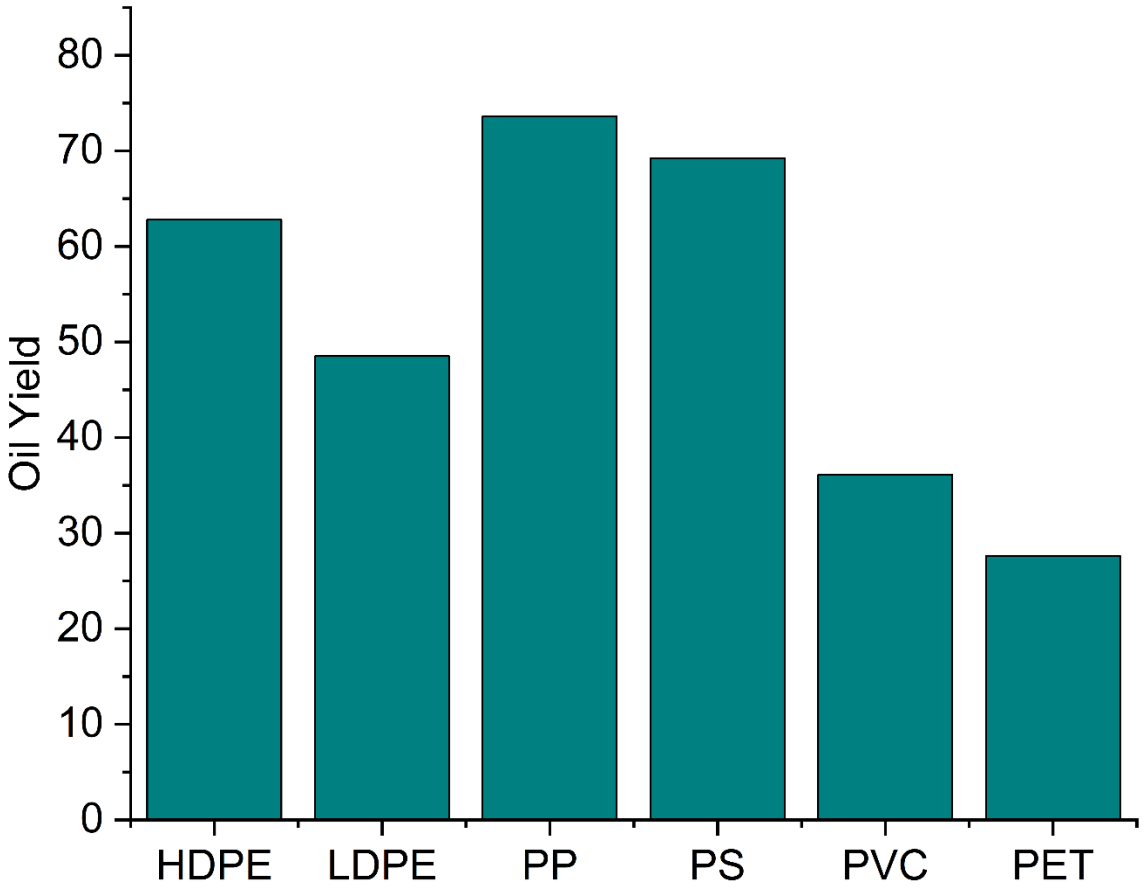

Figure B.3-9 Predict oil yield (mass percent) for the pyrolysis of pure plastics at 500 °C

Figure B.3-10 shows the effect of PET on a mixture of PP and LDPE.

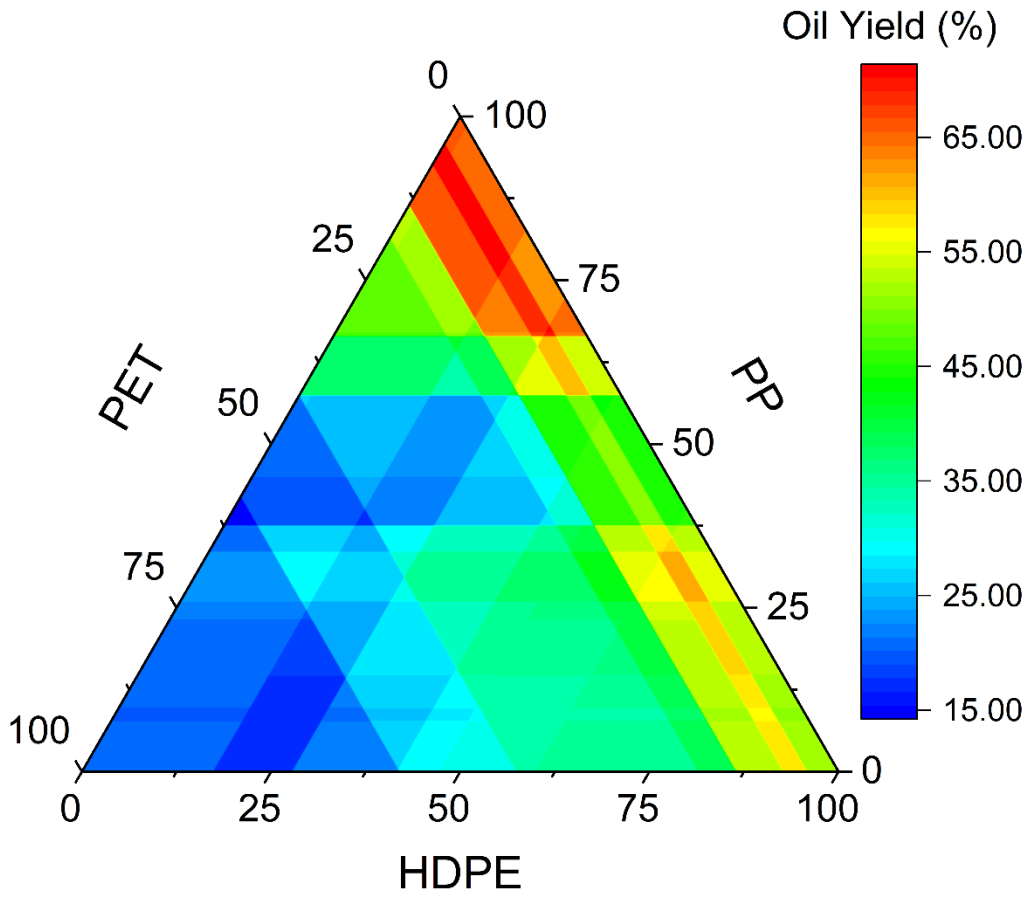

Figure B.3-10 Predicted oil yields for mixtures of LDPE, PP and PET pyrolyzed in a horizontal tube reactor at 500 ˚C, with a heating rate of 10 ˚C/min, a particle size of 13mm, plastics loading of 200g without catalyst.

Table B.3-5 and **Table B.3-6** provide the feed composition (**Table B.3-5**) and reaction parameters (**Table B.3-6**) used for the prediction of oil yields from the pyrolysis of real waste plastic found in the Rhine River in Europe.

Table B.3-5 Composition of Plastic Found in the Rhine River [137, 138]

Plastic Type	*Weight Percent in Mixture (%)*
HDPE	27
LDPE	0
PP	37
PS	26
PVC	2
PET	0

Table B.3-6 Estimated Reaction Parameters Used for Rhine River Oil Yields

Feature	*Value*
Particle Size	13 mm
Heating Rate	10 °C/min
Feed Size	200 g
Catalyst	None
Reactor Type	Horizontal Tube

3.5.1.5 *Thermodynamic Model Modifications*

The Monte Carlo (MC) model previously developed by the group [58] utilized oil yields and specific oil composition from data published in the literature. In this work the specific composition of the oil products is not known as new feeds are studied. In order to handle this, the exergy of combustion of the oil is calculated using an estimated HHV of the oil instead of the specific heats of combustion of the products. An average HHV of 41 MJ/kg was used and varied by ± 10% to capture how the feed composition could affect the HHV of the oil [193]. Other necessary modifications to the model included removing one of the water filter steps and removal of the RO as these were not necessary in fresh water. Finally, as the system would be stationary and not operating on a ship the exergy required for the boat engine was removed from the model. The full list of stochastic variables used in the MC simulation can be found in **Table B.3-7** and the constant variables used in the model can be found in **Table B.3-8**.

Table B.3-7 Uniform distribution of stochastic variables used in the MC model

Variable	*Minimum Value*	*Maximum Value*
Oil Yield (%) at 400 °C	47.6	65.8
Oil Yield (%) at 450 °C	43.9	62.1
Oil Yield (%) at 500 °C	46.1	64.3
Oil Yield (%) at 550 °C	36.5	54.7
Oil Yield (%) at 600 °C	35.6	53.8

Oil Yield (%) at 650 °C	35	53.2
HHV (MJ/kg)	36.9	45.1
Heat Exchanger efficiency	0.5	0.8
Dryer Efficiency	0.4	0.6
Ambient Water Temperature (K)	291	296
Heat of Combustion Variance	0.98	1.02

Table B.3-8 Constant Variables Energy Draw in the MC Model

Variable	*Value*
Pump (kW)	0.7457
Shredder (kW)	2.2
Conveyor Belt (kW)	0.372
Exergy Difference b/w polymer and fuel (kW)	1.36

Chapter 4: Predictive machine learning for thermal depolymerization of plastics and application to economic analysis of municipal recycling facilities

4.1 Introduction

Municipal solid waste (MSW) generation in the US is continually rising, with an estimated 292.4 million tons generated in 2018[4]. Waste plastic accounted for 12.2% of all MSW resulting in approximately 35.7 million tons of plastic waste. MSW is separated based on the fate of the materials, with recyclables (24% of MSW) being directed to Materials Recovery Facilities (MRFs). There are approximately 420 MRFs across the US that accept co-mingled wastes containing paper/paperboard, wood, metals, glass, rubbers/textiles and plastics[5]. The scale and composition of wastes varies from MRF to MRF but on average the MSW being sent to MRFs is composed of 5% plastics[4]. This means that only 9% of plastic waste generated annually ends up at a recycling facility.

Of the approximately 3.1 million tons of plastic at MRFs, only a portion will recycled due to factors such as contamination and poor recycling mechanisms for specific polymer types[194]. Developing technologies that can handle plastics that are currently landfilled will not only increase the amount of plastic recycled, by reducing confusion caused by which plastics can be recycled but also divert massive amounts of wastes from landfills that are rapidly filling. A promising family of technologies are thermal depolymerization technologies that can convert mixed plastic waste feedstocks into fuels. These technologies such as pyrolysis and hydrothermal liquefaction (HTL) use high temperatures to break the bonds in the polymer backbones and convert them into smaller molecules that can be used as fuels and chemicals[44, 195].

These thermal technologies have been proven to be effective depolymerization methods in the literature with oil yield typically being the primary metric of performance. If economically feasible, deploying thermal depolymerization systems across the US, either at MRFs or in their own facilities, would allow for the diversion of plastic from landfills and into usable products. These technologies however have been seen to be sensitive to both feedstock composition and reaction conditions, with relatively minor changes causing large impacts on oil yield which could in turn have significant impact on the process economics [196-198]. With 420 MRFs spread across 50 states experimentally determining the expected oil yield based on each specific plastic waste composition is not realistic. Instead, utilizing the extensive data already existing in the literature for both pyrolysis and HTL reactions allows for the development of machine learned models capable of predicting oil yields for any given feedstock and reaction conditions. Models such as these are valuable as they can aid in decision-making and optimization of resources.

Chapter 3 aimed to develop a machine learning model capable of accurately predicting oil yields from pyrolysis reactions for the "Big-Six" plastics. This model, although as accurate as could be expected, did have some limitations in its applicability, that this work aims to address, expanding the use of the model. Primarily the restriction of reaction type to pyrolysis means that it could not be used to understand the potential of HTL reactions. HTL is also a viable technology but is not as well studied as pyrolysis and enough data does not exist in the literature to make a model for HTL reactions alone. Creating a model capable of predicting both reactions allows for the learning from pyrolysis to be applied to HTL and predictions made for both. The other limitation of the previously developed model was its restriction to "Big Six" polymers. These plastics are the most commonly found in US MSW, but an increasing number of other plastics are

being developed and found in waste. Allowing for a wider range of feedstock compositions further increases the applicability of any model developed.

Along with oil yields, another key factor in understanding the economic potential of using thermal depolymerization technologies in the US is the scale of the process. The amount of plastic varies from state to state and at a more granular level, from MRF to MRF. While exhaustive data for the size and composition of MRFs across the US does not exist, recently published work analyzed the average composition and quantity of plastic in all 50 states[199]. Further, the quantity and composition of plastic collected at the 9 MRFs accepting plastic waste within the state of Massachusetts has also been reported[200]. While the composition does not vary greatly from state to state the quantity of plastic does which will impact the economics of deploying thermal depolymerization technologies. Techno-economic analysis (TEAs) of converting waste plastic into liquid products have been previously completed [29, 201, 202]. These studies have included processes to separate specific liquid products such as naphtha[29] or have looked at estimated plastic compositions at large scales[201]. They often rely on experimental data for the yield and composition of the product oil composition[202]. Other studies have analyzed the economics of converting waste plastic into high value products such as lubricants[203] or fuel gases such as hydrogen[204] or methanol[205] and ammonia[206]

This work aims to utilize machine learning models to predict the oil yields for the specific waste plastic compositions in all 50 states and 9 Massachusetts MRFs. These predicted yields will then be integrated with a techno-economic analysis to determine the minimum selling price of the product oil necessary to make the process economical. Through this work the use of integrated machine learning with traditional modeling techniques like TEAs will be demonstrated and their use as decision aiding tools highlighted.

4.2 Methods

Data Collection and Preparation

This work expands upon work the work previously published[104] and outlined in Chapter 3. The dataset used in the machine learning model is composed of the data set previously published for pyrolysis reactions of Big Six polymer as well as new data points for HTL and pyrolysis reaction of any plastic with an oxygen, nitrogen, or chlorine as the heteroatom. To allow for a wider range of polymer to be included outside of the Big Six, the classification of the polymer in the expanded data set is the elemental composition of the polymer (in % C, H, O, Cl and N) along with the molecular weight of the monomer. For polymer mixtures the elemental composition and molecular weight of the monomer were both calculated as the weighted average of the components. The inclusion of the molecular weight of the monomer allows for the differentiation of plastics that have the same elemental composition but are known to react differently (i.e. polyethylene and polypropylene).

Along with the composition of the polymer, the other features included in the model are reaction temperature (in degrees C), particle size (in mm), reaction time (in minutes), residence time (in seconds), presence of a catalysts(1 indicates yes, 0 indicates no), HTL or pyrolysis (1 indicates HTL, 0 indicates pyrolysis), and reactor type (1 indicates yes, 0 indicates no). Presence of a catalyst, HTL or pyrolysis and reactor type are all categorical variables and are therefore one-hot-encoded as indicated above. The reactor types included in the model are batch, fixed bed, fluidized bed, continuous horizontal tube, swept batch and semi batch reactors. Due to discrepancies on the naming of reactor type in the literature a series of rules were used to categorize the reactor type in the model. Regardless of how they are classified in the literature, any reactor that has a sweep gas removing products during reaction was classified as a swept batch reactor.

Semi-batch reactors were any reactors that did not use a sweep gas but had continuous removal of products during reaction. Literature classifications were kept for any reactors that fell outside these specific categories.

In order to allow for the inclusion of both reaction time and residence time when only one would be applicable depending on the reactor type a modified one-hot encoding was used. Whichever time definition did not apply (i.e. residence time for a batch reaction) was given a value of zero and the other definition would be the value reported in the literature. For swept batch reactions, reactor size and sweep gas flowrate was used to calculate the residence time, as most often total reaction time is reported and not the residence time within the reactor. Any data point that provides neither reaction time nor residence time (or the information necessary to calculate residence time) was excluded from the final dataset for lacking critical reaction details.

Data handling, splitting and evaluation was handled in the same manner explained in detail in Chapter 3.2. Random Forest (RF) was chosen as the machine learning model used in this work, due to its performance shown in Chapter 3, its relative simplicity of interpretation, its ability to handle small data and its ability to handle data that has not been normalized. Models were developed in Python 3.6[141] and scikit-learn 1.1.0 packages[142]

Techno-economic Analysis

Oil yields for each feedstock were predicted using the optimized RF model. Model features outside of feedstock composition were modeled based on average values found in the literature. These values can be seen in **Table 4-1**. The feedstock compositions can be found in the **Appendix C Table C.4-3** and **Table C.4-4**. For the composition of waste plastic in the state of Massachusetts, waste reported as commingled plastic was assumed to have the same composition as the state average reported by Milbrandt, et.al.[199]. Due to the well-established recycling pathways for PET and the known challenges of reacting PVC (chlorine by-products) it was assumed these plastics

were separated from the mixtures prior to reaction. This would be a relatively simple separation step to achieve as PET and PVC both have densities greater than water and could be removed with flotation separation. The composition of the plastic mixtures was readjusted to 100% after the removal of PET and PVC and the elemental composition and molecular weight of the monomer calculated.

Table 4-1 Reaction Conditions used in machine learning model predictions

Feature	*Value*
Temperature	500 °C
Particle Size	7.5 mm
Reaction Time	0 min
Residence Time	300 seconds
Catalysts	None
HTL	Pyrolysis
Reactor Type	Continuous Horizontal Tube

A simplified pyrolysis reactor system was developed in Aspen V.14 as seen in **Figure 4-1**. This process does not include pre-processing steps such as baling or flaking the polymers. Further information including process details can be found in **Appendix C**. For each scenario (i.e. state or specific MRF) the predicted oil yield from the machine learning model was fed into the Aspen model accounting for composition of the feedstock, composition of the pyrolysis oil (py-oil) and feed flowrate. It was assumed that the yield of gaseous product was 5% and the remainder was unreacted solid/char and pyrolysis oil. The total equipment cost, and annual utility cost were taken from Aspen economic predictions.

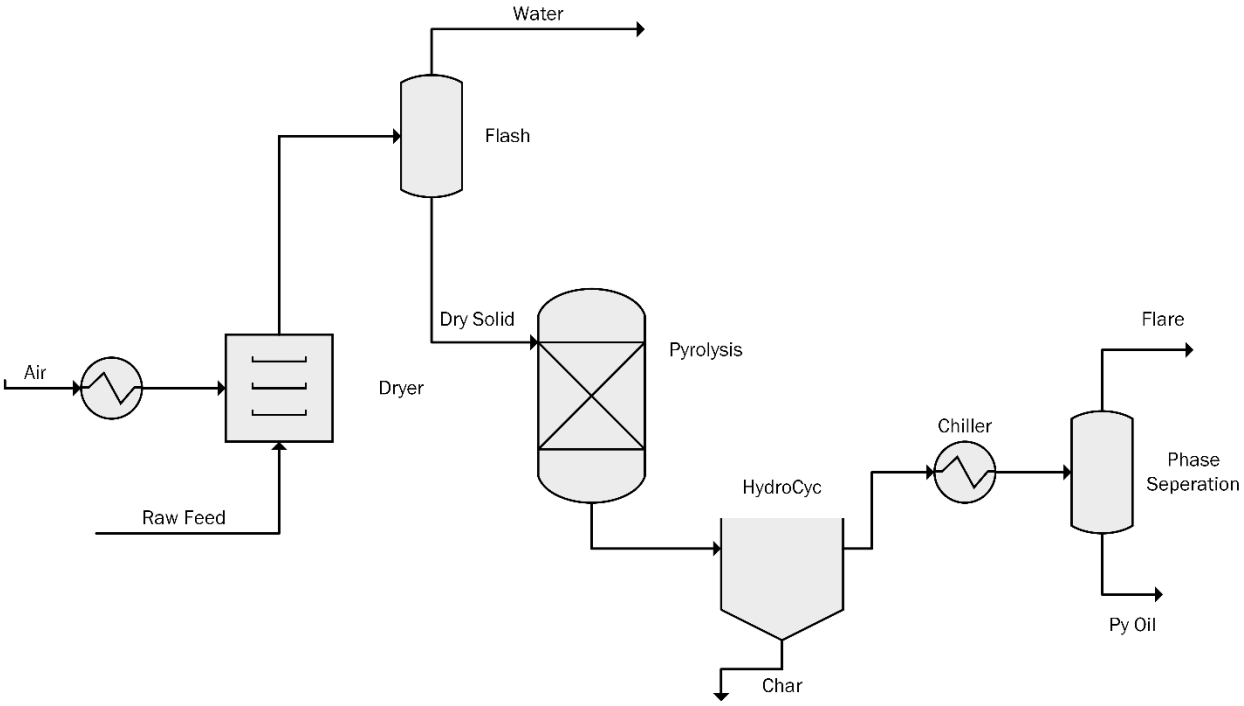

Figure 4-1 Process diagram for pyrolysis system including drying the feedstock, the pyrolysis reactor and separation of the residual solids, pyrolysis oil and waste gas.

The predictions for equipment cost and utility costs from Aspen were used in the techno-economic analysis. The parameters used to calculate the Total Capital Investment and assumptions used in calculating Net Present Value (NPV) can be found in **Appendix C Table C.4-6** and **Table C.4-7**. Annual operating costs comprised of the utilities predicted by Aspen, transportation costs and the cost of disposing of the residual solid/char after the reaction. The disposal cost was taken as the average tipping fee for the state based on what region of the country they are in [207]. The cost of transporting the waste plastic from the MRF to the pyrolysis reactor system was taken as $50/ton [208]. The minimum py-oil selling price was calculated for a NPV of zero over a 30-year plant life.

4.3 Results

Machine Learning Model

Previously published work analyzed a dataset that encompassed data for pyrolysis reactions of the Big Six plastics (high and low-density polyethylene, polypropylene, polystyrene, polyethylene terephthalate, and polyvinyl chloride)[104]. In this work the dataset is expanded to encompass both pyrolysis and HTL reactions and any polymer with a nitrogen, oxygen or chlorine atom as the heteroatom. The new dataset allows for the expansion of reactions and reaction conditions that can be predicted using a machine learned model and therefore the size of the dataset. The dataset used in this work had 442 datapoints and 18 features. The features included in the model were the elemental composition of the feedstock and the molecular weight of the monomer, reaction temperature, particle size, reaction time, residence time, catalysts, HTL and reactor type (batch, fixed bed, fluidized bed, continuous horizontal tube, swept batch and semi batch).

The expanded dataset was used to optimize a Random Forest model; the optimized hyperparameters can be seen in **Appendix C Table C.4-8**. The mean absolute error (MAE) of the test set for the optimal model was ±10.78%. The performance of the model on the test set can be visualized in **Figure 4-2.** A majority of the test set data falls within the ±10% region around the 1:1 line, however approximately 40% of the data falls outside of this region. The 1:1 line represents where the model prediction is equal to the reported experimental yield. **Figure 4-2** provides a visual representation of the MAE, showing that although much of the test set falls within the ±10% region, the data falling outside of this region, and some by a large margin, skew the MAE to a value greater than ±10%. It should also be noted that no trend exists between the data points falling outside these regions, indicating the model is not systematically inaccurate for specific conditions.

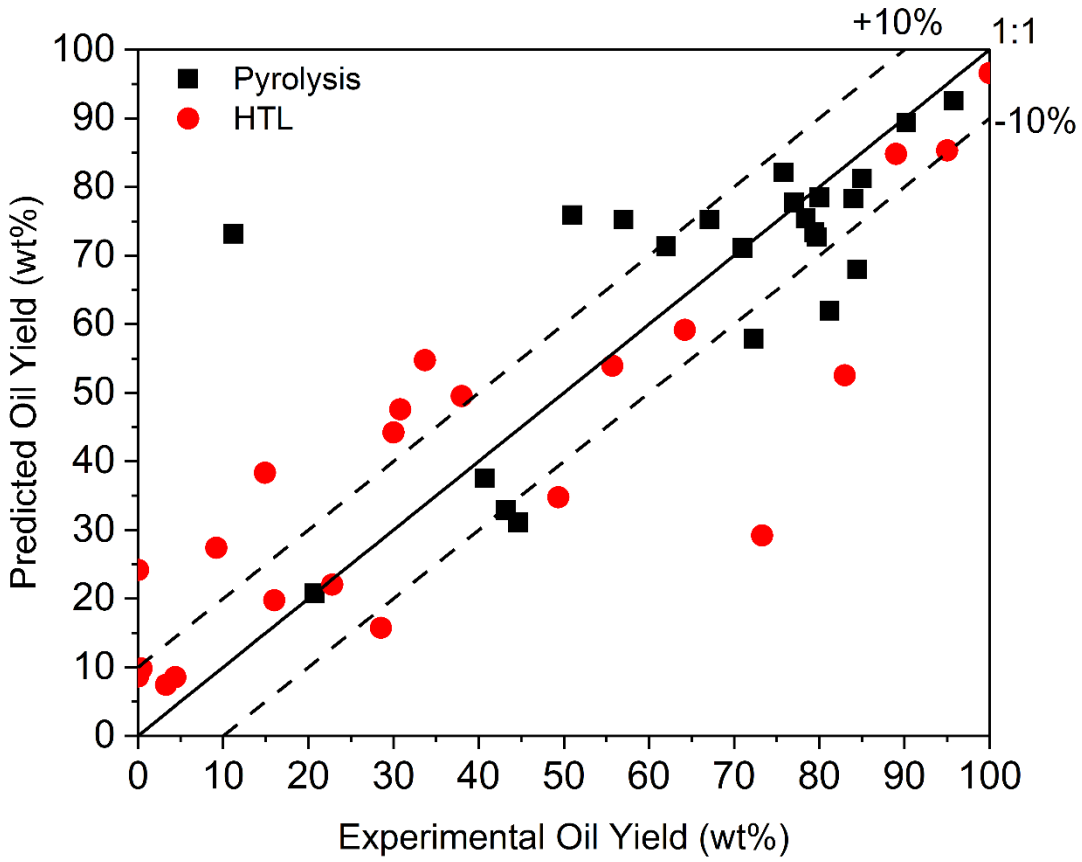

Figure 4-2 Parity plot of the predicted oil yield (wt%) vs the experimentally reported oil yield for the data test set. The data points for HTL vs pyrolysis reactions are identified, along with the ±10% region around the 1:1 line where the predicted oil yield is equal to the experimental oil yield.

The distribution of data type within the dataset can also be visualized through the test set seen in **Figure 4-2**. The dataset is comprised of approximately two thirds pyrolysis reactions and one third HTL reactions (as seen also in the **Appendix C Figure C.4-6**). This split in data represents the current state of the literature and research in the field. As the field advances and more data becomes available the dataset will be become more balanced between reaction types which should aid in reducing overall model error and increase the prediction accuracy of HTL reactions in particular. The current form of the data still shows the ability to predict both pyrolysis

and HTL reactions with accuracy. However, a higher percentage of pyrolysis reactions predictions lying inside of the ±10% region (30% vs 41% for HTL), and the data within this region is clustering more tightly around the 1:1 line indicates the model predicts these reactions with slightly more accuracy than the HTL reactions.

In comparison with the previously published work the MAE seen here is higher than the MAE for the dataset including pyrolysis reactions only (MAE of ±9.1%[104]). Although the dataset size increased by a factor of 1.4, by including HTL reactions, the variability and diversity between data points has increased. This indicates that there is a tradeoff between model accuracy and model applicability. Depending on the use of the model a more accurate but less applicable model may be better and likewise in other situations a more widely applicable model may be best. As a decision aiding tool for analyzing new feedstocks, being able to use a single model to explore a wide range of reaction conditions has significant value, especially when the loss of accuracy is less than 2%.

Technoeconomic Analysis

A key factor in the success of a new technology is if it is economically viable at scale. A technoeconomic analysis is a way to study the economic feasibility but the oil yield of the feedstock of interest must be known in order to complete the analysis. By integrating the machine learning model into the TEA, the oil yield of any feedstock can be predicted and used to understand the economics of that feedstock. To this end in this work the machine learning model was used to predict the oil yield based on the average composition of waste plastic in all 50 states[199] and a TEA was used to understand the minimum selling price (MSP)of the product in $/ton necessarily to make the process profitable.

As waste plastic is typically a dry feedstock (less than 1% moisture)[209] and the economics of its equipment is better understood[210-212], pyrolysis was chosen as the technology to be modeled,

although the same process could be applied for HTL reactions. In each state it was assumed that all of the waste plastic in the state can be collected and converted into pyrolysis oil in a single localized pyrolysis plant. The one exception to this assumption is for the state of Texas, which due to the quantity of plastic two plants of equal size were necessary.

Although every state has slight variations in the average composition of waste plastic the RF model predicted the oil yield of all 50 states as 64% ± 1.4%. This shows that the difference in plastic waste composition state to state is not large enough to make a major impact on the predicted oil yield. Instead, the primary feature that could impact the economics of deploying pyrolysis systems in various states will be the scale of such a system, as the quantity of plastic state to state varies drastically[199]. **Figure 4-3** shows the results of the TEA for all 50 states except for Connecticut, as CT primarily collects PET for recycling and the remaining plastic quantity was too low to be economically viable ($1,300/ton).

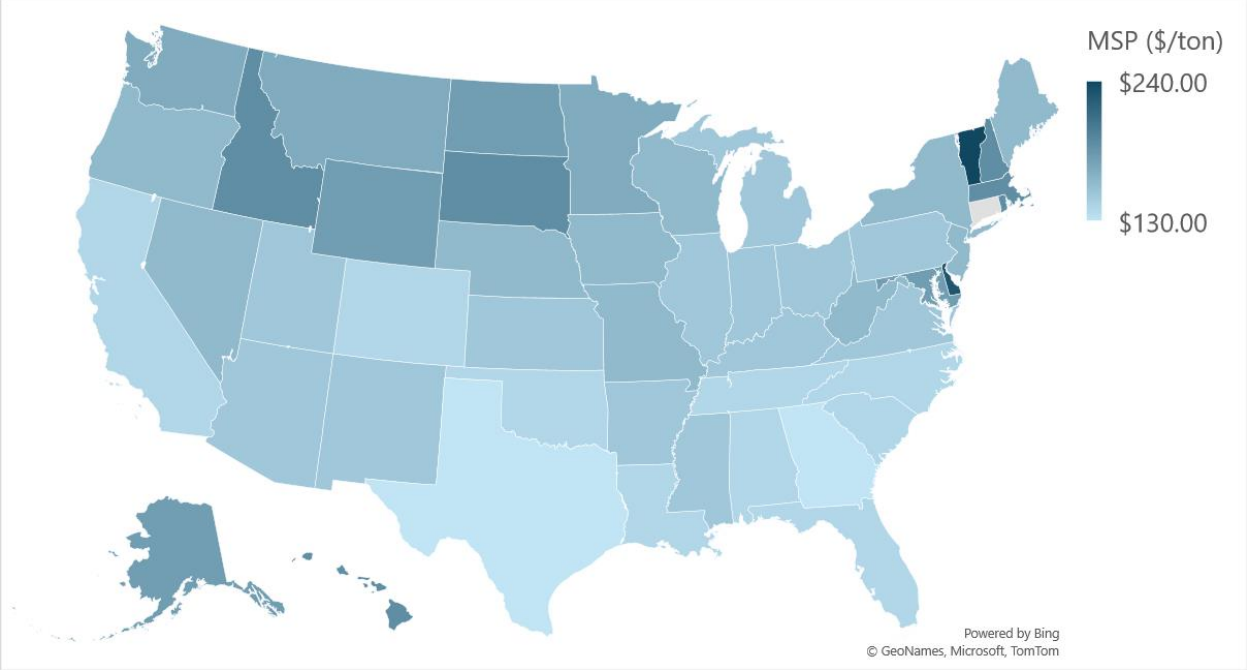

Figure 4-3 Predicted minimum selling price in $/ton of pyrolysis oil for each state if all waste plastic in the state is converted to oil in a single pyrolysis plant. Connecticut is not included due to the very low amount of non-PET plastic collected in the state.

Figure 4-3 indicates a regional dependence on the MSP, with states in the Northeast and Northern Plains regions having a higher MSP. States in the Southeast have a lower MSP on average. The regional grouping of MSP is due in part to scale (small states in the Northeast and lower populations in the Northern Plains) and also in part due to the higher cost of disposing of residual solids in those regions. The Northeast in particular has the highest average landfill tipping fee of any region in the US at $75.92/ton[207]. **Figure 4-3** shows that conversion of waste plastic into pyrolysis oil is economically promising in every state, considering the price of crude oil in the US is approximately $550/ton[213]. Interestingly the range in minimum selling prices does not correlate to the range in the quantity of waste plastics across the US. That is to say the range in the amount of plastic state to state is much more significant than the range in MSP. This difference cannot not be explained purely by the regional difference in tipping fees, as states such as Texas and Oklahoma have the same tipping fee, but Texas has 6 times as much waste plastic and the difference in MSP is less than $10/ton. The assumption that all of the waste plastic in the state will be collected into one centralized location makes the scale of the process large enough that the economy of scale plays a major role, and the individual scale of the state no longer has a significant impact on MSP. This effect can be seen in **Figure 4-4.**

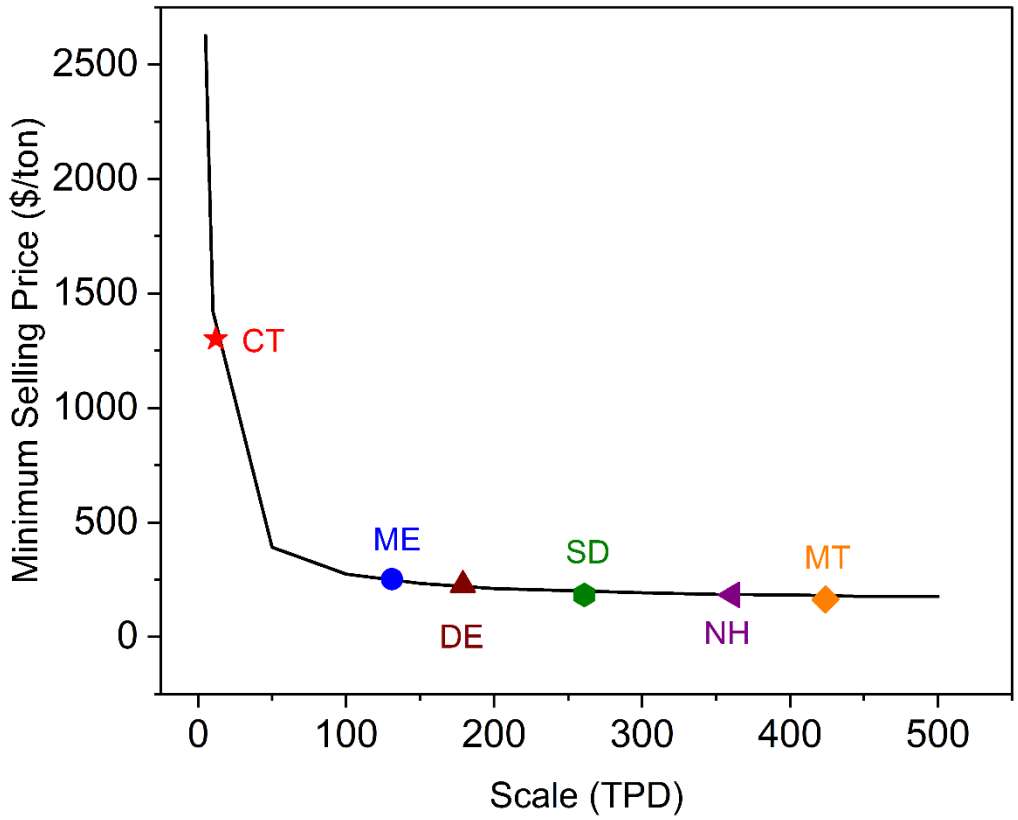

Figure 4-4 Minimum selling price in $/ton based on the scale of the pyrolysis plant in tons per day. The composition and predicted yield for the state of Massachusetts was used to demonstrate the economies of scale seen across all states. The scale and predicted MSP of select states are shown to follow the same trend as seen for the state of Massachusetts.

Figure 4-4 shows that there is a strong dependence on scale when the flowrate is less than 100 tons per day (TPD). **Figure 4-4** also shows that all flowrates greater than 350 TPD will have the same MSP regardless of the flowrate through the system. With the assumption of a single centralized pyrolysis plant, every state would have a flowrate greater than 100 TPD based on the quantity of waste plastic in the state, with the exception of CT. This means that the scale of the required pyrolysis plant state to state will have little to no impact on the MSP as can be seen in **Figure 4-3**. The slight regional dependence on scale can be been seen through the select states

scale and MSP highlighted in **Figure 4-4**, showing states in the Northeast and Northern Plains region fall below 350 TPD and have slight scale dependence.

While scale was shown to have little to no impact of the MSP, factors such as transportation and feedstock costs could have a major impact. A sensitivity analysis was completed in order to understand the effect of 8 major factors contributing to the MSP. This analysis can be seen in **Figure 4-5** for the case study of the state of Massachusetts. The values for each of these parameters can be seen in **Appendix C Table C.4-9.** The average MSP for the state of Massachusetts is predicted to be $190/ton. This average value assumes zero feedstock cost, and the analysis in **Figure 4-5** shows that the prediction of MSP is most sensitive to feedstock cost. If a negative feedstock cost is available (if for example landfill tipping fees are being offset at a MRF), the process can become even more cost effective. On the other hand, if a feedstock cost is charged the product will become more expensive. The MSP is also sensitive to how much it costs to transport the waste plastic to a recycling facility, indicating thought should be put into the location of conversion systems to limit the necessity of transportation. A key parameter not included in the analysis shown in **Figure 4-5** is yield, which is a factor that MSP can be very sensitive to. To understand the sensitivity of MSP on oil yield the MSP was plotted vs theoretical oil yields from 10-80% as seen in **Figure C.4-7**. This analysis indicated that the MSP decreases with increasing oil yields, suggesting optimizing of reactor conditions for optimal oil yields is beneficial when considering economic viability.

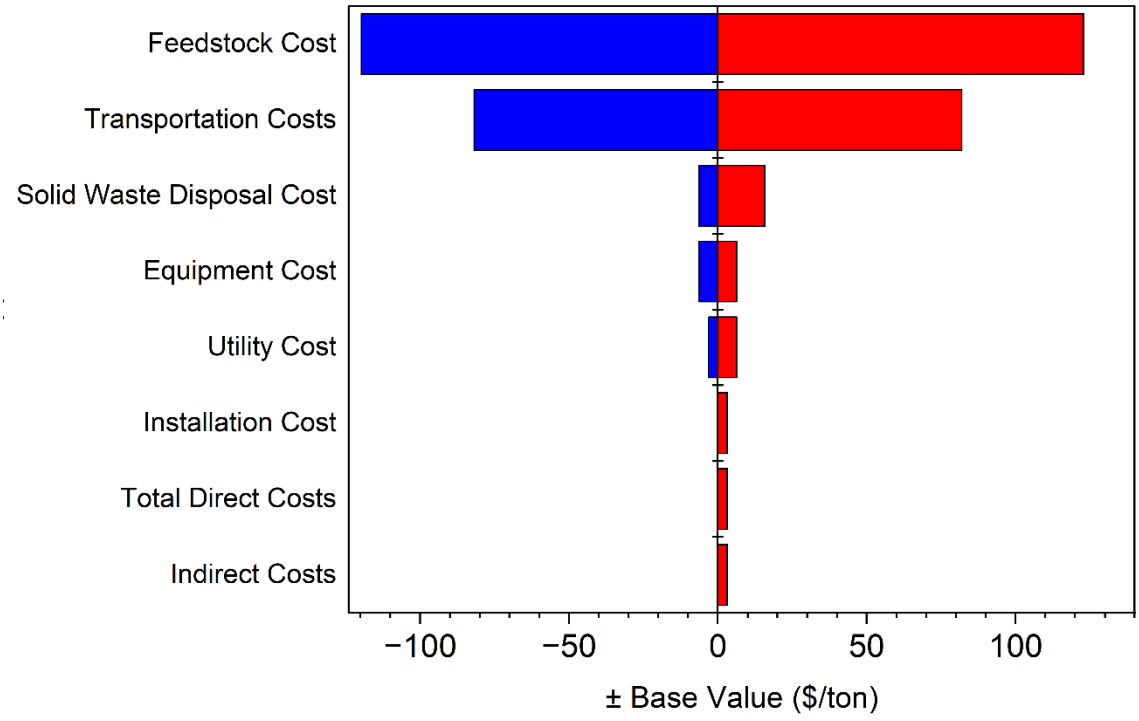

Figure 4-5 Sensitivity analysis of 8 key parameters effecting the predicted minimum selling price of products produced from pyrolysis of waste plastic for the case study of the state of Massachusetts. The average MSP is $190/ton and the sensitivity is expressed as ± dollar values off of the average MSP.

The assumption that all plastic is collected in a centralized location makes the pyrolysis plant scale large enough to make the process very economically promising but this assumption, especially in large states, may be unreasonable. If a centralized pyrolysis plant is not feasible, another logical location for waste plastic pyrolysis units is co-located with the MRFs that collect and sort the recycling wastes. Reliable data for the quantity and more importantly the composition of waste plastics at MRFs is not widely reported across the US. Data of this kind is reported for the state of Massachusetts and therefore Massachusetts was used as a case study in this work to understand the economics of co-locating the pyrolysis conversion system at the MRF.

There are 9 MRFs across Massachusetts that accept plastic wastes and of these 9, only 5 collect more than 1,000 tons per year once PET and PVC have been removed. 1,000 TPY was used

as the minimum threshold for co-locating a pyrolysis system in this work. The MSP for each of the remaining 5 MRFs along with their scale can be seen in **Table 4-2**. **Table 4-2** also shows the predicted MSP for the state of Massachusetts from **Figure 4-3** and the predicted MSP if the reported quantity and composition of plastic from all 9 MRFs was summed. There is a large difference in the quantity of plastic for the state from these two sources, indicating not only the challenges in differences in how data is reported, but also a potential large amount of plastic that is going directly to landfill in the trash and never reaching a MRF.

Table 4-2 Scale and minimum selling price for a pyrolysis system co-located with Municipal Recycling Facilities across the state of Massachusetts

Location Name	*Scale (ton/yr)*	*Minimum Selling Price ($/ton)*
Casella Auburn MRF	1,693	$2,810
Casella Charlestown	1,387	$3,300
El Harvey	1,091	$4,120
WM Avon MRF	1,323	$3,470
WM Billerica MRF	1,235	$3,690
Mass MRF Total[1]	8,580	$600
Mass Total[2]	117,500	$190

[1]Summation of the reported quantity of waste plastic collected at all 9 MRFs across the state.
[2]As used in **Figure 4-3****Figure 4-4** [199, 200]

It can be seen that in a smaller state like Massachusetts co-locating pyrolysis units with MRFs reduces the scale of each plant and greatly increases the required minimum selling price of the pyrolysis oil. With MSPs of greater than $3,000/ton in most locations using a pyrolysis conversion system at a MRF would not be economically viable and would argue for using a centralized pyrolysis plant. **Table 4-2** also shows that the more plastic that can be captured before

it ends up landfilled the better the economics of the py-oil becomes, but even under business as usual a centralized pyrolysis unit that takes waste plastics from MRFs would be highly feasible and a valid alternative to landfilling that plastic which cannot be otherwise recycled.

4.4 Conclusions

Through this work the integration of machine learning models with technoeconomic analysis methods has been demonstrated. Utilizing the extensive data existing in the literature allows for the development of accurate models capable of predicting oil yields for both pyrolysis and hydrothermal liquefaction reactions for any feedstock. These models can be used to predict the oil yield of new feedstocks of interests and these yields can be used to understand the economic viability of the feedstock. In this work it has been shown that converting waste plastic at centralized pyrolysis plants is economically feasible in all 50 states, except CT. Smaller plants are also viable with flowrates greater than 100 TPD and these models can be used to understand the viability for any desired scale and feedstock composition. The integration of machine learning allows for an understanding of economics before significant resources have been invested into experimental exploration of a potentially non-viable feedstock.

4.5 Appendix C

Table C.4-3 Feedstock Compositions and Quantity by State[199]

State	*C (wt%)*	*H (wt%)*	*O (wt%)*	*Cl (wt%)*	*N (wt%)*	*MW (g/mol)*
AK	86.14067	13.85933	0	0	0	37.77631
AL	86.34336	13.65664	0	0	0	39.14479
AR	86.14067	13.85933	0	0	0	37.77631
AZ	86.18932	13.81068	0	0	0	38.53002
CA	86.34529	13.65471	0	0	0	40.1815
CO	86.24671	13.75329	0	0	0	39.29557
CT	86.0382	13.9618	0	0	0	36.38491
DE	86.01806	13.98194	0	0	0	35.87506
FL	86.27706	13.72294	0	0	0	38.67796

GA	86.34552	13.65448	0	0	0	39.19558
HI	86.28353	13.71647	0	0	0	39.30113
IA	85.97548	14.02452	0	0	0	35.80615
ID	85.89517	14.10483	0	0	0	35.0168
IL	86.13153	13.86847	0	0	0	37.19476
IN	86.07457	13.92543	0	0	0	37.02895
KS	86.31109	13.68891	0	0	0	39.12453
KY	86.07167	13.92833	0	0	0	37.29557
LA	86.14067	13.85933	0	0	0	37.77631
MA	85.92159	14.07841	0	0	0	35.08492
MD	86.11668	13.88332	0	0	0	37.65784
ME	86.02928	13.97072	0	0	0	36.46361
MI	86.05922	13.94078	0	0	0	39.52348
MN	85.96159	14.03841	0	0	0	36.26306
MO	85.99021	14.00979	0	0	0	36.00349
MS	86.14067	13.85933	0	0	0	37.77631
MT	86.14067	13.85933	0	0	0	37.77631
NC	86.09496	13.90505	0	0	0	36.76766
ND	86.14067	13.85933	0	0	0	37.77631
NE	86.04655	13.95345	0	0	0	36.93052
NH	86.14067	13.85933	0	0	0	37.77631
NJ	86.27925	13.72075	0	0	0	38.88049
NM	86.14067	13.85933	0	0	0	37.77631
NV	86.2097	13.7903	0	0	0	37.87723
NY	86.00076	13.99924	0	0	0	36.22479
OH	86.12039	13.87961	0	0	0	37.86167
OK	86.14067	13.85933	0	0	0	37.77631
OR	85.95913	14.04087	0	0	0	36.11182
PA	86.20481	13.79519	0	0	0	37.927
RI	86.18693	13.81307	0	0	0	38.52952
SC	86.14067	13.85933	0	0	0	37.77631
SD	86.14067	13.85933	0	0	0	37.77631
TN	86.29608	13.70392	0	0	0	39.75856
TX	86.6502	13.3498	0	0	0	43.68308
UT	86.14067	13.85933	0	0	0	37.77631
VA	86.24945	13.75055	0	0	0	37.96748
VT	86.20992	13.79008	0	0	0	38.07041
WA	85.94659	14.05341	0	0	0	35.57341
WI	85.98095	14.01905	0	0	0	36.22733
WV	86.14067	13.85933	0	0	0	37.77631
WY	86.35128	13.64872	0	0	0	40.35329

Table C.4-4 Feedstock composition and quantity by Massachusetts MRF[200]

MRF	*C (wt%)*	*H (wt%)*	*O (wt%)*	*Cl (wt%)*	*N (wt%)*	*MW (g/mol)*
Casella Auburn MRF	85.6017	14.3983	0	0	0	29.96115
Casella Charlestown	85.6	14.4	0	0	0	31.30472
El Harvey	85.65767	14.34233	0	0	0	32.56617
Brockton Recyclery	85.6	14.4	0	0	0	37.0052
Repub Peabody	85.6	14.4	0	0	0	28.05
WM Avon MRF	85.6	14.4	0	0	0	33.14279
WM Billerica MRF	85.6	14.4	0	0	0	31.82512
WM RRT MRF	85.6	14.4	0	0	0	32.15935
ZWS Rochester	85.62655	14.37345	0	0	0	29.79255
Mass MRF Total	85.61	14.39	0	0	0	31.39

Aspen Model

The py-oil composition was assumed to be comprised of the model compounds of hexadecane and styrene to represent polyethylene/polypropylene components and polystyrene components respectively. The weight percent of each model compound was modeled such that it was equal to the weight percent of the combined PE/PP for hexadecane and PS for styrene.

The equipment cost predicted by Aspen for the state of the Massachusetts is shown below in **Table C.4-5**. The equipment cost increases with increasing process scale.

Table C.4-5 Sample Process Equipment Costs for the State of Massachusetts (16,319.41 kg/hr flowrate)

Equipment	Cost ($)
Flash Vessel	31,700
Chiller	28,700
Flash Vessel 2	27,200
Pyrolysis Reactor	702,500

Dryer	872,900
Heat Exchanger	23,800

Techno-economic Analysis

Parameters and factors used to calculate TCI and NPV in the technoeconomic analysis are detailed below in **Table C.4-6** and **Table C.4-7**

Table C.4-6 Estimation of the Total Capital Investment (TCI)[75]

Total Direct Costs (TDC)
1. Total Installed Cost (TIC) (2.2x equipment cost[214])
2. Buildings (1.0% TIC)
3. Site Development (9.0% TIC)
4. Additional Piping (4.5% TIC)
Indirect Costs
1. Prorated expenses (10% of TDC)
2. Home Office & construction fees (20% of TDC)
3. Field Expense (10% of TDC)
4. Project Contingency (10% of TDC)
5. Startup and permits (5% of TDC)
Fixed Capital Investment (FCI)
1. Total Direct Costs
2. Indirect Costs
Total Capital Investment (TCI)
1. Fixed Capital Investment
2. Working Capital (5% of FCI)

Table C.4-7 Assumptions made for the calculation of Net Present Value[75]

Parameter	Value
Equity	40%
Loan Interest	8.0%
Loan Term, years	10
Plant Depreciation Period, years	7
Construction Period, years	3
% Spent in Year -3	8%
% Spent in Year -2	60%
% Spent in Year -1	32%
Start-up Time, years	0.5
Revenues (% of Normal)	50%
Variable Costs (% of Normal)	75%
Fixed Cost (% of Normal)	100%
Internal Rate of Return	10%

Income Tax Rate	35%
Operating Hours Per Year	7,200

Machine Learning Model and Dataset

The hyperparameters from the optimized Random Forest model used throughout this work are outline in **Table C.4-8** and the breakdown of the dataset in terms of HTL vs pyrolysis and mixed plastic vs single stream plastic studies can be seen in **Figure C.4-6**.

Table C.4-8 Optimal random forest model hyperparameters

Hyperparameter	Value
Random State	186
Number of Estimators	152
Maximum Features	7
Maximum Depth	19
Min_sample_split	2
Min_samples_leaf	1

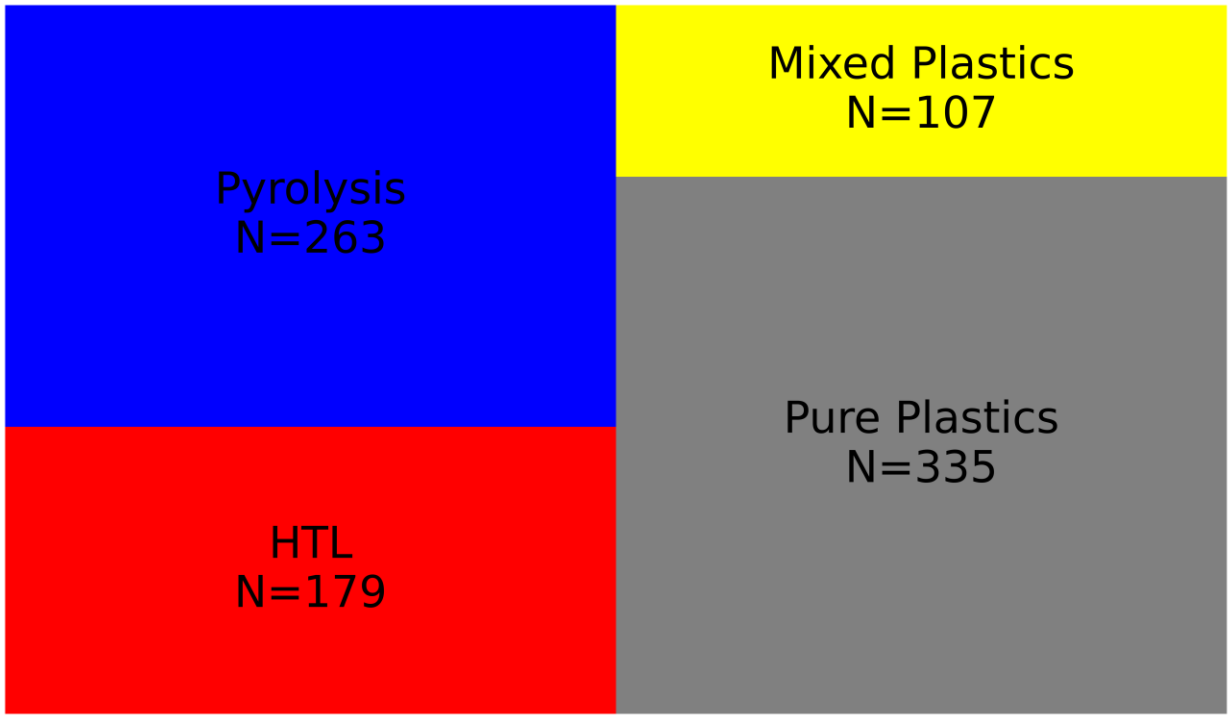

Figure C.4-6 Overview of dataset with N indicating the number of data points falling within each category.

Massachusetts Case Study

Table C.4-9 Minimum and Maximum Values for Sensitivity Analysis Parameters

TEA Parameters	Minimum Value	Maximum Value
Equipment Installation Cost Factor	1.98	2.42
Total Direct Costs (% of TIC)	105 %	125%
Indirect Costs (% of TDC)	45%	65%
Transportation Costs	$0/ton	$100/ton
Solid Waste Disposal Cost	$60/ton	$100/ton
Utility Cost (% of predicted cost)	-20%	20%
Equipment Cost (% of predicted Cost	-50%	50%
Feedstock Cost	-$75/ton	$75/ton

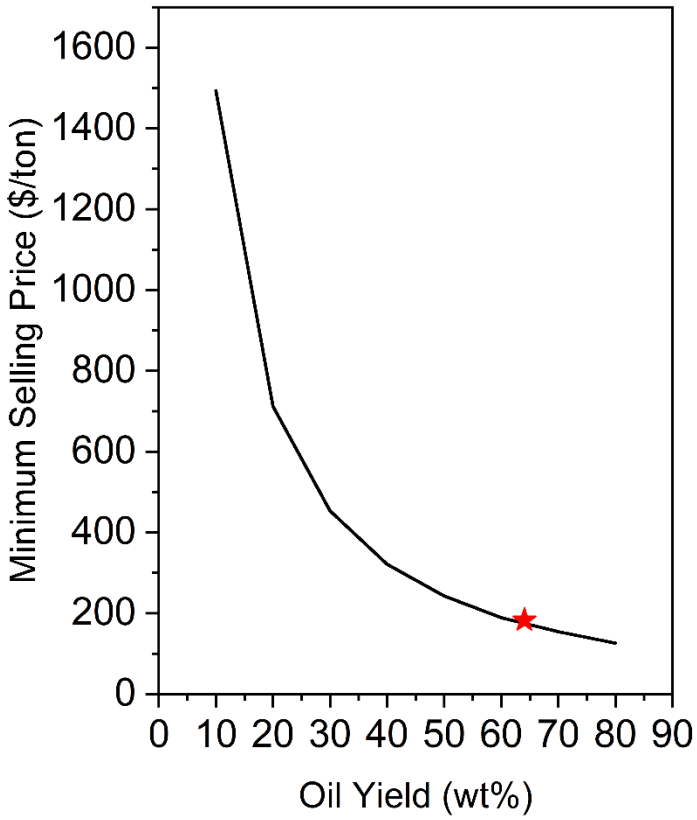

Figure C.4-7 Effect of predicted minimum selling price in $/ton for theoretical oil yields from 10% to 80%. The predicted MSP based on the oil yield predicted for the state of Massachusetts is indicated by the red star.

Chapter 5: Oxygenated monomer production from the depolymerization of polystyrene in the presence of a radical source

5.1 Introduction

Polystyrene, both expanded PS (EPS) and solid PS, is a versatile polymer used in packing materials, food containers, and other rigid containers and products[61]. Most of these products made from PS are single use in their application, meaning they are disposed of and not used again. Considering approximately 15 and a half million metric tons of polystyrene was produced globally in 2022[215], PS accounts for huge amounts of waste every year. Compounding the waste problem is the less than 1% of PS that is recycled globally[216]. Once a PS product is used it will end up either taking up valuable space in rapidly filling landfills[217] or as pollution in the environment, harming ecosystems[218-220]. As a stable polymer PS will take hundreds of years to fully decompose[61], but will undergo continuous environmental degradation into smaller and smaller micro plastics[221] further complicating any cleanup efforts.

Polystyrene traditionally has low recycling rates for a multitude of reasons. Due to the large volume and low density of PS, especially EPS, transportation costs for transport to recycling centers are high[222], which in turn increases the cost of any recycled material made. When polystyrene does make it to a recycling facility, the current recycling techniques available for polystyrene use toxic solvents[223] and there is limited use for the byproducts[224]. Dissolution by solvents is the most common way to recycle PS. Dissolution is able to separate contaminants from the polystyrene waste and also greatly reduce the volume, and therefore transportation costs, of the waste[222]. However, the solvents used are typically highly toxic and dangerous to work with in large quantities[223] and prevents the recovered material being converted back into food packaging[224], which significantly impacts the potential market for the post recycling materials.

These factors combine to make recycling of PS difficult resulting in an end product that is more expensive than virgin PS[223].

Alternative methods for recycling of PS are necessary to address the large amounts of PS waste generated. A promising new category of technologies are thermal depolymerization technologies. These technologies such as pyrolysis and hydrothermal liquefaction (HTL) use high temperatures to convert waste plastics, both mixed and pure plastics, into fuels, monomers and chemicals. Pyrolysis, which uses high temperatures in the absence of oxygen, has been studied extensively for the conversion of PS[225]. Oil yields, as oil is the primary product of interest, nearing 100%, indicating complete depolymerization of the PS, have been achieved with reaction temperatures greater than 450 °C[150, 182]. The pyrolysis oil produced from these reactions is comprised of single ring aromatic compounds such as toluene, ethylbenzene, alpha-methylstyrene and styrene monomers, along with styrene dimers and trimers[176, 179, 182]. Although the product distribution after pyrolysis is relatively simple and high conversion to styrene monomers and BTEX compounds (benzene, toluene, ethylbenzene and xylene) are possible[163, 179], pyrolysis performance is susceptible to contaminants[176]. This means significant preprocessing of the waste to remove contaminants is needed, increasing costs and impacting the economic viability.

HTL, which uses high temperature and high pressure, in the presence of sub- or supercritical water, has also been shown in the literature to convert PS into usable products[48, 226]. The presence of sub- or supercritical water allows HTL to operate at lower temperatures compared to pyrolysis (>350 °C). It should be noted studies have reported high oil yields at 350 °C, but the use of dimethyl chloride as a wash solvent can cause dissolution of unreacted PS, making separation of oil and dissolved solid impossible[70]. Along with lowering the reaction temperatures necessary for high oil yield, HTL also has the benefit of being less susceptible to contaminants[176]. These factors

mean that the preprocessing required for pyrolysis can be greatly reduced or eliminated for HTL reactions. However, a major drawback of PS HTL is the oil mixtures are much more complected than pyrolysis oil and the monomer recovery is limited[48]. With a lower monomer recovery rate, the products formed during HTL are not as valuable, hurting the process economics. Increasing the value of HTL byproducts would take advantage of the benefits of HTL over pyrolysis while addressing the major technological drawback of HTL.

It is proposed that adding an external oxidative radical source will promote the creation of high valued oxidative single ring aromatic compounds while also reducing the severity of conditions necessary for complete conversion of PS. The critical role of radicals in the depolymerization of polystyrene has been theorized for many years and shown in the pyrolysis literature[124, 227, 228], however how this role changes in hydrothermal liquefaction is not as well understood. In thermal depolymerization of PS, the major reaction is a radical induced beta-scission, where the radicals are formed primarily through random scission or hydrogen abstraction reactions[229]. The random scission and hydrogen abstracts reactions in pyrolysis have activations energies nearly three times are large as for beta-scission[124]. This means that the severity of conditions necessary for complete depolymerization are for the creation of radicals and not the main depolymerization mechanism. It is hypothesized that adding an external radical source to HTL reactions (called Radical Initiated Hydrothermal Liquefaction, RI-HTL) will initiate beta-scission at its lower activity energy without the need for the higher activation energy reactions. These radical sources should be inexpensive and green chemicals for RI-HTL to be an improvement on current recycling techniques.

In this work the effect of an external radical source added to HTL reactions, on reaction severity and product composition is explored. The role of radicals in traditional HTL is also explored.

5.2 Methods

Materials

Virgin polystyrene pellets with a weight-average molecular weight of 176,000 Da (Scientific Polymer Products, Inc., Ontario, NY) were used as the primary feedstock in this study. The radical source used was 30 wt% hydrogen peroxide (Fisher Scientific, USA). Deionized water (DI) was obtained from a Barnstead E-pure system.

Experimental

Thermal experiments were conducted in a 100 cm^3 Hastelloy Parr batch reactor with reaction temperatures ranging from 325 °C to 400 °C. For each run 5 g PS was loaded into the reactor, and 28 g of DI water were added for HTL reactions. For RI-HTL reactions hydrogen peroxide was added in O:C ratios ranging from 0.091 to 0.25 and DI water was added so that the reaction always had 28 g of water. After loading and sealing the reactor the headspace was purged with nitrogen three times to ensure an inert environment. The reactor was then pressurized to an initial pressure of 1000 psi for runs less than 400°C. At 400 °C the initial pressure was set to 850 psi to ensure the maximum operating pressure remained under 4,000 psi. High initial pressure was necessary to prevent small molecules repolymerizing in the reactor head cold spots during reaction. The reactor was continuously stirred using a Parr magnetic stirring drive during heat up, reaction and cool down. Reaction times from 0 to 20 minutes were studied where 0 minutes correlates to the time at which the reactor reaches the desired reaction temperature. The reactor was rapidly quenched to 20 °C using an ice bucket at the end of the reaction time. After quenching and depressurization, the reactor was weighed in order to determine the gravimetric gas yield.

Extraction of the reaction products was done in a 3-step process. The aqueous phase was removed from the residual solids and oils through vacuum filtration with 11-micron Whatman 1 filter paper. Under select conditions when oil also went through the filter paper with the aqueous

phase, the aqueous phase was centrifuged and removed from the oil phase through pipetting. The oil product that did not go through the filter was removed from the residual solid using a methanol solvent rinse. Methanol was chosen as the solvent as PS is insoluble in methanol, unlike many other common extraction solvents. This ensures that all oil recovered was formed during the reaction and is not dissolved residual solid. The oil/residual solid remaining in the filter paper after the aqueous phase extraction is rinsed with methanol until the methanol ran clear. The reactor was also rinsed and scraped repeatedly with methanol until the methanol ran clear. The remaining residual solid in the filter is weighed and dried in a 60 °C oven overnight to remove any residual methanol or water. The oil is separated from the methanol through rotary evaporation.

Analysis Techniques

The oil sample compositions were classified using gas chromatography mass spectroscopy (Shimadzu GCMS-QP2010 SE) on a RESTEK Rtx-5 column (30m, 0.25 mm ID). The GC-MS method temperature profile used was 33-290 °C with a ramp rate of 4 °C/min and a column flow rate of 0.61 mL/min. Specific components were quantified using GC-FID (Shimadzu GC-2010 Plus) on a RESTEK Rxi-5Sil column (30m, 0.25 mm ID). Oil samples were also analyzed on GCxGC-FID and GCxGC-MS, which was performed by Woods Hole Oceanographic Institution, in Woods Hole, MA. The molecular weights of the residual solids were determined through gel permeation chromatography. This analysis was performed by the University of Akron Testing Services.

Sensitivity Analysis

A severity factor was developed to quantify the severity of the reaction conditions including time, temperature and peroxide loading. The traditional severity factor for time and temperature developed by Chum, et.al.[230] was used as the base form and a second term accounting

for peroxide loading was added. The form of the severity factor used can be seen in **Equation 5-1.**

$$R_w = exp\left(\frac{T_R - 100}{\omega}\right)\Delta t + exp(P * k) \qquad \textbf{Eq 5-1}$$

Where T_R is the reaction temperature in °C, Δt is the reaction time, P is the peroxide loading in O:C ratio and ω and k are fit parameters, with values of 5.9 and 4.358 respectively. The fit parameters were estimated by minimizing the R^2 for severity vs oil yield.

5.3 Results

PS is known to depolymerize primarily through beta-scission reactions that are initiated by a radical[229]. These radicals are traditionally formed from other high activation energy reactions such as hydrogen abstraction and random scission. Adding an external radical source to reactions has the potential to initiate beta-scission reactions at less severe conditions, negating the need for higher activation energy reactions to create the radicals. Hydrogen peroxide was chosen as a radical source in this work for a multitude of reasons; hydrogen peroxide breaks down at approximately 250 °C [231] which is less than HTL reaction temperatures for PS, it is a green radical source as it decomposes into water and oxygen and it is not an expensive source. Hydrogen peroxide also has the added benefit of being an oxygen source which could create valuable oxygenated byproducts from the reaction. To understand both the role of radicals in traditional HTL reactions and the potential of radical initiated HTL, reactions were run over a series of temperatures, times and peroxide loadings.

Optimization of Reaction Conditions

Existing work in the literature has shown that supercritical conditions are necessary for high oil yields[48, 226], therefore in this work a subcritical temperature of 350 °C was chosen for initial studies. This allows for the potential benefit of RI-HTL to highlighted. **Figure 5-1** shows the oil and residual solid yields for traditional HTL and three different peroxide loadings relative

to the plastic loaded prior to reaction. Peroxide loading is represented as the ratio of oxygen in the hydrogen peroxide to the carbon in the polymer. At 350 °C the HTL reaction (0 peroxide loading) has zero oil yield, and the primary reaction product is residual solid. This residual solid has the appearance of unreacted PS. It should be noted that there are also two other reaction products, the aqueous phase and the gas phase, but the amount of carbon in the aqueous phase is negligible and the gas is less that 5 wt% and comprised of primarily methane. The lack of oil and minimal gas production indicates that under these conditions HTL does not cause depolymerization of PS. The ceiling temperature, the rate at which depolymerization is equal to repolymerization in a polymer, can give insight into what temperature conditions may be necessary for complete conversion. PS has a ceiling temperature of approximately 390 °C [232], which means that below this temperature the rate of repolymerization will be greater than depolymerization and oil will not be the primary product. It should be noted that the exact impact of water on the ceiling temperature of plastics is not yet well understood and the exact ceiling temperature of PS in a hydrothermal system may vary.

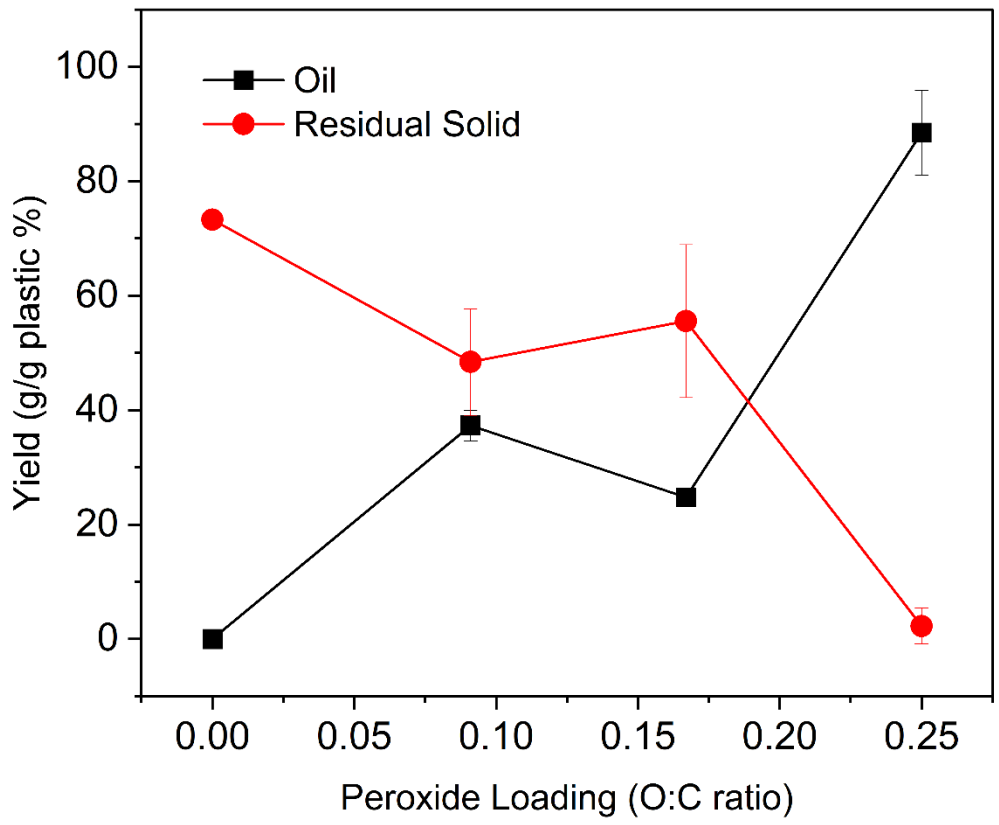

Figure 5-1 Effect of peroxide loading on oil and solid residue yields at 350 °C and 20 minutes for HTL (0 loading) and three different peroxide loadings

Going from HTL conditions to RI-HTL conditions, **Figure 5-1** shows an increase in oil yield and a decrease in residual solid, as the peroxide loading, and therefore quantity of radicals in the system, is increased. Both the 0.091 and 0.167 condition see an increase in oil yield compared to HTL, but residual solid remains the primary reaction product. This indicates that the presence of free radicals in the system has increased the depolymerization reaction as compared to HTL, but that the amount of radical is not sufficient for complete depolymerization. At a peroxide loading of 0.25 a complete flip in product distribution can be seen as compared to HTL. The oil yield at this condition is 88% ± 7% and the residual solid is less than 5% indicating near complete conversion of the PS into products. When sufficient radical is added to the system complete conversion can be achieved at conditions that result in no yield for HTL, proving external radicals

are capable of initiating depolymerization. This is a promising result but, temperature is known to be a critical factor in thermal depolymerization technologies, and understanding its effect combined with a radical source will allow for the optimization of reactor conditions and optimal technology performance.

Figure 5-2 shows the oil and solid residue yield for HTL and RI-HTL reactions with reaction temperatures from 325 °C to 400 °C. For both HTL and RI-HTL, an increase in oil yield is seen with increasing temperature with the exception of RI-HTL at 400 °C. The reduction of oil yield at 400 °C is due to the severity of reaction conditions being too high and the oil being further broken down into gas. The full mass balance including all four phases (oil, residual solid, gas and aqueous) can be seen in Appendix D **Figure D.5-9**. For subcritical conditions, other than 365 °C, HTL reactions do not result in any oil yield. While there is no oil produced at subcritical conditions, further analysis of the solid phase has shown significant chemistry has occurred within the solid. The molecular weight of the starting polymer is 176,000 Da and the molecular weight of the residual solid from HTL at 350 °C is 7,998 Da, indicating mid-chain depolymerization is occurring within the solid prior to oil production. Reactions at 365 °C show higher performance than the other subcritical conditions. This is believed to be from the water at these conditions (subcritical temperature by 9 degrees, but critical pressure) having near supercritical properties, explaining the higher performance of HTL at this temperature. For subcritical conditions, RI-HTL reactions with a 0.25 O:C ratio increase the oil yield compared to HTL. RI-HTL reactions at 350 °C result in a maximum benefit when compared to HTL increasing oil yield from less than 5% to greater than 85%.

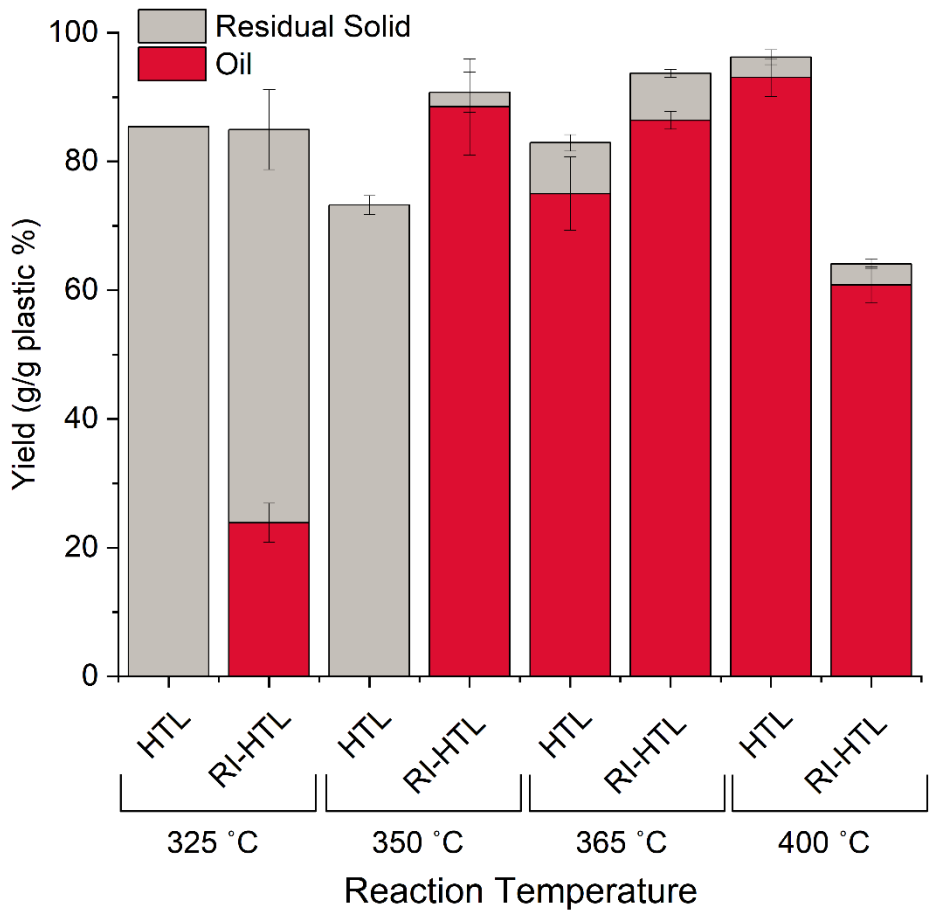

Figure 5-2 Yield in g/g plastic wt% of oil product and solid residue for HTL and RI-HTL reactions with reaction temperatures from 325 °C to 400 °C with a 20-minute reaction time. All RI-HTL runs had a O:C ratio of 0.25.

The performance of HTL reactions in the supercritical region improve significantly with HTL at 400 °C having equal yield with RI-HTL at 350 °C. At 365 °C, a near supercritical condition, HTL results in yields approximately 5% less than oil yield RI-HTL at 350°C. Although a 15-degree difference is not large, it correlates to a pressure difference of nearly 500 psi. A reduction in temperature of 15 degrees and pressure of 500 psi can drastically impact the materials and thickness of construction for reactors making the process less expensive and increase overall process safety. **Figure 5-1 Figure 5-2** established the optimal reaction conditions of 350 °C and

a 0.25 O:C ratio but further reduction of reaction condition severity could be achieved if the reaction time can be reduced.

Figure 5-3 shows the oil yield for reaction times ranging from 0 to 20 minutes at 350 °C and a 0.25 O:C ratio. With a 0-minute reaction time the oil yield is 40% ± 2%. This means that a portion of the PS is being depolymerized before the reaction temperature has been met. Considering the RI-HTL reaction at 325 °C resulted in 24% oil yield this result would be expected. As time increases to 10 and 15 minutes no increase in oil yield is observed. This result gives some insight into the depolymerization mechanism, as if the polymer was depolymerizing primarily through end-chain unzipping, as is seen for pyrolysis of PS, you would expect an increase in oil yield with reaction time. Instead, what was observed here was that there was a decrease in the molecular weight of the residual solid with time but no change in oil yield. This would suggest that the primary depolymerization mechanism in RI-HTL is mid-chain beta-scission and that with sufficient reaction time the chains will depolymerize down into small liquid molecules. The molecular weight for the 20-minute reaction is not reported as the amount of residual solid was less than could be captured and tested through GPC. The decrease in molecular weight of the residual solids can be seen visually in Appendix D **Figure D.5-10**. Further work is needed to fully understand the mechanism of both HTL and RI-HTL reactions, which will be expanded upon in Chapter 8.

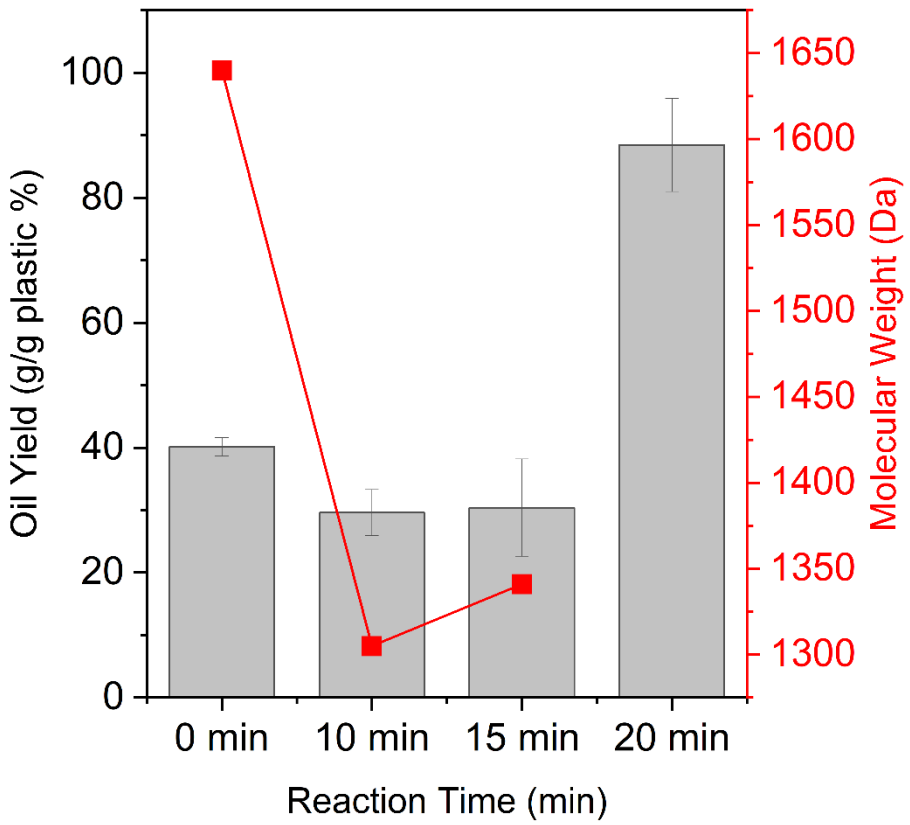

Figure 5-3 Oil yield and GPC determined molecular weight of the residual solid for reaction times from 0 to 20 minutes with a reaction temperature of 350 °C and a O:C ratio of 0.25. The molecular weight of the virgin PS was found to be 176 kDa.

In order to quantify how the severity of the reaction conditions change with the addition of hydrogen peroxide, a severity factor was developed as seen in **Equation 5-1.** This relationship was used to calculate the severity of all conditions analyzed above as seen in **Figure 5-4**. The region highlighted with the red box is the region in which RI-HTL and HTL reactions have similar oil yield performance. How the addition of hydrogen peroxide effects the severity in this region was of particular interest to fully quantify the change in severity. It can be seen that the severity of HTL at 365°C (severity of 21.8) is less than the severity of RI-HTL at 350°C with a peroxide loading of 0.25 (severity of 22.7). This indicates that although the severity of the temperature and pressure decreases, the overall reaction severity is slightly increased for RI-HTL.

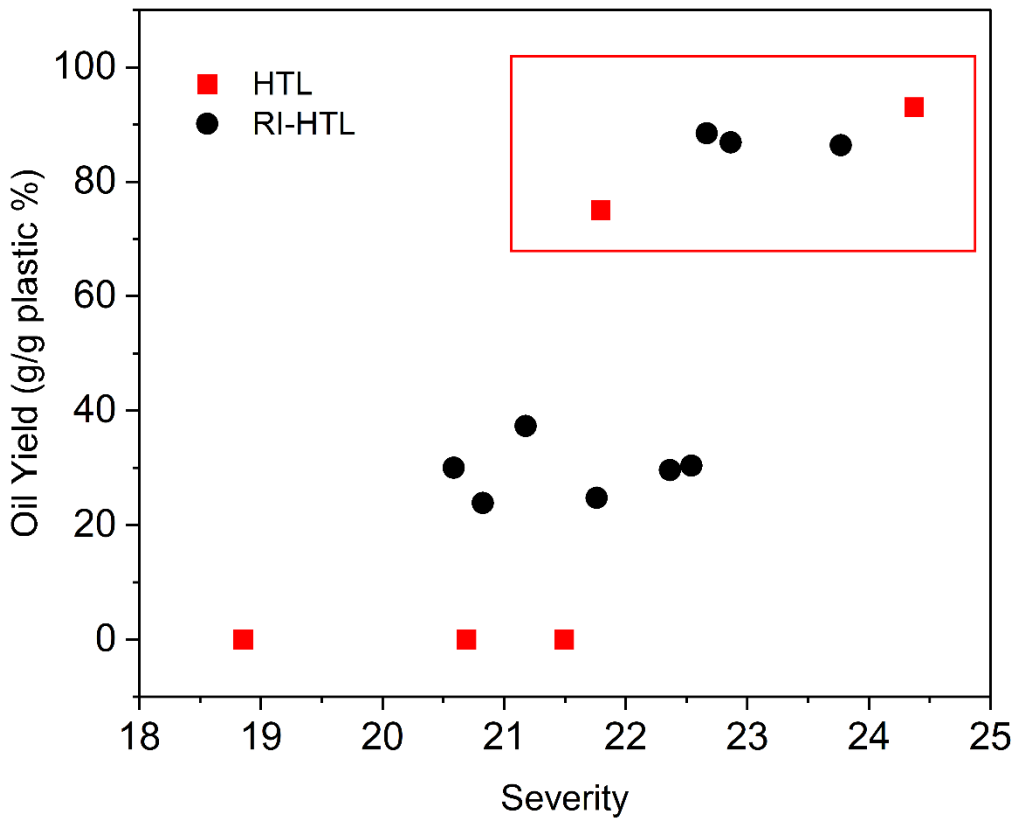

Figure 5-4 Severity analysis compared to oil yields for all reactions. The red box represents the region where RI-HTL and HTL have similar performance. The two HTL reactions within this box are at 365°C (severity factor of 21.8) and 400°C (severity factor of 24.4).

Compositional Understanding of RI-HTL Oils

The work completed in **Figure 5-1-5-3** established the optimal reactor conditions (350°C, 0.25 peroxide loading and 20-minute reaction time) for maximum oil yield from RI-HTL reactions. Although high yield is a critical factor, the composition of the oil is also critical for understanding the use and potential of any oils formed. The oil formed during the depolymerization is a complex mixture of aromatics, styrene monomers, styrene dimers and styrene trimers. To understand this complex mixture, representative samples for HTL and RI-HTL were analyzed using GCxGC-MS and GCxGC-FID and all samples were analyzed using GCMS.

Figure 5-5 shows the GCxGC-FID of the oil produced by an HTL reaction at 400 °C and a 20-minute reaction time. There are three distinct regions seen within the chromatogram, which have been identified as regions of single ring aromatics, two-ring aromatics, and three-ring aromatics. The single ring aromatic region which is in the region of 500s to 3000s in the first-dimension retention time is comprised primarily of styrene monomer and other simple one-ring aromatics such as toluene, ethylbenzene and alpha-methylstyrene. The second region from 3000s to 6500s is comprised of styrene dimers and other two-ring aromatics. The final region seen is comprised of styrene trimers and 3-ring aromatics. It should be noted that there are no oxygenated components found in the oil formed during HTL reactions. From the overlaid one-dimensional GC chromatogram and from the GCMS chromatogram seen in Appendix D **Figure D.5-11**, it can be seen that the one-dimensional GC is able to identify all major peaks within the oil.

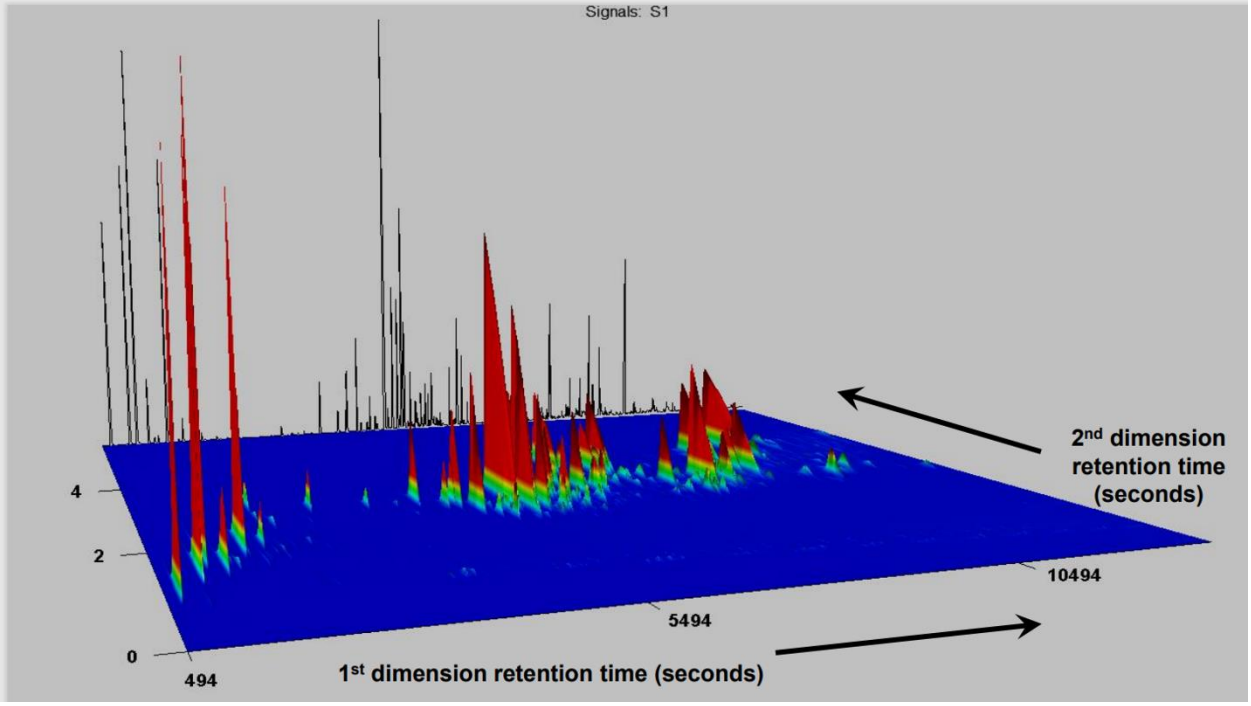

Figure 5-5 GCxGC-FID of HTL at 400 °C and 20-minute reaction time with the one-dimensional GC-FID chromatogram overlaid.

Figure 5-6 shows the GCxGC-FID for the RI-HTL reaction at 350 °C and a 5:1 C:O ratio. Once again three distinct regions correlating to single ring, two-ring and three-ring aromatics can be seen. Although the three key regions still exist, the single ring aromatics identified are primarily oxygenated aromatics such as benzaldehyde and acetophenone, with some styrene and other unoxygenated aromatics. The two and three-ring aromatic regions remain primarily unchanged. Once again, this representative two dimensional GC when compared to the overlaid one-dimensional GC-FID and the GCMS chromatogram seen in Appendix D **Figure D.5-12**, indicates all major peaks are being capture in the one-dimensional GC. **Figures 5-5 and 5-6** give confidence to the predictions made by GCMS and GCMS was used for all further analysis.

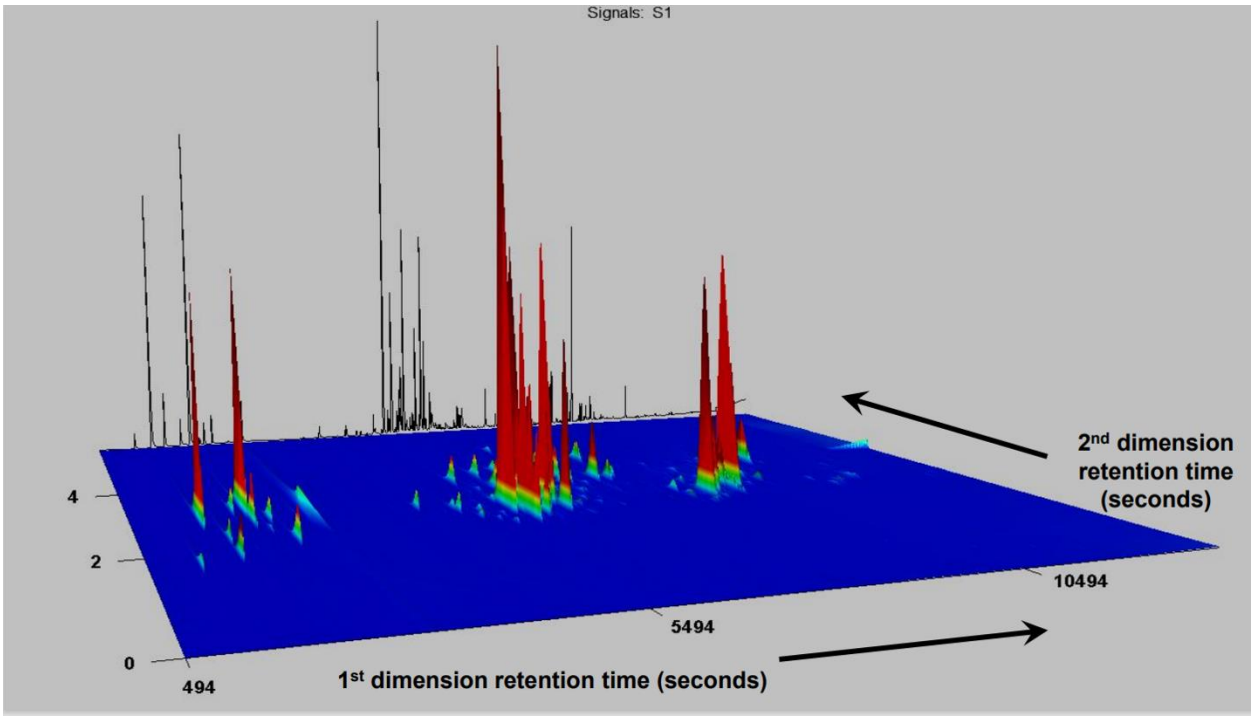

Figure 5-6 GCxGC-FID of RI-HTL at 350 °C, 0.167 O:C ratio and 20-minute reaction time with the one-dimensional GC-FID chromatogram overlaid.

As the hydrogen peroxide loading is increased more and more oxygen is added to the system ending up primarily in either the gas or oil phases. **Figure 5-7** tracks 5 key product

categories based on their percentage of the total area in the GCMS chromatogram. The correlating GCMS chromatograms can be seen in Appendix D **Figure D.5-12**. The product categories of interest are oxygenated single ring aromatics (such as benzaldehyde and acetophenone), single ring aromatics (such as styrene and toluene), two-ring aromatics (including styrene-dimers), oxygenated two-ring aromatics and three-ring aromatics (including styrene trimers). As the amount of hydrogen peroxide in the reaction increases, the amount of oxygenated single-ring aromatics found in the oil increases and the amount of unoxygenated single-ring aromatics decreases. There is also an interesting optimal recovery of single-ring aromatics when the peroxide loading is 0.167, however this also correlates to the lowest oil yield. The reason for this optimal requires further study that will be explained further in Chapter 8. **Figure 5-7** suggests that for optimal oil yield and maximum oxygenated single ring aromatics recovery a peroxide loading of 0.25 should be used.

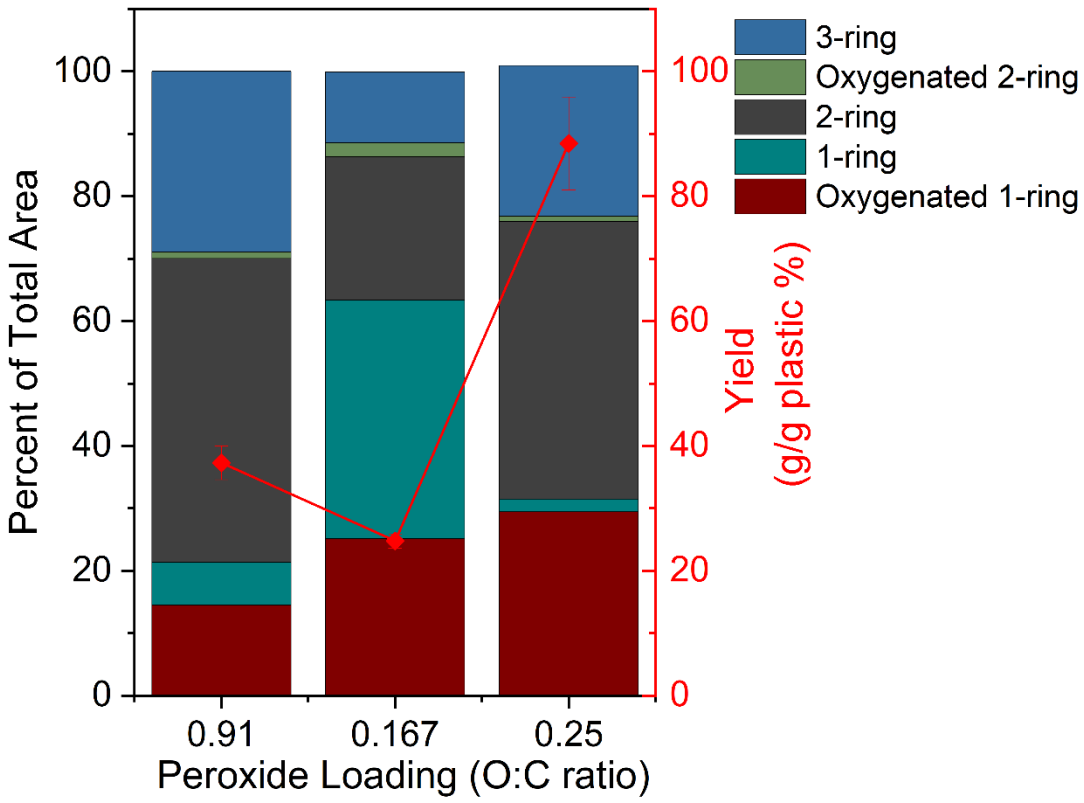

Figure 5-7 Effect of peroxide loading on oil composition and oil yield for reactions at 350 ˚C and 20-minute reaction time

Increasing the temperature with a constant peroxide loading will increase the severity of the reaction conditions and the effect of this severity on oil composition can be seen in **Figure 5-8**. The corresponding chromatograms can be seen in Appendix D **Figure D.5-13**. As the reaction temperature increases from 350°C to 365 °C, an increased degree of depolymerization can be seen in the increase in single ring aromatics, oxygenated or unoxygenated, and the corresponding decrease in two and three-ring aromatics. This suggests that at the high reaction temperature the two and three-ring aromatics are being further depolymerized into single ring aromatics. The amount of oxygenated single ring aromatics also decreases at 365 °C. At 400 °C the percentage of

the oil comprised of two and three ring aromatics increases, indicating that the gas produced (correlating to the drop in oil yield) comes primarily from the decomposition of the single ring compounds. **Figure 5-8** indicates that with relatively small changes in reaction temperature there is a tunability to the composition of the oil. The optimal temperature for high value oxygenated single ring aromatics is seen at 350 °C.

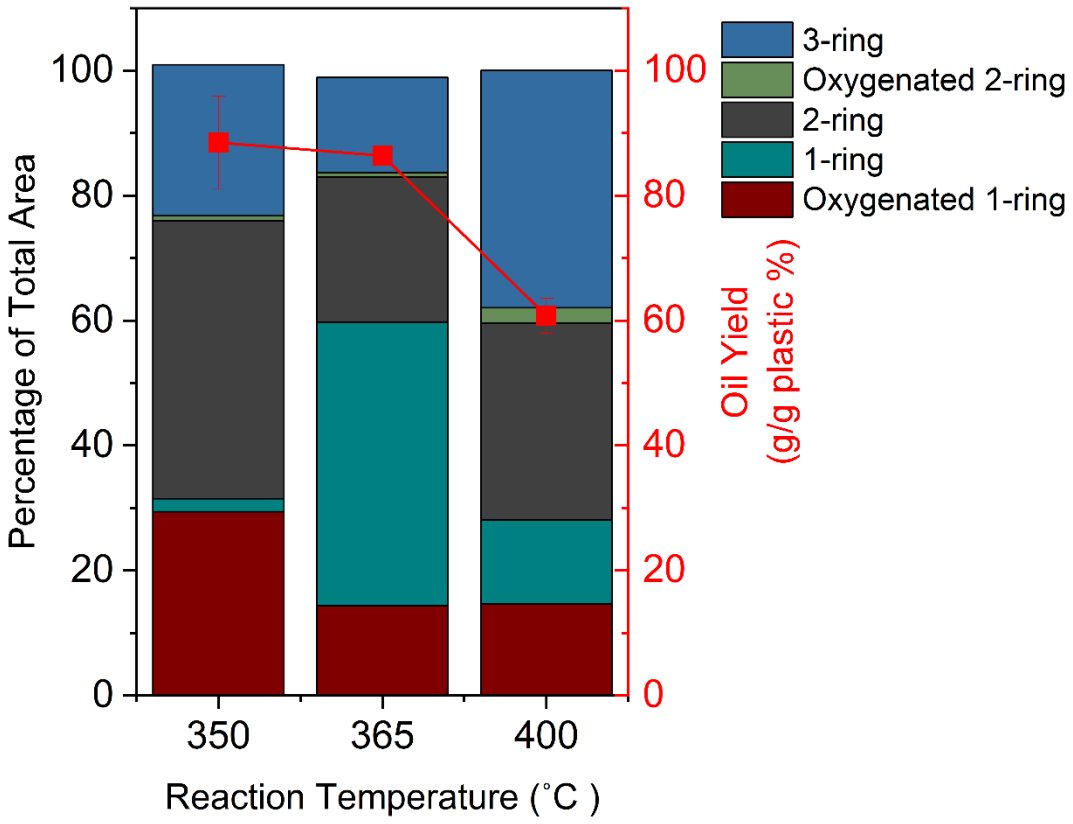

Figure 5-8 Effect of temperature on oil composition for a 0.25 peroxide loading and 20-minute reaction time based on the percentage of total area under their corresponding GCMS chromatogram.

Finally the effect of time on the composition of the oil was studied. It was seen in **Figure 5-3** that increasing reaction time did not correspond to increasing oil yield until 20 minutes, however it did correspond to an decrease in the molecular weight of the solid. **Figure D.5-14** and

Figure D.5-15 in Appendix D shows the compositonal changes in the oil with time. A minor decrease in the amount of oxygenated single ring aromtics was seen from 0 to 15 minutes, but no notable differences in the oil composition were observed. This suggests that as the reaction time progresses depolymerization happens primarily in the solid phase. Only once the solid phase has been almost entirely converted to oil does the composition of the oil start to have appreciable changes.

5.4 Conclusions

The work done in this study has shown the potential for radical initiated hydrothermal liquefaction to reduce the severity of reaction conditions necessary for complete depolymerization of polystyrene. It has shown that external radicals can eliminate the need for the high activation energy reactions that produce radicals in traditional HTL and initiate beta-scission at milder conditions. It has also demonstrated the potential of this technology to increase the value of the reaction products by producing high value oxygenated single ring aromatic compounds. The effect of reaction temperature, reaction time and radical loading on both oil and residual solid yields and oil compositions have been shown and an optimal reaction condition of 350 °C, 20-minutes and 3:1 loading has been demonstrated to result in highest oil yield and oxygenated single ring aromatic recovery.

5.5 Appendix D

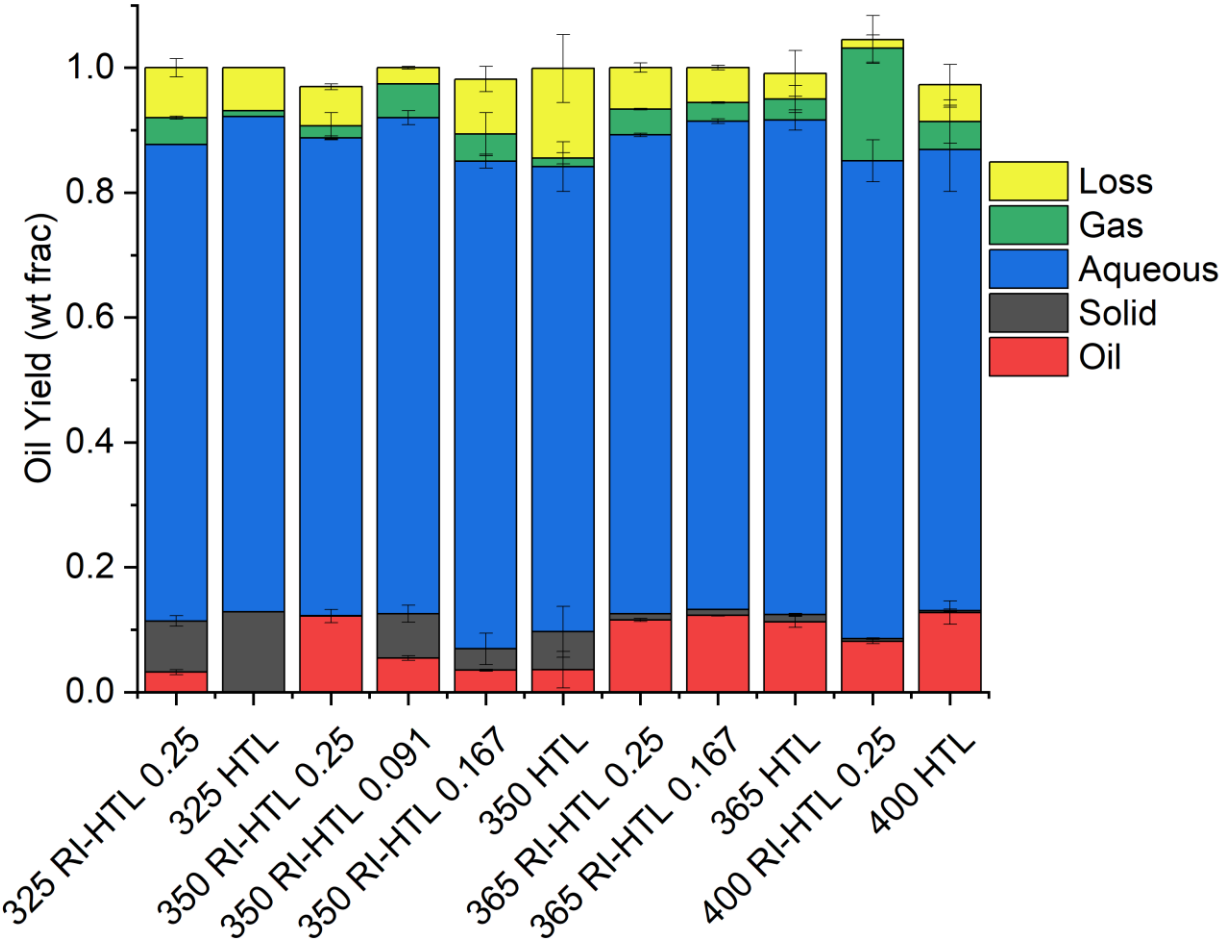

Figure D.5-9 Full mass balance for HTL and RI-HTL reactions with reaction temperatures from 325 °C to 400 °C

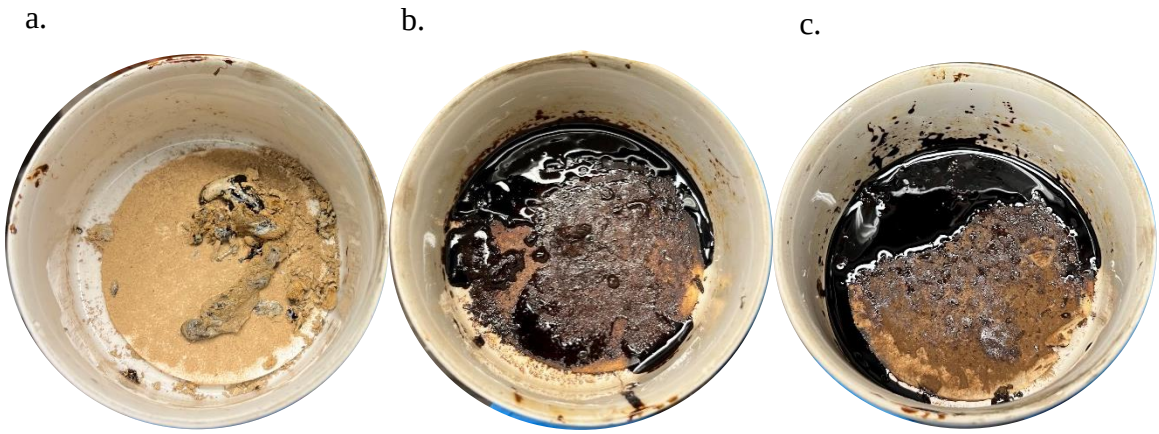

Figure D.5-10 Residual solid and wax from RI-HTL reactions at 350 °C and a 0.25 peroxide loading for a.) 0-minute reaction time, b.) 10-minute reaction time and c.) 15-minute reaction time.

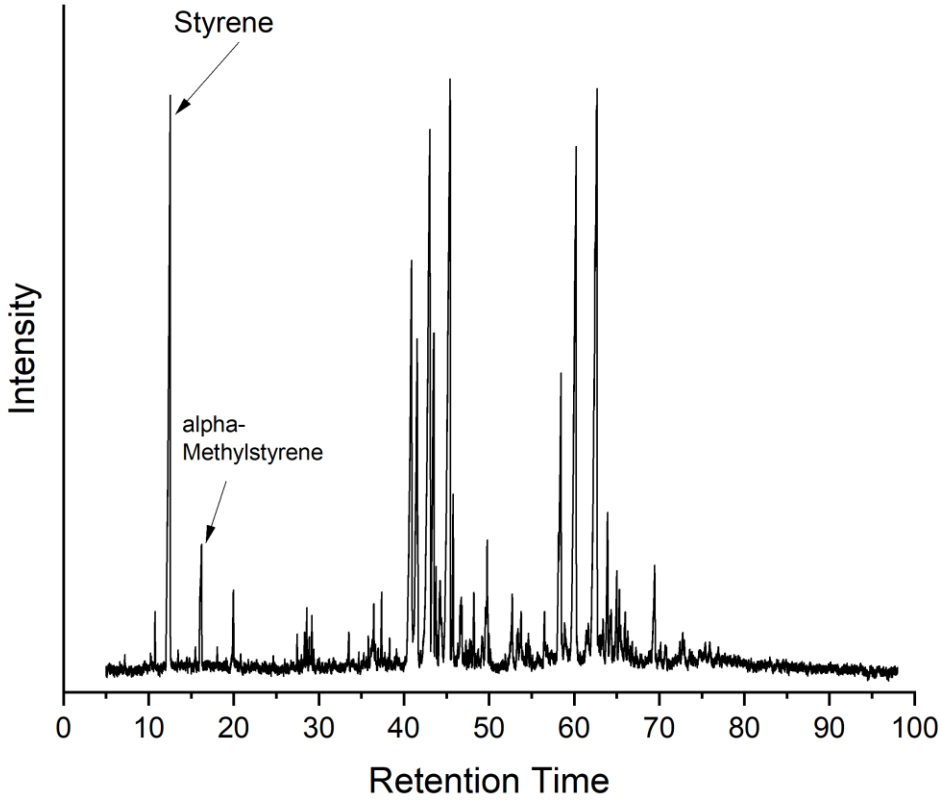

Figure D.5-11 GCMS chromatogram for HTL at 400 °C and 20-minute reaction time with select single ring aromatic compounds highlighted

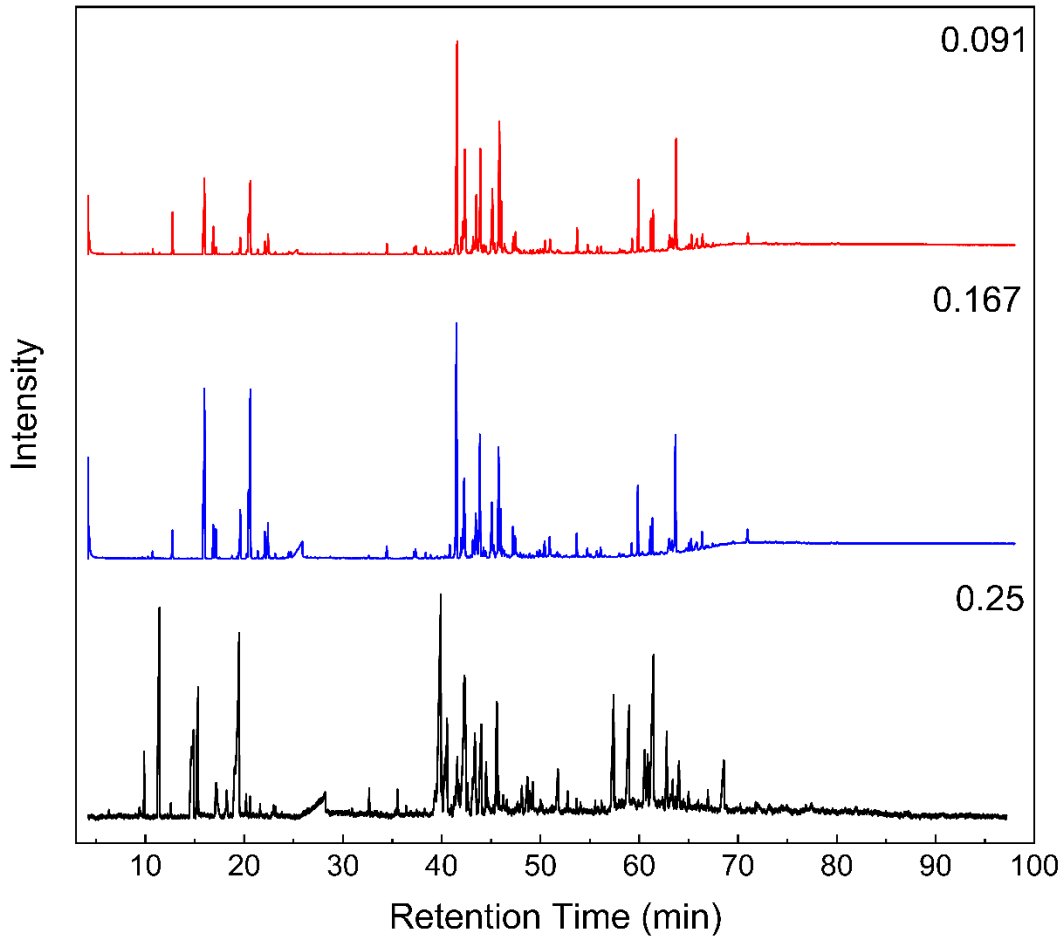

Figure D.5-12 GCMS chromatograms of RI-HTL reactions at 350 °C, 20-minute reaction for peroxide loadings of 0.091, 0.167 and 0.25

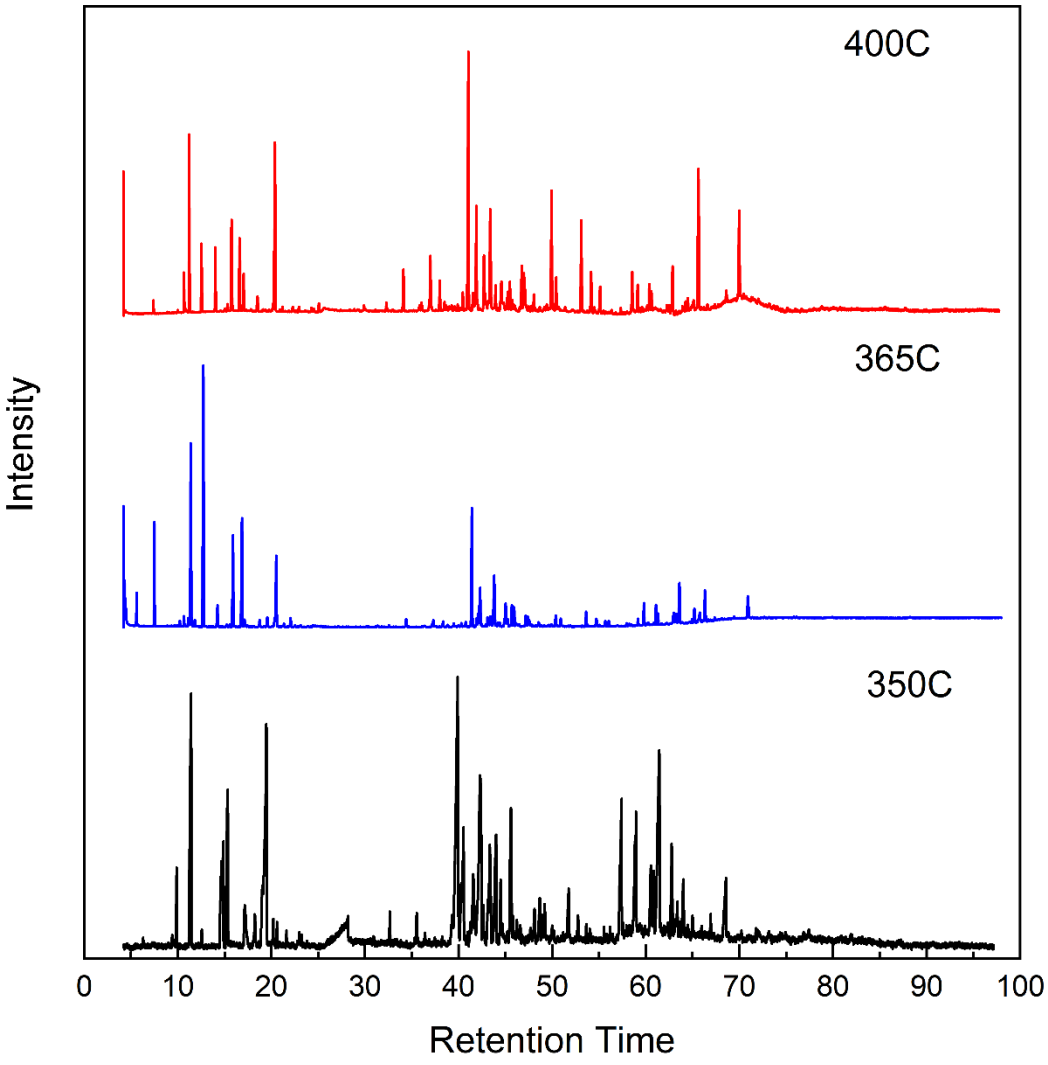

Figure D.5-13 GCMS chromatograms of RI-HTL reactions with 0.25 peroxide loading and 20 minute reaction times for various reaction temperatures.

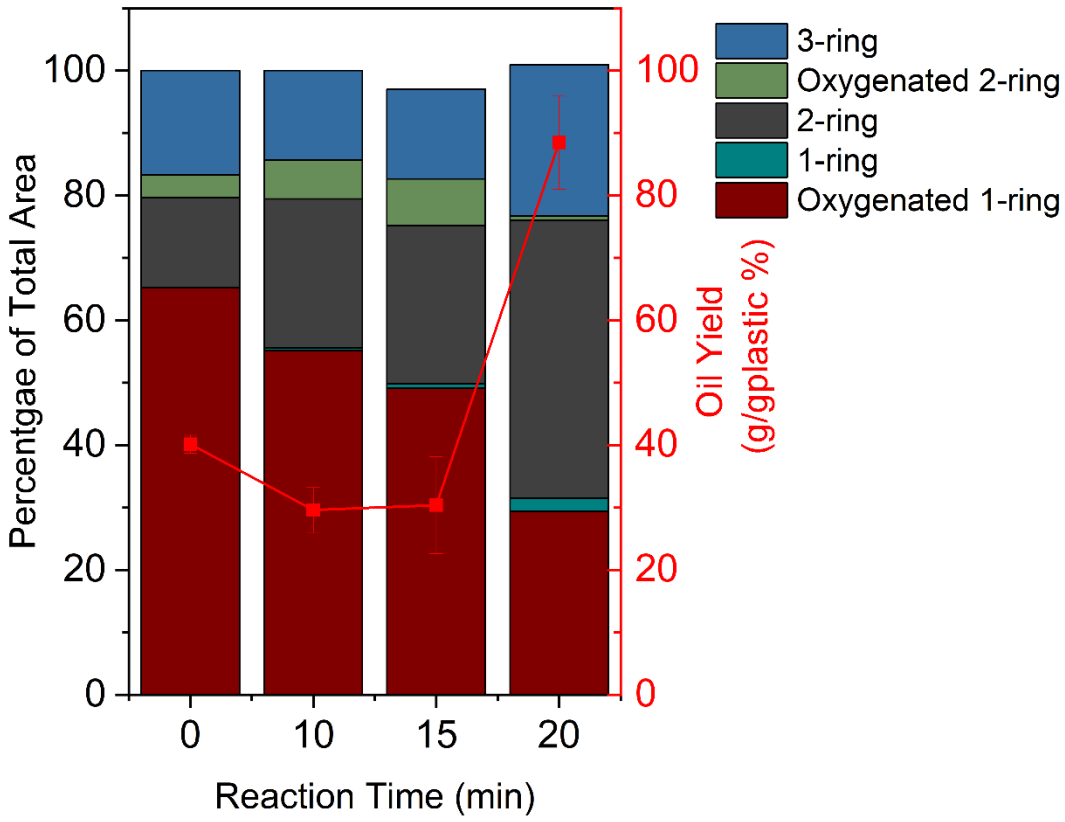

Figure D.5-14 Effect of reaction time of RI-HTL reactions at 350 °C and a 0.25 peroxide loading on the composition of the oil in percentage of the total area from GCMS analysis.

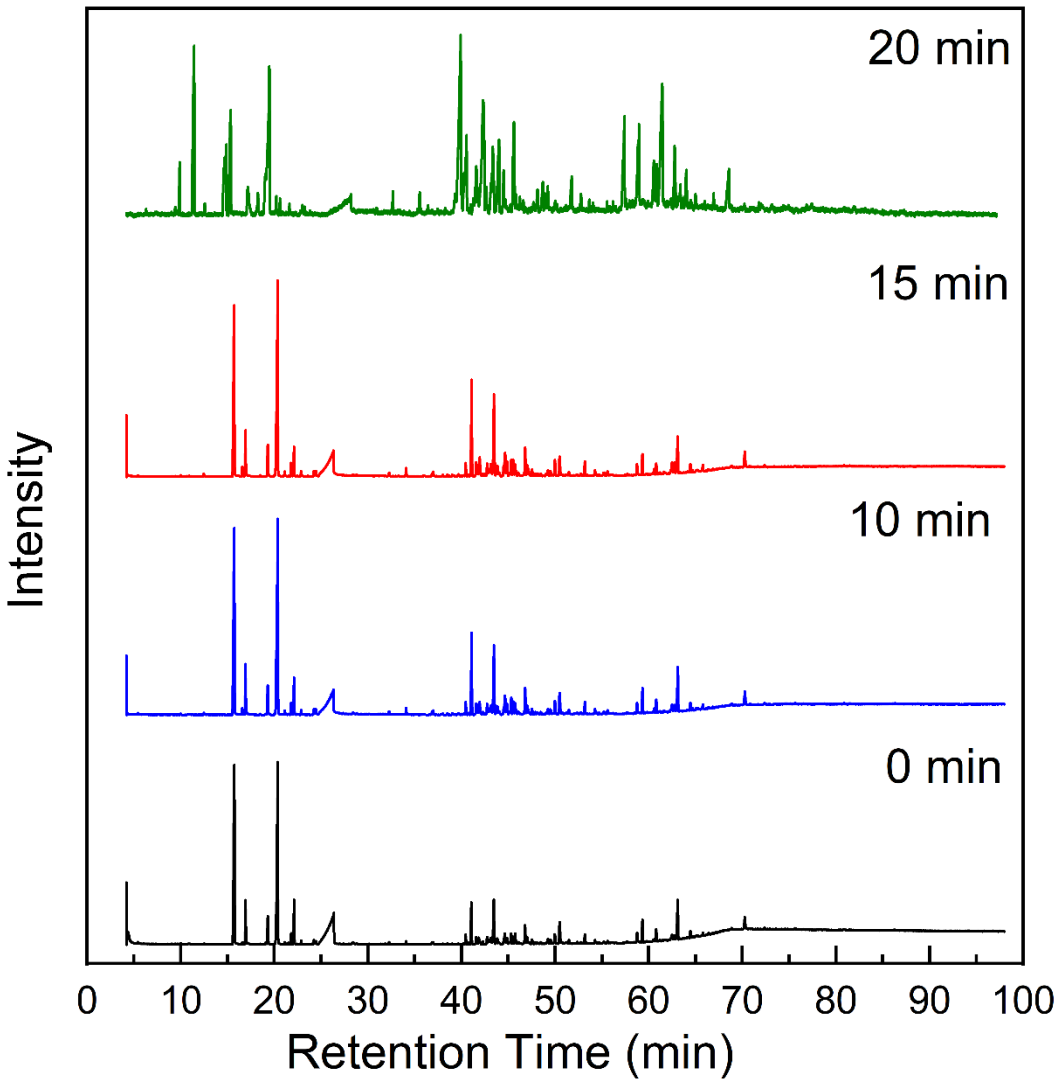

Figure D.5-15 GCMS chromatograms for RI-HTL reactions at 350 °C and a 0.25 peroxide loading at reaction times from 0 to 20 minutes.

Chapter 6: Data driven discovery of reaction pathways for understanding catalytic cracking of hydrocarbons in the presence of catalyst

6.1 Introduction

Polyethylene (PE) accounts for 42% of the plastic found in municipal solid waste in the United States[4]. Although high density polyethylene (HDPE) is one of the three plastics with a robust recycling market [3] its recycling rate is only approximately 30%[4]. Various factors like needing pure PE streams for recycling and sensitivity to contaminants (i.e., plastic additives, residual products, labels, etc.) contribute to this low recycling rate. On the other hand, low density polyethylene (LDPE) has limited recycling potential under current technologies[4]. The low recycling rate and high landfill rate has led to accumulation of PE waste in the environment [7, 233].

Addressing the issue of waste plastic will require a comprehensive strategy including development and greater use of biodegradable plastics[77], reduced waste,[76] and improved upcycling technologies. Even with all of these techniques there will still be waste plastic that must be valorized, since eventually it will accumulate defects and impurities that result in it reaching the end of its useful life [234]. Chemical recycling is a promising way to address this remaining waste fraction but further study is needed to bet understand these reactions, for optimal recycling.

Thermal cracking of polyethylene molecules via thermal processes such as pyrolysis and hydrothermal liquefaction (HTL) have showed promise in converting the long PE chains into shorter linear alkanes [169, 235-237]. These linear alkanes can be used as a diesel like fuel or be further upgraded using catalysts into valuable chemicals [238-240]. Using at least a portion of these fuels for chemical conversion is economically promising due to the higher value of the chemical products as compared to the fuel. The thermal conversion of PE into short linear alkanes has been studied significantly already [169, 235-237], and therefore this work aims to better understand the second half

of the previously described upgrading scheme, the upcycling of the short chain linear alkanes into valuable chemicals.

Upgrading these short chain linear alkanes into commercially viable yields of valuable products will require the use of catalysts. The oil that results from the thermal depolymerization of polyethylene is a highly complex mixture of alkanes, alkenes, aromatics and napthenes[183]. Catalytic upgrading allows for the conversion of these complex mixtures into specific desired products and with specific properties. Studies have demonstrated the power of catalytic upgrading of bio-oils for targeting BTEX (benzene, toluene, ethylbenzene and xylene) and other aromatic hydrocarbon compounds[241]. Catalysts have also been used to increase the quality of oils by increasing the higher heating value, reducing viscosity and increasing the C/H ratio [242]. The use of catalysts for upgrading of oils is therefore a beneficial process but further adds to the complexity of the system when needing to understand reaction kinetics.

Understanding reaction networks, including reaction rate constants, is required for reactor design and currently remains an unsolved challenge due to the complexity of the decomposition pathways. The decomposition products from the thermal conversion of PE span a large range of carbon numbers, with products primarily in the range from C7 to C18 reported,[243] and tracking the kinetics of each product during upgrading results in an immensely complex reaction network. To address this complexity this work utilizes dodecane as a model compound, as dodecane is a common short chain linear alkane produced during PE decomposition. Furthermore, the data used in this study looks at the supercritical cracking of dodecane in the presence of ZSM-5 [240], as ZSM-5 has been shown in previous studies to be a good catalyst for upgrading short chain alkanes[244, 245].

Historical approaches to modeling reaction networks often involve either attempting to reconstruct from elementary reactions [246] or group type models [240]. Group type models simplify the reaction network by grouping like products and tracking the product groups during the reaction, instead of tracking each individual product[247-249]. The products that are grouped together are determined through a combination of chemical knowledge, published models and a researchers "chemical intuition" of the system. However, this approach quickly becomes complex as the number of products increases, until the system is too complex for human intelligence. Utilizing data-drive methods, allows for the mathematical identification of similarity to form like product groups, allowing for the analysis of immensely complex systems.

A promising data-driven method for this type of identification is dendrograms. Dendrograms represent data from dimensional space as a tree with the vertical axis indicating similarity [57]. The branches at the bottom of the tree will be most similar to each other and become less similar with every node going up the tree. This method is promising for the application of group type modeling as it mathematically determines the similarity between products and offers multiple layers of possible groups depending on the desired number of product groups. Dendrograms also can work with data that has more features than data points, which is often the case in kinetic modeling data sets.

In this work dendrograms will be used to indicate similar product groups for use in a group type model for the supercritical cracking of dodecane in the presence of ZSM-5. These groups will then be used to model the reaction network for this reaction, including the optimal reaction pathway and the targeting of specific desirable products.

6.2 Methods

Algorithm Development

Traditionally in machine learning large amounts of data are required (>100,000 data points[52, 53]) and there are significantly more data points than features (i.e. more rows than columns), however for this application studying the supercritical cracking of dodecane in the presence of ZSM-5 the data has 6 rows corresponding to 6 time points and 21 columns corresponding to the time-dependent dodecane conversion and the carbon yield of 20 reaction products. This misbalance of data points to features limits the type of data-driven method that can be used. For this reason, dendrograms were chosen as they are an unsupervised classification method that can be used to determine the similarity between data. Dendrograms are a form of hierarchical clustering that represent data from dimensional space as a tree with the height of the tree representing similairty[57]. Similarity is typically calculated using one of four methods, single linkage, complete linkage, average linkage and centroid distance [57]. The similarity method that was used within the dendrogram algorithm was chosen to be average linkage. Equation 6.1 shows how average linkage is computed.

$$\boldsymbol{Similarity} = \frac{\boldsymbol{T_{rs}}}{(\boldsymbol{N_r} \times \boldsymbol{N_s})} \qquad \textbf{(6.1)}$$

Where T_{rs} is the sum of all the pairwise distances between cluster r and s, and N_s and N_r are the sizes of cluster s and r respectively[250]. The raw experimental data was fed into the hierarchy dendrogram package from scripy cluster in Python 3.6.9.

The data was also normalized in two different ways, a scale transform and a z-transform. The scale transform seen in Equation 6.2 normalized the data between the values of zero and one.

$$\boldsymbol{X_{i,j\,new}} = \frac{\boldsymbol{x_{i,j}}}{\boldsymbol{x_{i,max}}} \qquad \textbf{(6.2)}$$

Where $X_{i,j\ new}$ is the new x value, $x_{i,j}$ is the carbon yield value of x for product i at time j and $x_{i,max}$ is the maximum value of x for product i across all time points.

The z-transform, seen in Equation 6.3, standardizes the data such that the mean of the sample is zero[251].

$$Z_i = \frac{x_{i,j} - \bar{x}_i}{\sigma_i} \quad (6.3)$$

Where Z_i is the new value, $\bar{x}_i$ is the mean of the yields for product i and σ_i is the standard deviation of product i.

Data Selection

The dataset used in this study was chosen for two key reasons. The first was that dodecane is a common product formed during the depolymerization of PE and therefore a good model compound for understanding the upcycling potential of PE products. The second key reason this dataset was chosen was because the data has already been analyzed using group type modeling [240], providing an important comparison for the performance of data-driven methods.

Kinetic Model Development

The kinetic model used for the group type reaction modeling was a first order reaction. The model was developed in MATLAB and estimated the value of the group carbon yield by minimizing the error between experimental and calculated yields by changing the rate coefficients. The model tested all possible reaction pathways with the limitations of the C12 group being first and that only in series or in parallel reactions are allowed, no combinations were allowed in this study. The accuracy of the kinetic model was determined using two error metrics, Sum of Squared Error (SSE) and Maximum Absolute Error (MAE) as seen in Equations 6.5 and 6.6 respectively.

$$SSE = \sum\sum\left(C - C_{exp}\right)^2 \quad (6.4)$$

$$MAE = max\left|C - C_{exp}\right| \quad (6.5)$$

Where C is the calculated value of the carbon yield of the group and C_{exp} is the experimental carbon yield.

6.3 Results & Discussion

Identification of group type modeling groups using dendrograms

The previous study that the data in this work is sourced from created a kinetic model for the supercritical cracking of dodecane using group type modeling [240]. Zaker, et. al. used a combination of literature, knowledge of chemical groups and analysis of conversion to group the products into five groups; aromatic, aliphatic, heavies, coke and gas. These groups were then used for a kinetic study of dodecane cracking in the presence or absence of supercritical water. While a viable and established method for determining groups in group type modeling, this approach can be time consuming and is susceptible to human bias. This study aims to develop a rapid and unbiased mathematical method to group products in kinetic studies for group type modeling.

In order to develop this method the raw experimental data (seen in the **Appendix E Table E.6-4**) was fed into the dendrogram algorithm. Since dendrograms are an unsupervised method the time data associated with the carbon yields of each product is not fed to the algorithm. The resulting dendrogram can be seen in **Figure 6-1**. C12, which is the dodecane feed, is the most dissimilar compound in the data as its node has the largest distance indicated by the vertical axis. Dodecane should be dissimilar from its products as it the only component present at the start of the reaction, so this result matches what is expected. This is an initial indicator that although there is very little data the dendrogram is able to identify this dissimilarity. Once the dendrogram is created human intuition is needed in order to read and interpret the results. The dendrogram itself could be read such that each pairing, or individual compound is its own group, however this only reduces the number of groups by half or less which still leaves a fairly complex reaction to model. For this

reason, larger groups were identified from the dendrogram, by making the group cuts higher on the vertical axis.

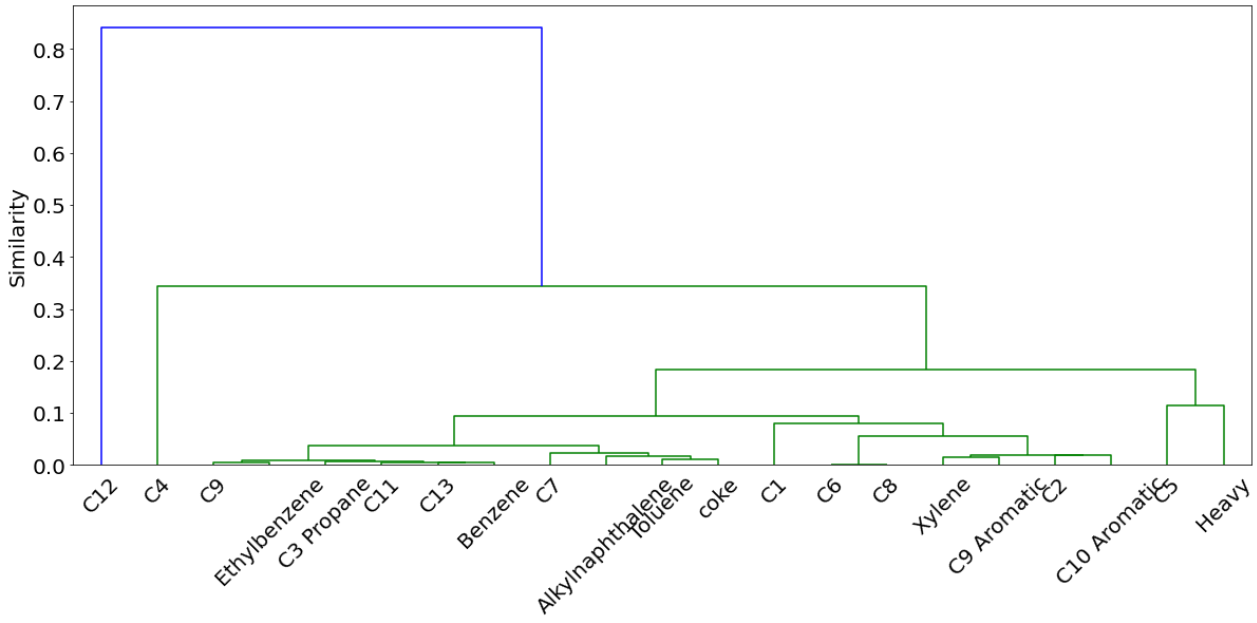

Figure 6-1 Dendrogram for the experimental carbon yield data from the supercritical cracking of dodecane computed using average linkage.

The groups that were indicated from **Figure 6-1** can be seen in **Table 6-1**. Group 3 consists of the products in the cluster directly to the left of the C5/Heavy cluster up to C1 and Group 4 consists of all the products from coke to C9. C4 was combined with the C5 and heavies cluster due to the insignificant difference in similarity. It should be noted that these groups are very different from those that were identified using the previous method described[240]. Non-mathematical methods group the gases, the aliphatic and the aromatic compounds in separate groups. In this analysis these compounds are distributed throughout the various groups.

Table 6-1 Groups indicated by experimental and z-transformed carbon yield dendrograms.

Group Number	*Experimental Carbon Yield*	*Z-Transformed Carbon Yield*
1	C12	C12
2	C4, C5 and Heavies	Benzene/C6
3	Small alkanes and aromatics (not benzene)	C11/C8/C7/C9
4	Large alkanes, benzene and coke	Small Alkanes, Aromatics, Heavies and Coke

In an attempt to determine if the lack of data was impacting the dendrogram, and therefore the group's, various fit methods were applied to the raw data to generate more artificial data between the experimental time points. Linear regression, piecewise linear regression and spline fitting were tested with 1,000 data points generated and the resulting dendrograms differed from Figure 1 in the scale of their vertical axis alone. This means that they indicated the same groups as the raw data, further strengthening the mathematical validity of the groups indicated above. The resulting dendrograms can be found in the **Appendix E Figure E.6-9Figure E.6-11**.

Due to the decision to create larger groups, further analysis tracking the carbon yield of each group over time was performed. This analysis, seen in **Figure 6-2**, confirms that these groups are physically different over time. If they were not physically different, i.e., the carbon yields of certain groups were the same as each other, it could indicate that cuts made in order to form the groups were made too high up on the dendrogram and the dissimilarities seen in the dendrogram have been lost.

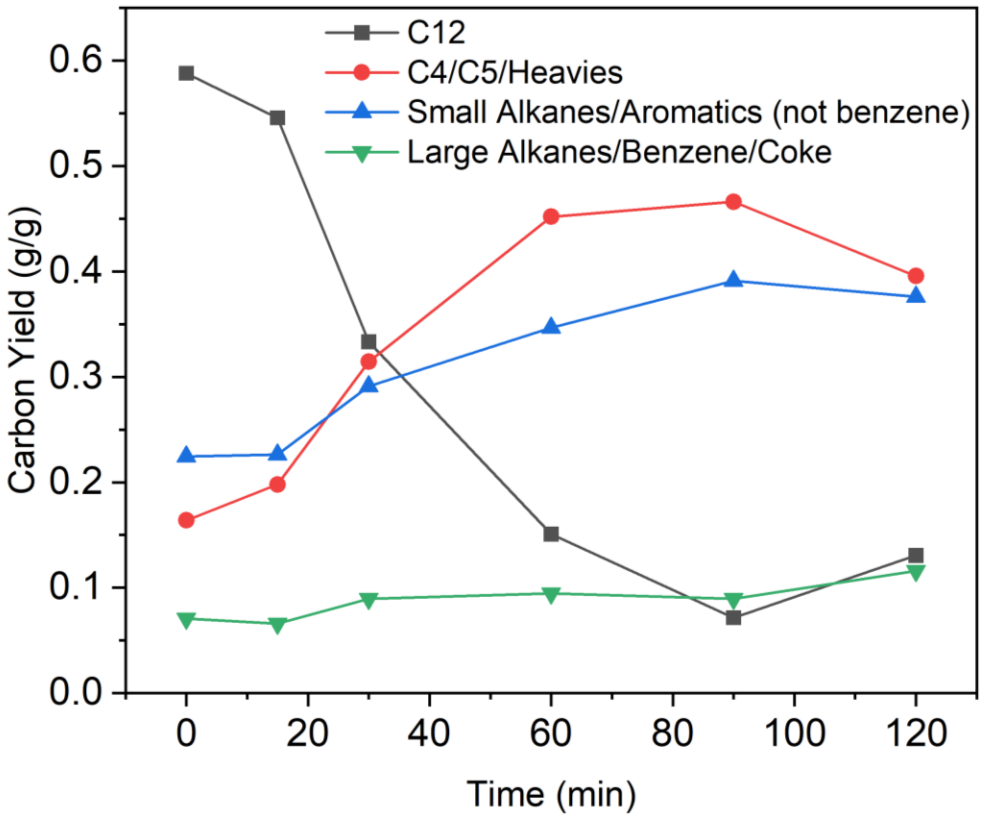

Figure 6-2 Concentration of each dendrogram indicated group over time

In addition to feeding the raw data into the dendrogram algorithm, the data was also normalized using both a scale transform and a Z-transform. By normalizing the data, the impact of the absolute value of carbon yields can be eliminated in order to determine if those values are more important in the dendrogram than the shape of the data over time. This normalized data was fed into the same dendrogram algorithm and the resulting dendrogram for the Z-transformed data can be seen in **Figure 6-3** and in **Figure E.6-12** for the scale transform data. As can be seen in **Figure 6-3** and the groups in **Table 6-1**, the dendrogram changes significantly as compared with the dendrogram using the raw data. This indicates that the absolute value of the carbon yields is the strongest factor impacting similarity when the raw data is used. Depending on the application this should be considered when determining which dendrogram to use.

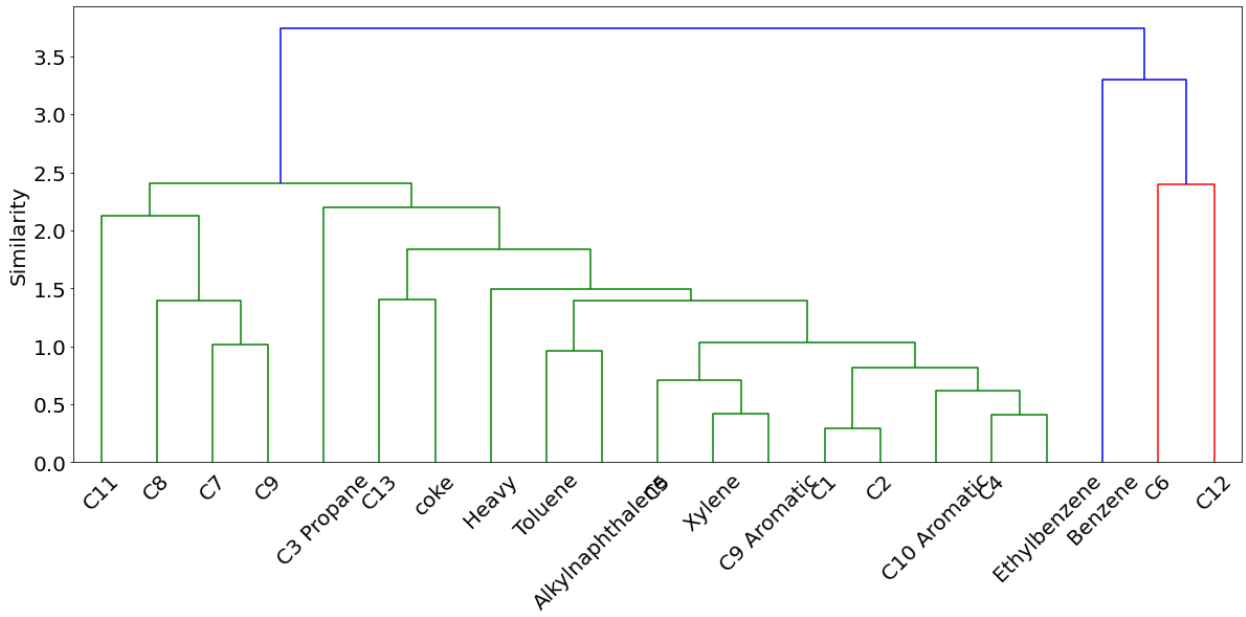

Figure 6-3 Dendrogram for the Z-transformed carbon yields of supercritical cracking of dodecane

Kinetic modeling utilizing dendrogram identified groupings

To test the accuracy of the groups that were indicated in the previous section, they were used in a kinetic model to predict the carbon yields of each group over time. Although the dendrograms can be used to group similar reaction products, they do not provide any information as to what order these groups are formed. Therefore, all possible reaction pathways were modeled with the only restrictions being C12 must be the first group and all following reactions occur either all in parallel or all in series.

The results of the kinetic modeling can be seen in **Table 6-2** for the groups indicated from **Figure 6-1** (Experimental Carbon Yield in Table 1). When considering the range of carbon yield for each group seen in **Figure 6-2** all of the reaction pathways give a decent fit depending on the required accuracy of the specific application. Some of the reaction pathways did have more accuracy than others especially reaction P and reactions S1 and S2.

Table 6-2 Sum of squared errors and average maximum absolute error for kinetic modeling of each possible reaction pathway

Reaction Pathway	**Reaction Name**	**Sum of Squared Errors**	**Average Max Absolute Error**
↗ 2 1 → 3 ↘ 4	P	0.0332	0.0582
1 → 2 → 3 → 4	S1	0.0337	0.0584
1 → 2 → 4 → 3	S2	0.0344	0.0589
1 → 4 → 2 → 3	S3	0.0466	0.0787
1 → 4 → 3 → 2	S4	0.0765	0.0776
1 → 3 → 2 → 4	S5	0.0703	0.0756
1 → 3 → 4 → 2	S6	0.0778	0.0819

For the lowest error reported in **Table 6-2** (reaction P) the calculated carbon yields were plotted verse time and verses the experimental yields as seen in **Figure 6-4**. **Figure 6-4a** shows the parity plot for this model with the solid line indicating the 1:1 line where calculated and experimental data are equal and the dotted lines showing ± 5%. Overall, there is a good clustering around the 1:1 line showing that the calculated yields are close to the experimental data. This trend can also be seen in **Figure 6-4b** where the calculated (solid line) carbon yields are tracked over time and the experimental yields are shown through the open circles. The calculated yields seem to have the most trouble matching the experimental data at the 60-minute time point, which could

be due to the fact that the standard deviation of the experimental data at 60 minutes is the highest of any time point.

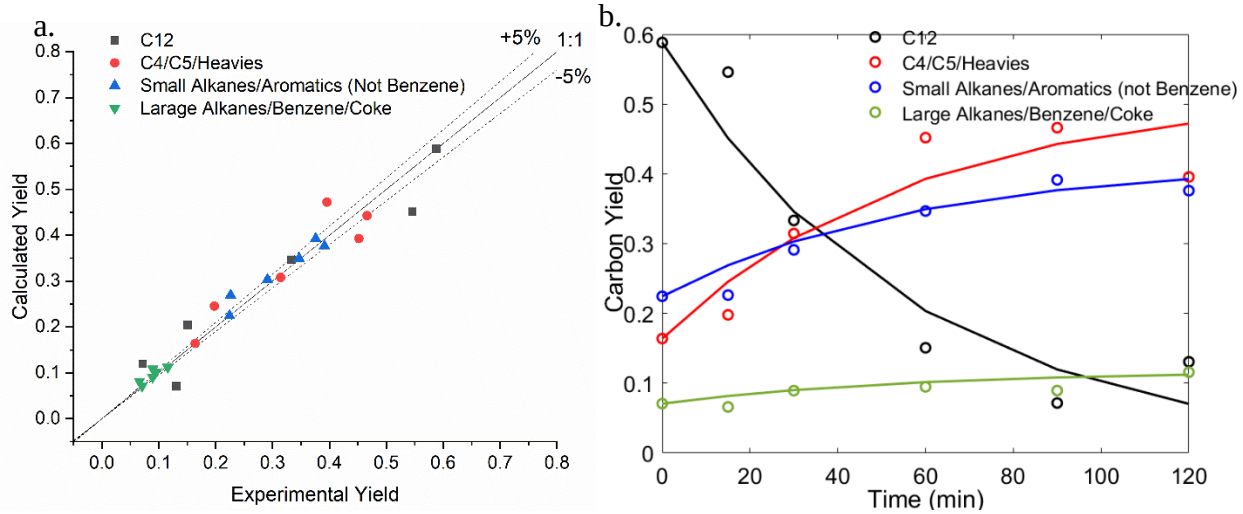

Figure 6-4 Kinetic modeling results for reaction P (all reactions in parallel) vs a.) the experimental carbon yields for each group and b.) time with the open circles indicating experimental data and the solid line being the calculated yields

Seeing the accuracy achieved with the four groups indicated from the dendrogram, the method was tested again but with three groups, combining groups 2 and 3. Testing three groups allowed for the determination of whether there was a lower limit on the number of groups modeled and still have accurate carbon yield predictions. The results of this analysis can be seen in **Appendix E Figure E.6-13** and

Table E.6-5. Once again, the reaction pathway of all reactions in parallel gave the lowest error with an SSE of 0.0322. The errors with three or four groups are very similar for the all reactions in parallel pathway indicating that this reaction pathway gave the most accurate prediction of carbon yields. For this reason, future sections will look at the reaction pathway of all reactions in parallel.

The same kinetic model was also used to model the groups that were indicated in **Figure 6-3** from the normalized carbon yield data. Again, the reaction pathway of all reaction in parallel gave the lowest SSE and these results can be seen in **Figure 6-5**. The SSE of these groups for all reactions in parallel was found to be 0.0414 which is higher than the kinetic model for the raw data. From **Figure 6-5** it can be seen that the change in overall model SSE is due to more of the data falling outside of the ±5% range. However, given that the SSE is only 5% of the maximum carbon yield value, this can still be considered an accurate model. This indicates that although different groups are indicated when the data is normalized, these groups can also be used to accurately model the kinetics.

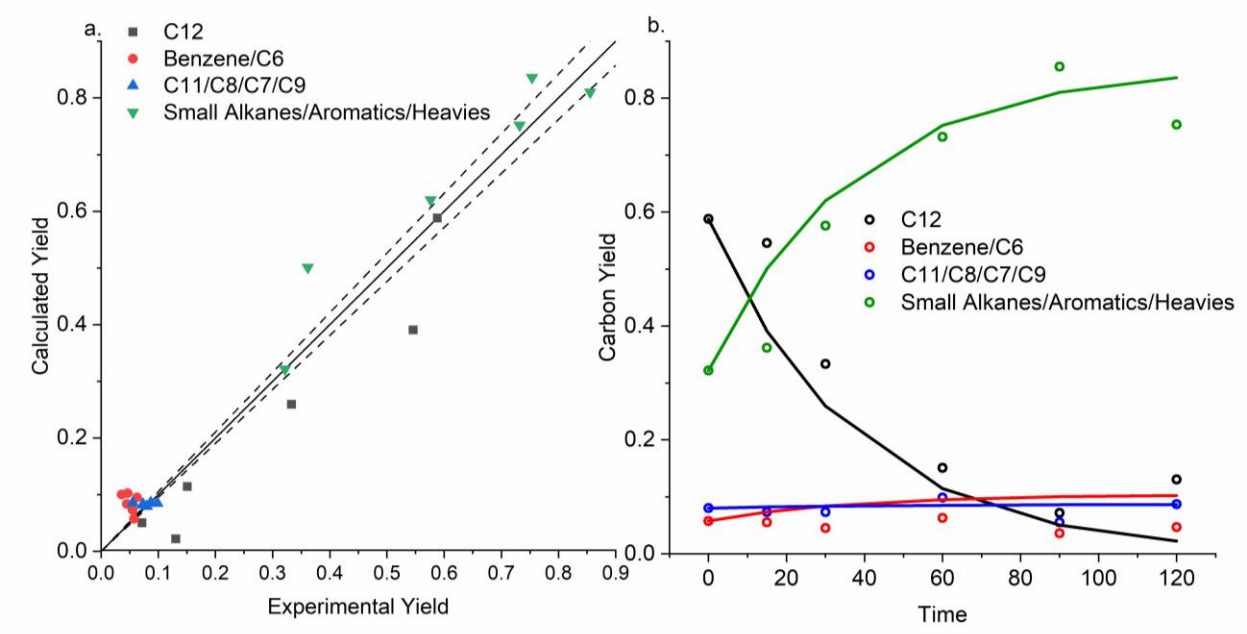

Figure 6-5 Kinetic modeling results for reaction P (all reactions in parallel) vs a.) the experimental carbon yields for each group and b.) time with the open circles indicating experimental data and the solid line being the calculated yields for the group indicated by the normalized carbon yield dendrogram

Targeted modeling of desired reaction products

One of the possible drawbacks of group type reaction modeling is the fact that it can conceal the yields of especially important products. The specific concentrations of individual products could be important for a variety of reasons whether they are of high economic value or a fouling product and being able to track them can be critical. In the previous section the aim was the minimize the error overall for all the groups, in this section the aim will be to minimize the error for specific targeted compounds without significantly impacting overall accuracy. To achieve this the same groups that were identified from the raw data dendrogram were used but the targeted product was pulled out of its group and made its own. The same kinetic model was then used to calculate the carbon yields of each group when all reactions occur in parallel.

The targeted compounds studied were toluene and xylene as toluene came out of group 4 and xylene came out of group 3. The targeted compounds became their own group, group 5. As can be seen in **Table 6-3** the maximum absolute error for the targeted compound groups is the lowest out of any group and the overall model SSE is within the same range as the analysis without the targeted groups. This can also be seen in **Figure 6-6**, with **Figure 6-6a** showing the parity plot and concentration over time for toluene and **Figure 6-6b** showing these plots for xylene. All groups have a good overall fit between the experimental and calculated carbon yields. This indicates that without sacrificing any overall model accuracy, specific targeted compounds of interest can be accurately modeled and tracked over the reaction time.

Table 6-3 Sum of Squared Errors and Individual Group Max Absolute Error for Targeting Toluene and Xylene

Compound	SSE	Group 1 MAE	Group 2 MAE	Group 3 MAE	Group 4 MAE	Group 5 MAE
Toluene	0.0329	0.0956	0.0745	0.0425	0.0189	.0074
Xylene	0.0324	0.0958	0.0746	0.0337	0.0170	.0107

a.

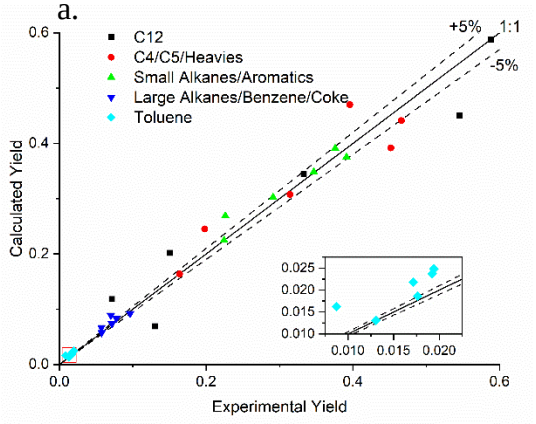

b.

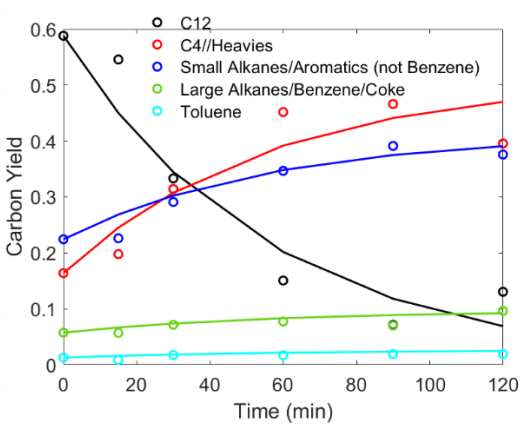

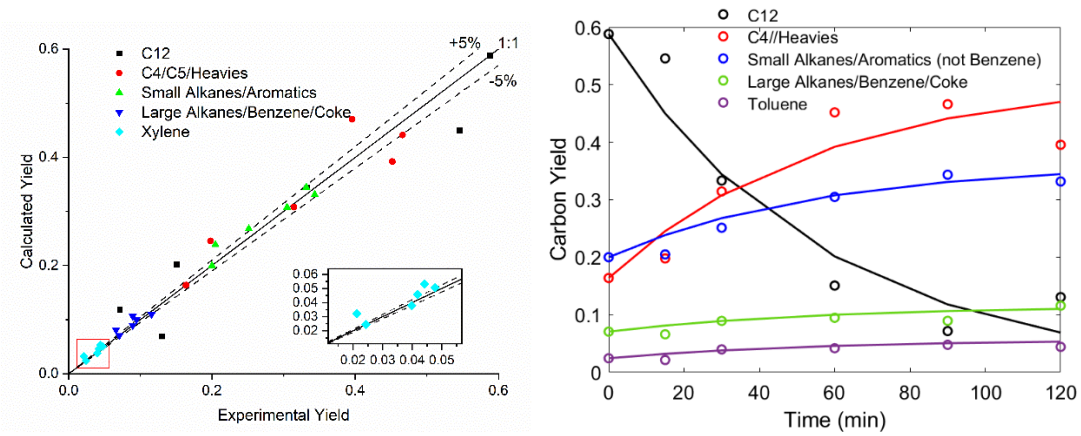

Figure 6-6 Parity and carbon yield over time plots for the targeting of desired compounds a.) toluene and b.) xylene

Method expansion to new datasets

The previous three sections have shown that the groups indicated by a dendrogram can be accurately used to model the kinetics of the supercritical cracking of dodecane using group type kinetic modeling. To test the validity of this method when applied to different datasets the same procedure was followed to model the supercritical cracking of dodecane in the presence of supercritical water. The presence of supercritical water changes the chemistry as the reaction is now hydrothermal instead of pyrolytic and therefore this can be considered a new dataset.

This data set tracks dodecane and 21 reaction product carbon yields over 6 time points. This data was once again fed into the dendrogram algorithm using average linkage and the resulting dendrogram can be seen in **Figure 6-7**. Once again C12 is the most dissimilar compound, which is a good indicator. In the presence of supercritical water, C12 is even more dissimilar than the products as compared to when there is no supercritical water. This is believed to be due to the fact that the carbon yields of the products are reduced in the presence of supercritical water.

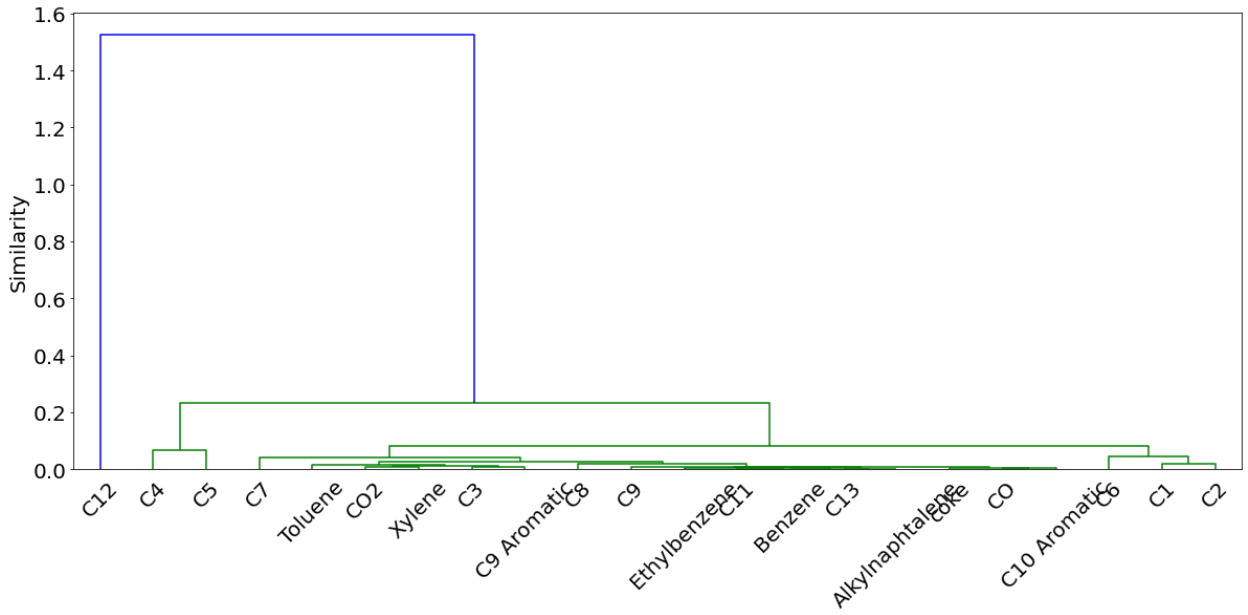

Figure 6-7 Dendrogram using average linkage of supercritical cracking of dodecane in the presence of supercritical water

Figure 6-7 indicates four groups, 1.) C12, 2.) C4 and C5, 3.) C1, C2 and C6 and 4.) everything else. However, when the concentrations of each group were plotted over time (**Figure E.6-14**) it can be seen that there was very little difference between the C1/C2/C6 group and the group of the remaining products. It was determined that these groups were not dissimilar enough (<5%) to separate and going forward the groups indicate by the dendrogram are as follows:

1.) C12

2.) C4 and C5

3.) Alkanes, aromatics, C1, C2 and C6

As all reactions occurring in parallel showed the lowest error in previous sections, this reaction pathway was used again to model the kinetics of this data set. The results can be seen in **Figure 6-8**, where **Figure 6-8a** shows the calculated yields verse the experimental and **Figure 6-8b** shows the yields over time. Once again, with the exception of one of the C12 predications, the data points on **Figure 6-8a** are clustered closely to the 1:1 line showing a good fit between

calculated and experimental carbon yields. This trend can also be seen in **Figure 6-8b**, where with the exception of the final C12 data point, there is close agreement between the calculated and experimental yields.

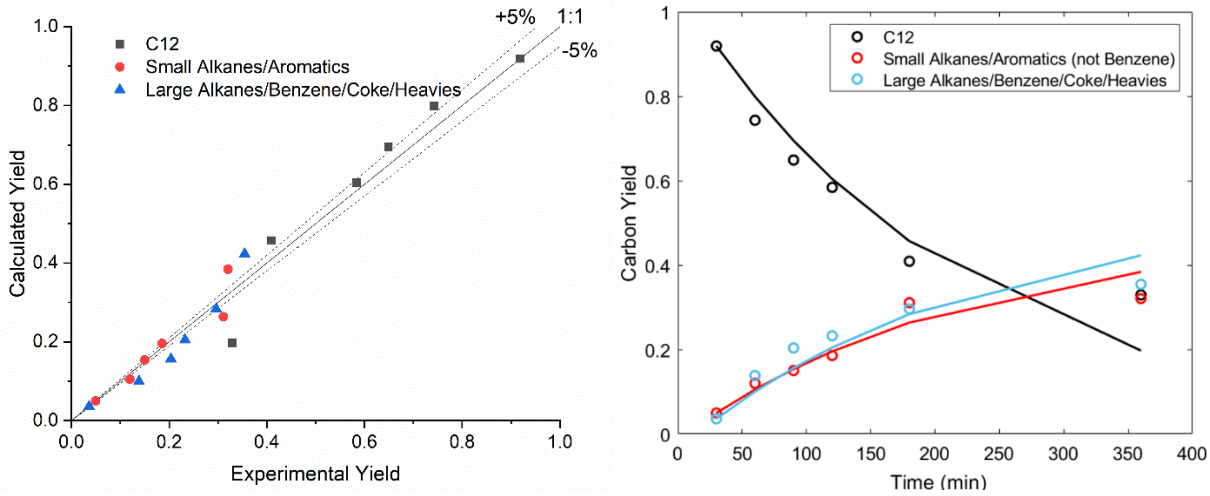

Figure 6-8 Kinetic modeling results for reaction P (all reactions in parallel) vs a.) the experimental carbon yields for each group and b.) time with the open circles indicating experimental data and the solid line being the calculated yields for the supercritical cracking of dodecane in the presence of supercritical water

6.4 Conclusion

Through this work it has been shown that the machine learning algorithm of dendrograms can be used to determine similarity within reaction products for the purpose of creating groups for group type kinetic modeling. These groups can then be used to accurately calculate the carbon yields over time and specific compounds of interest can still be individually tracked without reducing overall model accuracy. Use of this method is an alternative way to determine groups in group type kinetic modeling that eliminates the need for human and chemical intuition.

6.5 Appendix E

Table E.6-4 Raw Experimental Carbon Yields for Supercritical Dodecane Cracking in the Presence of ZSM-5[240]

Time	0	15	30	60	90	120
C1	0.031344	0.036597	0.058363	0.057159	0.104064	0.093325
C2	0.018537	0.021644	0.03507	0.035064	0.058302	0.059046
C3_propane	0	0	0.000626	0.000231	0.000264	0.000339
C4	0.106899	0.124813	0.164924	0.174162	0.231039	0.187319
C5	0.057025	0.073119	0.099562	0.122736	0.118234	0.121025
C6	0.054097	0.05056	0.043092	0.061143	0.031843	0.042762
C7	0.018467	0.018922	0.023451	0.030279	0.018906	0.030915
C8	0.054097	0.05056	0.043092	0.061143	0.031843	0.042762
C9	0.003772	0.001988	0.004845	0.005943	0.004006	0.007328
C11	0.003539	0.001877	0.001956	0.001065	0.000612	0.005929
C12	0.588101	0.545709	0.333201	0.150742	0.071616	0.130674
C13	0	0.002315	0.000319	0.002414	0.003099	0.003708
Benzene	0.003582	0.004649	0.002055	0.001783	0.004258	0.003834
Toluene	0.01305	0.00874	0.017626	0.017149	0.01923	0.019403
Ethylbenzene	0.003782	0.004428	0.005836	0.005433	0.007471	0.006463
Xylene	0.024378	0.021355	0.039799	0.041816	0.047776	0.044157
C9_aromatic	0.024621	0.02535	0.041513	0.049675	0.056171	0.052645
C10_aromatic	0.017396	0.020178	0.030116	0.040664	0.06126	0.041188
alkylnaphthalene	0.006611	0.004901	0.014337	0.011917	0.011625	0.016507
Heavy	0	0	0.049902	0.154947	0.11681	0.087235
Coke	0.0179	0.0182	0.018255	0.01857	0.01998	0.02139

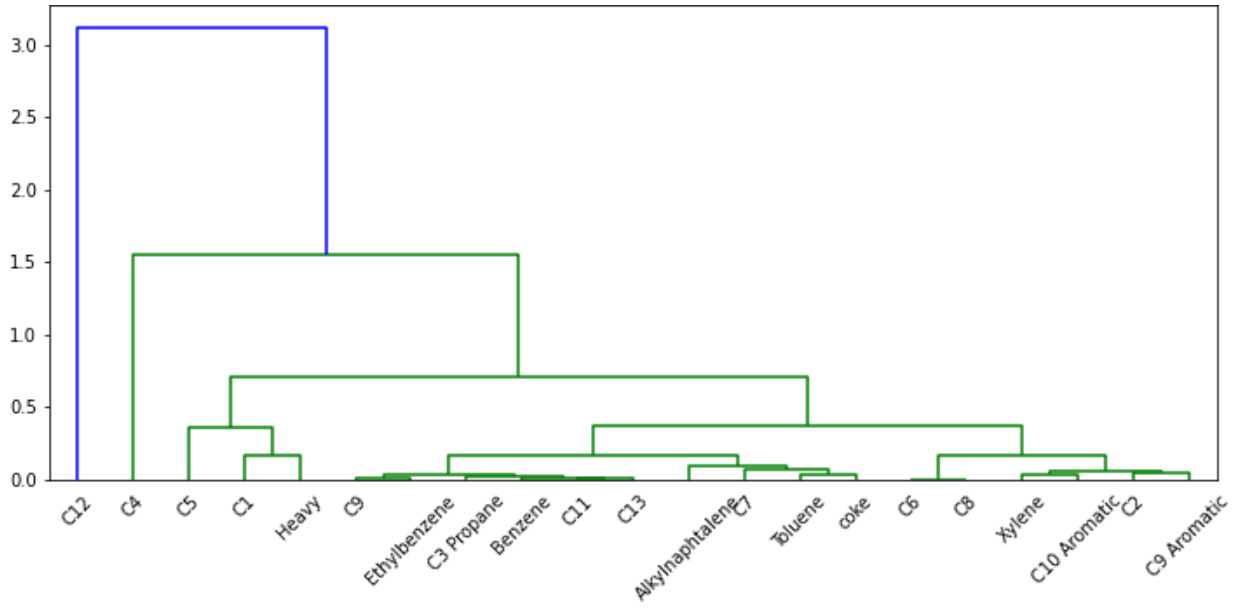

Figure E.6-9 Dendrogram for the carbon yields for supercritical cracking of dodecane with 1,000 artificial data points generated using linear regression.

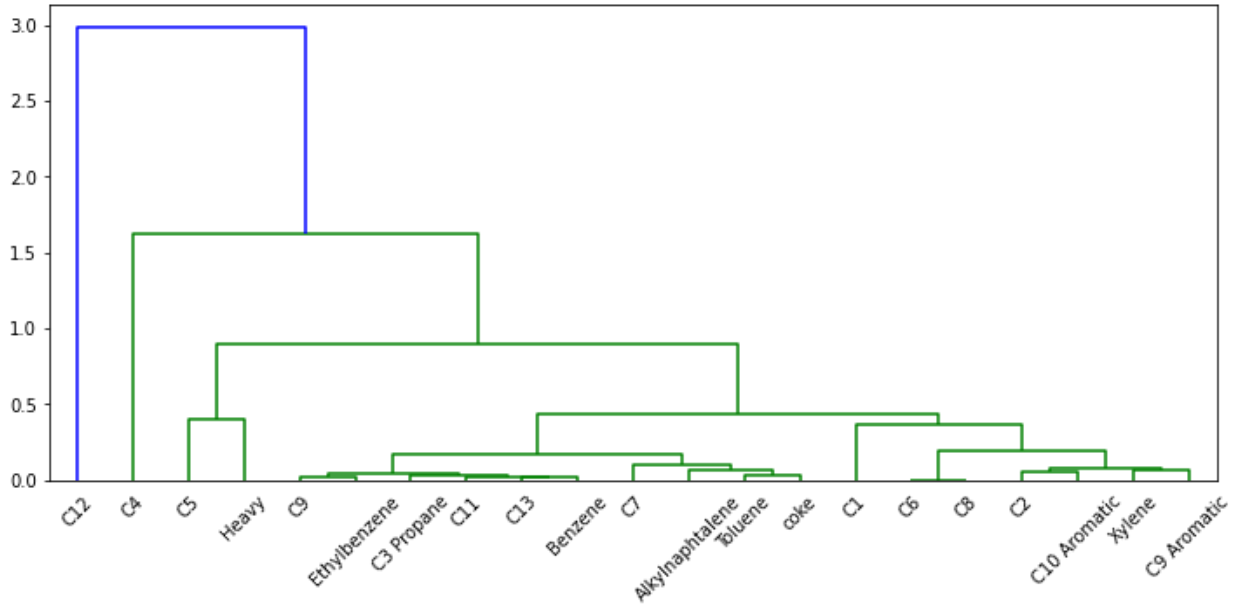

Figure E.6-10 Dendrogram for the carbon yields for supercritical cracking of dodecane with 1,000 artificial data points generated using piecewise linear regression.

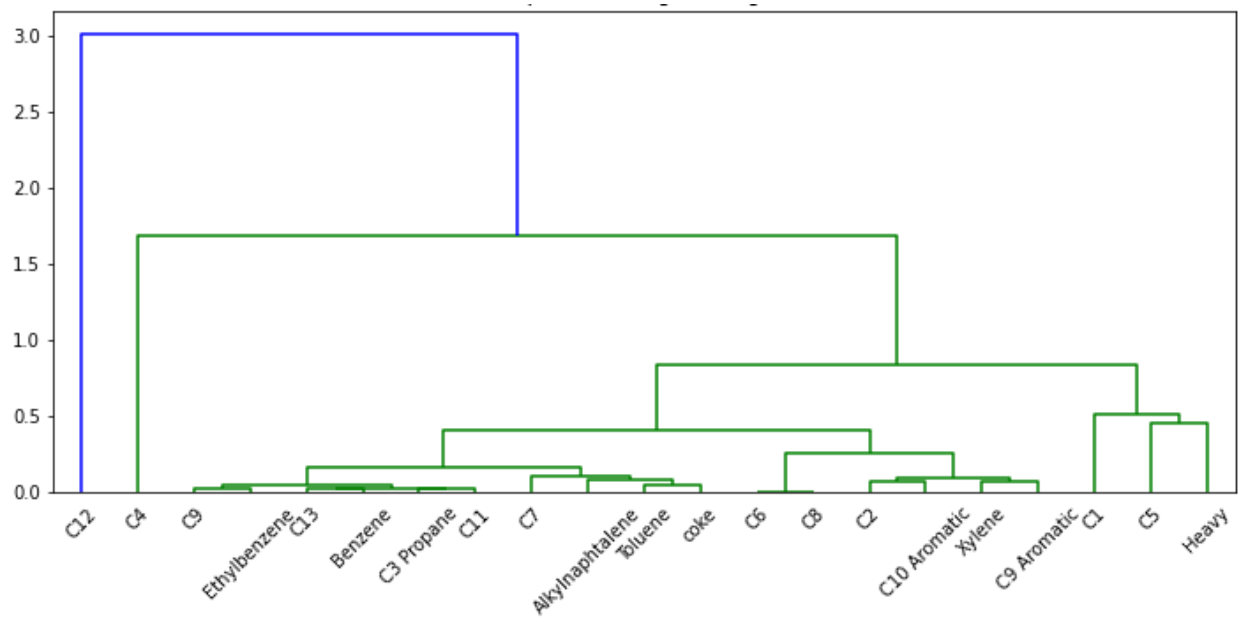

Figure E.6-11 Dendrogram for the carbon yields for supercritical cracking of dodecane with 1,000 artificial data points generated using Cubic Splines.

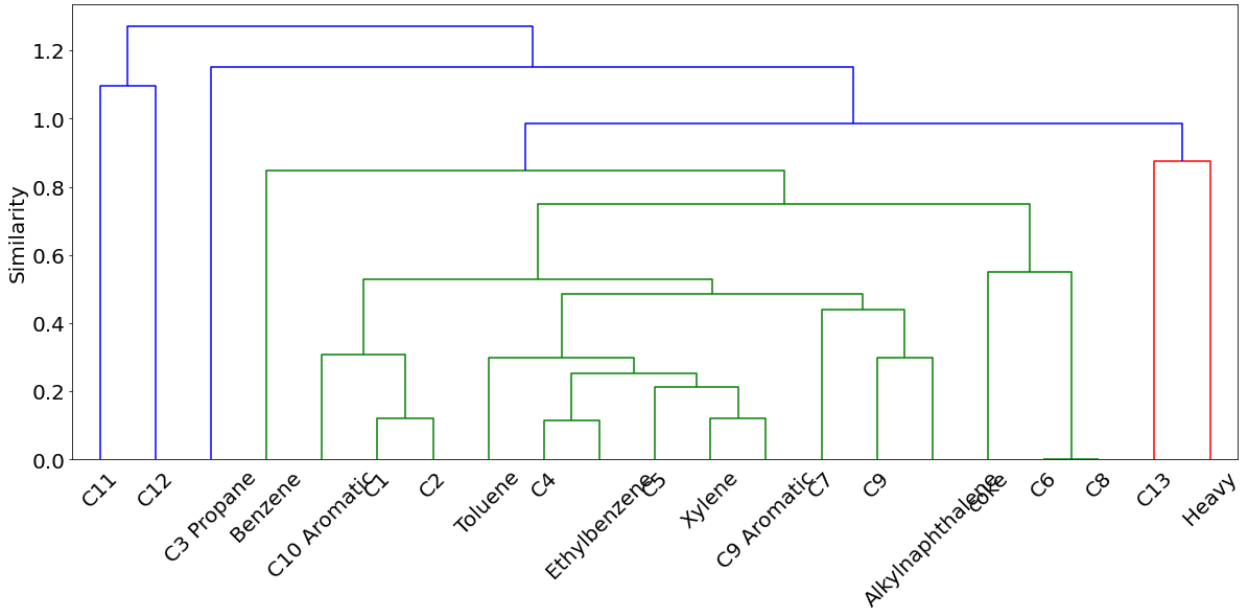

Figure E.6-12 Dendrogram for the supercritical cracking of dodecane in the presence of ZSM-5 when the data is normalized between 0 and 1 using a scale transform

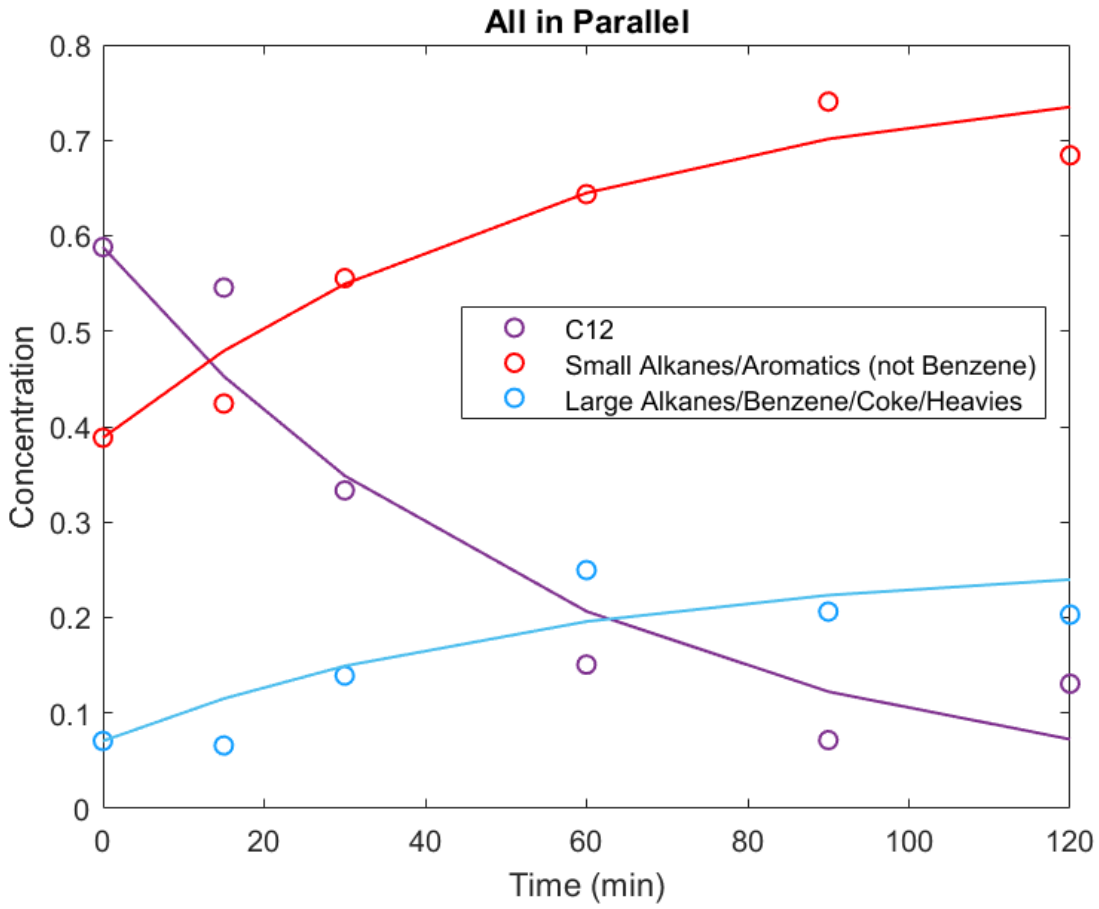

Figure E.6-13 Kinetic modeling results for reaction P (all reactions in parallel) with three groups vs. the time with the open circles indicating experimental data and the solid line being the calculated yields for the supercritical cracking of dodecane in the presence of supercritical water

Table E.6-5 Sum of squared errors and average maximum absolute error for kinetic modeling of each possible reaction pathway

Reaction Pathway	**Reaction Name**	**Sum of Squared Errors**	**Average Max Absolute Error**
↗ 2 1 ↘ 3	P	0.0332	0.0674
1 → 2 → 3	S1	0.0415	0.0847
1 → 3 → 2	S5	0.0619	0.0970

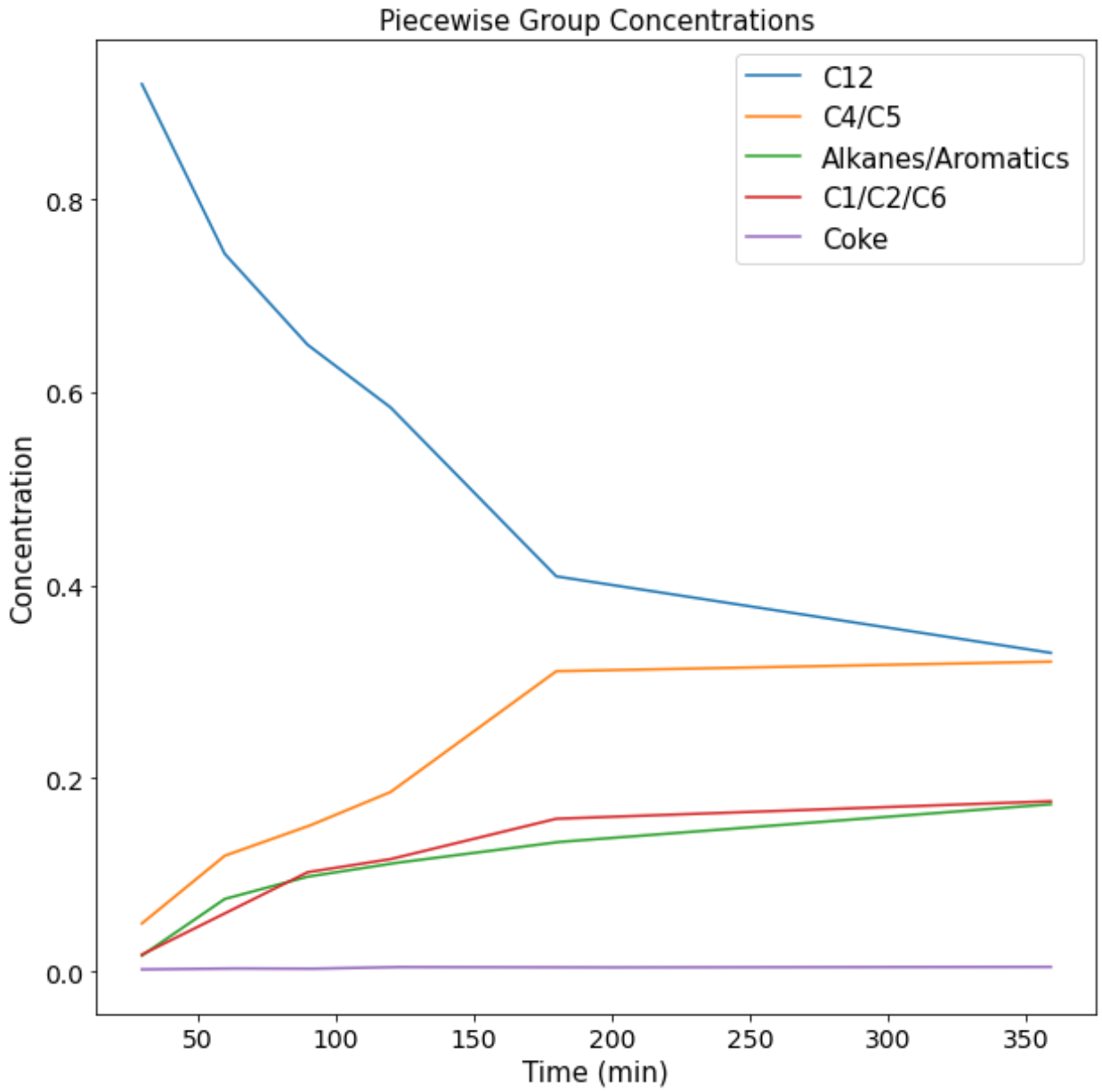

Figure E.6-14 Normalized concentration over time for the groups identified in **Figure 6-7** for SCDSCW

Chapter 7: Use of Machine Learning and Monte Carlo Analysis to Various Applications

The machine learning and Monte Carlo modeling techniques developed in this thesis were also be applied to other feedstocks and problems. This chapter will briefly outline the work done to apply these techniques to organic biomass feedstocks as well as a different application of polystyrene pyrolysis.

7.1 Wet Organic Biomass

HTL has been extensively studied for the conversion of wet organic biomass feedstocks into bio-oils. Diverting these wet organic biomasses away from landfills is important not only in terms of the limited space available in landfills, but also due to the emissions created when these feedstocks degrade in landfills. Utilizing the extensive data existing in the literature allows for the development of machine learning models that can predict oil yields for HTL of biomass feedstocks. Chen, et. al.[125] created a dataset of 525 data points for any wet organic biomass HTL data existing in the literature. The correct handling of data for small datasets was detailed extensively to highlight limitations of the work previously published. The dataset was used to optimize 8 different machine learning algorithms, of which Random Forest, XGBoost and ANN had the best performance. The performance of the model was benchmarked against models existing in the literature and the predictions applied to a technoeconomic analysis. The TEA showed that biocrude yield has a significant impact on Minimum Fuel Selling Price up until approximately 40%, after which the impact is greatly reduced.

The knowledge and methods developed in this thesis aided in the development of the data handling protocols outlined in this work, as well as the bench marking of model performance compared to other models in the literature.

7.2 Bamboo

Ekwe, et.al.[252] explored the mechanochemical pretreatment of *Bambusa vulgaris* for the creation of waste free renewable sugars. The Monte Carlo techniques developed in this thesis were applied to this problem to understand the amount of ethanol that could be created in Nigeria using mechanochemical pretreatment followed by subsequent fermentation. Uncertain parameters for glucose, and xylose yields along with available land were incorporated into the model. The results of the Monte Carlo model indicated that utilizing all marginal land not necessary for solar to grow bamboo, could offset 50-80% of Nigeria's domestic gasoline usage. With no more than 30% of arable land also used for bamboo growth, 100% of Nigeria's domestic gasoline usage could be offset using bamboo derived ethanol.

7.3 Distillation of Polystyrene to raw styrene

Chemical recycling of waste plastics will be an important part of the recycling portfolio necessary to address the worlds waste plastic problem. The products that can be produced from chemical recycling must be diverse and have markets available for the technologies to be viable. In this work the conversion of waste plastic back to styrene monomers through pyrolysis and two stage distillation was explored. Both the energy requirements and economics of the process was analyzed using a mixture of Aspen modeling and economic modeling. The learnings from this thesis were applied to the problem to account for uncertainty in the economic performance parameters. A Monte Carlo analysis was completed to get estimations and uncertainties for the Levelized Production Costs, as well as Total Product Cost and Total Capital Investment, for plant scales from 15 to 120 tons per day. Levelized productions costs less than $3/ kg of styrene produced were achievable with scales greater than 60 tons per day regardless of product feedstock costs. This work indicated the potential of using pyrolysis to convert waste polystyrene back into styrene monomer, a promising result for the development of circular plastics recycling.

Chapter 8: Future Work

The work in this thesis has added to the knowledge of how thermal depolymerization technologies can be used to expand waste plastic recycling capabilities. However, there is still work to be done before wide spread deployment of these technologies is feasible. As promising as pyrolysis and hydrothermal liquefaction are, the impact of real waste contaminants such as additives, colorants and plasticizers, which are often trade secrets, is just starting to be understood. Large scale deployment of thermal depolymerization technologies is currently limited by two major factors: understanding the impact of real waste and associated contaminants on not only reaction yields, but also product compositions and finding markets for byproducts. In this chapter suggestions will be made for how to overcome these limitations at all three scales studied in this thesis; oceans, rivers and MRFs.

It was shown that fuel created from theoretical ocean plastics in an onboard HTL conversion system can thermodynamically fuel self-powered ocean cleanup. This work relied on studies published in the literature that used virgin polymers. Although HTL is known to be able to handle contaminants, the exact composition of fuels created from real ocean plastics cannot be known without more study. These plastics will have the inherent additive contaminants all real waste plastic has along with organic matter containment from its exposure to the environment. Acquiring waste from the GPGP would allow for experimental optimization of reaction conditions for optimal oil yield.

Along with optimizing oil yields, it is critical to also understand the composition of the oils made from real GPGP waste. A compositional understanding of both the waste and the oil will expand the fields knowledge of how real waste composition effects oil composition. For self-powered ocean cleanup to be feasible the oil properties cannot change drastically with feedstock

composition changes. It is also important for more study to be done on how the oils created act in a marine diesel engine. If a traditional marine diesel engine cannot use blue diesel directly research into modified engines may be necessary. A reliable fuel that the selected engine can efficiently consume is required for deployment. The research done using real waste will help overcome the major remaining questions about the feasibility of self-powered ocean cleanup.

Similar to ocean plastics, river plastics will have organic contaminants that could impact the performance of pyrolysis reactions. Plastics found at MRFs on the other hand may have contaminants in the form of residual product and label contaminants. Regardless of its origin and specific contaminants the models developed in this work are made with data that is almost entirely for virgin plastics. Even the mixtures that have been studied are typically created using virgin polymers. This means that if contaminants have a major role in the performance of thermal depolymerization technologies, the models developed in this work will not be able to account for and predict these impacts. Addressing this limitation is a two-fold approach, the first of which is continuing research being done on real waste streams, as it was for ocean plastics. The models developed here can be used to choose the best real waste feeds to do further research on. Careful analysis of both oil yield and oil composition along with reporting of the yields of the other phases (i.e. gas, residual solid and aqueous when applicable) of these feedstocks will enhance the quality and amount of data existing in the literature. The results should be compared to the predictions made to understand the potential impact contaminants have on oil yield and understand if the models created here are accurate for real waste. As more and more data become available, the datasets can be expanded and the models re-run to increase accuracy and applicability of the predictions that can be made. Continuous improvement of the models as the field continues to advance will only increase the power and knowledge that can be gained from them.

Along with increasing the amount of data for real wastes, improvements to the way data is reported in the literature will allow for the development of more accurate models. Currently, in the field there is no agreed upon definition of what constitutes oil. Some papers report all liquid product as oil, while others will distinguish between heavy and light phases of oil. This results in comparisons not always being one to one and incorporating inherent error into any model trained on the data. Along with varying oil definitions, there is also large variability in the extraction processes used from research group to research group. Complete uniformity in the experimental process is not realistic, nor is it necessarily a good idea as it could limit research progression, but uniformity in reporting the processes used is necessary. This will allow for a better understanding within the field on how these experimental decisions impact process performance. A complete understanding of the process at the lab scale experimental level will aid in scale up of these thermal conversion technologies along with allowing for the development of more accurate models by reducing the inherent error in the dataset.

For systems designed to consume HTL or pyrolysis derived fuels directly, such as self-powered ocean cleanup or river-based conversion systems, understanding potential product markets is unnecessary. While also true at MRFs, where fuel generated could be used to offset any liquid fuel consumption at the facility, creating products with higher values than diesel fuel will improve the technoeconomic performance. To create the highest value products, a fundamental understanding of the technology is necessary. The work outlined in chapter 5 of this thesis began the process of understanding the critical role of radicals in the depolymerization of polystyrene. However, more work is required to fully understand the depolymerization mechanism in the presence of sub- or supercritical water and how it differs from the more well understood pyrolysis mechanism. There are two key areas that need more study, the first of which is the impact of time

on HTL reactions, at conditions that create oil (365 °C or 400 °C) and at conditions that do not generate any oil (350 °C). At both of these conditions, study of the solid phase is required to fully understand the mechanism. It was seen for RI-HTL that changes in the molecular weight of the solid were occurring even when oil yield was not changing.

A time study at 350 °C is important because initial studies of HTL at 350 °C with a 20-minute reaction time showed that although no oil was created, the molecular weight of the residual solid was significantly reduced. Reactions with reaction times less than 20 minutes will verify the hypothesis that the molecular weight of the solid is reducing with time, indicating that the presence of water in HTL promotes mid-chain scission, as compared to in pyrolysis where the primary mechanism is end-chain unzipping. Increasing the reaction time past 20 minutes will also give insight into whether 350 °C is a severe enough condition to produce oil in traditional HTL reactions if enough time is given.

Further study at either 365 °C or 400 °C will aid in understanding the mechanism of HTL depolymerization and also aid in understanding if RI-HTL fundamentally changes the depolymerization mechanism or just promotes it at less severe conditions. It is hypothesized, based on the knowledge of thermal depolymerization of PS, that radicals initiate beta-scission reactions which are the primary depolymerization mechanism. It was hypothesized that RI-HTL will initiate these reactions and not fundamentally change the depolymerization mechanism. Therefore, it would be expected that a time study at an HTL condition that produces oil would have the same behavior as RI-HTL at 350°C. RI-HTL at 350°C showed a decrease in the molecular weight of the residual solid with no increase in oil yield. A similar result for HTL would strongly suggest that the key depolymerization mechanism in the presence of water is mid-chain scission as stated previously.

The other key area that needs more study is understanding the role of oxygen in RI-HTL and answering whether RI-HTL is dominated by radicals or by oxidation reactions. Initial studies were completed using a radical source that did not have oxygen (dimethyl diphenyl butane) which showed promising oil yield performance, but DMDB was too stable and partially remained in the oil product after reaction making determining oil yield difficult. Oxidative runs were also completed where HTL reactions at 350°C were charged with oxygen in quantities equaling a O:C ratio of 0.091. These runs did not result in any oil yield but did result in visible decay of the residual solid. These results strongly suggest that it is a combination of both radical initiated and oxidative chemistry but more studies with various radical and oxygen sources are needed to confirm this theory.

This work has shown the importance of understanding not only the oil produced in these reactions but also the residual solids. In the literature for HTL of polymers, analysis of the solid phase is rarely if ever completed. There is significant room for research into not only the state of these residual solids in the reaction but also the best ways to analyze them. Not studying the residual solid phase leaves a massive gap in the fields understanding of HTL depolymerization mechanisms, which negatively impacts the ability to tune the reaction for production of specific desired compounds.

Production of fuels from waste plastics is a promising way to handle end of life plastics and mixtures that cannot be separated but production of higher value products is also important. Production of higher value products, such as oxygenated single-ring aromatics has been demonstrated in this work but finding a market for these products could be difficult. Future work that demonstrates how these compounds can be used to create high value products, potentially without the need for extensive distillation to separate products, will aid in deployment of these

systems. Proof that these oils can be used to create products will promote further investment in the field and expand the market potential.

Finally, in this work RI-HTL was demonstrated for polystyrene which is a polymer that cannot currently be recycled and therefore an important polymer to understand. However, polystyrene accounts for only approximately 6% of US waste plastic. Understanding how other polymer types respond to RI-HTL can further expand its potential impact. It is also important to further the research for both mixed plastic feedstocks and real waste feedstocks to once again understand the potential impact of contaminants on the process performance.

Although there are limitations that exists in the current understanding of thermal depolymerization technologies, deployment of these technologies is feasible with little effort. This work has shown that these technologies are not only thermodynamically feasible, but also economically feasible. With a limited amount of future research to understand the effect of contaminants on performance, these technologies can be widely deployed and greatly reduce the amount of plastic going to landfills and ending up polluting the environment. These technologies are only one part of a multi-faceted approach to eliminating waste plastic that must also include research into biodegradable polymers, enhanced and truly circular recycling and a reduction in the world’s reliance on plastic.

Chapter 9: Conclusions

The studies performed here have combined computational methods, including machine learning, with experimental work to demonstrate the potential of thermal depolymerization technologies as a viable waste plastic recycling method. Utilizing computational methods, such as thermodynamic modeling and machine learning are critical for optimizing experimental resources and driving deployment of these technologies within the next decade. This work identified key areas that can benefit from the incorporation of machine learning models, along with ways to increase the value of byproducts.

In order to create a valuable fuel product from waste plastic, the fuel must have an energy quantity greater than the energy consumed to create said fuel. This work developed a method to analyze the thermodynamic potential of a feedstock, while accounting for uncertainty in process parameters. It was shown that both self-powered ocean cleanup and self-powered conversion of river plastics is thermodynamically feasible. Furthermore, this work has shown how machine learning models can be combined with thermodynamic modeling, allowing for the thermodynamic potential of any new feedstock to be studied, regardless of the availability of experimental work completed at those conditions.

Along with thermodynamic feasibility, understanding the economic potential of new feedstocks is a critical aspect for widescale deployment of thermal depolymerization technologies. This work was able to combine machine learning models with a technoeconomic analysis to demonstrate how machine learning can be used to rapidly predict the oil yield of a new feedstock. These predictions can then be integrated into Aspen and a technoeconomic analysis to predict the minimum selling price of any products produced. Pyrolysis of waste plastic in nearly all 50 states was found to be economically feasible.

This work identified methods to identify, track and produce select desired reaction products through machine learning modeling. It was once again demonstrated how machine learning can be integrated into traditional kinetic modeling techniques and produce equally accurate predications while eliminating a reliance on a specific researcher's chemical intuition and decision making. This further supports that machine learning can be effectively used in chemical engineering in a variety of ways, and future work should continue to expand how machine learning is applied in the field.

Lastly, this work created high value oxygenated single-ring aromatic compounds during HTL reactions of polystyrene by adding an oxygenated external radical source, hydrogen peroxide. It has also reduced the severity of conditions necessary for complete depolymerization of polystyrene, an important advancement in both technology and safety. This RI-HTL technology has been demonstrated for the first time in this work. RI-HTL has the potential to change the HTL deployment landscape by creating new products with higher economic value than the fuels traditionally made from waste plastics HTL.

The work presented here begins to shed light on the thermodynamic and economic viability of deploying thermal conversion technologies to convert waste plastics to valuable products. It also advances the fields knowledge of how machine learning can be integrated into traditional chemical engineering problems. Through continued research in both machine learning and the depolymerization mechanism for plastics in the presence of water, deployment of thermal depolymerization technologies will become less expensive and more common.

Chapter 10: References

1. Annual production of plastics worldwide from 1950 to 2020. In *Statista*, Plastics Europe (PEMRG): 2021.

2. Geyer, R.; Jambeck, J. R.; Law, K. L., Production, use, and fate of all plastics ever made. *Science Advances* **2017,** *3* (7), 1-5.

3. Shen, L.; Worrell, E., Chapter 13- Plastic Recycling. In *Handbook of Recycling*, Worrell, E.; Reuter, M. A., Eds. Elsevier: 2014; pp 179-190.

4. Advancing Sustainable Materials Management: Facts and Figures 2018. Agency, U. S. E. P., Ed. Office of Land and Emergency Management: 2018.

5. Recycling Infrastructure and Market Opportunities Map. https://www.epa.gov/circulareconomy/recycling-infrastructure-and-market-opportunities-map#02 (accessed 1/26/22024).

6. Jambeck, J. R.; Geyer, R.; Wilcox, C.; Siegler, T. R.; Perryman, M.; Andrady, A.; Narayan, R.; Law, K. L., Plastic waste inputs from land into the ocean. *Science* **2015,** *347* (6223), 768-771.

7. Cozar, A.; Echevarria, F.; Gonzalez-Gordillo, J. I.; Irigoien, X.; Ubeda, B.; Hernandez-Leon, S.; Palma, A. T.; Navarro, S.; Garcia-de-Lomas, J.; Ruiz, A.; Fernandez-de-Puelles, M. L.; Duarte, C. M., Plastic debris in the open ocean. *PNAS* **2013,** *111* (28), 10239-10244.

8. Li, W. C.; Tse, H. F.; Fok, L., Plastic waste in the marine environment: A review of sources, occurrence and effects. *Science of The Total Environment* **2016,** *566-567*, 333-349.

9. Rhines, P. B.; Young, W. R., A theory of wind-driven circulation. I. Mid-ocean gyres. **1982**.

10. Leal Filho, W.; Hunt, J.; Kovaleva, M., Garbage Patches and Their Environmental Implications in a Plastisphere. *Journal of Marine Science and Engineering* **2021,** *9* (11), 1289.

11. Lebreton, L.; Slat, B.; Ferrari, F.; Sainte-Rose, B.; Aitken, J.; Marthouse, R.; Hajbane, S.; Cunsolo, S.; Schwarz, A.; Levivier, A.; Noble, K.; Debeljak, P.; Maral, H.; Schoeneich-Argent, R.; Brambini, R.; Reisser, J., Evidence That the Great Pacific Garbage Patch Is Rapidly Accumulating Plastic. *Scientific Reports* **2018,** *8* (1), 1-15.

12. Barnes, D. K. A.; algani, F.; Thompson, R. C.; Barlaz, M., Accumulation and gradmentation of plastic debris in global environments. *Philosophical Transactions of the Royal Society B: Biological Sciences* **2009,** *364*, 1985-1998.

13. Eriksen, M.; Maximenko, N.; Thiel, M.; Cummins, A.; Lattin, G.; Wilson, S.; Hafner, J.; Zellers, A.; Rifman, S., Plastic pollution in the South Pacific subtropical gyre. *Marine Pollution Bulletin* **2013,** *68* (1), 71-76.

14. Galgani, F.; Leaute, J. P.; Moguedet, P.; Souplet, A.; Verin, Y.; Carpentier, A.; Goraguer, H.; Latrouite, D.; Andral, B.; Cadiou, Y.; Mahe, J. C.; Poulard, J. C.; Nerisson, P., Litter on the Sea Floor Along European Coasts. *Marine Pollution Bulletin* **2000,** *40* (6), 516-527.

15. Derraik, J. G. B., The pollution of the marine environment by plastic debris: a review. *Marine Pollution Bulletin* **2002,** *44* (9), 842-852.

16. Romeo, T.; Pietro, B.; Pedà, C.; Consoli, P.; Andaloro, F.; Fossi, M. C., First evidence of presence of plastic debris in stomach of large pelagic fish in the Mediterranean Sea. *Marine pollution bulletin* **2015,** *95* (1), 358-361.

17. Azzarello, M. Y.; Van Vleet, E. S., Marine birds and plastic pollution. *Marine Ecology Progress Series* **1987,** *37* (2/3), 295-303.

18. Schuyler, Q.; Hardesty, B. D.; Wilcox, C.; Townsend, K., Global analysis of anthropogenic debris ingestion by sea turtles. *Conservation biology* **2014,** *28* (1), 129-139.

19. Gall, S. C.; Thompson, R. C., The impact of debris on marine life. *Marine pollution bulletin* **2015,** *92* (1-2), 170-179.

20. van Emmerik, T.; Schwarz, A., Plastic debris in rivers. *Wiley Interdisciplinary Reviews: Water* **2020,** *7* (1), e1398.

21. Lebreton, L. C. M.; Zwet, J. v. d.; Damsteeg, J.-W.; Slat, B.; Andrady, A.; Reisser, J., River plastic emissions to the world's oceans. *Nature Communications* **2017,** *8*, 1-10.

22. Calcar, C. J. v.; Emmerik, T. H. M. v., Abundance of plastic debris across European and Asian rivers. *Environmental Research Letters* **2019,** *14*, 1-9.

23. Dris, R.; Gasperi, J.; Rocher, V.; Saad, M.; Renault, N.; Tassin, B., Microplastic contamination in an urban area: a case study in Greater Paris. *Environmental Chemistry* **2015,** *12* (5), 592-599.

24. Zhao, S.; Zhu, L.; Wang, T.; Li, D., Suspended microplastics in the surface water of the Yangtze Estuary System, China: first observations on occurrence, distribution. *Marine pollution bulletin* **2014,** *86* (1-2), 562-568.

25. Rech, S.; Macaya-Caquilpán, V.; Pantoja, J.; Rivadeneira, M.; Campodónico, C. K.; Thiel, M., Sampling of riverine litter with citizen scientists—findings and recommendations. *Environmental monitoring and assessment* **2015,** *187*, 1-18.

26. Yonkos, L. T.; Friedel, E. A.; Perez-Reyes, A. C.; Ghosal, S.; Arthur, C. D., Microplastics in four estuarine rivers in the Chesapeake Bay, USA. *Environmental science & technology* **2014,** *48* (24), 14195-14202.

27. Lechner, A.; Keckeis, H.; Lumesberger-Loisl, F.; Zens, B.; Krusch, R.; Tritthart, M.; Glas, M.; Schludermann, E., The Danube so colourful: a potpourri of plastic litter outnumbers fish larvae in Europe's second largest river. *Environmental pollution* **2014,** *188*, 177-181.

28. Pressley, P. N.; Levis, J. W.; Damgaard, A.; Barlaz, M. A.; DeCarolis, J. F., Analysis of material recovery facilities for use in life-cycle assessment. *Waste Management* **2015,** *35*, 307-317.

29. Yadav, G.; Singh, A.; Dutta, A.; Uekert, T.; DesVeaux, J. S.; Nicholson, S. R.; Tan, E. C. D.; Mukarakate, C.; Schaidle, J. A.; Wrasman, C. J.; Carpenter, A. C.; Baldwin, R. M.; Román-Leshkov, Y.; Beckham, G. T., Techno-economic analysis and life cycle assessment for catalytic fast pyrolysis of mixed plastic waste. *Energy & Environmental Science* **2023,** *16* (9), 3638-3653.

30. Sarafraz, A.; Alvarez, N.; Toussaint, J.; Rangel, F.; Giggetts, L.; Wilborne, S., Towards Eliminating Recycling Confusion: Mixed Plastics and Electronics Case Study. *Technology Innovation for the Circular Economy: Recycling, Remanufacturing, Design, System Analysis and Logistics* **2024**, 103.

31. Hopewell, J.; Dvorak, R.; Kosior, E., Plastics recycling: challenges and opportunities. *Philosophical Transactios of the Royal Society B* **2009,** *364* (1526), 2115-2126.

32. Schyns, Z. O. G.; Shaver, M. P., Mechanical Recycling of Packaging Plastics: A Review. *Macromolecular Rapid Communications* **2021,** *42* (3), 2000415.

33. Oblak, P.; Gonzalez-Gutierrez, J.; Zupančič, B.; Aulova, A.; Emri, I., Processability and mechanical properties of extensively recycled high density polyethylene. *Polymer Degradation and Stability* **2015,** *114*, 133-145.

34. Ragaert, K.; Delva, L.; Van Geem, K., Mechanical and chemical recycling of solid plastic waste. *Waste Management* **2017,** *69*, 24-58.

35. Vogt, B. D.; Stokes, K. K.; Kumar, S. K., Why is Recycling of Postconsumer Plastics so Challenging? *ACS Applied Polymer Materials* **2021,** *3* (9), 4325-4346.

36. Anuar Sharuddin, S. D.; Abnisa, F.; Wan Daud, W. M. A.; Aroua, M. K., A review on pyrolysis of plastic wastes. *Energy Conversion and Management* **2016,** *115*, 308-326.

37. Singh, R. K.; Ruj, B.; Sadhukhan, A. K.; Gupta, P., Impact of fast and slow pyrolysis on the degradation of mixed plastic waste: Product yield analysis and their characterization. *Journal of the Energy Institute* **2019,** *92* (6), 1647-1657.

38. Abbas-Abadi, M. S.; Haghighi, M. N.; Yeganeh, H., Evaluation of pyrolysis product of virgin high density polyethylene degradation using different process parameters in a stirred reactor. *Fuel processing technology* **2013,** *109*, 90-95.

39. Marcilla, A.; Beltrán, M. I.; Navarro, R., Thermal and catalytic pyrolysis of polyethylene over HZSM5 and HUSY zeolites in a batch reactor under dynamic conditions. *Applied Catalysis B: Environmental* **2009,** *86* (1), 78-86.

40. Shah, J.; Jan, M. R., Thermo-catalytic pyrolysis of polystyrene in the presence of zinc bulk catalysts. *Journal of the Taiwan Institute of Chemical Engineers* **2014,** *45* (5), 2494-2500.

41. Kaminsky, W.; Schlesselmann, B.; Simon, C., Thermal degradation of mixed plastic waste to aromatics and gas. *Polymer Degradation and Stability* **1996,** *53* (2), 189-197.

42. Demirbas, A., Pyrolysis of municipal plastic wastes for recovery of gasoline-range hydrocarbons. *Journal of Analytical and Applied Pyrolysis* **2004,** *72* (1), 97-102.

43. Byrappa, K.; Yoshimura, M., *Handbook of hydrothermal technology*. William Andrew: 2012.

44. Laredo, G. C.; Reza, J.; Meneses Ruiz, E., Hydrothermal liquefaction processes for plastics recycling: A review. *Cleaner Chemical Engineering* **2023,** *5*, 100094.

45. Chen, W.-T.; K., J.; Wang, N.-H., Use of supercritical water for the liquefaction of polypropylene into oil. *ACS Sustainable Chem. Eng.* **2019,** *7*, 3749-3758.

46. Zhang, H.; Su, X.; Sun, D.; Zhang, R.; Bi, J., Investigation on degradation of polyethylene to oil in a continuous supercritical water reactor. *J Fuel Chem Technol* **2007,** *35* (4), 487-491.

47. Williams, P. T.; Slaney, E., Analysis of products from the pyrolysis and liquefaction of single plastics and waste plastic mixtures. *Resources, Conservation and Recycling* **2007,** *51*, 754-769.

48. Kwak, H.; Shin, H.-T.; Bae, S.-Y.; Kumazawa, H., Characteristics and kinetics of degradation of polystyrene in supercritical water. *Journal of applied polymer science* **2006,** *101* (1), 695-700.

49. Tagaya, H.; Katoh, K.; Kadokawa, J.-i.; Chiba, K., Decomposition of polycarbonate in subcritical and supercritical water. *Polymer Degradation and Stability* **1999,** *64* (2), 289-292.

50. Jin, K.; Vozka, P.; Kilaz, G.; Chen, W.-T.; Wang, N.-H. L., Conversion of polyethylene waste into clean fuels and waxes via hydrothermal processing (HTP). *Fuel* **2020,** *273*, 117726.

51. Cheng, Q.; Wang, S.; Yan, C., Sequential Monte Carlo simulation for robust optimal design of cooling water system with quantified uncertainty and reliability. *Energy* **2017,** *118*, 489-501.

52. Dastile, X.; Celi, T.; Potsane, M., Statistical and machine learning models in credit scoring:A systematic literature survey. *Applied Soft Computing* **2020,** *91*, 106263.

53. Stockwell, D. R.; Peterson, A. T., Effects of sample size on accuracy of species dsitribution models. *Ecological Modeling* **2002,** *148*, 1-13.

54. Aierzhati, A.; Stablein, M. J.; Wu, N. E.; Kuo, C.-T.; Si, B.; Kang, X.; Zhang, Y., Experimental and model enhancement of food waste hydrothemal liquefaction with combined effects of biochemicl composition and reaction conditions. *Bioresource Technology* **2019,** *284*, 139-147.

55. Sheng, L.; Wang, X.; Yang, X., Prediction model of biocrude yield and nitrogen heterocyclic compounds analysis by hydrothermal liquefaction of microalgae with model compounds. *Bioresource Technology* **2018,** *247*, 14-20.

56. Liaw, A.; Wiener, M., Classification and regression by randomForest. *R news* **2008,** *2*, 18-22.

57. James, G.; Witten, D.; Hastie, T.; Tibshirani, R., *An Introduction to Statistical Learning with Applications in R*. Springer: New York, 2013.

58. Belden, E. R.; Kazantzis, N. K.; Reddy, C. M.; Kite-Powell, H.; Timko, M. T.; Italiani, E.; Herschbach, D. R., Thermodynamic feasibility of shipboard conversion of marine plastics to blue diesel for self-powered ocean cleanup. *Proceedings of the National Academy of Sciences* **2021,** *118* (46), e2107250118.

59. Cressey, D., Bottles, bags, ropes and toothbrushes: the struggle to track ocean plastics. *Nature* **2016,** *536* (7616), 263-265.

60. Efferth, T.; Paul, N. W., Threats to Human Health by Great Ocean Garbage Patches. *The Lancet Planetary Health* **2017,** *1* (8), e301-e303.

61. Ward, C. P.; Reddy, C. M., We need better data about the environmental persistence of plastic goods. *PNAS* **2020,** *117* (26), 14618-14621.

62. Chamas, A.; Moon, H.; Zheng, J.; Qiu, Y.; Tabassum, T.; Jang, J. H.; Abu-Omar, M.; Scott, S. L.; Suh, S., Degradation Rates of Plastics in the Environment. *ACS Sustainable Chem. Eng.* **2020,** *8*, 3494-3511s.

63. The Ocean Cleanup. https://theoceancleanup.com/ (accessed Jun 1, 2020).

64. Hohn, S.; Acevedo-Trejos, E.; Abrams, J. F.; Moura, J. F. d.; Spranz, R.; Merico, A., The long-term legacy of plastic mass production. *Science of The Total Environment* **2020,** *746*, 1-8.

65. Brambini, R., Dommergues B., Maral H., Sainte-Rose B., Hydrodynamics and capture efficiency of plastic cleanup booms: Part I, experiments and dynamic analysis. *Proceedings of the ASME 2017 36th International Conference on Ocean, Offshore and Arctic Engineering* **2017**, 1-10.

66. Zhao, P.; Yuan, Z.; Zhang, J.; Song, X.; Wang, C.; Guo, Q.; Ragauskas, A. J., Supercritcal water co-liquefaction of LLDPE and PP into oil: properties and synergy. *Sustainable Energy & Fuels* **2021,** *5*, 575-583.

67. Kalnes, T.; Marker, T.; Shonnard, D. R., Green Diesel: A Second Generation Biofuel. *International Journal of Chemical Reactor Engineering* **2007,** *5* (1).

68. Tester, J. A.; Modell, M., *Thermodynamics and Its Applications*. 3rd ed.; Prentice Hall PTR: Upper Saddle River, New Jersey, 1997.

69. Madani, K.; Lund, J. R., A Monte-Carlo game theoretic approach for Multi-Criteria Decision Making under uncertainty. *Advances in Water Resources* **2011,** *34*, 607-616.

70. Seshasayee, M. S.; Savage, P. E., Oil from plastic via hydrothermal liquefaction: Production and characterization. *Applied Energy* **2020,** *278*, 1-12.

71. Notteboom, T.; Cariou, P. In *Fuel surcharge practices of container shipping lines: Is it about cost recovery or revenue-making?*, IAME 2009, Copenhagen, Copenhagen, 2009.

72. Janssen, H., Monte-Carlo based uncertainty analysis: Sampling efficiency and sampling convergence. *Reliability Engineering & System Safety* **2013,** *109*, 123-132.

73. Anene, A. F.; Fredrksen, S. B.; Saetre, K. A.; Tokheim, L.-A., Experimental study of thermal and catalytic pyrolysis of plastic waste components. *Sustainability* **2018,** *10*, 3979.

74. Liang, J.-H.; Wan, X.; Rose, K. A.; Sullivan, P. P.; McWilliams, J. C., Horizontal dispersion of buoyant materials in the ocean surface boundary layer. *Journal of Physical Oceanography* **2018,** *28* (9), 2103-2125.

75. Snowden-Swan, L.; Zhu, Y.; Jones, S.; Elliott, D.; Schmidt, A.; Hallen, R.; Biling, J.; Hart, T.; Fox, S.; Maupin, G., Hydrothermal liquefaction and upgrading of municipal wastewater treatment plant sludge: A preliminary techno-economic analysis. Energy, U. S. D. o., Ed. Pacific Northwest National Laboratory: 2016.

76. Xanthos, D.; Walker, T. R., International policies to reduce plastic marine pollution from single-use plastics (plastic bags and microbeads): A review. *Marine Pollution Bulletin* **2017,** *118*, 17-26.

77. Thompson, R. C.; Moore, C. J.; Saal, F. S. V.; Swan, S. H., Plastics, the Environment and Human Health: Current Consensus and Future Trends. *Philosophical Transactions of the Royal Society B: Biological Sciences* **2009,** *364* (1526), 2153-2166.

78. Mani, M.; Subash, C.; Nagarajan, G., Performance, emission and combustion characterisitcs of a DI diesel engine using waste plastic oil. *Applied Thermal Engineering* **2009,** *29* (13), 2738-2744.

79. Kass, M. D.; Janke, C. J.; Connatser, R. M.; Samual A. Lewis, S.; Keiser, J. R.; Gaston, K., Compatibility Assessment of Fuel System Infrastructure Plastics with Bio-oil and Diesel Fuel. *Energy Fuels* **2018,** *32* (1), 542-553.

80. Knott, B. C.; Erickson, E.; Allen, M. D.; Gado, J. E.; Graham, R.; Kearns, F. L.; Pardo, I.; Topuzlu, E.; Anderson, J. J.; Austin, H. P.; Dominick, G.; Johnson, C. W.; Rorrer, N. A.; Szostkiewicz, C. J.; Copié, V.; Payne, C. M.; Woodcock, H. L.; Donohoe, B. S.; Beckham, G. T.; McGeehan, J. E., Characterization and engineering of a two-enzyme system for plastic depolyermization. *PNAS* **2020,** *117* (41), 25476-25485.

81. Taniguchi, I.; Yoshida, S.; Hiraga, K.; Miyamoto, K.; Kimura, Y.; Oda, K., Biodegradation of PET: Current Status and Application Aspects. *ACS Catal.* **2019,** *9* (5), 4089-4105.

82. IPCC *Climate Change 2014: Synthesis Report. Contribution of Working Groups I, II and III to the Fifth AssessmentReport of the Intergovernmental Panel on Climate Change*; IPCC: Geneva, Switzerland, 2014; p 151.

83. McGill, R.; Remley, W.; Winther, K. *Alternative Fuels for Marine Applications*; IEA Advanced Motor Fuels Implementing Agreement: 2013.

84. Hoang, A. T.; Pham, V. V., A review on fuels used for marine diesel engines. *Journal of Mechanical Engineering Research & Developments (JMERD)* **2018,** *41* (4), 22-32.

85. Kotchenruther, R. A., The effects of marine vessel fuel sulfur regulations on ambient $PM_{2.5}$ at coastal and near coastal monitoring sites in the U.S. *Atmospheric Environment* **2017,** *151*, 52-61.

86. 4, T. C. I. T. S., ISO 8217:2017 Petroleum products- Fuels (class F)- Specifications of marine fuels. 6 ed.; Standardization, I. O. f., Ed. 2017.

87. @Risk. 7.5.011460.0 ed.; Palisade: 2016.

88. Sandvik SAF 2507. https://www.materials.sandvik/en-us/materials-center/material-datasheets/tube-and-pipe-seamless/sandvik-saf-2507/#:~:text=Sandvik%20SAF%202507%C2%AE%20is,to%20pitting%20and%20crevice%20corrosion (accessed 6/25/2020).

89. Berglin, E. J.; Enderlin, C. W.; Schmidt, A. J., Review and assessment of commercial vendors/options for feeding and pumping biomass slurries for hydrothermal liquefaction. Pacific Northwest Laboratory: Richland, Washington, 2012.

90. Akhtar, J.; Amin, N. A. S., A review on process conditions for otimum bio-oil yield in hydrothermal liquefaction of biomass. *Renewable and Sustainable Energy Reviews* **2011,** *15*, 1615-1624.

91. Roberts, D. E.; Walton, W. W.; Jessup, R. S., Heats of combustion and solution of liquid styrene and solid polystyrene, and the heat of polymerization of styrene. *Journal of Research of the National Bureau of Standards* **1947,** *38*, 627-635.

92. Chang, S. S., Heat capacities of polyethylene from 2 to 360 K. II. Two high density linear polyethylene samples and thermodynamic properties of crystalline linear polyethylene. *Journal of Research of the National Bureau of Standards-A. Physics and Chemistry* **1974,** *78* (A.3), 387-400.

93. Farah, S.; Kunduru, K. R.; Basu, A.; Domb, A. J., Molecular weight determination of polyethylene terephthalate. In *Poly (Ethylene Terephthalate) Based Blends, Composites and Nanocomposites*, Elsevier: Waltham, MA, 2015; pp 143-165.

94. Chang, S. S., Heat capacity and thermodynamic properties of Poly(Vinyl Chloride). *Journal of Research of the National Bureau of Standards* **1977,** *82* (1), 9-18.

95. Acree, W. E. J.; Chickos, J. S., Thermochemical Data. In *NIST Chemistry WebBook, NIST Standard Reference Database Number 69*, Burgess, D. R. J., Ed. National Institute of Standards and Technology: Gaithersburg MD, 20899.

96. Daifullah, A. H. A.; Mohamed, M. M., Degradation of benzene, toluene ethylbenzene and p-xylene (BTEX) in aqueous soltuions using UV/H2O2 system. *J Chem. Technol. Biotechnol* **2004,** *79*, 468-474.

97. Coquelet , C.; Valtz, A.; Richon, D., Solubility of ethylbenzene and xylene in pure water and aqueous alkanolamine solutions. *J. Chem. Thermodynamics* **2008,** *40*, 942-948.

98. Lane, W. H., Determination of the solubility of styrene in water and of water in styrene. *Industrial and Engineering Chemistry* **1946,** *18* (5), 295-296.

99. Toluene. Sigma-Aldrich: St. Louis, MO, Feb 20, 2020.

100. Akca, E.; Gursel, A., A review of superalloys and IN718 nickel-based INCONEL superalloy. *Periodicals of Engineering and Natural Sciences* **2015,** *3* (1), 15-27.

101. Lhotsky, O.; Krakorova, E.; Masi, P.; Zebrak, R.; Linhartova, L.; Kresinova, Z.; Kaslik, J.; Steinova, J.; Rodsand, T.; Filipova, A.; Petru, K.; Kroupova, K.; Cajthaml, T., Pharmaceuticals, benzene, toluene, and chlorobenzene removal from contaminated groundwater by combined UV/H_2O_2 photo-oxidation and aeration. *Water Research* **2017,** *120*, 245-255.

102. Acree, W. E. J.; Chickos, J. S., Thermophysical Properties of Fluid Systems. In *NIST Chemistry WebBook, NIST Standard Reference Database Number 69*, Lemmon, E. W. M., M. O.; Friend, D. G.,, Ed. National Institute of Standards and Technology: Gaithersburg MD, 20899.

103. Fishing vessel operations. http://www.fao.org/3/ah827e/AH827E06.htm.

104. Belden, E. R.; Rando, M.; Ferrara, O. G.; Himebaugh, E. T.; Skangos, C. A.; Kazantzis, N. K.; Paffenroth, R. C.; Timko, M. T., Machine Learning Predictions of Oil Yields

Obtained by Plastic Pyrolysis and Application to Thermodynamic Analysis. *ACS Engineering Au* **2022**.

105. Annual production of plastics worldwide from 1950 to 2020 (on millions metric tons). https://www.statista.com/statistics/282732/global-production-of-plastics-since-1950/ (accessed July 26, 2022).

106. Plastics: Material- Specific Data. https://www.epa.gov/facts-and-figures-about-materials-waste-and-recycling/plastics-material-specific-data (accessed Jul 26, 2022).

107. Chen, H. L.; Nath, T. K.; Chong, S.; Foo, V.; Gibbins, C.; Lechner, A. M., The plastic waste problem in Malaysia: management, recycling and disposal of local and global plastic waste. *SN Applied Sciences* **2021,** *3* (4), 437.

108. Cole, M.; Lindeque, P.; Fileman, E.; Halsband, C.; Goodhead, R.; Moger, J.; Galloway, T. S., Microplastic Ingestion by Zooplankton. *Environmental Science & Technology* **2013,** *47* (12), 6646-6655.

109. Barboza, L. G. A.; Dick Vethaak, A.; Lavorante, B. R. B. O.; Lundebye, A.-K.; Guilhermino, L., Marine microplastic debris: An emerging issue for food security, food safety and human health. *Marine Pollution Bulletin* **2018,** *133*, 336-348.

110. Filiciotto, L.; Rothenberg, G., Biodegradable Plastics: Standards, Policies, and Impacts. *ChemSusChem* **2021,** *14* (1), 56-72.

111. Schmidt, C.; Krauth, T.; Wagner, S., Export of Plastic Decris by Rivers into the Sea. *Environmental Science & Technology* **2017,** *51*, 12246-12253.

112. Al-Salem, S. M.; Lettieri, P.; Baeyens, J., Recycling and recovery routes of plastic solid waste (PSW): A review. *Waste Management* **2009,** *29* (10), 2625-2643.

113. Joseph, B.; James, J.; Kalarikkal, N.; Thomas, S., Recycling of medical plastics. *Advanced Industrial and Engineering Polymer Research* **2021,** *4* (3), 199-208.

114. Thiounn, T.; Smith, R. C., Advances and approaches for chemical recycling of plastic waste. *Journal of Polymer Science* **2020,** *58* (10), 1347-1364.

115. Advancing Sustainable Materials Management: Facts and Figures 2018. https://www.epa.gov/sites/default/files/2021-01/documents/2018_ff_fact_sheet_dec_2020_fnl_508.pdf (accessed December 2021).

116. Chen, H.; Wan, K.; Zhang, Y.; Wang, Y., Waste to Wealth: Chemical Recycling and Chemical Upcycling of Waste Plastics for a Great Future. *ChemSusChem* **2021,** *14* (19), 4123-4136.

117. Ellis, L. D.; Rorrer, N. A.; Sullivan, K. P.; Otto, M.; McGeehan, J. E.; Román-Leshkov, Y.; Wierckx, N.; Beckham, G. T., Chemical and biological catalysis for plastics recycling and upcycling. *Nature Catalysis* **2021,** *4* (7), 539-556.

118. Valero, A.; Valero, A., Thermodynamic Rarity and Recyclability of Raw Materials in the Energy Transition: The Need for an In-Spiral Economy. *Entropy* **2019,** *21* (9), 1-14.

119. Qureshi, M. S.; Oasmaa, A.; Pihkola, H.; Deviatkin, I.; Tenhunen, A.; Mannila, J.; Minkkinen, H.; Pohjakallio, M.; Laine-Ylijoki, J., Pyrolysis of plastic waste: Opportunities and challenges. *Journal of Analytical and Applied Pyrolysis* **2020,** *152*, 104804.

120. Elliott, D. C.; Biller, P.; Ross, A. B.; Schmidt, A. J.; Jones, S. B., Hydrothermal liquefaction of biomass: Developments from batch to continuous process. *Bioresource Technology* **2015,** *178*, 147-156.

121. Quesada, L.; Calero, M.; Martín-Lara, M. Á.; Pérez, A.; Blázquez, G., Production of an Alternative Fuel by Pyrolysis of Plastic Wastes Mixtures. *Energy & Fuels* **2020,** *34* (2), 1781-1790.

122. Harmon, R. E.; SriBala, G.; Broadbelt, L. J.; Burnham, A. K., Insight into Polyethylene and Polypropylene Pyrolysis: Global and Mechanistic Models. *Energy & Fuels* **2021,** *35* (8), 6765-6775.

123. Kruse, T. M.; Levine, S. E.; Wong, H.-W.; Duoss, E.; Lebovitz, A. H.; Torkelson, J. M.; Broadbelt, L. J., Binary mixture pyrolysis of polypropylene and polystyrene: A modeling and experimental study. *Journal of Analytical and Applied Pyrolysis* **2005,** *73* (2), 342-354.

124. M. Kruse, T.; Sang Woo, O.; J. Broadbelt, L., Detailed mechanistic modeling of polymer degradation: application to polystyrene. *Chemical Engineering Science* **2001,** *56* (3), 971-979.

125. Cheng, F.; Belden, E. R.; Li, W.; Shahabuddin, M.; Paffenroth, R. C.; Timko, M. T., Accuracy of predictions made by machine learned models for biocrude yields obtained from hydrothermal liquefaction of organic wastes. *Chemical Engineering Journal* **2022,** *442* (1), 1-13.

126. Zhu, X.; Li, Y.; Wang, X., Machine learning prediction of biochar yield and carbon contents in biochar based on biomass characteristics and pyrolysis conditions. *Bioresource Technology* **2019,** *288*, 121527.

127. Ascher, S.; Watson, I.; You, S., Machine learning methods for modelling the gasification and pyrolysis of biomass and waste. *Renewable and Sustainable Energy Reviews* **2022,** *155*, 111902.

128. Gruber, F.; Grahlert, W.; Wollmann, P.; Kaskel, S., Classification of black plastics waste using fluorescence imaging and machine learning. *Recycling* **2019,** *4* (4), 1-17.

129. Yang, Y.; Zhang, X.; Yin, J.; Yu, X., Rapid and nondestructive on-site classification method for consumer-grade plastics based on partable NIR spectrometer and machine learning. *Journal of Spectroscopy* **2020,** *2020*, 6631234.

130. Stefas, D.; Gyftokostas, K.; Bellou, E.; Couris, S., Laser-induced breakdown spectroscopy assisted by machine learning for plastics/polymers identification. *Atoms* **2019,** *7* (3), 79-92.

131. Lu, H.; Diaz, D. J.; Czarnecki, N. J.; Zhu, C.; Kim, W.; Shroff, R.; Acosta, D. J.; Alexander, B. R.; Cole, H. O.; Zhang, Y.; Lynd, N. A.; Ellington, A. D.; Alper, H. S., Machine learning-aided engineering of hydrolases for PET depolymerization. *Nature* **2022,** *604* (7907), 662-667.

132. Yel, E.; Tezel, G.; Uymaz, S. A., ANN modelling for prediciting the water absorption of composites with waste plastic pyrolysis char fillers. *Data Science and Applications* **2018,** *1* (1), 45-51.

133. Abnisa, F.; Anuar Sharuddin, S. D.; bin Zanil, M. F.; Wan Daud, W. M. A.; Indra Mahlia, T. M., The Yield Prediction of Synthetic Fuel Production from Pyrolysis of Plastic Waste by Levenberg–Marquardt Approach in Feedforward Neural Networks Model. *Polymers* **2019,** *11* (11), 1853.

134. Mighani, M.; Shahi, A.; Antonioni, G., *Catalytic Pyrolysis of Plastic Waste Products: Time Series Modeling Using Least Square Support Vector Machine and Artificial Neural Network*. 2017.

135. Okada, S.; Ohzeki, M.; Taguchi, S., Efficient partition of integer optimization problems with one-hot encoding. *Scientific Reports* **2019,** *9* (1), 13036.

136. Aieb, A.; Madani, K.; Scarpa, M.; Bonaccorso, B.; Lefsih, K., A new approach for processing climate missing databases applied to daily rainfall data in Soummam watershed, Algeria. *Heliyon* **2019,** *5* (2), e01247.

137. Mani, T.; Hauk, A.; Walter, U.; Burkhardt-Holm, P., Microplastics profile along the Rhine River. *Scientific Reports* **2015,** *5*, 1-7.

138. Vriend, P.; Calcar, C. v.; Kooi, M.; Landman, H.; Pikaar, R.; Emmerik, T. v., Rapid Assessment of Floating Macroplastic Transport in the Rhine. *Frontiers in Marine Science* **2020,** *7*, 1-8.

139. Zhang, S., Nearest neighbor selection for iteratively kNN imputation. *Journal of Systems and Software* **2012,** *85*, 2541-2552.

140. Nadkarni, P., Core Technologies: Data Mining and "Big Data". In *Clinical Research Computing A Practitioner's Handbook*, 2016; pp 187-204.

141. Van Rossum, G.; Drake, F. L. *Python 3 Reference Manual*, CreateSpace: Scotts Valley, CA, 2009.

142. Pedregosa, F.; Varoquaux, G.; Gramfort, A.; Michel, V.; Thirion, B.; Grisel, O.; Blondel, M.; Prettenhofer, P.; Weiss, R.; Dubourg, V.; Vanderplas, J.; Passos, A.; Cournapeau, D.; Brucher, M.; Perrot, M.; Duchesnay, E., Scikit-learn: Machine Learning in Python. *JMLR* **2011,** *12* (85), 2825-2830.

143. Williams, E. A.; Williams, P. T., The pyrolysis of individual plastics and a plastic mixture in a fixed bed reactor. *Journal of Chemical Technology & Biotechnology* **1997,** *70* (1), 9-20.

144. Alberg, D.; Last, M.; Kandel, A., Knowledge discovery in data streams with regression tree methods. *WIREs Data Mining and Knowledge Discovery* **2012,** *2* (1), 69-78.

145. MacKay, D. J. C., Hyperparameters: Optimize, or Integrate Out? In *Maximum Entropy and Bayesian Methods: Santa Barbara, California, U.S.A., 1993*, Heidbreder, G. R., Ed. Springer Netherlands: Dordrecht, 1996; pp 43-59.

146. Olive, D. J., Multiple Linear Regression. In *Linear Regression*, Olive, D. J., Ed. Springer International Publishing: Cham, 2017; pp 17-83.

147. Sakata, Y.; Uddin, M. A.; Muto, A., Degradation of polyethylene and polypropylene into fuel oil by using solid acid and non-acid catalysts. *Journal of Analytical and Applied Pyrolysis* **1999,** *51* (1), 135-155.

148. Zolghadr, A.; Sidhu, N.; Mastalski, I.; Facas, G.; Maduskar, S.; Uppili, S.; Go, T.; Neurock, M.; Dauenhauer, P. J., On the Method of Pulse-Heated Analysis of Solid Reactions (PHASR) for Polyolefin Pyrolysis. *ChemSusChem* **2021,** *14* (19), 4214-4227.

149. Scott, D. S.; Czernik, S. R.; Piskorz, J.; Radlein, D. S. A. G., Fast Pyrolysis of Plastic Wastes. *Energy & Fuels* **1990,** *4*, 407-411.

150. Encinar, J. M.; González, J. F., Pyrolysis of synthetic polymers and plastic wastes. Kinetic study. *Fuel Processing Technology* **2008,** *89* (7), 678-686.

151. Odejobi, O. J.; Oladunni, A. A.; Sonibare, J. A.; Abegunrin, I. O., Oil yield optimization from co-pyrolysis of low-density polyethylene (LDPE), polystyrene (PS) and polyethylene terephthalate (PET) using simplex lattice mixture design. *Fuel Communications* **2020,** *2-5*, 100006.

152. Dhahak, A.; Hild, G.; Rouaud, M.; Mauviel, G.; Burkle-Vitzthum, V., Slow pyrolysis of polyethylene terephthalate: Online monitoring of gas production and quantitative analysis of waxy products. *Journal of Analytical and Applied Pyrolysis* **2019,** *142*, 104664.

153. Smith, R. L.; Takkellapati, S.; Riegerix, R. C., Recycling of Plastics in the United States: Plastic Material Flows and Polyethylene Terephthalate (PET) Recycling Processes. *ACS Sustainable Chemistry & Engineering* **2022,** *10* (6), 2084-2096.

154. Wang, C.-Q.; Wang, H.; Liu, Y.-N., Separation of polyethylene terephthalate from municipal waste plastics by froth flotation for recycling industry. *Waste Management* **2015,** *35*, 42-47.

155. Wal, M. v. d.; Meulen, M. v. d.; Tweehuijsen, G.; Peterlin, M.; Palatinus, A.; Virsek, M. K.; Coscia, L.; Krzan, A. *SFRA0025: Identification and Assessment of Riverine Input of (Marine) Litter*; Final Report for the European Commission DG Environment under Framework Contract No ENV.D.2/FRA/2012/0025: 2015.

156. IEA Production forecast of thermoplastics worldwide from 2020 to 2050, by type (in million metric tons). https://www.statista.com/statistics/1192886/thermoplastics-production-volume-by-type-globally/ (accessed Agust 25, 2022).

157. Carbon Dioxide Emissions Coefficients. https://www.eia.gov/environment/emissions/co2_vol_mass.php (accessed August 2022).

158. IEA Global Energy Review 2021. https://www.iea.org/reports/global-energy-review-2021 (accessed August 2022).

159. Papadis, E.; Tsatsaronis, G., Challenges in the decarbonization of the energy sector. *Energy* **2020,** *205*, 118025.

160. Bagri, R.; Williams, P. T., Catalytic pyrolysis of polyethylene. *Journal of Analytical and Applied Pyrolysis* **2002,** *63* (1), 29-41.

161. Zhao, D.; Wang, X.; Miller, J. B.; Huber, G. W., The Chemistry and Kinetics of Polyethylene Pyrolysis: A Process to Produce Fuels and Chemicals. *ChemSusChem* **2020,** *13* (7), 1764-1774.

162. Al-Salem, S. M., Thermal pyrolysis of high density polyethylene (HDPE) in a novel fixed bed reactor system for the production of high value gasoline range hydrocarbons (HC). *Process Safety and Environmental Protection* **2019,** *127*, 171-179.

163. Pinto, F.; Costa, P.; Gulyurtlu, I.; Cabrita, I., Pyrolysis of plastic wastes. 1. Effect of plastic waste composition on product yield. *Journal of Analytical and Applied Pyrolysis* **1999,** *51* (1), 39-55.

164. Seo, Y.-H.; Lee, K.-H.; Shin, D.-H., Investigation of catalytic degradation of high-density polyethylene by hydrocarbon group type analysis. *Journal of Analytical and Applied Pyrolysis* **2003,** *70* (2), 383-398.

165. Kumar, S.; Singh, R. K., Recovery of hydrocarbon liquid from waste high density polyethylene by thermal pyrolysis. *Brazilian Journal of Chemical Engineering* **2011,** *28* (4), 659-667.

166. Abnisa, F.; Anuar Sharuddin, S. D.; Bin Zanil, M. F.; Wan Daud, W. M. A.; Indra Mahlia, T. M., The Yield Prediction of Synthetic Fuel Production from Pyrolysis of Plastic Waste by Levenberg-Marquardt Approach in Feedforward Neural Networks Model. *Polymers (Basel)* **2019,** *11* (11).

167. Ludlow-Palafox, C.; Chase, H. A., Microwave-Induced Pyrolysis of Plastic Wastes. *Industrial & Engineering Chemistry Research* **2001,** *40* (22), 4749-4756.

168. Quesada, L.; Pérez, A.; Godoy, V.; Peula, F. J.; Calero, M.; Blázquez, G., Optimization of the pyrolysis process of a plastic waste to obtain a liquid fuel using different mathematical models. *Energy Conversion and Management* **2019,** *188*, 19-26.

169. Ahmad, I.; Khan, M. I.; Khan, H.; Ishaq, M.; Tariq, R.; Gul, K.; Ahmad, W., Pyrolysis study of polypropylene and polyethylene into premium oil products. *International Journal of Green Energy* **2015,** *12*, 663-671.

170. Anene, A. F.; Fredriksen, S. B.; Sætre, K. A.; Tokheim, L.-A., Experimental Study of Thermal and Catalytic Pyrolysis of Plastic Waste Components. *Sustainability* **2018,** *10* (11).

171. FakhrHoseini, S. M.; Dastanian, M., Predicting Pryolysis Producst of PE, PP and PET Using NRTL Activity Coefficient Model. *Journal of Chemistry* **2013,** *2013*.

172. Uddin, M. A.; Koizumi, K.; Murata, K.; Sakata, Y., Thermal and catalytic degradation of structurally different types of polyethylene into fuel oil. *Polymer Degradation and Stability* **1997,** *56* (1), 37-44.

173. Miandad, R.; Barakat, M. A.; Aburiazaiza, A. S.; Rehan, M.; Ismail, I. M. I.; Nizami, A. S., Effect of plastic waste types on pyrolysis liquid oil. *International Biodeterioration & Biodegradation* **2017,** *119*, 239-252.

174. Bajus, M.; Hajekova, E., Thermal Cracking of the Model Seven Components Mixed Plastics into Oils/Waxes. *Petroleum & Coal* **2010,** *52* (3), 164-172.

175. Mlynková, B.; Hájeková, E.; Bajus, M., Copyrolysis of oils/waxes of individual and mixed polyalkenes cracking products with petroleum fraction. *Fuel Processing Technology* **2008,** *89* (11), 1047-1055.

176. Williams, P. T.; Slaney, E., Analysis of products from the pyrolysis and liquefaction of single plastics and waste plastic mixtures. *Resources, Conservation and Recycling* **2007,** *51* (4), 754-769.

177. Williams, P. T.; Williams, E. A., Fluidised bed pyrolysis of low density polyethylene to produce petrochemical feedstock. *Journal of Analytical and Applied Pyrolysis* **1999,** *51* (1), 107-126.

178. Mastral, F. J.; Esperanza, E.; Berrueco, C.; Juste, M.; Ceamanos, J., Fluidized bed thermal degradation products of HDPE in an inert atmosphere and in air–nitrogen mixtures. *Journal of Analytical and Applied Pyrolysis* **2003,** *70* (1), 1-17.

179. Muhammad, C.; Onwudili, J. A.; Williams, P. T., Thermal Degradation of Real-World Waste Plastics and Simulated Mixed Plastics in a Two-Stage Pyrolysis–Catalysis Reactor for Fuel Production. *Energy & Fuels* **2015,** *29* (4), 2601-2609.

180. Singh, R. K.; Ruj, B., Time and temperature depended fuel gas generation from pyrolysis of real world municipal plastic waste. *Fuel* **2016,** *174*, 164-171.

181. Mastral, F. J.; Esperanza, E.; García, P.; Juste, M., Pyrolysis of high-density polyethylene in a fluidised bed reactor. Influence of the temperature and residence time. *Journal of Analytical and Applied Pyrolysis* **2002,** *63* (1), 1-15.

182. Liu, Y.; Qian, J.; Wang, J., Pyrolysis of polystyrene waste in a fluidized-bed reactor to obtain styrene monomer and gasoline fraction. *Fuel Processing Technology* **2000,** *63* (1), 45-55.

183. Onwudili, J. A.; Insura, N.; Williams, P. T., Composition of products from the pyrolysis of polyethylene and polystyrene in a closed batch reactor: Effects of temperature and residence time. *Journal of Analytical and Applied Pyrolysis* **2009,** *86* (2), 293-303.

184. Martynis, M.; Mulyazmi; Winanda, E.; Harahap, A. N., Thermal Pyrolysis of Polypropylene Plastic Waste into Liquid Fuel: Reactor Performance Evaluation. *IOP Conference Series: Materials Science and Engineering* **2019,** *543*.

185. Papuga, S.; Gvero, P.; Vukic, L., Temperature and time influence on the waste plastics pyrolysis in the fixed bed reactor. *Thermal Science* **2015,** *20*.

186. López, A.; de Marco, I.; Caballero, B. M.; Laresgoiti, M. F.; Adrados, A., Influence of time and temperature on pyrolysis of plastic wastes in a semi-batch reactor. *Chemical Engineering Journal* **2011,** *173* (1), 62-71.

187. Ajibola, A. A.; Omoleye, J. A.; Efeovbokhan, V. E., Catalytic cracking of polyethylene plastic waste using synthesised zeolite Y from Nigerian kaolin deposit. *Applied Petrochemical Research* **2018,** *8* (4), 211-217.

188. Jadhao, S. B.; Seethamraju, S., Pyrolysis Study of mixed plastics waste. *IOP Conference Series: Materials Science and Engineering* **2020,** *736* (4), 042036.

189. Panda, A. K.; Alotaibi, A.; Kozhevnikov, I. V.; Shiju, N. R., Pyrolysis of Plastics to Liquid Fuel Using Sulphated Zirconium Hydroxide Catalyst. *Waste and Biomass Valorization* **2020,** *11* (11), 6337-6345.

190. Sembiring, F.; Purnomo, C. W.; Purwono, S., Catalytic Pyrolysis of Waste Plastic Mixture. *IOP Conference Series: Materials Science and Engineering* **2018,** *316*, 012020.

191. Miandad, R.; Rehan, M.; Barakat, M. A.; Aburiazaiza, A. S.; Khan, H.; Ismail, I. M. I.; Dhavamani, J.; Gardy, J.; Hassanpour, A.; Nizami, A.-S., Catalytic Pryolysis of Plastic Waste: Moving Toward Pyrolysis Based Biorefineries. *Frontiers in Energy Research* **2019,** *7*.

192. Ding, K.; Liu, S.; Huang, Y.; Liu, S.; Zhou, N.; Peng, P.; Wang, Y.; Chen, P.; Ruan, R., Catalytic microwave-assisted pyrolysis of plastic waste over NiO and HY for gasoline-range hydrocarbons production. *Energy Conversion and Management* **2019,** *196*, 1316-1325.

193. Joshi, C. A.; Seay, J. R., Total generation and combustion emissions of plastic derived fuels: A trash to tank approach. *Environmental Progress & Sustainable Energy* **2020,** *39* (5).

194. Merrington, A., 9 - Recycling of Plastics. In *Applied Plastics Engineering Handbook (Second Edition)*, Kutz, M., Ed. William Andrew Publishing: 2017; pp 167-189.

195. Eze, W. U.; Umunakwe, R.; Obasi, H. C.; Ugbaja, M. I.; Uche, C. C.; Madufor, I. C., Plastics waste management: A review of pyrolysis technology. *Clean Technol. Recycl* **2021,** *1* (1), 50-69.

196. Zhang, Y.; Brown, T. R.; Hu, G.; Brown, R. C., Techno-economic analysis of two bio-oil upgrading pathways. *Chemical Engineering Journal* **2013,** *225*, 895-904.

197. Zhu, Y.; Biddy, M. J.; Jones, S. B.; Elliott, D. C.; Schmidt, A. J., Techno-economic analysis of liquid fuel production from woody biomass via hydrothermal liquefaction (HTL) and upgrading. *Applied Energy* **2014,** *129*, 384-394.

198. Meyer, P. A.; Snowden-Swan, L. J.; Jones, S. B.; Rappé, K. G.; Hartley, D. S., The effect of feedstock composition on fast pyrolysis and upgrading to transportation fuels: Techno-economic analysis and greenhouse gas life cycle analysis. *Fuel* **2020,** *259*, 116218.

199. Milbrandt, A.; Coney, K.; Badgett, A.; Beckham, G. T., Quantification and evaluation of plastic waste in the United States. *Resources, Conservation and Recycling* **2022,** *183*, 106363.

200. Adamczyk, T. Massachusetts Landfills, Transfer Stations, Compost Sites & Recycling Facilities. https://www.mass.gov/lists/massachusetts-landfills-transfer-stations-compost-sites-recycling-facilities (accessed 1/26/2024).

201. Almohamadi, H.; Alamoudi, M.; Ahmed, U.; Shamsuddin, R.; Smith, K., Producing hydrocarbon fuel from the plastic waste: Techno-economic analysis. *Korean Journal of Chemical Engineering* **2021,** *38* (11), 2208-2216.

202. Fivga, A.; Dimitriou, I., Pyrolysis of plastic waste for production of heavy fuel substitute: A techno-economic assessment. *Energy* **2018,** *149*, 865-874.

203. Cappello, V.; Sun, P.; Zang, G.; Kumar, S.; Hackler, R.; Delgado, H. E.; Elgowainy, A.; Delferro, M.; Krause, T., Conversion of plastic waste into high-value lubricants: techno-economic analysis and life cycle assessment. *Green Chemistry* **2022,** *24* (16), 6306-6318.

204. Al-Qadri, A. A.; Ahmed, U.; Abdul Jameel, A. G.; Zahid, U.; Usman, M.; Ahmad, N., Simulation and modelling of hydrogen production from waste plastics: technoeconomic analysis. *Polymers* **2022,** *14* (10), 2056.

205. Afzal, S.; Singh, A.; Nicholson, S. R.; Uekert, T.; DesVeaux, J. S.; Tan, E. C.; Dutta, A.; Carpenter, A. C.; Baldwin, R. M.; Beckham, G. T., Techno-economic analysis and life cycle assessment of mixed plastic waste gasification for production of methanol and hydrogen. *Green Chemistry* **2023,** *25* (13), 5068-5085.

206. Palone, O.; Gagliardi, G. G.; Mechelli, M.; Cedola, L.; Borello, D., Techno-economic analysis of sustainable methanol and ammonia production by chemical looping hydrogen generation from waste plastic. *Energy Conversion and Management* **2023,** *292*, 117389.

207. *Analysis of MSW Landfill Tipping Fees-2022*; Environmental Research & Education Foundation: 2023.

208. Secondary Marterials Pricing - Plastics. RecyclingMarkets.net.

209. Chari, S.; Sebastiani, A.; Paulillo, A.; Materazzi, M., The Environmental Performance of Mixed Plastic Waste Gasification with Carbon Capture and Storage to Produce Hydrogen in the U.K. *ACS Sustainable Chemistry & Engineering* **2023,** *11* (8), 3248-3259.

210. Wright, M. M.; Daugaard, D. E.; Satrio, J. A.; Brown, R. C., Techno-economic analysis of biomass fast pyrolysis to transportation fuels. *Fuel* **2010,** *89*, S2-S10.

211. Jones, S.; Meyer, P.; Snowden-Swan, L.; Padmaperuma, A.; Tan, E.; Dutta, A.; Jacobson, J.; Cafferty, K. *Process design and economics for the conversion of lignocellulosic biomass to hydrocarbon fuels: fast pyrolysis and hydrotreating bio-oil pathway*; National Renewable Energy Lab.(NREL), Golden, CO (United States): 2013.

212. Dutta, A.; Iisa, M. K.; Talmadge, M.; Mukarakate, C.; Griffin, M. B.; Tan, E. C.; Wilson, N.; Yung, M. M.; Nimlos, M. R.; Schaidle, J. A. *Ex situ catalytic fast pyrolysis of lignocellulosic biomass to hydrocarbon fuels: 2019 state of technology and future research*; National Renewable Energy Lab.(NREL), Golden, CO (United States); Argonne …: 2020.

213. U.S. Crude Oil First Purchase Price. https://www.eia.gov/dnav/pet/hist/LeafHandler.ashx?n=pet&s=f000000__3&f=m (accessed 2/13/2024).

214. Peters, M. S.; Timmerhaus, K. D.; West, R. E.; Timmerhaus, K.; West, R., *Plant design and economics for chemical engineers*. McGraw-hill New York: 1968; Vol. 4.

215. Production capacity of polystyrene worldwise in 2022 and 2026. https://www.statista.com/statistics/1065889/global-polystyrene-production-capacity/ (accessed 02/05/2024).

216. Energy Information Administration:Official energy statistics from the US government. www.eia.doe.gov (accessed 02/05/2024).

217. Thompson, J.; Watson, R. Time is Running Out:The U.S. Landfill Capacity Crisis. https://sweepstandard.org/time-is-running-out-the-u-s-landfill-capacity-crisis/#:~:text=Based%20on%20data%20collected%20by,could%20be%20only%20half%20that. (accessed 2/9/2024).

218. Galloway, T. S.; Cole, M.; Lewis, C., Interactions of microplastic debris throughout the marine ecosystem. *Nature Ecology & Evolution* **2017,** *1* (5), 0116.

219. Lambert, S.; Wagner, M., Microplastics Are Contaminants of Emerging Concern in Freshwater Environments: An Overview. In *Freshwater Microplastics : Emerging Environmental Contaminants?*, Wagner, M.; Lambert, S., Eds. Springer International Publishing: Cham, 2018; pp 1-23.

220. de Souza Machado, A. A.; Kloas, W.; Zarfl, C.; Hempel, S.; Rillig, M. C., Microplastics as an emerging threat to terrestrial ecosystems. *Global Change Biology* **2018,** *24* (4), 1405-1416.

221. Meides, N.; Menzel, T.; Poetzschner, B.; Löder, M. G. J.; Mansfeld, U.; Strohriegl, P.; Altstaedt, V.; Senker, J., Reconstructing the Environmental Degradation of Polystyrene by Accelerated Weathering. *Environmental Science & Technology* **2021,** *55* (12), 7930-7938.

222. Cella, R. F.; Mumbach, G. D.; Andrade, K. L.; Oliveira, P.; Marangoni, C.; Bolzan, A.; Bernard, S.; Machado, R. A. F., Polystyrene recycling processes by dissolution in ethyl acetate. *Journal of Applied Polymer Science* **2018,** *135* (18), 46208.

223. García, M. T.; Duque, G.; Gracia, I.; de Lucas, A.; Rodríguez, J. F., Recycling extruded polystyrene by dissolution with suitable solvents. *Journal of Material Cycles and Waste Management* **2009,** *11* (1), 2-5.

224. Gutiérrez, C.; García, M. T.; Gracia, I.; de Lucas, A.; Rodríguez, J. F., The Selective Dissolution Technique as Initial Step for Polystyrene Recycling. *Waste and Biomass Valorization* **2013,** *4* (1), 29-36.

225. Maafa, I. M., Pyrolysis of Polystyrene Waste: A Review. *Polymers* **2021,** *13* (2), 225.

226. Lilac, W., Lee S. , Kinetics and mechanisms of styrene monomer recovery from waste polystyrene by supercritical water partial oxidation. *Advances in Environmental Research* **2001,** *6* (1), 9-16.

227. Kruse, T. M.; Wong, H.-W.; Broadbelt, L. J., Modeling the Evolution of the Full Polystyrene Molecular Weight Distribution during Polystyrene Pyrolysis. *Industrial & Engineering Chemistry Research* **2003,** *42* (12), 2722-2735.

228. Levine, S. E.; Broadbelt, L. J., Reaction pathways to dimer in polystyrene pyrolysis: A mechanistic modeling study. *Polymer Degradation and Stability* **2008,** *93* (5), 941-951.

229. Guyot, A., Recent developments in the thermal degradation of polystyrene—A review. *Polymer Degradation and Stability* **1986,** *15* (3), 219-235.

230. Chum, H. L.; Johnson, D. K.; Black, S. K.; Overend, R. P., Pretreatment-catalyst effects and the combined severity parameter. *Applied biochemistry and biotechnology* **1990,** *24*, 1-14.

231. Lin, C. C.; Smith, F. R.; Ichikawa, N.; Baba, T.; Itow, M., Decomposition of hydrogen peroxide in aqueous solutions at elevated temperatures. *International Journal of Chemical Kinetics* **1991,** *23* (11), 971-987.

232. Mark, J. E., Polymer data handbook. *(No Title)* **2009**.

233. Hahladakis, J. N.; Velis, C. A.; Weber, R.; Iacovidou, E.; Purnell, P., An overview of chemical additives present in plastics: Migration, release, fate and environmental ompact during their use, disposal and recycling. *Journal of Hazardous Materials* **2018,** *344*, 179-199.

234. Galati, A.; Scalenghe, R., Plastic end-of-life alternatives, with a focus on the agricultural sector. *Current Opinion in Chemical Engineering* **2021,** *32*, 1-10.

235. Moriya, T., Enomoto H., Characteristic of polyethylene cracking in supercritical water compared to thermal cracking. *Polymer Degradation and Stability* **1999,** *65*, 373-386.

236. Su, X.; Zhao, Y.; Zhang, R.; Bi, J., Investigation on degradation of polyehtylene to oils in supercritcal water. *Fuel Processing Technology* **2003,** *85*, 1249-1258.

237. Aboulkas, A.; harfi, K. E.; Bouadili, A. E., Thermal degradation behaviors of polyethylene and polypropylene. Part 1: Pyrolysis kinetics and mechanisms. *Energy Conversion and Management* **2010,** *51*, 1363-1369.

238. Celik, G.; Kennedy, R. M.; Hackler, R. A.; Ferrandon, M.; Tennakoon, A.; Patnaik, S.; LaPointe, A. M.; Ammal, S. C.; Heyden, A.; Perras, F. A.; Pruski, M.; Scott, S. L.; Poeppelmeier, K. R.; Sadow, A. D.; Delferro, M., Upcycling single-use polyehtylene into high-quality liquid products. *ACS Cent. Sci.* **2019,** *5* (11), 1795-1803.

239. Tennakoon, A.; Wu, X.; Paterson, A. L.; Patnaik, S.; Pei, Y.; LaPointe, A. M.; Ammal, S. C.; Hackler, R. A.; Heyden, A.; Slowing, I. I.; Coates, G. W.; Delferro, M.; Peters, B.; Huang, W.; Sadow, A. D.; Perras, F. A., Catalytic upcycling of high-density polyethylene via a procesive mechanism. *Nature Catalysis* **2020,** *3*, 893-901.

240. Zaker, A.; Guerra, P.; Tompsett, G. A.; Huang, X.; Bond, J. Q.; Timko, M. T., Chemicals from heavy oils by ZSM-5 catalysis in supercritical water: Model compound and reaction engineering. *AIChE Journal* **2020,** *66* (7), 1-12.

241. Kim, B.-S.; Kim, Y.-M.; Jae, J.; Watanabe, C.; Kim, S.; Jung, S.-C.; Kim, S. C.; Park, Y.-K., Pyrolysis and catalytic upgrading of Citrus unshiu peel. *Bioresource Technology* **2015,** *194*, 312-319.

242. Shakya, R.; Adhikari, S.; Mahadevan, R.; Hassan, E. B.; Dempster, T. A., Catalytic upgrading of bio-oil produced from hydrothermal liquefaction of Nannochloropsis sp. *Bioresource Technology* **2018,** *252*, 28-36.

243. Hai-feng, Z.; Xiao-li, S.; Dong-kai, S.; Rong, Z.; Ji-cheng, B., Investigation on degradation of polyethylene to oil in a continuous supercritcal water reactor. *Journal of fuel chemistry and technology* **2007,** *35* (4), 487-491.

244. Torri, C.; Fabbri, D.; Garcia-Alba, L.; Brilman, D. W. F., Upgrading of oils derived from hydrothermal treatment of microalgae by catalytic cracking over H-ZSM-5: A comparative Py–GC–MS study. *Journal of Analytical and Applied Pyrolysis* **2013,** *101*, 28-34.

245. Zhang, J.; Ma, M.; Chen, Z.; Zhang, X.; Yang, H.; Wang, X.; Feng, H.; Yu, J.; Gao, S., Production of monocyclic aromatics and light olefins through ex-situ catalytic pyrolysis of low-density polyethylene over Ga/P/ZSM-5 catalyst. *Journal of the Energy Institute* **2023,** *108*, 101235.

246. Liu, X.; Li, X.; Liu, J.; Wang, Z.; Kong, B.; Gong, X.; Yang, X.; Lin, W.; Guo, L., Study of high density polyethylene (HDPE) pyrolysis with reactive molecular dynamics. *Polymer Degradation and Stability* **2014,** *104*, 62-70.

247. Jacob, S. M.; Gross, B.; Voltz, S. E.; Weekman Jr, V. W., A lumping and reaction scheme for catalytic cracking. *AIChE Journal* **1976,** *22* (4), 701-713.

248. Abul-Hamayel, M. A., Kinetic modeling of high-severity fluidized catalytic cracking☆. *Fuel* **2003,** *82* (9), 1113-1118.

249. Meng, X.; Xu, C.; Gao, J.; Li, L., Catalytic pyrolysis of heavy oils: 8-lump kinetic model. *Applied Catalysis A: General* **2006,** *301* (1), 32-38.

250. Hierarchical Clustering. https://www.solver.com/xlminer/help/hierarchical-clustering-intro (accessed November, 18, 2021).

251. Lohninger, H., Fundamentals of Statistics EpinaDataLab: Epina E-book. http://www.statistics4u.info/fundstat_eng/ee_ztransform.html (accessed 1/4/2022).

252. Ekwe, N. B.; Tyufekchiev, M. V.; Salifu, A. A.; Tompsett, G. A.; LeClerc, H. O.; Belden, E. R.; Onche, E. O.; Ates, A.; Schmidt-Rohr, K.; Yuan, S.; Zheng, Z.; Soboyejo, W. O.; Timko, M. T., Mechanochemical Pretreatment for Waste-Free Conversion of Bamboo to Simple Sugars: Utilization of Available Resources for Developing Economies. *Advanced Sustainable Systems* **2022,** *6* (4), 2100286.